

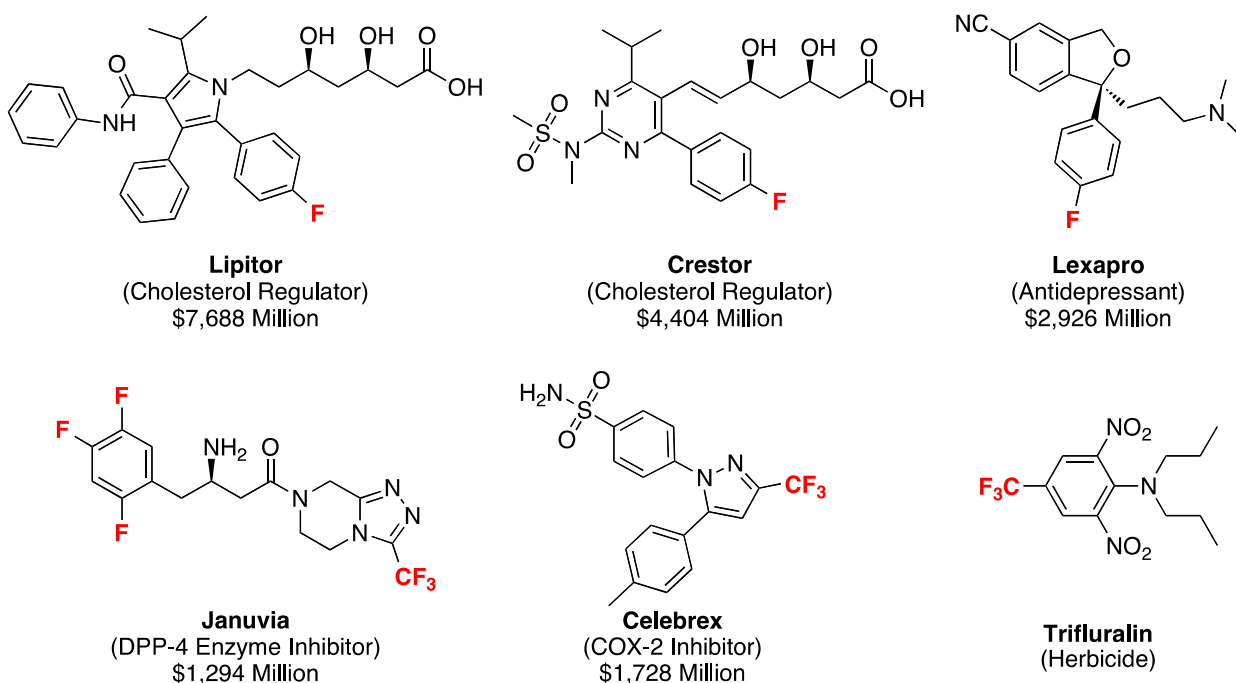
CHAPTER 1

Introduction

1.1 Significance of Fluorine

Due to its highest electronegativity, fluorine is a privileged functional motif in pharmaceutical, agrochemical, and materials science.¹ Currently, approximately 20% of all pharmaceuticals include at least one fluorine atom, and this is even higher for agrochemicals (~30%) (Scheme 1.1).^{2,3} In materials science, fluorocarbon based polymers represent a multibillion industry with increasing demand and continuous growth.⁴

Scheme 1.1 Representative Examples of Pharmaceuticals (and their annual sales in 2011), and Agrochemical Featuring Aryl-F and CF₃ Motifs.



In the design of pharmaceuticals and agrochemicals, incorporation of fluorine into a lead organic molecule enables the tuning of its biological properties.¹ For example, due to their electron withdrawing properties, fluorine or trifluoromethyl motifs lower the susceptibility of surrounding functionalities to cytochrome P450 enzymatic oxidation. Additionally, they can be used to directly block sites vulnerable to oxidation. A number of studies have also shown a direct impact of F upon the binding affinity and selectivity of biologically active molecules.^{1b} Several examples of top selling pharmaceuticals featuring F and/or CF₃ groups are shown in **Scheme 1.1**.

Although fluorine is the 13th most abundant element in earth's crust, it is only found in mineral form, which hinders its uptake in biological systems. As such, synthetic methods are needed to access the organofluorine compounds. To date, nucleophilic substitution is one of the most common ways to access C–F bonds.⁵ However, the high solvation energy of the fluoride ion in aqueous media results in a tightly bound hydration shell of water molecules, resulting in poor nucleophilicity. Meticulous exclusion of water can expose the naked fluoride as a strong nucleophile. However, the high basicity of anhydrous fluoride can limit its functional group tolerance.

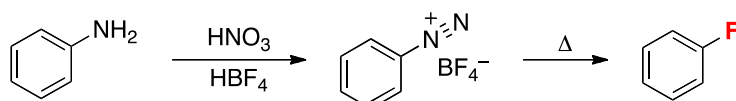
1.2 Organic Synthetic Methods for Organofluorine Molecules

Conventionally, two strategies have been used for the synthesis of aryl–F and CF₃ containing molecules: the functional group conversion method and the building-block method. In the functional group conversion method, a starting C–H or C–X (X = halide, OH, etc...) bond in a molecule reacts with a highly reactive fluorinating reagent, such as elemental fluorine (F₂), hydrogen fluoride (HF), or inorganic fluoride (SbF₅).^{6,7} These transformations are straightforward and have ideal atom economy. However, this strategy suffers from several drawbacks. First, the reactive nature of these fluorinating reagents render them incompatible with the majority of functional groups, which limits the substrate scope to simple molecules. Second, chemo- or regio-selectivity cannot be controlled during these processes. Finally, the handling of these highly reactive and hazard reagents requires special apparatus and skills, which hinders their application on a

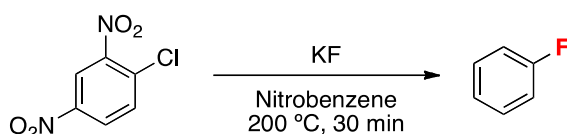
laboratory scale. Despite all of the difficulties mentioned above, the low cost of the fluorinating reagents made this the most attractive strategy for industrial operations.

Two of the most commonly used aromatic fluorination methods are the Balz-Schiemann reaction⁸ and the Halex process.⁶ The Balz-Schiemann reaction is a two-step functional group conversion method that converts aniline to aryl fluorides via diazonium fluoroborates as reaction intermediates (**Scheme 1.2**). The Halex process is a halogen exchange reaction that generates electron poor aryl-F from aryl-Cl through nucleophilic aromatic substitution (**Scheme 1.3**). Additionally, nucleophilic fluorination of diaryliodonium substrates has been demonstrated under thermal conditions, albeit with low reactivity and selectivity.

Scheme 1.2 Balz-Schiemann Reaction



Scheme 1.3 Halex Chemistry

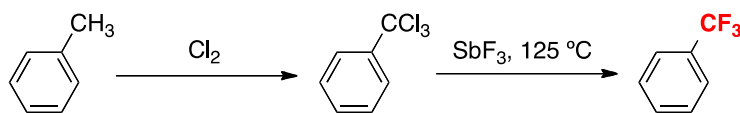


Scheme 1.4 Fluorination of Diaryliodonium Salt



On the industrial scale, trifluoromethylated arenes are mainly produced by the Swarts reaction, which was developed in 1892.⁷ This transformation involves a two-step conversion of toluene derivatives to benzotrifluorides via: (1) radical chlorination followed by (2) nucleophilic substitution with an inorganic fluoride (e.g. SbF₃) or anhydrous hydrogen fluoride (**Scheme 1.5**).⁷

Scheme 1.5 Swarts Reaction



The employment of highly reactive reagents and harsh conditions limits the substrate scope of this methodology to simple arenes. The two-step transformation is not straightforward or atom economical. Besides, the generation of six times as much chlorine waste as the desired product is undoubtedly costly. Thus, the development of mild and flexible alternative methods for the installation of F and CF₃ groups, particularly at late stages in the synthesis of complex molecules, is highly desirable.

Besides constructing a CF₃ unit from several single fluorination steps, the development of strategies that transfer CF₃ as a “package” has become a field of interest.^{5,9} A wide variety of CF₃ reagents have been developed, and can be classified into three groups, including nucleophilic, electrophilic, and radical CF₃ precursors.

A second strategy to construct an organofluorine compound is to start from a commercial F- or CF₃-containing simple building block as the core structure, and add the remaining parts around it. However, this method is strictly limited by the available chemical catalogues.

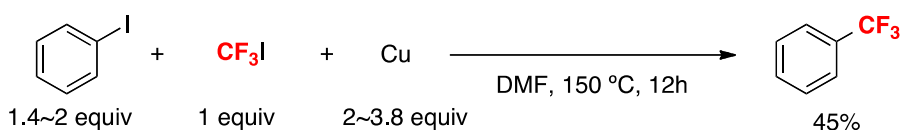
1.3 Transition Metal Based Methods for Ar-F and Ar-CF₃ Bond Formation

Aryl-F and aryl-CF₃ bonds are two of the strongest bonds known. Therefore, the formation of these motifs should be thermodynamically favorable. However, the high activation barriers for the aryl-F and aryl-CF₃ coupling render them kinetically inaccessible. A perfect solution to address these thermodynamically feasible but kinetically difficult transformations is the employment of a catalyst. In theory, a catalyst, such as transition metal, could be tuned by its surrounding ligands or oxidation state, to efficiently lower the activation barrier, and thereby access these bonds under mild conditions. Indeed, over the past decade, transition metal catalyzed/mediated aromatic fluorination¹⁰ and trifluoromethylation^{5,9} have become fields of great research interest.

1.3.1. Transition Metal Based Aromatic Trifluoromethylation

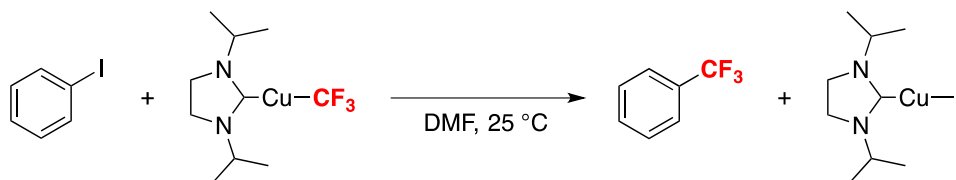
Copper is the most widely studied catalyst for transition metal catalyzed/mediated aromatic trifluoromethylation reactions.^{10c,11,12} In a pioneering report by McLoughlin and co-workers, benzotrifluoride was generated by reacting iodobenzene and CF₃I in the presence of copper at 150 °C.¹³ An *in situ* generated CuCF₃ was proposed to be the reactive intermediate. Since this initial report, many groups have expanded the CF₃ sources used for this reaction to those that are much easier to handle, such as TMSCF₃. The substrate scope has also been extended to sterically hindered, and heterocyclic systems. In several examples, the less reactive bromo-substituted aromatic could be converted to a CF₃ group as well.

Scheme 1.6 First Cu-Mediated Aryl–CF₃ Coupling via CuCF₃ Intermediate



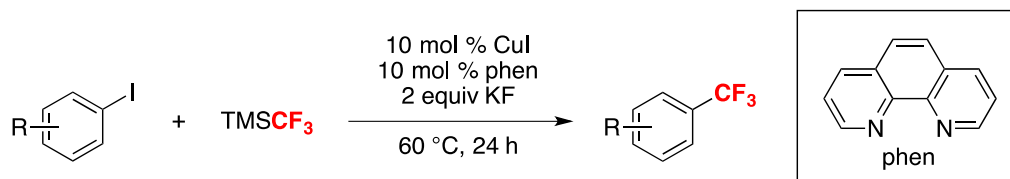
A major advance in the area of Cu-promoted trifluoromethylation was made in 2008, when Vicic reported the first example of an isolable, crystallographically characterized Cu^I–CF₃ complex.^{11a,b} This complex, which is supported by an *N*-heterocyclic carbene ligand, was shown to react with aryl iodides under mild conditions (25 °C, 112 h) to liberate trifluoromethylated products (**Scheme 1.7**). While related Cu-mediated trifluoromethylations were known prior to this report,^{10,11,12,13} these previous systems generally involved ill-defined “Cu–CF₃” intermediates.

Scheme 1.7 Reaction of First Well-Defined Cu–CF₃ Complex with Aryl Iodide



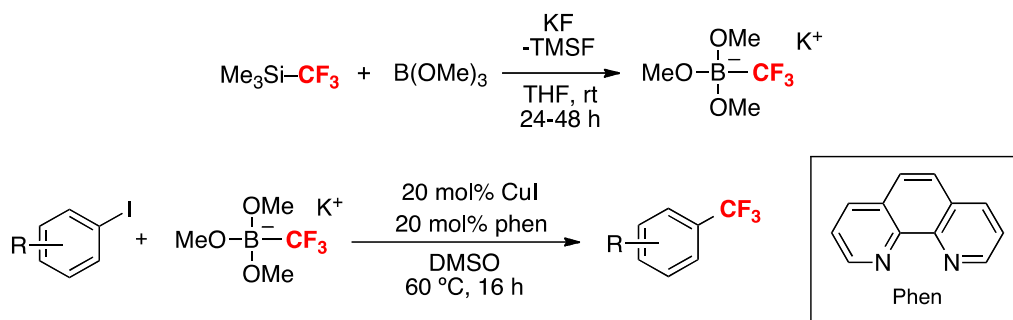
A final significant advance in the field of Cu-based trifluoromethylation was a report by Amii in 2009.^{12a} This work demonstrated the first copper *catalyzed* trifluoromethylation of aryl iodides. As shown in **Scheme 1.8**, 1,10-phenanthroline (phen) was used as a supporting ligand for Cu in conjunction with TMSCF₃ as the CF₃ source. A variety of electron deficient aryl iodides underwent trifluoromethylation under these conditions.

Scheme 1.8 First Cu-Catalyzed Trifluoromethylation of ArI



One of the limitations of current Cu-catalyzed/mediated trifluoromethylation of aryl iodides is their poor reactivity with electron rich substrates. Recently, Gooßen and co-workers prepared potassium (trifluoromethyl)trimethoxyborate from the reaction of TMSCF₃, KF, and B(OMe)₃ (**Scheme 1.9**).^{12c} This new nucleophilic CF₃ reagent is an easy to handle crystalline solid and allows efficient conversion of electron-rich aryl iodides to aryl-CF₃ products.

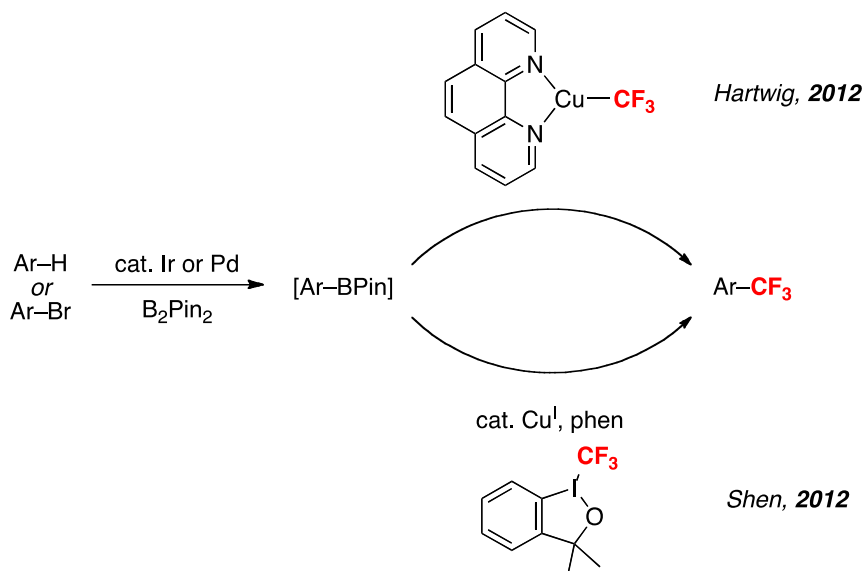
Scheme 1.9 Cu-Catalyzed Aryl-CF₃ Coupling with KB(OMe)₃CF₃



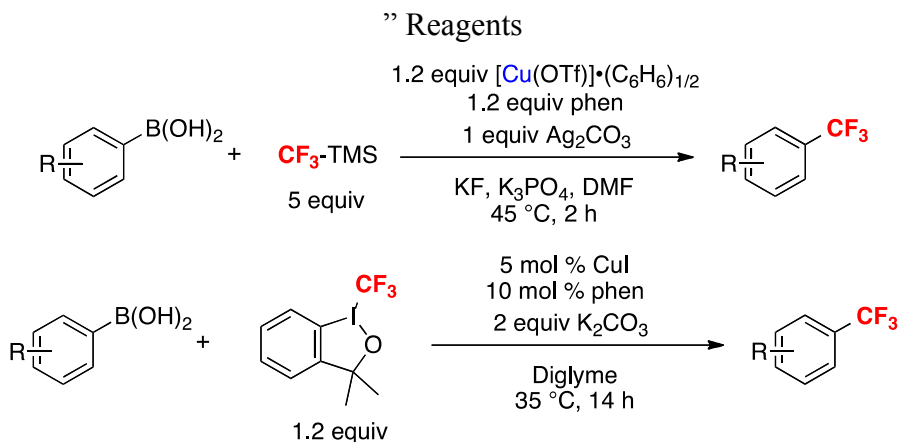
Aryl boronic acids and their derivatives have become an important class of substrates for Cu-catalyzed aromatic trifluoromethylation. Aryl boronic acids undergo facile transmetalation to form the Cu(aryl) intermediates under mild reaction conditions.

Moreover, aryl boronic acids can be easily prepared from aryl-halides, aryl triflates, or directly from aryl C–H bonds through Ir catalyzed borylation reactions. Notably, one pot trifluoromethylation of arenes or bromoarenes via cross-coupling of *in situ* formed aryl-BPin and Cu–CF₃ complexes has been reported by Hartwig and Shen.^{11i,12g}

Scheme 1.10 Cu-Based Fluorination of Ar–H or Ar–Br via Ar–BPin Intermediates



Scheme 1.11 Cu-Based Fluorination of Arylboronic Acids using “CF₃⁺” or “CF₃[−]” Reagents



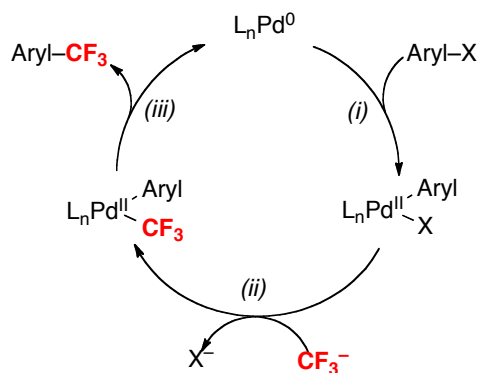
Cu-catalyzed/mediated trifluoromethylation of aromatic boronic acids has been reported using nucleophilic (TMSCF₃)^{11c,11e,11i,11j,12i} and electrophilic CF₃ reagents (Togni or Umemoto’s reagents).^{11f,12d,e} These transformations are generally believed to proceed

via nucleophilic or electrophilic transfer of the CF₃ group onto the Cu center, respectively. Although these transformations do not require harsh reaction conditions and have shown broad generality, the high cost of the exotic CF₃ reagents undoubtedly limits their application on a large scale. *As such, a challenge of current Cu-based trifluoromethylation methods is the development of mild and versatile protocols that employ cost effective CF₃ precursors. Advances in this area are described in **Chapter 2** of this thesis.*

Another major difficulty associated with Cu-catalyzed trifluoromethylation of aryl boronic acids is the generation of protodeboronated products. Most reported boronic acid trifluoromethylation protocols employ inert atmosphere conditions and dry solvents to minimize the formation of these unwanted side products. However, even under these meticulously controlled conditions, significant quantities (2-10%) of protodeboronated products are commonly observed and are very challenging to separate from the desired aryl-CF₃ products. *Therefore, the development of a practical trifluoromethylation protocol that is easy to setup, enables simple product isolation, and precludes formation of protodeboronated side products is highly desirable. Advances in this area are described in **Chapter 2** of this thesis.*

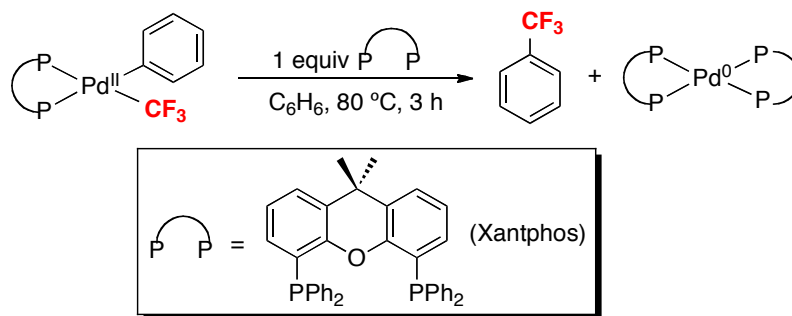
Palladium catalyzed cross-couplings have found broad application in aryl C-C bond formation. As shown in **Scheme 1.12**, in theory, Pd-catalyzed aromatic trifluoromethylation reactions should be able to proceed through the following steps: (i) initial formation of Pd(aryl) complexes via oxidative addition, C-H activation or transmetallation, (ii) transmetallation of a CF₃ group to Pd to form an Pd(aryl)(CF₃) intermediate, and (iii) reductive elimination of the aryl-CF₃ product from Pd(aryl)(CF₃). However, the realization of this proposed catalytic cycle is hindered by the challenging reductive elimination of aryl-CF₃ from Pd^{II}.

Scheme 1.12 Pd-Catalyzed Arene Trifluoromethylation via a Pd^{0/II} Mechanistic Pathway



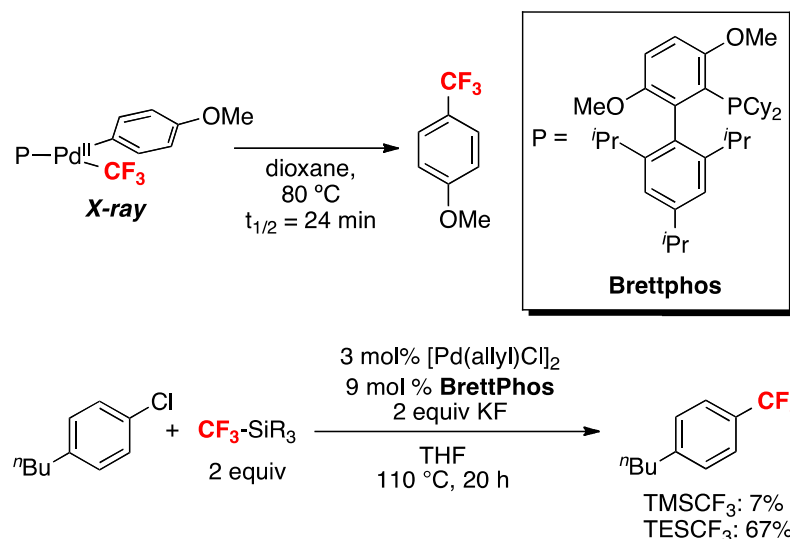
Tremendous effort has been directed at addressing this challenge.^{10c,14,15} For example, in 2006, Grushin demonstrated that (Xantphos)Pd(Ph)(CF₃) undergoes stoichiometric Ph–CF₃ bond-forming reductive elimination to release trifluorotoluene under relatively mild conditions (80 °C, 3 h, **Scheme 1.13**).^{14b,c} This was the first reported example of selective aryl–CF₃ coupling from a Pd center. The properties of the Xantphos ligand, particularly its large bite angle, were hypothesized to play an important role in this novel transformation.

Scheme 1.13 Aryl–CF₃ Coupling from (Xantphos)Pd(Ph)(CF₃)



More recently, Buchwald demonstrated a second example of aryl–CF₃ coupling from Pd^{II} using Brettphos,^{15b} which had been shown to facilitate other difficult reductive eliminations from Pd (**Scheme 1.14**). Notably, further development of this model system led to the first Pd-catalyzed trifluoromethylation of aryl chlorides using TESCF₃.

Scheme 1.14 Pd-Catalyzed Trifluoromethylation of Aryl Chlorides



Both Grushin and Buchwald's ligand approaches represent significant advances in Pd-catalyzed trifluoromethylation reactions via Pd^{0/II} catalytic cycles. However, the requirement of these expensive ligands and high temperatures still limits their widespread application. *An alternative approach to address aryl-CF₃ coupling from Pd could be synthetically valuable and could offer the potential for achieving complementary reactivity. Advances in this area are described in Chapter 4 of this thesis.*

Most Cu- and Pd-based trifluoromethylation have focused on transforming prefunctionalized substrates to the trifluoromethylated products. While a few reports demonstrated Pd-catalyzed selective C-H trifluoromethylation, current methods still have significant limitations. The conversion of trifluoromethylating reagents to a more reactive intermediate that can engage in direct C-H trifluoromethylation of non-prefunctionalized substrates represents a desirable alternative approach. *Advances in this area are described in Chapter 3 of this thesis.*

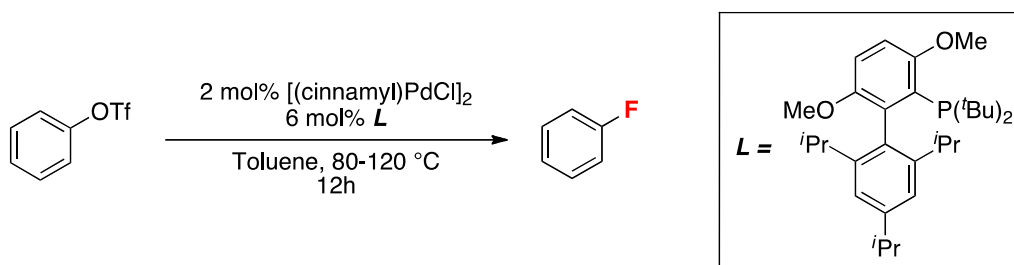
1.3.2. Transition Metal Based Aromatic Fluorination:

Research towards aryl-F bond formation has largely focused on using palladium and silver as catalysts.^{16,17,18,19,20} More recently, copper, an earth abundant first row transition metal has become an attractive alternative toward aryl-F coupling.^{21,22,23}

Pd-catalyzed aromatic fluorination can be achieved through a Pd^{0/II} or Pd^{II/IV} mechanistic cycle. Similar to the aryl–CF₃ coupling, the challenge associated with Pd catalyzed aromatic fluorination is the aryl–F bond-forming reductive elimination step from Pd(aryl)(F).

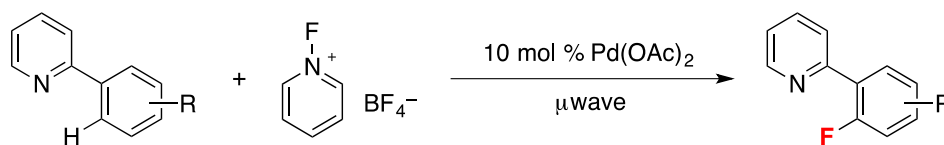
The first aryl C–F bond-forming reductive elimination from (L)Pd^{II}(Ar)(F) compound was demonstrated by Buchwald and co-workers (**Scheme 1.15**).^{19c} A bulky phosphorus ligand, ^tBuBrettPhos, played a key role in inducing the desired aryl–F coupling. Further development based on this initial success led to the first and only Pd-catalyzed conversion of aryl triflates to arylfluorides using Brettphos as a ligand.^{19c}

Scheme 1.15 Pd-Catalyzed Fluorination of Aryl Chlorides

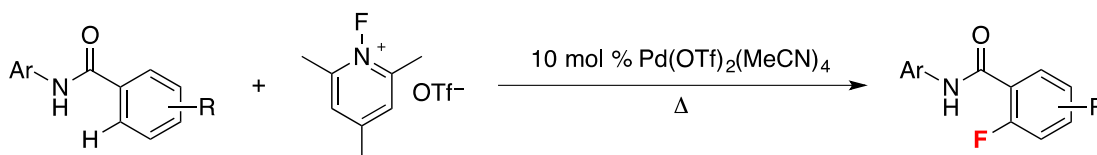


In 2006, our group reported the first Pd-catalyzed selective fluorination of aryl C–H bonds using an *N*-fluoropyridinium oxidant as an electrophilic fluorinating reagent (**Scheme 1.16**). In order to control the regioselectivity, a nitrogen-based directing group was attached to the aryl ring. While bonded to the Pd, this directing motif positions a specific C–H bond close to the Pd center, thus affording selective functionalization. A proposed catalytic cycle of this transformation is shown in **Scheme 1.18**. More recently, related reports by Yu’s group extended the applicable directing groups to triflamide and even *N*-arylamides (**Scheme 1.17**). In particular, the *N*-arylamide auxiliary could be easily converted to other functional groups, such as carboxylic acids, as a handle for further functionalization.

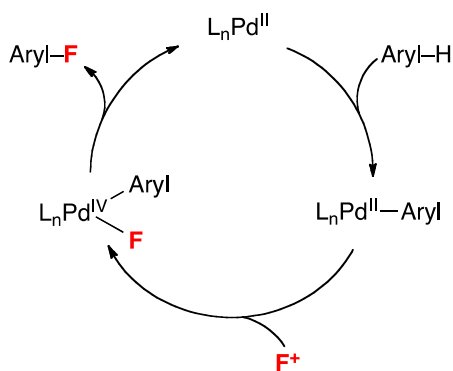
Scheme 1.16 Pyridine Directed Pd-Catalyzed C–H Fluorination Reaction



Scheme 1.17 *N*-Arylamide Directed Pd-Catalyzed C–H Fluorination Reaction



Scheme 1.18 Pd-Catalyzed Arene Fluorination via a Pd^{II/IV} Mechanistic Pathway

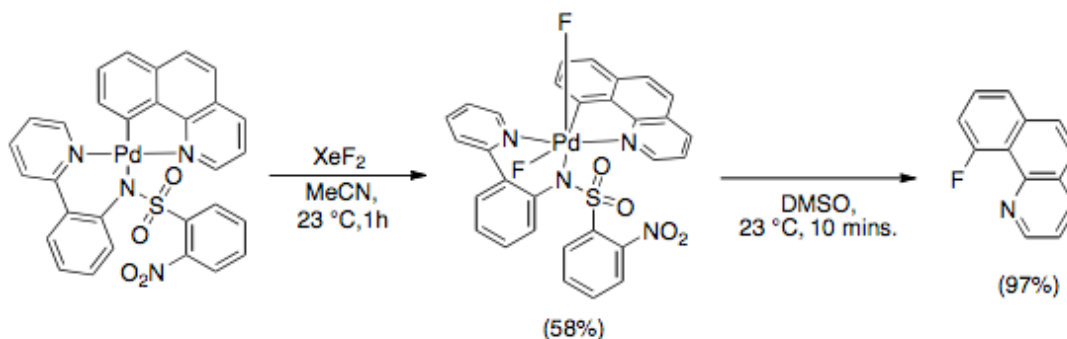


Our group and others have isolated and characterized several Pd^{IV}(aryl)(F) complexes.¹⁶ Detailed mechanistic investigations of aryl–F coupling from these species have afforded useful information that could be applicable to the development of novel fluorination reactions via related high valent Pd(aryl)(F) intermediates.

In 2008, Ritter and co-workers reported a fluorination of aryl boronic acids via stoichiometric Pd(aryl) complexes using an electrophilic F⁺ oxidant. The authors suggested that fluorination was achieved via aryl–F reductive elimination from Pd^{IV}(aryl)(F) intermediates.^{16f} More recently, the mechanism of these aryl–F couplings was systematically studied.^{16d} Reductive elimination from a cationic Pd^{IV}(aryl)(F) was proposed to be the rate-determining step. The ancillary pyridyl-sulfonamide ligand was believed to be crucial for the aryl–F coupling, likely due to its coordination mode and electronic contribution to Pd. Based on these mechanistic insights, a late stage

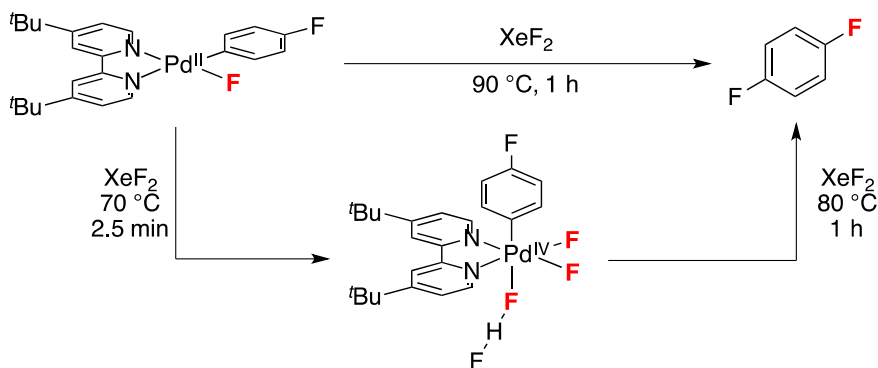
fluorination of positron emission tomography (PET) tracers via this strategy has been reported.^{16c}

Scheme 1.19 Aryl–F Coupling from Ritter’s Pd^{IV}(aryl)(F) Complex



More recently, our group reported the synthesis of a stable Pd^{IV}(Ar)(F)₂(FHF) complex that undergoes aryl–F bond formation in the presence of “F⁺” sources.^{16c} Unlike the example reported by Ritter, this Pd^{IV}(aryl)(F) complex includes an aryl ligand that is not part of a chelate. Therefore, it provides an ideal model for the development of novel methods for Pd-catalyzed fluorination of aryl–X (X = H, halide, OTf, B, Sn, Si, etc...)

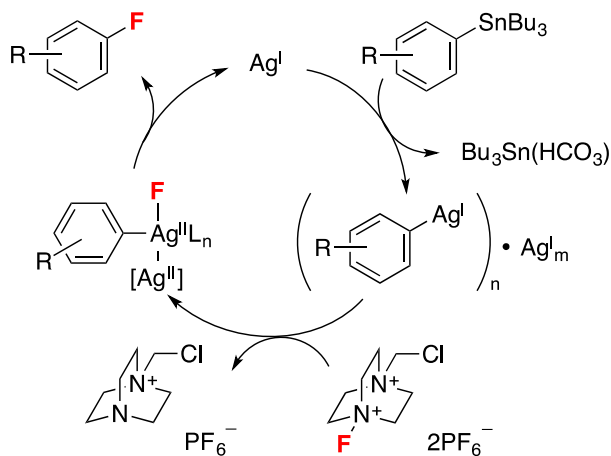
Scheme 1.20 Aryl–F Coupling from Sanford’s Pd^{IV}(aryl)(F) Complex



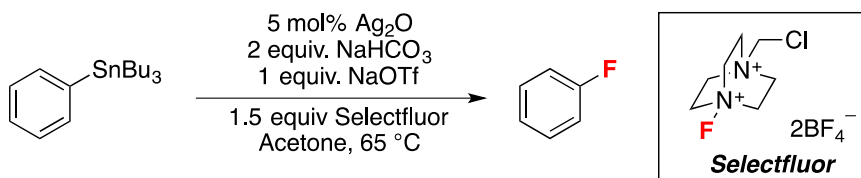
Silver mediated fluorination of aryl stannanes was first developed by Ritter and co-workers.²⁰ Reactions of aryl stannanes, 2 equivalents of AgOTf, and Selectfluor (an electrophilic fluorinating reagent) afforded the corresponding aryl–fluorides at room

temperature in 20 min.^{20a} This strategy has been successfully applied to the late-stage fluorination of complex molecules^{20c} and PET tracers.²⁴ The mechanism of this transformation was proposed to involve the oxidation of an *in situ* formed (Aryl–Ag)(AgOTf) adduct with Selectfluor, followed by reductive elimination from a high oxidation state Ag(aryl)(F) intermediate (**Scheme 1.21**). However, no direct mechanistic evidence has been demonstrated. Further optimization of the reaction conditions afforded a silver catalyzed fluorination of aryl stannanes using 5 mol% of Ag₂O as catalyst (**Scheme 1.22**).^{20c} More recently, silver mediated fluorinations of less toxic substrates, such as aryl boronic acids^{20b} and aryl silanes,^{20d} have been developed.

Scheme 1.21 Proposed Mechanism of Silver-Catalyzed Fluorination of Aryl Stannanes



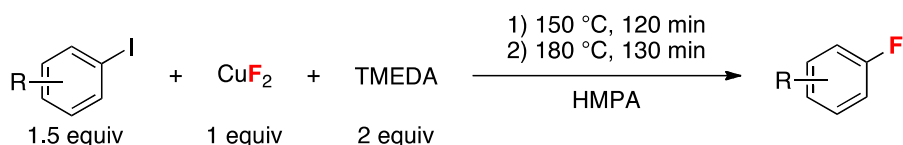
Scheme 1.22 Silver-Catalyzed Fluorination of Aryl Stannanes



Over the last 3 years, copper mediated fluorination has become a rapidly developing field of research.^{21,22,23} The low cost of copper compared to other noble metals mentioned earlier renders it an attractive alternative. However, early development of copper mediated transformations has been limited by the difficulties of design and characterization of stable Cu(aryl)(F) intermediates. Tremendous efforts have focused on

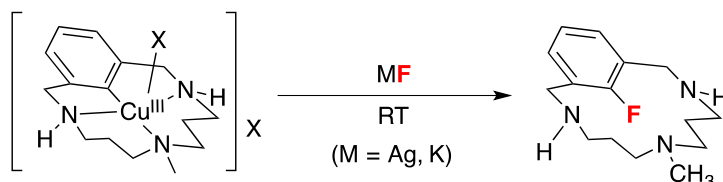
studies of poorly controlled and largely undefined Cu–F mediated fluorinations. For example, a patent by Grushin described the fluorination of haloarenes by CuF₂/TMEDA; however, few details were provided (**Scheme 1.23**).²¹

Scheme 1.23 Fluorination of Aryl iodide by CuF₂/TMEDA

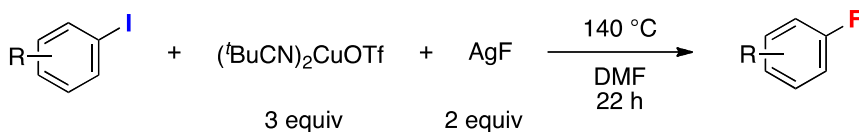


In a seminal report published in 2011, Ribas and co-workers reported the first proof-of-concept example of aryl–F bond forming reductive elimination from a macrocyclic aryl–Cu^{III} complex at room temperature (**Scheme 1.24**). This is the first example of facile aryl–F coupling from a well-defined Cu^{III}(aryl)(X) intermediate.²² Inspired by this initial discovery, Hartwig and co-workers extended the substrate scope of this transformation by developing a Cu-mediated conversion of aryl iodides to aryl fluorides via a putative arylcopper(III) fluoride intermediate (**Scheme 1.25**).^{23a} However, this method still suffers from several disadvantages. Expensive fluoride source (AgF) and excess amounts of substrates were required for achieving high yields. Moreover, the harsh conditions required (140 °C) and the strong basicity of fluoride limit the functional group tolerance of this method.

Scheme 1.24 Aryl Fluoride Bond Formation from Cu^{III}(aryl)(X)



Scheme 1.25 Cu-Mediated Fluorination of Aryl Iodides



Despite recent advances in the field of Cu-mediated aromatic fluorination, current methods are conducted under high temperatures that limited their substrate scope to simple arenes. *Therefore, the development of a practical Cu-based fluorination protocol that is applicable to a broad range of substrates under mild reaction conditions is highly desirable. Advances in this area are described in **Chapter 5** of this thesis.*

1.4 References

1. (a) Schlosser, M. *Angew. Chem. Int. Ed.* **2006**, *45*, 5432; (b) Müller, K.; Faeh, C.; Diederich, F. *Science* **2007**, *317*, 1881; (c) Hagmann, W. K. *J. Med. Chem.* **2008**, *51*, 4359; (d) Kirk, K. L. *Org. Process Res. Dev.* **2008**, *12*, 305; (e) Purser, S.; Moore, P. R.; Swallow, S.; Gouverneur, V. *Chem. Soc. Rev.* **2008**, *37*, 320.
2. Thayer, A. M. *Chem. Eng. News.* **2006**, *84*, 15.
3. Top Pharmaceuticals Poster Njardarson Group. <http://cbc.arizona.edu/njardarson/group/sites/default/files/Top> 200 Pharmaceutical Products by US Retail Sales in 2011_small_0.pdf (accessed Mar. 1st, 2013)
4. Global fluoropolymer market report. <http://www.acmite.com/market-reports/chemicals/global-fluoropolymer-market-report.html> (accessed Mar. 9th, 2013)
5. Furuya, T.; Kamlet, A. S.; Ritter, T. *Nature* **2011**, *473*, 470.
6. (a) Gottlieb, H. B. *J. Am. Chem. Soc.* **1936**, *58*, 532; (b) Adams, D. J.; Clark, J. H. *Chem. Soc. Rev.* **1999**, *28*, 225.
7. Swarts, F. *Bull. Acad. R. Belg.* **1892**, *24*, 309.
8. (a) Balz, G.; Schiemann, G. *Ber. Deutsch. Chem. Ges.* **1927**, *60*, 1186; (b) Swain, C. G.; Rogers, R. J. *J. Am. Chem. Soc.* **1975**, *97*, 799.
9. (a) Tomashenko, O. A.; Grushin, V. V. *Chem. Rev.* **2011**, *111*, 4475; (b) Roy, S.; Gregg, B. T.; Gribble, G. W.; Le, V.-D. *Tetrahedron* **2011**, *67*, 2161; (c) Anbarasan, P.; Neumann, H.; Beller, M. *Angew. Chem. Int. Ed.* **2011**, *50*, 519; (d) Besset, T.; Schneider, C.; Cahard, D. *Angew. Chem. Int. Ed.* **2012**, *51*, 5048; (e) Ye, Y.; Sanford, M. S. *Synlett* **2012**, *23*, 2005; (f) Studer, A. *Angew. Chem. Int. Ed.* **2012**, *51*, 8950.
10. (a) Hollingworth, C.; Gouverneur, V. *Chem. Commun.* **2012**, *48*, 2929; (b) Furuya, T.; Kamlet, A. S.; Ritter, T. *Nature* **2011**, *473*, 470; (c) Grushin, V. V. *Acc. Chem. Res.* **2010**, *43*, 160; (d) Brown, J. M.; Gouverneur, V. *Angew. Chem., Int. Ed.* **2009**, *48*, 8610.
11. (a) Dubinina, G. G.; Furutachi, H.; Vivic, D. A. *J. Am. Chem. Soc.* **2008**, *130*, 8600; (b) Dubinina, G. G.; Ogikubo, J.; Vivic, D. A. *Organometallics* **2008**, *27*, 6233; (c) Chu, L.; Qing, F.-L. *Org. Lett.* **2010**, *12*, 5060; (d) McReynolds, K. A.; Lewis, R. S.; Ackerman, L. K. G.; Dubinina, G. G.; Brennessel, W. W.; Vivic, D. A. *J. Fluorine Chem.* **2010**, *131*, 1108; (e) Senecal, T. D.; Parsons, A. T.; Buchwald, S. L. *J. Org. Chem.* **2011**, *76*, 1174; (f) Zhang, C. P.; Wang, Z. L.; Chen, Q. Y.; Zhang, C. T.; Gu, Y. C.; Xiao, J. C. *Angew. Chem. Int. Ed.* **2011**, *50*, 1896; (g) Tomashenko, O. A.; Escudero, E. C.; Belmonte, M. M.; Grushin, V. V. *Angew. Chem. Int. Ed.* **2011**, *50*, 7655; (h) Morimoto, H.; Tsubogo, T.; Litvinas, N. D.; Hartwig, J. F. *Angew. Chem. Int. Ed.* **2011**, *50*, 3793; (i) Litvinas, N. D.; Fier, P. S.; Hartwig, J. F. *Angew. Chem. Int. Ed.* **2012**, *51*, 536; (j) Zanardi, A.; Novikov, M. A.; Martin, E.; Benet-Buchholz, J.; Grushin, V. V. *J. Am. Chem. Soc.* **2011**, *133*, 20901; (k) Kremlev, M. M.; Mushta, A. I.; Tyrra, W.; Yagupolskii, Y. L.; Naumann, D.; Möller, A. *J. Fluorine Chem.* **2012**, *133*, 67; (l) Khan, B. A.; Buba, A. E.; Goößen, L. J. *Chem. Eur. J.* **2012**, *18*, 1577.
12. (a) Oishi, M.; Kondo, H.; Amii, H. *Chem. Commun.* **2009**, 1909; (b) Shimizu, R.; Egami, H.; Nagi, T.; Chae, J.; Hamashima, Y.; Sodeoka, M. *Tetrahedron Lett.* **2010**, *51*, 5947; (c) Knauber, T.; Arikani, F.; G, R.; Goossen, L. J. *Chem. Eur. J.* **2011**, *17*, 2689; (d) Xu, J.; Luo, D.-F.; Xiao, B.; Liu, Z.-J.; Gong, T.-J.; Fu, Y.; Liu, L. *Chem. Commun.* **2011**, *47*, 4300; (e) Liu, T.; Shen, Q. *Org. Lett.* **2011**, *13*, 2342; (f) Li, Y. C., T.; Wang, H.; Zhang, R.; Jin, K.; Wang, X.; Duan, C. *Synlett* **2011**, *12*, 1713; (g) Liu, T.; Shao, X.;

- Wu, Y.; Shen, Q. *Angew. Chem. Int. Ed.* **2012**, *51*, 540; (h) Chu, L.; Qing, F.-L. *J. Am. Chem. Soc.* **2011**, *134*, 1298; (i) Jiang, X.; Chu, L.; Qing, F.-L. *J. Org. Chem.* **2012**, *77*, 1251.
13. McLoughlin, V. C. R.; Thrower, J. *Tetrahedron* **1969**, *25*, 5921.
14. (a) Grushin, V. V.; Marshall, W. J. *J. Am. Chem. Soc.* **2006**, *128*, 4632; (b) Grushin, V. V.; Marshall, W. J. *J. Am. Chem. Soc.* **2006**, *128*, 12644; (c) Bakmutov, V. I.; Bozoglian, F.; Gomez, K.; Gonzalez, G.; Grushin, V. V.; Macgregor, S. A.; Martin, E.; Miloserdov, F. M.; Novikov, M. A.; Panetier, J. A.; Romashov, L. V. *Organometallics* **2012**, *31*, 1315; (d) Ball, N. D.; Kampf, J. W.; Sanford, M. S. *J. Am. Chem. Soc.* **2010**, *132*, 2878; (e) Ye, Y.; Ball, N. D.; Kampf, J. W.; Sanford, M. S. *J. Am. Chem. Soc.* **2010**, *132*, 14682; (f) Ball, N. D.; Gary, J. B.; Ye, Y.; Sanford, M. S. *J. Am. Chem. Soc.* **2011**, *133*, 7577.
15. (a) Wang, X.; Truesdale, L.; Yu, J.-Q. *J. Am. Chem. Soc.* **2010**, *132*, 3648; (b) Cho, E. J.; Senecal, T. D.; Kinzel, T.; Zhang, Y.; Watson, D. A.; Buchwald, S. L. *Science* **2010**, *328*, 1679; (c) Mu, X.; Chen, S.; Zhen, X.; Liu, G. *Chem. Eur. J.* **2011**, *17*, 6039; (d) Loy, R. N.; Sanford, M. S. *Org. Lett.* **2011**, *13*, 2548; (e) Mu, X.; Wu, T.; Wang, H.-Y.; Guo, Y.-L.; Liu, G. *J. Am. Chem. Soc.* **2011**, *134*, 878.
16. For examples of C–F bond formation from Pd(IV)(R)(F) complexes, see: (a) McMurtrey, K. B.; Racowski, J. M.; Sanford, M. S. *Org. Lett.* **2012**, *14*, 4094. (b) Racowski, J. M.; Kampf, J. W.; Sanford, M. S. *Angew. Chem., Int. Ed.* **2012**, *51*, 3414. (c) Ball, N. D.; Kampf, J. W.; Sanford, M. S. *J. Am. Chem. Soc.* **2010**, *132*, 2878. (d) Furuya, T.; Benitez, D.; Tkatchouk, E.; Strom, A. E.; Tang, P.; Goddard, W. A.; Ritter, T. *J. Am. Chem. Soc.* **2010**, *132*, 3793. (e) Lee, E.; Kamlet, A. S.; Powers, D. C.; Neumann, C. N.; Boursalian, G. B.; Furuya, T.; Choi, D. C.; Hooker, J. M.; Ritter, T. *Science* **2011**, *334*, 639. (f) Furuya, T.; Ritter, T. *J. Am. Chem. Soc.* **2008**, *130*, 10060.
17. Hull, K. L.; Anani, W. Q.; Sanford, M. S. *J. Am. Chem. Soc.* **2006**, *128*, 7134.
18. (a) Chan, C. S. L.; Wasa, M.; Wang, X.; Yu, J.-Q. *Angew. Chem., Int. Ed.* **2011**, *50*, 9081; (b) Wang, X.; Mei, T. S.; Yu, J.-Q. *J. Am. Chem. Soc.* **2009**, *131*, 7520.
19. (a) Maimone, T. J.; Milner, P. J.; Kinzel, T.; Zhang, Y.; Takase, M. K.; Buchwald, S. L. *J. Am. Chem. Soc.* **2011**, *133*, 18106; (b) Noel, T.; Maimone, T. J.; Buchwald, S. L. *Angew. Chem., Int. Ed.* **2011**, *50*, 8900; (c) Watson, D. A.; Su, M.; Teverovskiy, G.; Zhang, Y.; Garcia-Fortanet, J.; Kinzel, T.; Buchwald, S. L. *Science* **2009**, *321*, 1661.
20. (a) Furuya, T.; Strom, A. E.; Ritter, T. *J. Am. Chem. Soc.* **2009**, *131*, 1662; (b) Furuya, T.; Ritter, T. *Org. Lett.* **2009**, *11*, 2860; (c) Tang, P.; Furuya, T.; Ritter, T. *J. Am. Chem. Soc.* **2010**, *132*, 12150; (d) Tang, P.; Ritter, T. *Tetrahedron* **2011**, *67*, 4449.
21. For an example of fluorination of haloarenes by CuF₂/TMEDA, see: Grushin, V. Process for Preparing Fluoroarenes from Haloarenes. U.S. Patent 7,202,388, 2007.
22. (a) Casitas, A.; Canta, M.; Sola, M.; Costas, M.; Ribas, X. *J. Am. Chem. Soc.* **2011**, *133*, 19386; (b) Yao, B.; Wang, Z.-L.; Zhang, H.; Wang, D.-X.; Zhao, L.; Wang, M.-X. *J. Org. Chem.* **2012**, *77*, 3336.
23. (a) Fier, P. S.; Hartwig, J. F. *J. Am. Chem. Soc.* **2012**, *134*, 10795; (b) Fier, P. S.; Luo, J.; Hartwig, J. F. *J. Am. Chem. Soc.* **2013**, *135*, 2552.
24. Stenhagen, I. S. R.; Kirjavainen, A. K.; Forsback, S. J.; Jorgensen, C. G.; Robins, E. G.; Luthra, S. K.; Solin, O.; Gouverneur, V. *Chem. Commun.* **2013**, *49*, 1386.

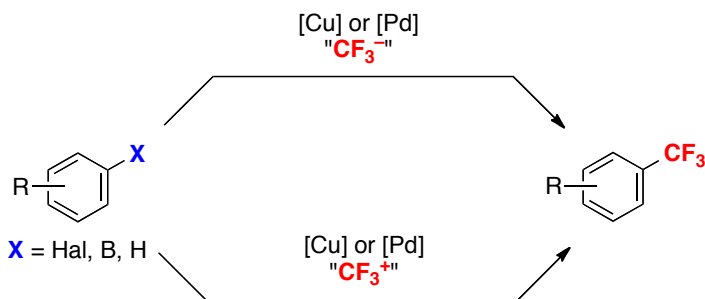
CHAPTER 2

Cu-Based Trifluoromethylation of Arylboronic Acids with CF₃ Radicals

2.1 Background

Trifluoromethyl substituents are widely prevalent in pharmaceuticals and agrochemicals.¹ As such, the development of mild and versatile synthetic methods for generating carbon–CF₃ bonds has become a field of intense interest. Over the past three years, a variety of Pd^{2,3} and Cu^{4,5}-based cross-coupling-type protocols have been developed for the trifluoromethylation of aryl halides, aryl boronic acids, and aromatic carbon–hydrogen bonds. As exemplified in **Scheme 2.1**, these transformations typically involve “CF₃⁻”^{3b,4e,4l,5i} or “CF₃⁺”^{3a,4f,5d,e} reagents, and are believed to proceed via nucleophilic or electrophilic transfer of the CF₃ group to the metal center.

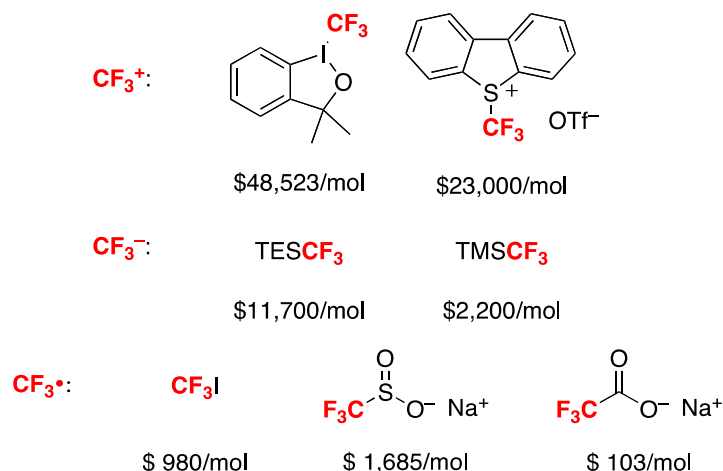
Scheme 2.1. Cu/Pd-Based Trifluoromethylation of Ar–X



Despite these important advances, most current strategies for aryl–CF₃ cross-coupling suffer from the relatively high cost of most of the CF₃⁻/CF₃⁺ reagents (e.g., *S*-(trifluoromethyl)thiophenium salts,^{3a,4f,5d} Togni’s reagent,^{5b,5e,5g} or TESCF₃),^{3b,5a} limited

functional group tolerance in the presence of these highly nucleophilic/electrophilic reagents,^{3c,5a,b} and the requirement for high temperatures in some systems.^{2b,3a,b,4d}

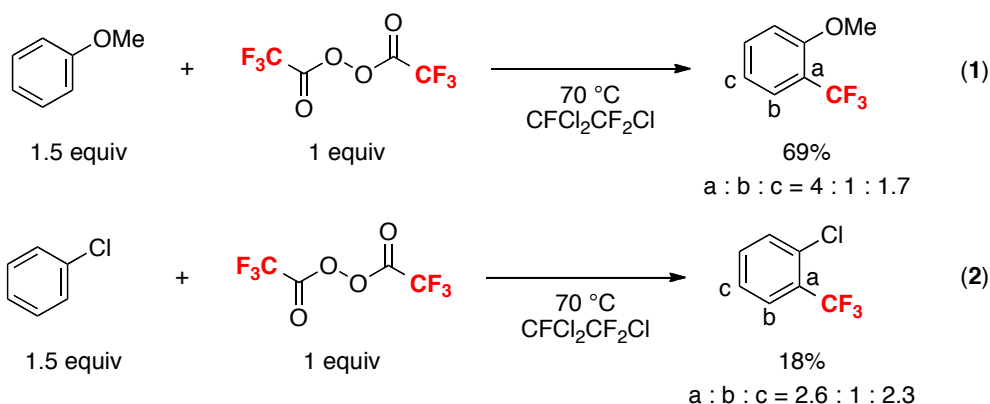
Scheme 2.2. Cost of Several Representative CF_3^- , CF_3^+ and CF_3^\bullet Reagents



One attractive approach to begin to address these limitations would be to access alternative and potentially complementary mechanistic manifolds. We reasoned that a CF_3^\bullet pathway, instead of CF_3^- or CF_3^+ strategies, would be particularly interesting, since CF_3 radical is a neutral and kinetically more reactive CF_3 source.

CF_3 radical-based aromatic C–H trifluoromethylation approaches have been demonstrated in the literature previously. However, these methods generally require inconvenient electrochemical or photochemical activation procedures,⁶ or utilize potentially explosive reagents, like peroxides, at elevated temperatures.⁷ An additional challenge associated with traditional trifluoromethylations with CF_3^\bullet is poor site selectivity and limited substrate scope. For example, while reaction of bis(trifluoroacetyl) peroxide with electron rich arenes afforded the trifluoromethylated products in good yields (**Scheme 2.3**, eq 1), significantly diminished reactivity was observed for electron-poor substrates (**Scheme 2.3**, eq 2).⁷ In both cases, the regio-selectivity of trifluoromethylation was controlled only by the substitution pattern on the substrates.

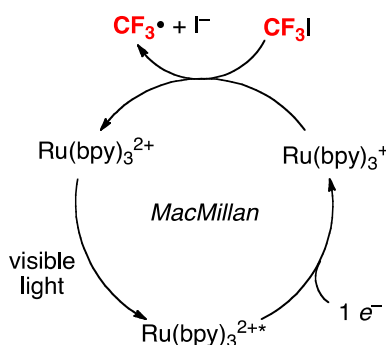
Scheme 2.3. Examples of Traditional Trifluoromethylations with $\text{CF}_3\cdot$



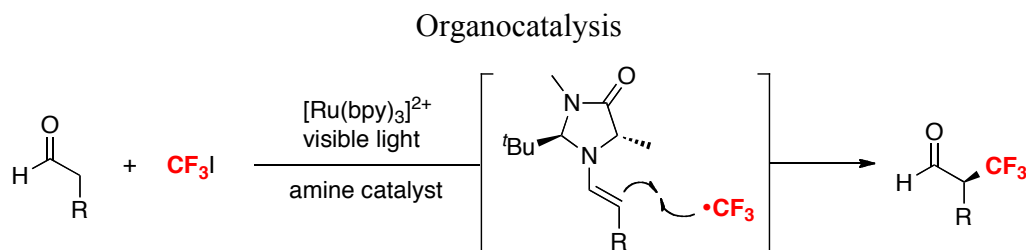
2.2 Design Plan

Our proposed mechanistic manifold requires mild and readily available sources of $\text{CF}_3\cdot$. Gratifyingly, a survey of the literature revealed several procedures that afford $\text{CF}_3\cdot$ under mild, neutral conditions from commercially available and relatively inexpensive reagents (**Scheme 2.1**). For example, CF_3I is a readily available chemical that is significantly less expensive than many common trifluoromethylating reagents (**Scheme 2.1**). Despite these advantages, it has not been employed previously in transition metal-catalyzed cross-coupling reactions. We reasoned that this might be due to the relatively low kinetic reactivity of CF_3I with transition metal aryl/alkyl complexes. However, we noted several recent reports by MacMillan demonstrating the conversion of CF_3I into more reactive $\text{CF}_3\cdot$ under mild conditions through visible light irradiation in the presence of $\text{Ru}(\text{bpy})_3^{2+}$, a commercial photocatalyst, and a reductant (**Scheme 2.4**).⁸ For example, enantioselective radical α -trifluoromethylation of various aldehydes was achieved by merging $\text{CF}_3\cdot$ generation with organocatalysis (**Scheme 2.5**).⁸

Scheme 2.4. Transfer of CF_3I to $\text{CF}_3\cdot$ via Ru-Catalyzed Photocatalysis

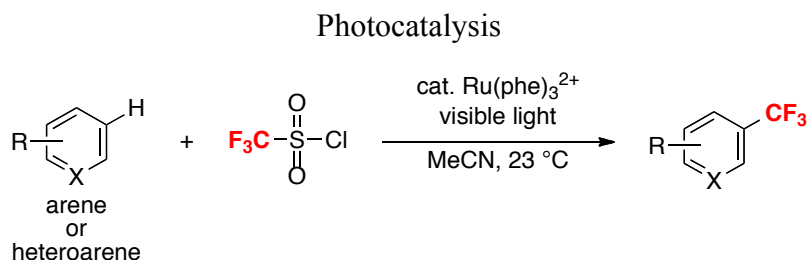


Scheme 2.5. Enantioselective Trifluoromethylation of Aldehydes by $\text{CF}_3\cdot$ via Photoredox



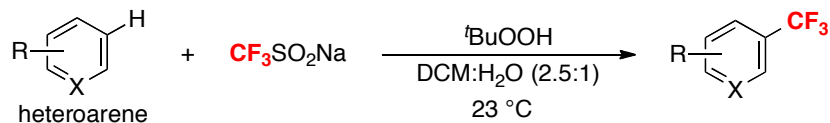
MacMillan also reported an elegant study of radical trifluoromethylation of a broad range of unactivated arenes and heteroarenes under mild condition using $\text{CF}_3\text{SO}_2\text{Cl}$ and $\text{Ru}(\text{phen})_3^{2+}$ as $\text{CF}_3\cdot$ precursor.⁹ Compared to the previously employed CF_3I , $\text{CF}_3\text{SO}_2\text{Cl}$ undergoes more facile SET with $\text{Ru}(\text{phen})_3^{2+*}$, resulting in a $\text{CF}_3\text{SO}_2\text{Cl}$ anion that then readily collapses to release $\text{CF}_3\cdot$. Moreover, the competitive aryl iodination, an unproductive direct coupling of the arene with $\text{I}\cdot$ resulting from the homolysis of $\text{CF}_3\text{-I}$, is avoided.

Scheme 2.6. Trifluoromethylation of Arenes and Heteroarenes via Ru-Catalyzed



In addition to using a Ru photocatalysis system to generate $\text{CF}_3\cdot$, several recent reports have shown that the combination of NaSO_2CF_3 (Langlois' reagent) and *tert*-butyl hydroperoxide (TBHP) generates trifluoromethyl radicals at room temperature in the presence of ambient air/moisture.^{10,11} Recently, this *in situ* generated $\text{CF}_3\cdot$ has been shown to react with electron-rich arenes and heterocycles to afford mixtures of isomeric C–H trifluoromethylation products (**Scheme 2.7**).¹¹

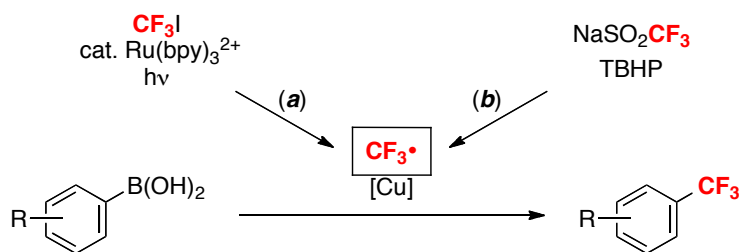
Scheme 2.7 Trifluoromethylation of Heteroarenes with $\text{CF}_3\cdot$ Derived from NaSO_2CF_3 and TBHP



An important challenge associated with developing selective trifluoromethylation reactions using $\text{CF}_3\cdot$ is the issue of site selectivity, since $\text{CF}_3\cdot$ can effect C–H trifluoromethylation via radical aromatic substitution (see more discussions in **Chapter 3**). Thus, a key challenge for this approach is to identify a system in which reaction of $\text{CF}_3\cdot$ with a metal catalyst is faster than the competing uncatalyzed C–H trifluoromethylation. We selected Cu-based catalysts to achieve this goal based on the fact that: (1) they are susceptible to rapid $1e^-$ oxidation reactions, and (2) prior work has demonstrated Cu-based trifluoromethylation under conditions much milder than that using other transition-metals, such as Pd, Ni, and Pt.

In this chapter, we discuss the design and development of two trifluoromethylation protocols based on this new mechanistic design, namely combining Cu-based cross-coupling with $\text{CF}_3\cdot$ to achieve mild and versatile trifluoromethylation methods (**Scheme 2.8**). The first half of the chapter discusses our efforts to combined Cu-catalyzed trifluoromethylation of aryl boronic acids with the generation of $\text{CF}_3\cdot$ using CF_3I , $\text{Ru}(\text{bpy})_3^{2+}$, and visible light.¹² Further development of this system revealed a much more practical Cu-mediated method for the trifluoromethylation of boronic acids that uses $\text{NaSO}_2\text{CF}_3/\text{TBHP}$ as the $\text{CF}_3\cdot$ precursor.¹³

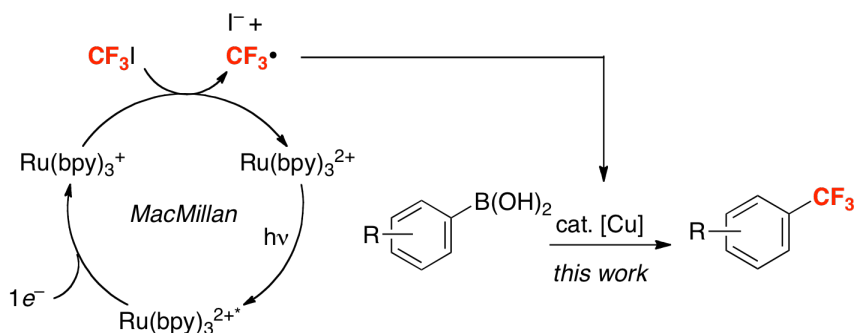
Scheme 2.8. Cu-Mediated Trifluoromethylation of Aryl Boronic Acids using CF_3 Radical



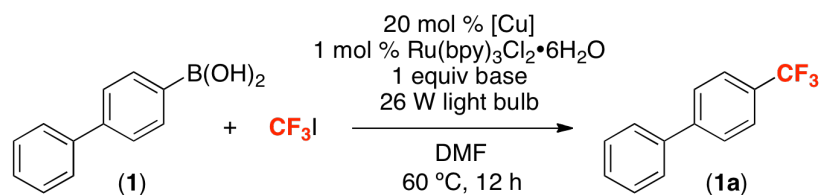
2.3 Merging Cu-Catalyzed Cross-Coupling and $\text{CF}_3\cdot$ from Ru-Catalyzed Photocatalysis

Our initial investigation of the proposed mechanistic manifold focused on the merger of visible light photocatalysis (to generate $\text{CF}_3\cdot$) with Cu catalysis (to generate reactive Cu–aryl species) (**Scheme 2.9**).⁸

Scheme 2.9. Proposed New Pathway for Radical Trifluoromethylation of Boronic Acids via Cu/Ru Visible Light Photocatalysis



Reaction Optimization: We choose 1,1'-biphenyl-4-ylboronic acid (substrate **1**) for initial studies because its reactivity with CF_3^+ or CF_3^- reagents has been previously demonstrated, and the corresponding CF_3 -containing product **1a** is a non-volatile, easy to handle solid. We were delighted to find that Cu/Ru photocatalysis using CF_3I as the trifluoromethylating reagent provided product **1a** in modest to excellent yields under a number of conditions (**Table 2.1**). The addition of base (to promote transmetalation) proved to be essential. Evaluation of a variety of different bases revealed that K_2CO_3 afforded a significant increase in yield. Copper(I) catalysts generally performed better than Cu^{II} salts, and the highest yield of **1a** (76%) was obtained with CuOAc. The optimal conditions were as follows: 1 equiv of boronic acid **1**, 5 equiv of CF_3I , 1 equiv of K_2CO_3 , 20 mol % of CuOAc, and 1 mol % of $\text{Ru}(\text{bpy})_3\text{Cl}_2\cdot 6\text{H}_2\text{O}$ with irradiation from two 26 W household light bulbs. The major side product was 4-iodo-1,1'-biphenyl (formed in 9% yield under the optimal conditions).

Table 2.1. Optimization of Reaction Between **1** and CF₃I^[a]

Entry	[Cu]	Base	Yield
1	Cu(OTf) ₂	K ₂ CO ₃	14%
2	[Cu(OTf)] ₂ ·C ₆ H ₆	K ₂ CO ₃	28%
3	CuI	K ₂ CO ₃	34%
4	Cu	K ₂ CO ₃	40%
5	Cu(OAc) ₂	K ₂ CO ₃	68%
6	CuOAc	K ₂ CO ₃	76%
7	CuOAc	NaOAc	34%
8	CuOAc	KF	50%
9	CuOAc	-	6%

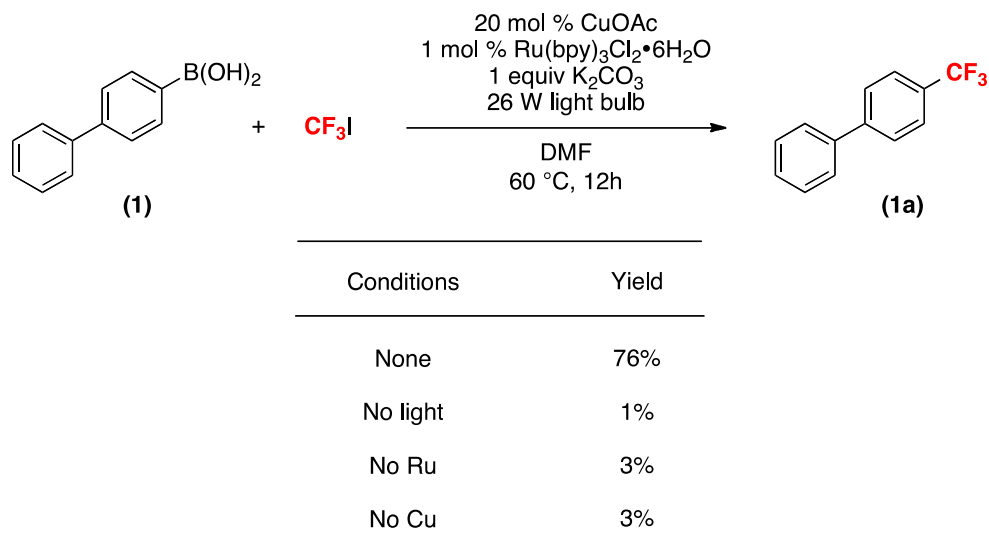
^[a] General conditions: substrate (0.05 mmol, 1 equiv), CF₃I (5 equiv), [Cu] (0.2 equiv), Ru(bpy)₃Cl₂·6H₂O (0.01 equiv), base (1 equiv), DMF (0.17 M in substrate), 60 °C, 12 h, 26 W compact fluorescent light bulb. ¹⁹F NMR yield.

This Cu/Ru-catalyzed coupling between **1** and CF₃I is practical and easily scalable. The reaction in **Table 2.1**, entry 6 was performed on a 0.05 mmol scale and provided 76% yield as determined by ¹⁹F NMR spectroscopy and GCMS. Nearly identical isolated yields were obtained on both 1 and 5 mmol scales (72% and 70% isolated yields, respectively).

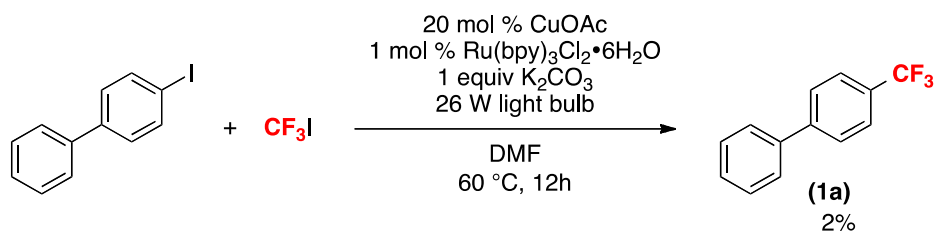
A variety of control reactions were conducted to establish the role of each component of the reaction mixture. As shown in **Table 2.2**, when CuOAc, Ru(bpy)₃Cl₂·6H₂O or light was excluded under otherwise identical conditions, ≤3% yield of **1a** was obtained. These results clearly indicate the necessity of all three components to achieve high yields under these conditions, consistent with the major pathway to **1a** proceeding via dual Ru/Cu catalysis (*vide infra*). The iodinated side product 4-iodo-1,1'-biphenyl was also subjected to the reaction conditions to establish whether it is an

intermediate in the boronic acid trifluoromethylation process (**Scheme 2.10**). Only 2% of the aryl-CF₃ product was formed, strongly suggesting that the major pathway to **1a** does not involve an iodinated intermediate.

Table 2.2. Control Reactions for Radical Trifluoromethylation of Boronic Acids via Cu/Ru Visible Light Photocatalysis

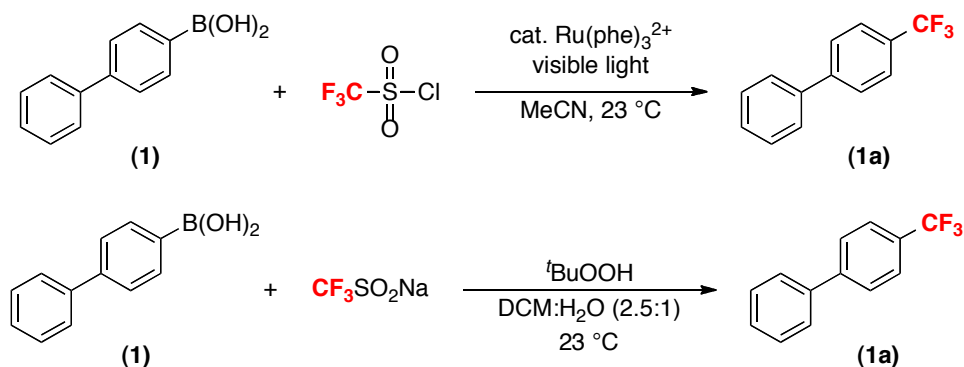


Scheme 2.10. Control Reaction with 4-Iodo-1,1'-biphenyl



Finally, the reactivity of boronic acid substrate **1** was investigated under conditions reported by MacMillan and Baran to promote C–H trifluoromethylation reactions via *in situ* generation of CF₃•.^{9,11} In both cases, <2% of **1a** was observed (**Scheme 2.11**). These results indicate that **1a** is not formed by the direct reaction of CF₃• with the boronic acid.

Scheme 2.11. Investigations of the Reactivity of **1a** toward Radical Trifluoromethylation under MacMillan and Baran's Conditions



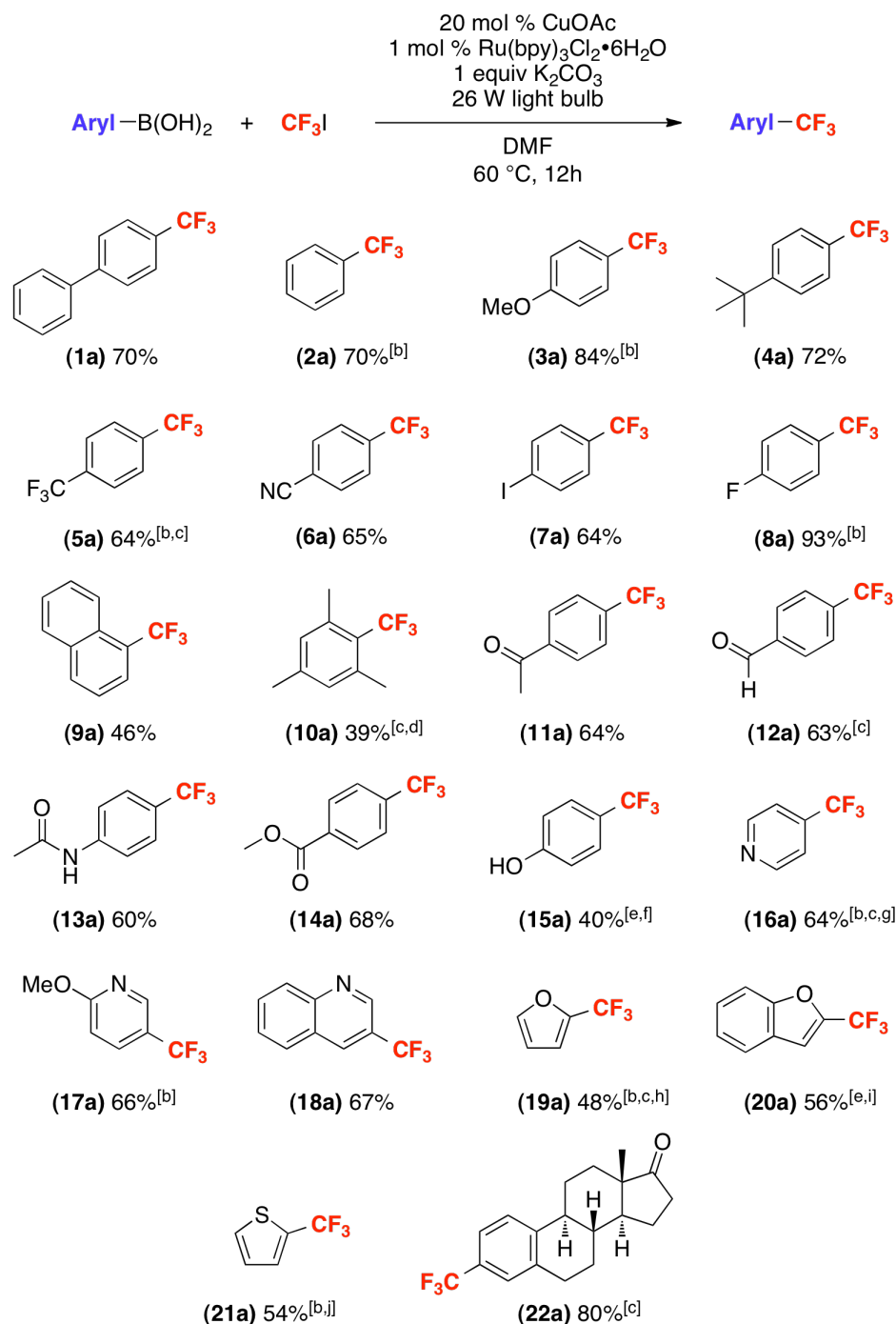
Substrate Scope: This transformation was next applied to a variety of different aryl- and heteroaryl boronic acid derivatives. Representative examples are shown in **Scheme 2.12** and were selected to highlight not only the broad scope but also the limitations of this method.¹⁴ Aromatic boronic acids bearing both electron-donating (*t*-butyl, methoxy) as well as electron-withdrawing (cyano, trifluoromethyl, fluoro, methyl ester) substituents underwent trifluoromethylation in high yields. A variety of different potentially reactive functional groups (aromatic alcohols, ketones, aldehydes, esters, and amides) were well-tolerated. A boronic acid embedded in the estrone framework underwent trifluoromethylation to generate **22a** in 80% isolated yield. Most remarkably, 4-iodo-phenylboronic acid underwent selective trifluoromethylation to form **7a**, leaving the aryl iodide intact for subsequent functionalization. This demonstrates the complementarity of this method to many other Cu-catalyzed trifluoromethylation protocols.^{5a,5c,5f} Furthermore, it provides additional evidence against the possibility of aryl iodide intermediates in this transformation.

The use of sterically hindered substrates such as 1-naphthyl and 2,4,6-trimethylphenyl boronic acid is typically challenging for copper-mediated cross-coupling reactions.¹⁵ As shown in **Scheme 2.12**, similar effects are seen in the current transformation, with products **9a** and **10a** being formed in modest yields (46% and 39%, respectively). In these cases, competing protodeboronation was problematic, and the major side product was naphthalene or mesitylene, respectively.

Heteroaromatic substrates are of particular relevance to the pharmaceutical and agrochemical industries due to the prevalence of heteroarenes in biologically active compounds.¹⁶ Boronic acids derived from pyridine, quinoline, furan, and thiophene all underwent trifluoromethylation in modest to good yields. In some of these cases modification of the catalyst loading and/or reaction temperature was required to achieve optimal yield. Importantly, in all of these substrates, trifluoromethylation of the boronic acid moiety out-competed uncatalyzed C–H trifluoromethylation of the heterocycle with $\text{CF}_3\bullet$. Thus, this method provides an attractive route for the site-selective installation of CF_3 substituents into these scaffolds.

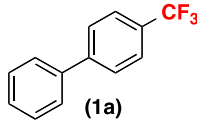
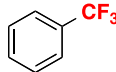
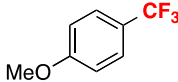
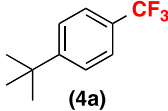
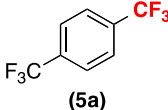
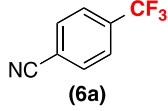
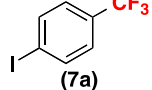
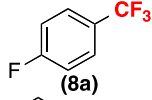
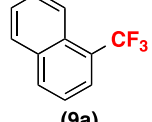
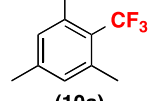
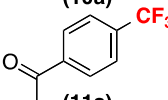
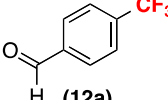
Control reactions (without Cu, Ru, or visible-light) were conducted for all the substrates shown in **Scheme 2.12** to ensure that each reaction component is required for this trifluoromethylation protocol. As shown in **Table 2.3**, when Cu was excluded from the reaction, only small amount of trifluoromethylated products (0-6%) were formed. Larger background reactions were observed for benzofuran and thiophene boronic acids (23 and 17%, respectively). In both cases, protodeboronation is the major reaction pathway. We believe the background reactions are a result of direct reactions of $\text{CF}_3\bullet$ with these reactive heterocycles. When Ru catalyst and/or light are excluded, small amounts of $\text{CF}_3\bullet$ could be generated from thermal homolytic cleavage of the $\text{CF}_3\text{-I}$ bond, resulting in the aryl- CF_3 products.

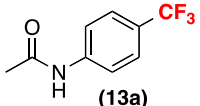
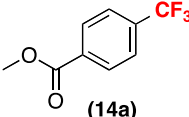
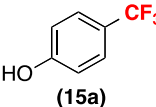

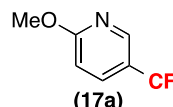
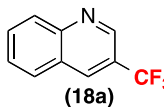
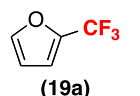
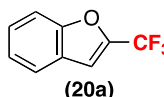
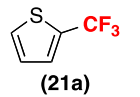
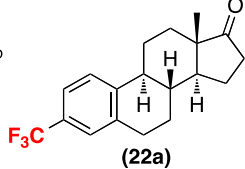
Scheme 2.12. Substrate Scope for Cu/Ru-Catalyzed Trifluoromethylation of Boronic Acids^[a]



^[a] General conditions: substrate (1 equiv), CF₃I (5 equiv), [Cu] (0.2 equiv), Ru(bpy)₃Cl₂•6H₂O (0.01 equiv), K₂CO₃ (1 equiv), DMF (0.17 M in substrate), 60 °C, 12 h, 26 W compact fluorescent light bulb; Isolated yield ($\geq 95\%$ purity). ^[b] ¹⁹F NMR yield. ^[c] 0.5 equiv of CuOAc. ^[d] Isolated as a 1:1 mixture with inseparable protodeboronated product. ^[e] 0.1 equiv of CuOAc. ^[f] Isolated as a 10:1 mixture with inseparable protodeboronated product. ^[g] 3 equiv of CF₃I. ^[h] Reaction run at 70 °C. ^[i] Reaction run at 40 °C. ^[j] 0.05 equiv of CuOAc.

Table 2.3. Control Reactions for Cu/Ru-Catalyzed Trifluoromethylation of Boronic Acids^[a]

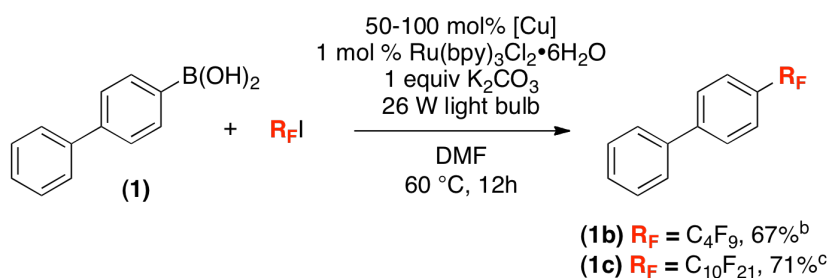
Entry	Product	Yield	Without Cu cat	Without Ru cat	Without light
1	 (1a)	80%	3%	3%	1%
2	 (2a)	70%	5%	0%	0%
3	 (3a)	84%	5%	1%	0%
4	 (4a)	86%	2%	1%	3%
5 ^b	 (5a)	64%	2%	11%	2%
6	 (6a)	84%	1%	22%	2%
7	 (7a)	73%	2%	13%	8%
8	 (8a)	93%	1%	20%	4%
9	 (9a)	57%	6%	2%	0%
10 ^b	 (10a)	45%	4%	4%	0%
11	 (11a)	70%	4%	14%	0%
12 ^b	 (12a)	74%	4%	5%	2%

Entry	Product	Yield	Without Cu cat	Without Ru cat	Without light
13	 (13a)	67%	4%	5%	1%
14	 (14a)	86%	4%	15%	2%
15 ^c	 (15a)	50%	3%	1%	0%
16 ^{b,d}	 (16a)	64%	2%	21%	3%
17	 (17a)	66%	2%	10%	1%
18	 (18a)	70%	5%	34%	13%
19 ^{c,e}	 (19a)	48%	7%	2%	0%
20 ^{c,f}	 (20a)	72%	23%	15%	1%
21 ^g	 (21a)	54%	17%	7%	0%
22 ^b	 (22a)	87%	0%	29%	1%

^[a] General conditions: substrate (0.05 mmol, 1 equiv), CF₃I (5 equiv), [Cu] (0.2 equiv), Ru(bpy)₃Cl₂•6H₂O (0.01 equiv), K₂CO₃ (1 equiv), DMF (0.17 M in substrate), 60 °C, 12 h, 26 W compact fluorescent light bulb. ^[b] ¹⁹F NMR yield. ^[c] 0.5 equiv of CuOAc. ^[d] 0.1 equiv of CuOAc. ^[e] Reaction run at 70 °C. ^[f] Reaction run at 40 °C. ^[g] 0.05 equiv of CuOAc.

Related conditions could also be applied to analogous perfluoroalkylation reactions. This is a significant advantage of the current method, since perfluoroalkyl analogues of other common trifluoromethylating reagents (*e.g.*, R_3SiCF_3 , *S*-(trifluoromethyl)thiophenium salts, or Togni's reagent) are expensive and/or not commercially available. As shown in **Scheme 2.13**, perfluorobutyl and perfluorodecyl iodides react with **1** to afford products **1b** and **1c** in good yields under the Cu/Ru catalyzed conditions.

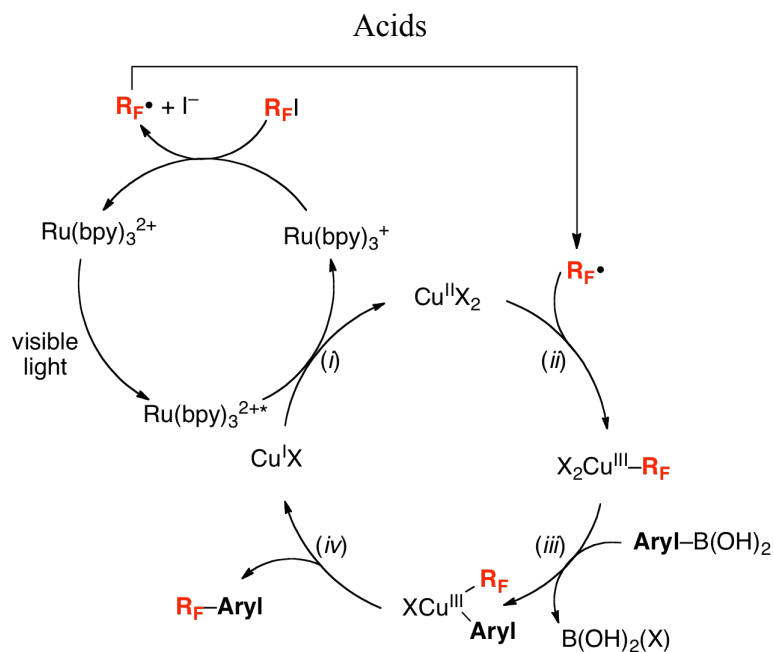
Scheme 2.13. Perfluoroalkylation of **1** Catalyzed by Cu/Ru^[a]



^[a] General conditions: substrate (1 equiv), CuOAc (0.5-1 equiv) Ru(bpy)₃Cl₂·6H₂O (0.01 equiv), K₂CO₃ (1 equiv), DMF (0.17 M in substrate), 60 °C, 12 h, 26 W compact fluorescent light bulb; Isolated yield. ^[b] 5 equiv of C₄F₉I, 0.5 equiv of CuOAc. ^[c] 1.2 equiv of C₁₀F₂₁I, 1 equiv of CuOAc.

Proposed Reaction Mechanism: While a detailed mechanistic picture of this transformation remains to be elucidated, a possible set of catalytic cycles is shown in **Scheme 2.14**. In this sequence, photoexcitation of Ru(bpy)₃²⁺ to Ru(bpy)₃^{2+*} is followed by 1e⁻ reduction by Cu^I to generate Ru(bpy)₃⁺ and Cu^{II}.¹⁷ Reduction of CF₃I by Ru(bpy)₃⁺ then affords CF₃•. Notably, the available reduction potential data indicates that both of these reactions should be thermodynamically favorable.^{18,19,20} The CF₃• could then react with Cu^{II} to generate a Cu^{III}(CF₃) intermediate. Subsequent base-promoted transmetalation between Cu^{III} and the aryl boronic acid would afford Cu^{III}(aryl)(CF₃), which could undergo aryl–CF₃ bond-forming reductive elimination to release the organic product and regenerate the Cu^I catalyst.²¹

Scheme 2.14. Possible Mechanism for Cu/Ru-Catalyzed Trifluoromethylation of Boronic Acids

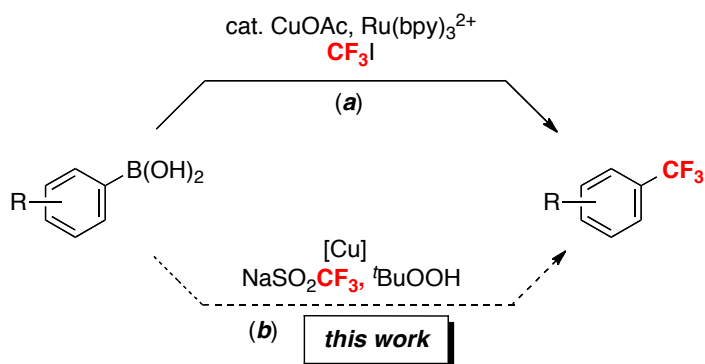


2.4 Practical Cu-Mediated Trifluoromethylation of Arylboronic Acids with NaSO₂CF₃/TBHP

The successful development of a Cu-catalyzed trifluoromethylation of aryl boronic acids with CF₃I in the presence of a photocatalyst and visible light demonstrated the feasibility of achieving selective aryl-CF₃ bond formation by merging CF₃• with a Cu-aryl intermediate.¹² The high selectivity and mild conditions associated with this process led us to consider more practical sources of CF₃• for Cu-mediated boronic acid trifluoromethylation. In particular, we are intrigued by a recent report by Baran and coworkers showing that the combination of NaSO₂CF₃ (Langlois' reagent) and TBHP generates trifluoromethyl radicals at room temperature in the presence of ambient air/moisture.¹⁰⁻¹¹

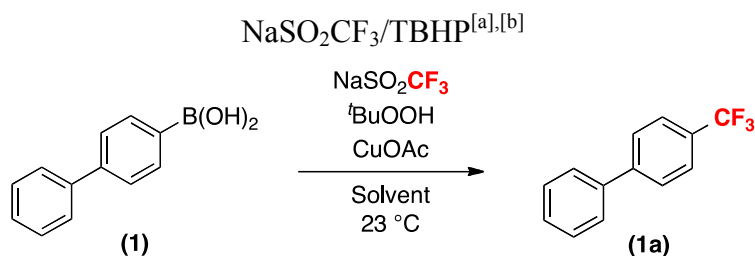
We reasoned that in the presence of a Cu salt, the CF₃• generated from NaSO₂CF₃ and TBHP could instead be harnessed to achieve site selective trifluoromethylation of a boronic acid (**Scheme 2.15**). The second half of this chapter demonstrates the feasibility of this approach and the development of a general, mild, and highly practical protocol for Cu-mediated trifluoromethylation of Aryl-B(OH)₂ with NaSO₂CF₃ and TBHP.¹³

Scheme 2.15. Cu-Mediated Trifluoromethylation with NaSO₂CF₃/TBHP



Reaction Optimization: Based on the work described above, we started by exploring the Cu-mediated reaction of [1,1'-biphenyl]-4-ylboronic acid (**1**) with NaSO₂CF₃ and TBHP in the presence of 20 mol % of CuOAc. The initial reactions are performed at room temperature in DCM/H₂O, the same conditions reported by Baran and co-workers. Gratifyingly, the desired trifluoromethylated product (**1a**) was formed in 18% yield. The yield increased to 47% in the presence of 1 equiv of CuOAc. This is particularly interesting in light of our earlier discovery showing that there is no direct C–H trifluoromethylation between **1a** and CF₃• (generated by NaSO₂CF₃/TBHP) in the absence of Cu (**Scheme 2.11**).

Optimization of solvent (as shown in **Table 2.4**) showed that the use of a 5:5:4 mixture of MeOH, DCM and H₂O resulted in an increase of yield to 71%. Furthermore, an extensive evaluation of copper salts revealed that CuCl provides 80% yield of **1a** on a 0.05 mmol scale (**Table 2.5**, entry 14).

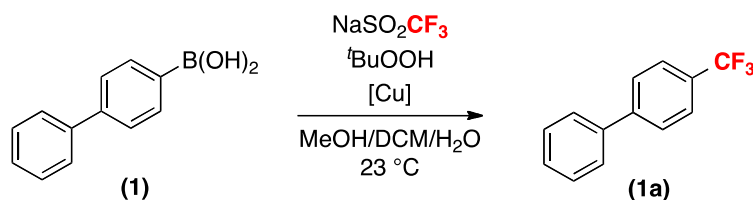
Table 2.4. Solvent Screen for Cu-Mediated Trifluoromethylation of **1** with

Entry	Solvent	Yield of 1a
1	<i>t</i> BuOH	14%
2	DMA	17%
3	THF	18%
4	MeCN	19%
5	Ethyl acetate	21%
6	EtOH	22%
7	DCM	33%
8	Hexane	41%
9	Nitrobenzene	41%
10	Acetone	45%
11	Benzene	46%
12	MeOH	62%
13 ^[c]	MeOH/DCM	71%

^[a] General conditions: substrate **1** (1 equiv, 0.05 mmol), CuOAc (1 equiv), NaSO₂CF₃ (3 equiv), TBHP (5 equiv) in 0.2 mL solvent and 0.08 mL H₂O at 23 °C for 12 h. ^[b] Yields determined by ¹⁹F NMR analysis. ^[c] Solvent ratio = 1:1.

There are several important features of this protocol that highlight its practicality. First, the reactions are all set up on the bench top at room temperature, without any purification of commercial solvents/reagents. Second, protodeboronation is not observed under these conditions, and the only detectable by-product is 4-hydroxybiphenyl. Third, the reaction scales well, proceeding in 85% isolated yield on 0.5 mmol scale.

Table 2.5. Copper Salt Screen for Cu-Mediated Trifluoromethylation of **1** with NaSO₂CF₃/TBHP^{[a],[b]}



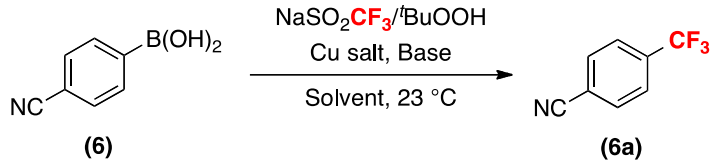
Entry	[Cu]	Yield of 1a
1	CuO	0%
2	Cu(OTf) ₂	4%
3	CuI	6%
4	Cu(TFA) ₂	6%
5	(MeCN) ₄ CuPF ₆	15%
6	(MeCN) ₄ CuBF ₄	18%
7	Cu(OH) ₂	24%
8	[CuOTf]•1/2C ₆ H ₆	31%
9	Cu(OAc) ₂	55%
10	Cu ₂ O	45%
11	Cu	67%
12	CuBr	70%
13	CuOAc	71%
14	CuCl	80%

^[a] General conditions: substrate **1** (1 equiv, 0.05 mmol), [Cu] (1 equiv), NaSO₂CF₃ (3 equiv), TBHP (5 equiv) in DCM/MeOH/H₂O (5:5:4 ratio) at 23 °C for 12 h. ^[b] Yields determined by ¹⁹F NMR analysis.

While electron-neutral and rich boronic acids showed excellent reactivity under the optimal conditions from **Scheme 2.16** (*vide infra*), several electron deficient derivatives did not. For example, (4-cyanophenyl)boronic acid (**6**) reacted to afford **6a** in only 36% yield. In collaboration with Stefan Künzi, I began to optimize the reaction conditions for electron deficient substrates (**Table 2.6**). We reasoned that the lower yields might be due to slower transmetalation of the electron deficient boronic acid. Consistent with this proposal, the addition of 1 equiv of NaHCO₃ (which is expected to accelerate transmetalation) led to an increase in yield to 46%. Further evaluation of different Cu

sources showed that the substitution of CuCl with (MeCN)₄CuPF₆ resulted in the best yield of **6a** (59%).

Table 2.6. Optimization for Electron Poor Boronic Acids^{[a][b]}

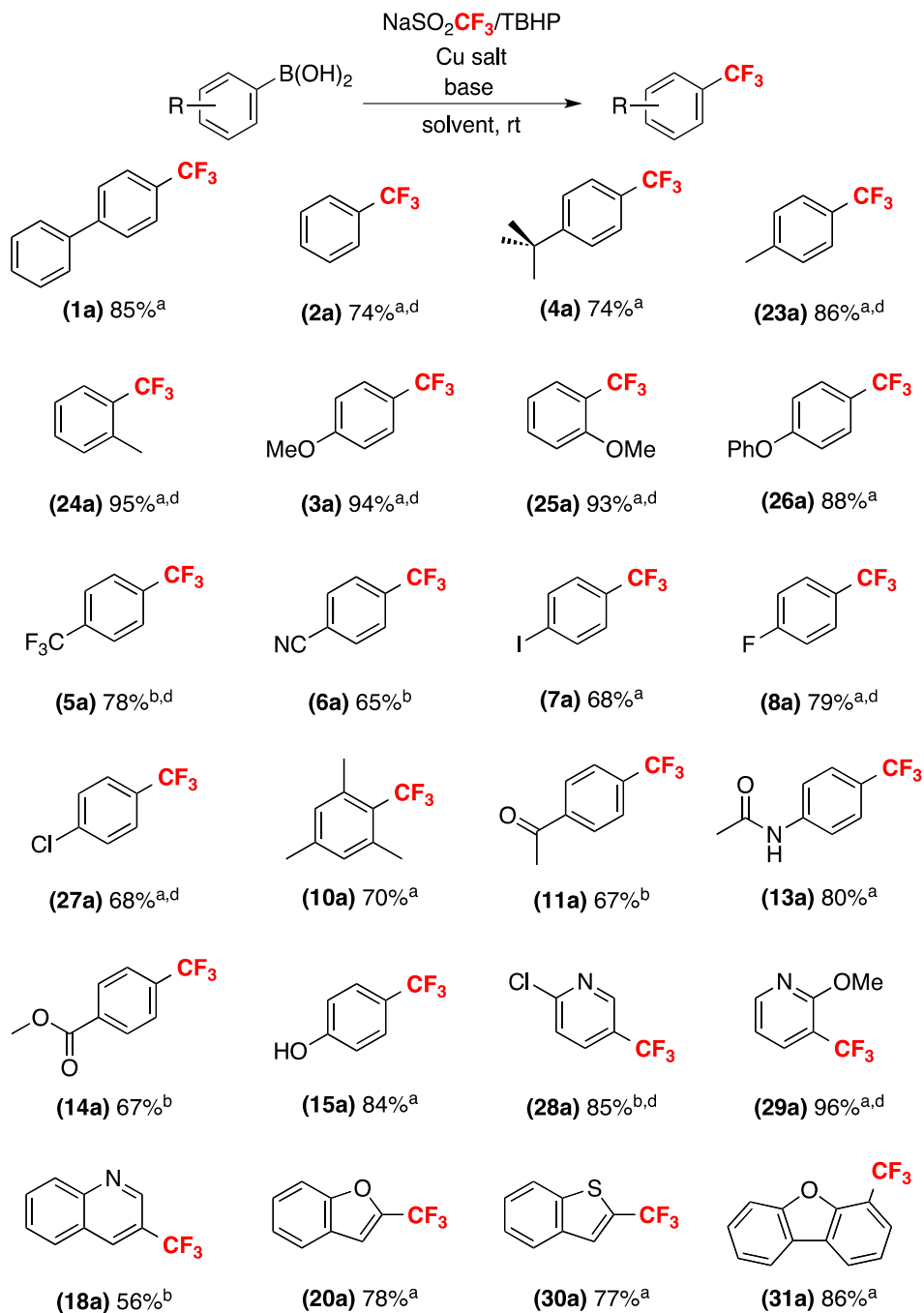


entry	copper salt	base	yield
1 ^c	CuCl	–	36%
2 ^c	CuCl	NaHCO ₃	46%
3 ^d	(MeCN) ₄ CuPF ₆	–	42%
4 ^{d,e}	(MeCN) ₄ CuPF ₆	–	38%
5 ^d	(MeCN) ₄ CuPF ₆	NaHCO ₃	49%
6 ^{d,e}	(MeCN) ₄ CuPF ₆	NaHCO ₃	59%

^[a] General conditions: substrate **6** (1 equiv, 0.05 mmol), [Cu] (1 equiv), base (1 equiv), NaSO₂CF₃ (3 equiv), TBHP (5 equiv) at 23 °C for 12 h. ^[b] Yields determined by ¹⁹F NMR analysis. ^[c] Solvent = MeOH/DCM/H₂O (5:5:4 ratio). ^[d] Solvent = MeOH. ^[e] 4 equiv TBHP.

Substrate Scope: With these two sets of conditions in hand, we next explored the full substrate scope of Cu-mediated trifluoromethylation with NaSO₂CF₃ and TBHP. As shown in **Scheme 2.16**, arenes bearing electron-donating alkyl, alkoxy, or phenoxy substituents reacted in excellent yield under the CuCl-mediated conditions (conditions a). Trifluoromethylation of electron deficient substrates (eg, cyano, trifluoromethyl, and carbonyl-substituted aryl boronic acids) afforded the desired products in good to excellent yield in the presence of (MeCN)₄CuPF₆ and NaHCO₃ (conditions b).²² Interestingly, the reaction of (4-iodophenyl)boronic acid resulted in exclusive trifluoromethylation of the C–B bond, leaving the C–I linkage intact. Sterically hindered boronic acid derivatives, which are generally challenging substrates for Cu-mediated cross-couplings,¹⁵ afforded good to excellent yields in this transformation (cf, products **10a**, **24a**, **25a**, **29a** and **31a**). Moreover, the reaction is compatible with diverse functional groups, including enolizable ketones, esters, amides, and phenols. Finally, heteroaryl boronic acids based on pyridine, quinoline, thiophene and furan afforded moderate to excellent yield. Notably, trifluoromethylation of the C–B bond outcompeted free radical C–H trifluoromethylation in all of these substrates.

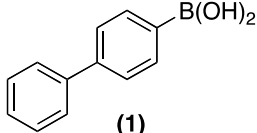
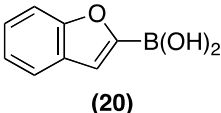
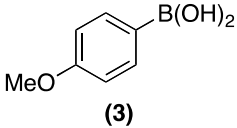
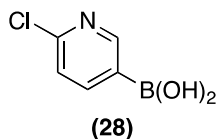
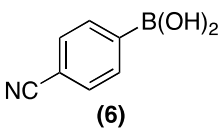
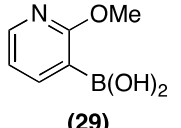
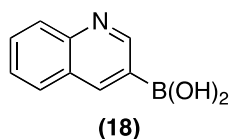
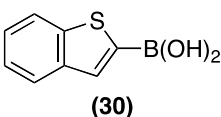
Scheme 2.16. Substrate Scope of Copper-Mediated Trifluoromethylation of Aryl Boronic Acids with NaSO₂CF₃/TBHP^[c]



^[a] Reaction conditions: substrate (1 equiv, 0.5 mmol), CuCl (1 equiv), NaSO₂CF₃ (3 equiv), TBHP (5 equiv) in DCM/MeOH/H₂O (5:5:4 ratio) at 23 °C for 12 h. ^[b] Reaction conditions: substrate (1 equiv), (MeCN)₄CuPF₆ (1 equiv), NaSO₂CF₃ (3 equiv), NaHCO₃ (1 equiv), TBHP (4 equiv) in MeOH at 23 °C for 12 h. ^[c] Isolated yield. ^[d] Yields determined by ¹⁹F NMR analysis.

Control reactions (without Cu added) were performed for all the substrates listed on **Table 2.7**. Only trace amounts (<2%) of the CF₃ containing product were observed in most cases. 2-(Trifluoromethyl)benzofuran was obtained in 5% yield in this control reaction.

Table 2.7. Reaction of Aryl–B(OH)₂ with NaSO₂CF₃/TBHP^[c]

Substrate	Yield	Substrate	Yield
	<1% ^a		5% ^a
	<1% ^a		0% ^b
	<2% ^b		<2% ^a
	<1% ^b		<1% ^a

^[a] Reaction conditions: substrate (1 equiv, 0.05 mmol), NaSO₂CF₃ (3 equiv), and TBHP (5 equiv) in DCM/MeOH/H₂O at 23 °C for 12 h. ^[b] Reaction conditions: substrate (1 equiv, 0.05 mmol), NaSO₂CF₃ (3 equiv), NaHCO₃ (1 equiv), and TBHP (4 equiv) in MeOH at 23 °C for 12 h. ^[c] Yields determined by ¹⁹F NMR analysis.

As noted above, most previously reported boronic acid trifluoromethylation protocols require inert atmosphere conditions and dry solvents. Even under these controlled conditions, significant quantities (2-10%) of protodeboronated products are commonly observed and are very challenging to separate/purify from the desired Aryl–CF₃ products. In contrast, all of the trifluoromethylation reactions in **Scheme 2.16** were insensitive to ambient air/moisture and were set up on the benchtop without purification of commercial reagents and/or solvents. Despite the presence of water, protodeboronation of the boronic acid was not detected under these conditions. This makes product isolation

extremely straightforward, as the major side-product (the corresponding hydroxylated arene) is readily removable by extraction or column chromatography.

2.5 Conclusions

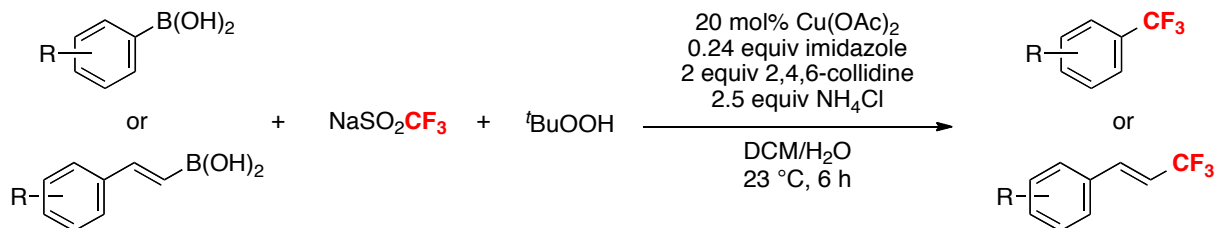
In summary, this chapter describes the development of two mild and versatile Cu-based trifluoromethylation methods using $\text{CF}_3\cdot$ precursors. Our Cu/Ru-catalyzed trifluoromethylation/perfluoroalkylation of aryl boronic acids takes advantage of visible light photoredox catalysis to generate $\text{R}_F\cdot$ under mild conditions and merges it with copper-catalyzed aryl boronic acid functionalization.¹² This combination enabled a method for the trifluoromethylation of a wide variety of aromatic and heteroaromatic substrates bearing many common functional groups. Most importantly, this transformation demonstrates the feasibility of achieving Cu-catalyzed trifluoromethylation via a radical pathway. Furthermore, it represents a new example of combining organometallic and photoredox catalysis to achieve synthetically useful organic transformations.²³

Based on that initial proof-of-concept discovery, we developed a highly practical copper-mediated trifluoromethylation of a variety of aryl and heteroaryl boronic acids with $\text{CF}_3\cdot$, which is generated *in situ* from NaSO_2CF_3 and TBHP.¹³ These reactions are easy to set up under ambient conditions, and product purification is similarly straightforward. Both protocols represent significant synthetic advances for the selective preparation of trifluoromethylated compounds.

2.6 Subsequent Developments and Outlook

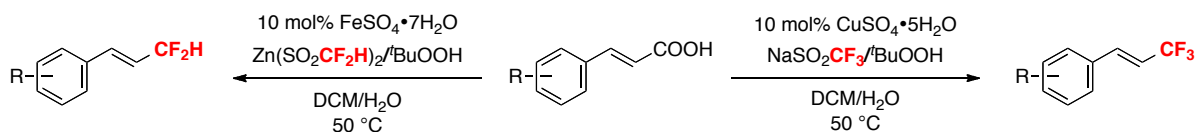
Since the initial publication of our work, the combination of transition metal catalysis and trifluoromethyl radicals has been utilized by a number of others for accessing trifluoromethyl-substituted aromatics and alkenes. For example, soon after we reported the Cu-mediated aromatic trifluoromethylation of aryl boronic acids with NaSO_2CF_3 and TBHP, a closely related transformation was reported by Beller (**Scheme 2.17**).²⁴ Beller and co-workers evaluated a wide variety of Pd and Cu catalysts under radical trifluoromethylation reaction conditions. Extensive screening led to the initial discovery of Cu-mediated trifluoromethylation of aryl boronic acids with NaSO_2CF_3 and TBHP. For example, 22% 1-methoxy-4-(trifluoromethyl)benzene was obtained using 20 mol % of $\text{Cu}(\text{OAc})_2$. Several additives, including imidazole, 2,4,6-collidine, and NH_4Cl , were empirically identified to improve the yields of this transformation. The most dramatic increase in yield came from increasing the amount of the trifluoromethylating reagent and oxidant (to 7 equiv of NaSO_2CF_3 and 16.1 equiv of TBHP). A relatively limited set of electronically varied arylboronic acids were subjected to the Cu-catalyzed trifluoromethylation conditions and afforded modest to good yields (with 1-4 turnovers of the Cu catalyst). Heterocyclic boronic acids (of dibenzofuran, benzofuran and Boc-protected indole) led to modest yields of the corresponding trifluoromethylated products (34-63%). Despite the advantage of using just 20 mol % of Cu catalyst, the requirement for superstoichiometric quantities of the more expensive CF_3 reagent and the low efficiency could limit the application of this catalytic trifluoromethylation reaction. Notably, several electronically various vinylboronic acids were also examined under the Beller's trifluoromethylation conditions and CF_3 -substituted alkenes were obtained in good yields. In most cases, (*E*)-alkenes was formed with high selectivity. The origin of this selectivity was attributed to the higher stability of (*E*)-alkenes compared to the *Z* isomers.

Scheme 2.17. Beller's Example of Cu-Catalyzed Trifluoromethylation of Aryl- and Vinylboronic Acids with $\text{CF}_3\cdot$ Derived from $\text{NaSO}_2\text{CF}_3/\text{TBHP}$



Efforts towards combining transition metal catalysis and $\text{CF}_3\cdot$ and $\text{CF}_2\text{H}\cdot$ have proven successful in the context of copper and iron-catalyzed decarboxylative trifluoromethylation and difluoromethylation of α,β -unsaturated carboxylic acids using NaSO_2CF_3 and $\text{Zn}(\text{SO}_2\text{CF}_2\text{H})_2$ (**Scheme 2.18**).²⁵ Prior to this work, trifluoromethyl-substituted (*E*)-alkenes had typically been prepared via the reaction of expensive “ CF_3^+ ” or “ CF_3^- ” reagents with vinyl boronic acids^{5d,e,24} and borates,²⁶ vinyl iodides,²⁷ vinyl sulfonates,²⁸ α,β -unsaturated carboxylic acids,²⁹ or alkynes.³⁰ The use of bench stable, and cost effective NaSO_2CF_3 and $\text{Zn}(\text{SO}_2\text{CF}_2\text{H})_2$ reagents led to the development of convenient and practical alternatives to afford tri- and difluoromethyl-substituted (*E*)-alkenes.

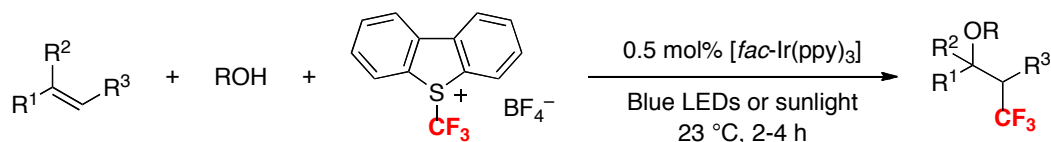
Scheme 2.18. Cu- and Fe-Catalyzed Decarboxylative Tri- and Difluoromethylation of α,β -Unsaturated Carboxylic Acids with NaSO_2CF_3 and $\text{Zn}(\text{SO}_2\text{CF}_2\text{H})_2$



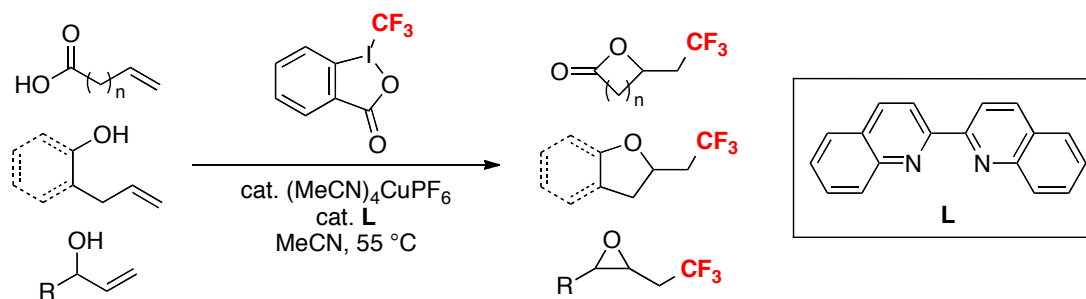
The activation of CF_3 precursors via photoredox catalysis has also become an increasingly important strategy for C– CF_3 bond formation. For example, recently, Akita and co-workers revealed the oxytrifluoromethylation of alkenes using Umemoto's reagent in the presence of a photocatalyst and light (**Scheme 2.19**).³¹ This radical transformation is efficient toward activated alkenes, such as styryl substrates and electron-rich alkenes, and is compatible with a broad range of O nucleophiles, such as alcohols and carboxylic acids. The efficient generation of trifluoromethyl radical is

critical for achieving high efficiency under mild conditions (2-4 hours, at room temperature). Recently, Buchwald and co-workers reported a Cu-catalyzed intramolecular oxytrifluoromethylation of unactivated alkenes using Togni's "CF₃⁺" reagent (**Scheme 2.20**).³² Slightly higher temperature (55 °C) is required for high efficiency. A radical mechanism is also proposed for this transformation.

Scheme 2.19. Photoredox Oxytrifluoromethylation of Alkenes with CF₃•

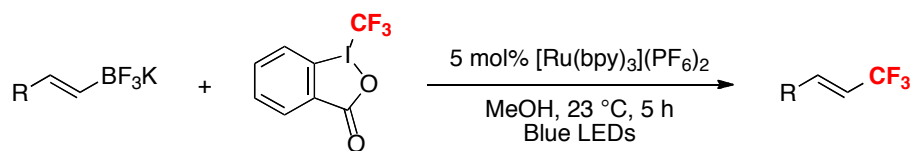


Scheme 2.20. Intramolecular Oxytrifluoromethylation of Unactivated Alkenes



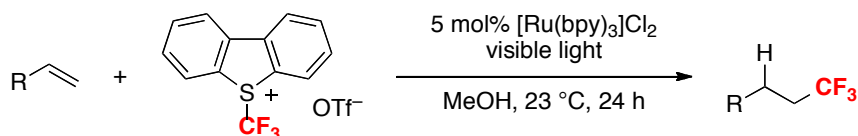
Another example of applying CF₃• derived from Ru-catalyzed photocatalysis to a trifluoromethylation reaction was recently realized in the context of synthesizing CF₃-substituted alkenes from vinyltrifluoroborates (**Scheme 2.21**).³³ A wide variety of vinyl borates, including heteroaryl groups like thiophene, pyridine, quinoline and benzothiazole, were successfully converted to the CF₃-containing products. The combination of Togni's reagent and [Ru(bpy)₃](PF₆)₂ proved to be superior to the previous Ir/Umemoto system for this transformation.

Scheme 2.21. Photoredox Trifluoromethylation of Vinyltrifluoroborates with $\text{CF}_3\cdot$



Most recently, Gouverneur and co-workers reported a visible-light induced hydrotrifluoromethylation of unactivated alkenes using the Umemoto reagent in the presence of a Ru photocatalyst (**Scheme 2.22**). Postulating that the net fluoroform addition could be achieved by addition of CF_3 radical, followed by H atom extraction from a separate reducing agent, the authors explored the reactions of unactivated alkenes in the presence of reducing agents under photocatalysis conditions. Again, the use of the Umemoto reagent precluded atom transfer radical addition (addition of CF_3 , and I to alkenes) that is typically observed with CF_3I , and as well as oxytrifluoromethylation (addition of CF_3 , and O nucleophile to alkenes) that is typically seen with the Togni reagents.

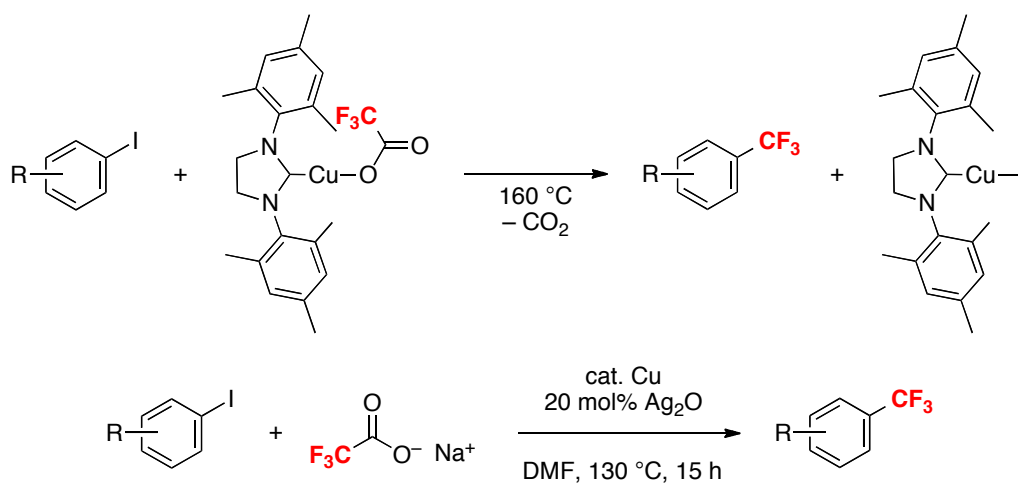
Scheme 2.22. Photoredox Trifluoromethylation of Vinyltrifluoroborates with $\text{CF}_3\cdot$



Trifluoroacetate salts, such as NaTFA and KTFA, are easy to handle, white crystalline powders that are considerably less costly than most commonly used trifluoromethylating reagents. In fact, their cost is even lower than fluoroform (CF_3H),³⁴ the most atom economical reagent for installing a CF_3 motif. Despite these significant advantages, the current state of the art for decarboxylative trifluoromethylation using trifluoroacetate salts involves generating “ $\text{CF}_3\cdot$ ” via heating the substrates at $>150\text{ }^\circ\text{C}$ in the presence of super-stoichiometric amounts of Cu.³⁵ In 2010, Vacic reported the first decarboxylative trifluoromethylation of aryl halides using a well-defined (NHC)Cu(TFA) complex.^{4d} However, no enhanced reactivity was observed compared to the conventional “ligandless” Cu(TFA) complex.^{35a,b} In a very exciting recent report from Li and Duan,

the first Cu-catalyzed decarboxylative trifluoromethylation of aryl iodides with NaTFA was achieved. In this system, Ag₂O was used as a catalytic promoter.^{5f} A broad range of substrates bearing electron withdrawing and even electron donating substituents underwent trifluoromethylation in good yields at 130 °C. The authors proposed that the activation energy for the decarboxylation of NaTFA to generate AgCF₃ *in situ* was lower than that for the formation of CuCF₃.

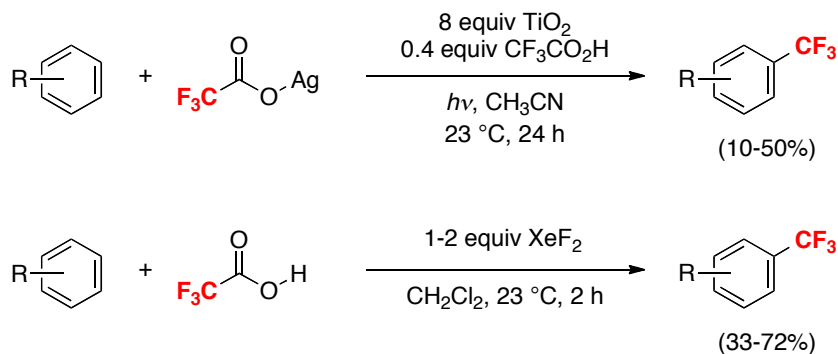
Scheme 2.23. Cu-Assisted Decarboxylative Trifluoromethylation using (NHC)Cu(TFA) and NaTFA



Trifluoroacetates have also been successfully used as a CF₃• precursor under oxidative conditions. Several studies have reported the radical trifluoromethylation of aromatic molecules via Kolbe electrolysis with NaTFA.³⁶ Moreover, TiO₂ has been successfully used to induce the generation of CF₃• from AgTFA under photochemical conditions.³⁷ The oxidation of trifluoroacetate by TiO₂ afforded the trifluoroacetate radical, which liberates CF₃• upon CO₂ elimination. The subsequent reaction of arenes and heteroarenes with CF₃• then forms the corresponding products in moderate to good yields. However, high efficiency was only achieved using a super-stoichiometric quantity of TiO₂ in conjunction with irradiation from a Hg lamp, which severely limits its application. Finally, XeF₂ has also been successfully used as an oxidant for the generation of trifluoromethyl radical from TFA.³⁸ Intriguingly, both the photolytic and

the chemically induced oxidative trifluoromethylations were performed at room temperature!

Scheme 2.24. Radical Arene Trifluoromethylation by the Oxidation of AgTFA or TFA



As mentioned above, while trifluoroacetate is an ideal CF_3^- precursor, the high activation barrier for the decarboxylation of CF_3CO_2^- generally requires high temperatures, which limits its broad application. On the contrary, radical trifluoromethylation of organic substrates using trifluoroacetates could be a viable pathway, since the preformed TFA radical should be more kinetically reactive towards decarboxylation and release of CF_3^\bullet . Future work could focus on the development of a chemical and/or photochemical systems that induce the facile formation of $\text{CF}_3\text{CO}_2^\bullet$ under mild conditions. Efficient reactivity between the CF_3^\bullet generated from trifluoroacetates and organic substrates, and/or a combination of CF_3^\bullet with previously developed transition-metal-catalyzed cross-coupling strategies should generate robust protocols that are highly desirable in the industrial sector.

2.7 Experimental Procedures and Characterization Data

General Procedures

NMR spectra were obtained on a Varian vnmrs 700 (699.76 MHz for ^1H ; 175.95 MHz for ^{13}C ; 658.43 for ^{19}F), Varian vnmrs 500 (500.10 MHz for ^1H ; 125.75 MHz for ^{13}C , 470.56 MHz for ^{19}F), Varian Inova 500 (499.90 MHz for ^1H ; 125.70 MHz for ^{13}C), or a Varian MR400 (400.52 MHz for ^1H ; 100.71 for ^{13}C , 376.87 MHz for ^{19}F) spectrometer. ^1H and ^{13}C chemical shifts are reported in parts per million (ppm) relative to TMS, with

the residual solvent peak used as an internal reference. ^{19}F NMR spectra are referenced based on the internal standard 1,3,5-trifluorobenzene, which appears at -107.40 ppm. Multiplicities are reported as follows: singlet (s), doublet (d), doublet of doublets (dd), doublet of doublets of doublets (ddd), doublet of triplets (dt), triplet (t), triplet of doublets (td), triplet of triplets (tt), quartet (q), quintet (quin), multiplet (m), and broad resonance (br). Melting points were determined with a Mel-Temp 3.0, a Laboratory Devices Inc, USA instrument, and are uncorrected. HRMS data were obtained on a Micromass AutoSpec Ultima Magnetic Sector mass spectrometer. GCMS analysis was performed on a Shimadzu GCMS-QP2010 plus gas chromatograph mass spectrometer. The products were separated on a 30 m length by 0.25 mm id, RESTEK XTI-5 column coated with a 0.25 μm film. Helium was employed as the carrier gas, with a constant column flow of 1.5 mL/min. The injector temperature was held constant at 250 $^{\circ}\text{C}$. Kugelrohr distillations were performed on a Buchi Glass Oven B-580 Kugelrohr.

Materials and Methods.

CuOAc , $(\text{MeCN})_4\text{CuPF}_6$, and CuCl were obtained from Strem Chemical. Aryl boronic acids were obtained from Frontier Scientific. 1,3,5-Trifluorobenzene, 4-(trifluoromethyl)benzotrifluoride, and iodobenzotrifluoride were obtained from Oakwood Products. 4-Fluorobenzotrifluoride and 4-(trifluoromethyl)pyridine were obtained from Matrix Scientific. Trifluorotoluene was obtained from Acros. Potassium carbonate was obtained from Fisher Scientific. $\text{CF}_3\text{SO}_2\text{Na}$, and 4-(trifluoromethyl)anisole were obtained from SynQuest Laboratories. $\text{Ru}(\text{bpy})_3\text{Cl}_2 \cdot 6\text{H}_2\text{O}$, $\text{Ru}(\text{phen})_3\text{Cl}_2$, $\text{CF}_3\text{SO}_2\text{Cl}$, 1,4-bis(trifluoromethyl)benzene, 4-(trifluoromethyl)phenol, estrone and dry DMF, DMA, DMSO, 1,4-dioxane, diglyme and NMP were obtained from Sigma Aldrich. NaHCO_3 was obtained from Fisher Scientific. $\text{CF}_3\text{SO}_2\text{Na}$ was obtained from Matrix Scientific. TBHP (70% aqueous solution) was obtained from Alfa Aesar.

For the Cu/Ru-Catalyzed trifluoromethylation system (**Section 2.3**), all syntheses were conducted using standard Schlenk techniques or in a nitrogen atmosphere glovebox unless otherwise stated. For the Cu-Mediated radical trifluoromethylation using $\text{NaSO}_2\text{CF}_3/\text{TBHP}$ (**Section 2.4**), all syntheses were conducted on the benchtop without purification of commercial reagents and/or solvents. Copper(I) salts were removed from

the glovebox approximately once every two weeks and stored in N₂ flushed vials on the bench top.

Experimental Details.

Preparation of CF₃I Stock Solution:

DMF (20 mL) was added to a Schlenk graduated cylinder under nitrogen (see picture below for apparatus). The vessel and solvent were weighed. Next, CF₃I was bubbled through the DMF solution using a long needle until the total volume of the solution reached approximately 25 mL. The vessel was sealed weighed again. The concentration of the CF₃I stock solution was then calculated based on the mass of CF₃I added and the total volume of the solution.



Figure 2.1. Schlenk Graduated Cylinder with CF₃I Stock Solution

Reactivity of Aryl Boronic Acid under MacMillan's Reaction Conditions⁹

In a glovebox, substrate **1** (9.9 mg, 0.05 mmol, 1 equiv), Ru(phen)₃Cl₂ (0.36 mg, 0.0005 mmol, 0.01 equiv), and K₂HPO₄ (26.1 mg, 0.15 mmol, 3 equiv) were weighed into a 4 mL vial. MeCN (0.4 mL) was added. The vial was fitted with a screw cap containing a silicone septum and removed from the glove box. The CF₃SO₂Cl (10.64 μL, 2 equiv) was added by syringe, and the vial was sealed with parafilm and placed in a water bath at room temperature with two 26 W compact fluorescent light bulbs (one on either side of the vial approximately 5 cm away). The reaction mixture was allowed to stir for 24 h. The reaction was quenched with water (1 mL) and extracted with ethyl acetate (2 x 1 mL) and CH₂Cl₂ (1 x 1 mL). The combined organic layers were dried over MgSO₄. 1,3,5-trifluorobenzene and naphthalene (0.05 mmol, 1 equiv) were added as internal standards, and the reaction was analyzed by ¹H NMR and ¹⁹F NMR spectroscopy. The starting material **1** was recovered in nearly quantitative yield, and trifluoromethylated product **1a** was formed in less than 2% yield.

Reactivity of Aryl Boronic Acid under Baran's Reaction Conditions¹¹

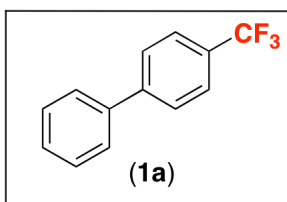
To a solution of substrate **1** (49.5 mg, 0.25 mmol, 1.0 equiv) and sodium trifluoromethylsulfinate (117 mg, 0.75 mmol, 3.0 equiv) in dichloromethane (1 mL) and water (0.4 mL) at 0 °C was slowly added tert-butylhydroperoxide (70% solution in water, 0.17 mL, 1.25 mmol, 5.0 equiv) with vigorous stirring. The reaction was warmed to room temperature and stirred for 24 h. The resulting solution was partitioned between dichloromethane (2 mL) and saturated sodium bicarbonate (2 mL). The organic layer was separated, and the aqueous layer was extracted with dichloromethane (3 × 2 mL). The combined organic layers were dried over MgSO₄. 1,3,5-trifluorobenzene and naphthalene (0.25 mmol, 1 equiv) were added as internal standards, and the reaction was analyzed by ¹⁹F NMR spectroscopy and GCMS. No trifluoromethylated product was observed. 4-Hydroxybiphenyl was formed in 75% yield.

Synthesis and Characterization of Products in Scheme 2.10

Standard Procedure for Trifluoromethylation of Aryl Boronic Acids

In a glovebox, the boronic acid substrate **1** (0.25 mmol, 1 equiv), CuOAc (6 mg, 0.05 mmol, 0.2 equiv), Ru(bpy)₃Cl₂•6H₂O (1.85 mg, 0.0025 mmol, 0.01 equiv), and K₂CO₃

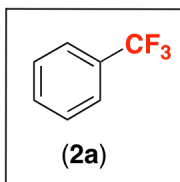
(35 mg, 0.25 mmol, 1 equiv) were weighed into a 20 mL vial. CF₃I (1.25 mmol, 5 equiv) was added to the reaction vial as a stock solution in DMF. Additional DMF was added to make the total volume 1.5 mL. The vial was sealed with a Teflon-lined cap, removed from the glove box, and placed in an oil bath at 60 °C with two 26 W compact fluorescent light bulbs (one on either side of the vial approximately 5 cm away). The reaction mixture was allowed to stir for 12 h. The resulting red solution was cooled to room temperature. 1,3,5-Trifluorobenzene (0.25 mmol, 1 equiv) was added as an internal standard, and the reaction was analyzed by ¹⁹F NMR spectroscopy. GCMS analysis was performed on a Shimadzu GCMS-QP2010 plus gas chromatograph mass spectrometer. The products were separated on a 30 m length by 0.25 mm id, RESTEK XTI-5 column coated with a 0.25 μm film. Helium was employed as the carrier gas, with a constant column flow of 1.5 mL/min. The injector temperature was held constant at 250 °C. The GC oven temperature program was as follows: 40 °C hold 6 min, ramp 15 °C/min to 250 °C, and hold for 3 min.



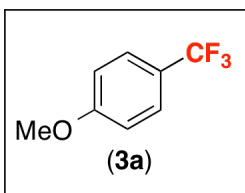
The reaction was performed on a 0.25 mmol scale using the standard procedure. The trifluoromethylated product **1a** was formed in 80% yield. The product showed a ¹⁹F NMR signal at -62.4 ppm in DCE (lit. -62.4 ppm in CDCl₃).^{5d} The identity of the product was further confirmed by GCMS analysis, where the product peak was observed at 15.28 min.

This reaction of substrate **1** was also conducted on a 5 mmol scale. For the 5 mmol scale reaction, substrate **1** (0.99 g, 5 mmol, 1 equiv), CuOAc (122 mg, 1 mmol, 0.2 equiv), K₂CO₃ (0.69 g, 5 mmol, 1 equiv), Ru(bpy)₃Cl₂•6H₂O (37.4 mg, 0.05 mmol, 0.01 equiv), CF₃I (25 mmol, 5 equiv) and DMF (30 mL) were used. The reaction was conducted in a 250 mL round bottom flask, and the yield was determined to be 82% by ¹⁹F NMR spectroscopy. The reaction mixture was then diluted with Et₂O (50 mL), and the resulting mixture was washed with water (3 x 50 mL) and brine (1 x 50 mL) and then dried over magnesium sulfate. The solvent was removed by rotary evaporation, and the product was purified by column chromatography on silica gel using pentane as the eluent. Compound

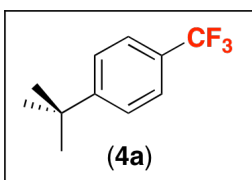
1a was obtained as white crystalline solid (776 mg, 70% yield, mp = 64.0-64.4 °C). The ^1H , ^{13}C and ^{19}F NMR spectroscopic data were identical to that reported previously in the literature.³



The reaction was performed on a 0.25 mmol scale using the standard procedure. The ^{19}F NMR spectral data for **2a** matched that of an authentic sample (Acros, s, -62.3 ppm). The trifluoromethylated product was formed in 70% yield. The identity of the product was further confirmed by GCMS analysis, where the product peak was observed at 3.64 min.



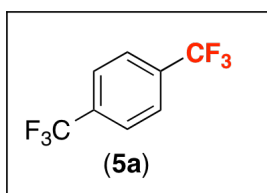
The reaction was performed on a 0.25 mmol scale using the standard procedure. The ^{19}F NMR spectral data for **3a** matched that of an authentic sample (SynQuest Labs, s, -61.0 ppm). The trifluoromethylated product was formed in 84% yield. The identity of the product was further confirmed by GCMS analysis, where the product peak was observed at 10.28 min.



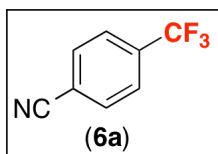
The reaction was performed on a 0.25 mmol scale using the standard procedure. The trifluoromethylated product **4a** was formed in 86% yield. The product showed a ^{19}F NMR signal at -61.8 ppm in DCE (lit. -62.2 ppm in CDCl_3).^{4c} The identity of the product was further confirmed by GCMS analysis, where the product peak was observed at 11.30 min.

This reaction of substrate **4** was also conducted on a 1 mmol scale. For the 1 mmol scale reaction, substrate **4** (178 mg, 1 mmol, 1 equiv), CuOAc (24 mg, 0.2 mmol, 0.2 equiv), K_2CO_3 (138 mg, 1 mmol, 1 equiv), $\text{Ru}(\text{bpy})_3\text{Cl}_2 \cdot 6\text{H}_2\text{O}$ (7.4 mg, 0.01 mmol, 0.01 equiv), CF_3I (5 mmol, 5 equiv) and DMF (6 mL) were used. The reaction was conducted in a 25 mL round bottom flask. The reaction mixture was then diluted with Et_2O (40 mL), and the resulting mixture was washed with water (2 x 40 mL), saturated aqueous CaCl_2 (1 x

40 mL), and brine (1 x 40 mL) and then dried over magnesium sulfate. The solvent was removed by rotary evaporation at 0 °C, and the product was purified by Kugelrohr distillation at 80 °C at 10 mm Hg. The isolated product **4a** (145 mg, 72% yield) was 96% pure, and contained traces (4%) of the corresponding protodeboronation byproduct *tert*-butylbenzene, which was not easily separable by chromatography on silica gel. The ¹H, ¹³C and ¹⁹F NMR spectroscopic data were identical to that reported previously in the literature.^{4c}



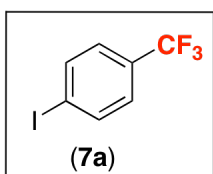
The reaction was performed on a 0.25 mmol scale using 50 mol % of CuOAc (15 mg, 0.125 mmol, 0.5 equiv) under otherwise identical conditions to the standard procedure. The ¹⁹F NMR spectral data for **5a** matched that of an authentic sample (Aldrich, s, -62.8 ppm). The trifluoromethylated product was formed in 64% yield. The identity of the product was further confirmed by GCMS analysis, where the product peak was observed at 3.56 min.



The reaction was performed on a 0.25 mmol scale using the standard procedure. The ¹⁹F NMR spectral data for **6a** matched that of an authentic sample (Oakwood, s, -63.1 ppm). The trifluoromethylated product was formed in 84% yield. The identity of the product was further confirmed by GCMS analysis, where the product peak was observed at 10.37 min.

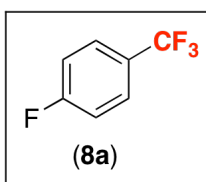
This reaction of substrate **6** was also conducted on a 1 mmol scale. For the 1 mmol scale reaction, substrate **6** (147 mg, 1 mmol, 1 equiv), CuOAc (24 mg, 0.2 mmol, 0.2 equiv), K₂CO₃ (138 mg, 1 mmol, 1 equiv), Ru(bpy)₃Cl₂•6H₂O (7.4 mg, 0.01 mmol, 0.01 equiv), CF₃I (5 mmol, 5 equiv) and DMF (6 mL) were used. The reaction was conducted in a 25 mL round bottom flask. The reaction mixture was then diluted with Et₂O (40 mL), and the resulting mixture was washed with water (2 x 40 mL), saturated aqueous CaCl₂ (1 x 40 mL), and brine (1 x 40 mL) and then dried over magnesium sulfate. The solvent was removed by rotary evaporation at 0 °C, and the product was purified by Kugelrohr distillation at 90 °C at 10 mm Hg. The isolated product **6a** (112 mg, 65% yield) was 97%

pure, and contained traces (3%) of the corresponding protodeboronation byproduct benzonitrile. If necessary, the protodeboronation product can be completely removed by subsequent column chromatographic purification on silica gel using 2% diethyl ether in pentane as the eluent. After this second purification, compound **6a** was obtained as a white solid (89 mg, 52% yield). The ^1H , ^{13}C and ^{19}F NMR spectroscopic data were identical to the authentic sample.



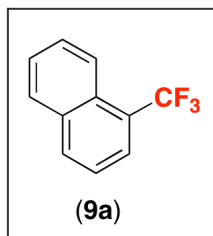
The reaction was performed on a 0.25 mmol scale using the standard procedure. The ^{19}F NMR spectral data for **7a** matched that of an authentic sample (Oakwood, s, -62.5 ppm). The trifluoromethylated product was formed in 73% yield. The identity of the product was further confirmed by GCMS analysis, where the product peak was observed at 11.49 min.

This reaction of substrate **7** was also conducted on a 1 mmol scale. For the 1 mmol scale reaction, substrate **7** (248 mg, 1 mmol, 1 equiv), CuOAc (24 mg, 0.2 mmol, 0.2 equiv), K_2CO_3 (138 mg, 1 mmol, 1 equiv), $\text{Ru}(\text{bpy})_3\text{Cl}_2 \cdot 6\text{H}_2\text{O}$ (7.4 mg, 0.01 mmol, 0.01 equiv), CF_3I (5 mmol, 5 equiv) and DMF (6 mL) were used. The reaction was conducted in a 25 mL round bottom flask. The reaction mixture was then diluted with Et_2O (40 mL), and the resulting mixture was washed with water (2 x 40 mL), saturated aqueous CaCl_2 (1 x 40 mL), and brine (1 x 40 mL) and then dried over magnesium sulfate. The solvent was removed by rotary evaporation at 0°C , and the product was purified by Kugelrohr distillation at 100°C at 10 mm Hg. The isolated product **7a** (174 mg, 64% yield) was 96% pure, and contained traces (4%) of the corresponding protodeboronation byproduct iodobenzene, which was not easily separable by chromatography on silica gel. The ^1H , ^{13}C and ^{19}F NMR spectroscopic data were identical to the authentic sample.



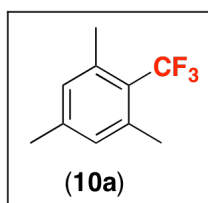
The reaction was performed on a 0.25 mmol scale using the standard procedure. The ^{19}F NMR spectral data for **8a** matched that of an authentic sample (Matrix Scientific, s, 3F, -61.6 ppm; m, 1F, -107.5 ppm). The trifluoromethylated product was formed in 93% yield. The

identity of the product was further confirmed by GCMS analysis, where the product peak was observed at 3.42 min.



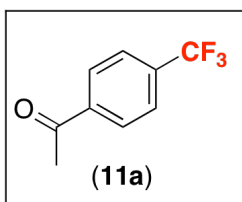
The reaction was performed on a 0.25 mmol scale using the standard procedure. The trifluoromethylated product **9a** was formed in 57% yield. The product showed a ^{19}F NMR signal at -59.3 ppm in DCE (lit. -59.72 ppm in CDCl_3).^{5d} The identity of the product was further confirmed by GCMS analysis, where the product peak was observed at 13.51 min.

This reaction of substrate **9** was also conducted on a 1 mmol scale. For the 1 mmol scale reaction, substrate **9** (172 mg, 1 mmol, 1 equiv), CuOAc (24 mg, 0.2 mmol, 0.2 equiv), K_2CO_3 (138 mg, 1 mmol, 1 equiv), $\text{Ru}(\text{bpy})_3\text{Cl}_2 \cdot 6\text{H}_2\text{O}$ (7.4 mg, 0.01 mmol, 0.01 equiv), CF_3I (5 mmol, 5 equiv) and DMF (6 mL) were used. The reaction was conducted in a 25 mL round bottom flask. The reaction mixture was then diluted with Et_2O (40 mL), and the resulting mixture was washed with water (2 x 40 mL), saturated aqueous CaCl_2 (1 x 40 mL), and brine (1 x 40 mL) and then dried over magnesium sulfate. The solvent was removed by rotary evaporation at 0°C , and the product was purified by Kugelrohr distillation at 120°C at 10 mm Hg. Compound **9a** was obtained as a 5:1 mixture with the protodeboronation product naphthalene (103 mg in total, 46% yield for **9a**). Subsequent purification of this sample by column chromatography on silica gel using pentane as the eluent afforded **9a** as a pure clear liquid (79 mg, 40% yield). The ^1H , ^{13}C and ^{19}F NMR spectroscopic data were identical to that reported previously in the literature.^{5d}



The reaction was performed on a 0.25 mmol scale using 50 mol % of CuOAc (15 mg, 0.125 mmol, 0.5 equiv) under otherwise identical conditions to the standard procedure. The trifluoromethylated product **10a** was formed in 45% yield. The product showed a ^{19}F NMR signal at -53.2 ppm in DCE (lit. -55.0 ppm in CDCl_3).^{5f,39} The identity of the product was further confirmed by GCMS analysis, where the product peak was observed at 11.45 min.

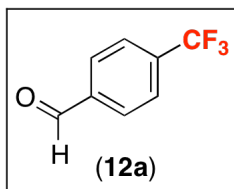
This reaction of substrate **10** was also conducted on a 1 mmol scale. For the 1 mmol scale reaction, substrate **10** (164 mg, 1 mmol, 1 equiv), CuOAc (60 mg, 0.5 mmol, 0.5 equiv), K₂CO₃ (138 mg, 1 mmol, 1 equiv), Ru(bpy)₃Cl₂•6H₂O (7.4 mg, 0.01 mmol, 0.01 equiv), CF₃I (5 mmol, 5 equiv) and DMF (6 mL) were used. The reaction was conducted in a 25 mL round bottom flask. The reaction mixture was then diluted with Et₂O (40 mL), and the resulting mixture was washed with water (2 x 40 mL), saturated aqueous CaCl₂ (1 x 40 mL), and brine (1 x 40 mL) and then dried over magnesium sulfate. The solvent was removed by rotary evaporation at 0 °C, and the product was purified by Kugelrohr distillation at 90 °C at 10 mm Hg. Compound **10a** was obtained as a 1:1 mixture with the inseparable protodeboronation product mesitylene as a clear liquid (119 mg in total, 39% yield for **10a**). The ¹H, ¹³C and ¹⁹F NMR spectroscopic data were identical to that reported previously in the literature.^{5f}



The reaction was performed on a 0.25 mmol scale using the standard procedure. The trifluoromethylated product **11a** was formed in 70% yield. The product showed a ¹⁹F NMR signal at –62.7 ppm in DCE (lit. –63.0 ppm in CDCl₃).^{4c} The identity of the product was further confirmed by GCMS analysis, where the product peak was observed at 11.68 min.

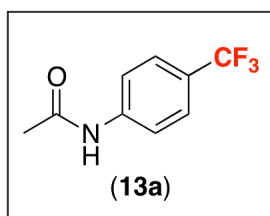
This reaction of substrate **11** was also conducted on a 1 mmol scale. For the 1 mmol scale reaction, substrate **11** (164 mg, 1 mmol, 1 equiv), CuOAc (24 mg, 0.2 mmol, 0.2 equiv), K₂CO₃ (138 mg, 1 mmol, 1 equiv), Ru(bpy)₃Cl₂•6H₂O (7.4 mg, 0.01 mmol, 0.01 equiv), CF₃I (5 mmol, 5 equiv) and DMF (6 mL) were used. The reaction was conducted in a 25 mL round bottom flask. The reaction mixture was then diluted with Et₂O (40 mL), and the resulting mixture was washed with water (2 x 40 mL), saturated aqueous CaCl₂ (1 x 40 mL), and brine (1 x 40 mL) and then dried over magnesium sulfate. The solvent was removed by rotary evaporation at 0 °C, and the product was purified by Kugelrohr distillation at 100 °C at 10 mm Hg. The isolated product **11a** (120.0 mg, 64% yield) was 95% pure, and contained traces (5%) of the corresponding protodeboronation byproduct

acetophenone, which was not easily separable by chromatography on silica gel. The ^1H , ^{13}C and ^{19}F NMR spectroscopic data were identical to that reported previously in the literature.^{4c}



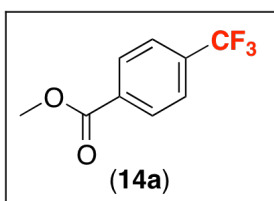
The reaction was performed on a 0.25 mmol scale using 50 mol % of CuOAc (15 mg, 0.125 mmol, 0.5 equiv) under otherwise identical conditions. The trifluoromethylated product **12a** was formed in 74% yield. The product showed a ^{19}F NMR signal at -62.8 ppm in DCE (lit. -62.7 ppm in CDCl_3).⁴⁰ The identity of the product was further confirmed by GCMS analysis, where the product peak was observed at 10.18 min.

This reaction of substrate **12** was also conducted on a 1 mmol scale. For the 1 mmol scale reaction, substrate **12** (150 mg, 1 mmol, 1 equiv), CuOAc (60 mg, 0.5 mmol, 0.5 equiv), K_2CO_3 (138 mg, 1 mmol, 1 equiv), $\text{Ru}(\text{bpy})_3\text{Cl}_2 \cdot 6\text{H}_2\text{O}$ (7.4 mg, 0.01 mmol, 0.01 equiv), CF_3I (5 mmol, 5 equiv) and DMF (6 mL) were used. The reaction was conducted in a 25 mL round bottom flask. The reaction mixture was then diluted with Et_2O (40 mL), and the resulting mixture was washed with water (2 x 40 mL), saturated aqueous CaCl_2 (1 x 40 mL), and brine (1 x 40 mL) and then dried over magnesium sulfate. The solvent was removed by rotary evaporation at 0°C , and the product was purified by Kugelrohr distillation at 100°C at 10 mm Hg. The isolated product **12a** (110.0 mg, 63% yield) was 95% pure, and contained traces (5%) of the corresponding protodeboronation byproduct benzaldehyde, which was not easily separable by chromatography on silica gel. The ^1H , ^{13}C and ^{19}F NMR spectroscopic data were identical to that reported previously in the literature.⁴⁰



The reaction was performed on a 0.25 mmol scale using the standard procedure. The trifluoromethylated product **13a** was formed in 67% yield. The product showed a ^{19}F NMR signal at -63.5 ppm in DCE (lit. -62.3 ppm in CDCl_3).^{4h} The identity of the product was further confirmed by GCMS analysis, where the product peak was observed at 15.48 min.

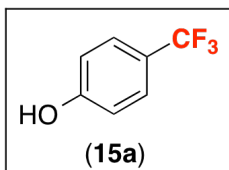
This reaction of substrate **13** was also conducted on a 1 mmol scale. For the 1 mmol scale reaction, substrate **13** (179 mg, 1 mmol, 1 equiv), CuOAc (24 mg, 0.2 mmol, 0.2 equiv), K₂CO₃ (138 mg, 1 mmol, 1 equiv), Ru(bpy)₃Cl₂•6H₂O (7.4 mg, 0.01 mmol, 0.01 equiv), CF₃I (5 mmol, 5 equiv) and DMF (6 mL) were used. The reaction was conducted in a 25 mL round bottom flask. The reaction mixture was then diluted with Et₂O (40 mL), and the resulting mixture was washed with water (2 x 40 mL), saturated aqueous CaCl₂ (1 x 40 mL), and brine (1 x 40 mL) and then dried over magnesium sulfate. The solvent was removed by rotary evaporation at 0 °C, and the product was purified by Kugelrohr distillation at 150 °C at 10 mm Hg. The isolated product **13a** (121.0 mg, 60% yield) was 95% pure, and contained traces (5%) of the corresponding protodeboronation byproduct *N*-phenylacetamide, which was not easily separable by chromatography on silica gel. The ¹H, ¹³C and ¹⁹F NMR spectroscopic data were identical to that reported previously in the literature.^{4h}



The reaction was performed on a 0.25 mmol scale using the standard procedure. The trifluoromethylated product **14a** was formed in 86% yield. The product showed a ¹⁹F NMR signal at –62.7 ppm in DCE (lit. –62.9 ppm in CDCl₃).^{4c} The identity of the product was further confirmed by GCMS analysis, where the product peak was observed at 11.93 min.

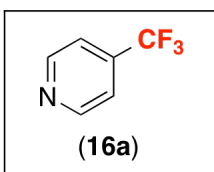
This reaction of substrate **14** was also conducted on a 1 mmol scale. For the 1 mmol scale reaction, substrate **14** (180 mg, 1 mmol, 1 equiv), CuOAc (24 mg, 0.2 mmol, 0.2 equiv), K₂CO₃ (138 mg, 1 mmol, 1 equiv), Ru(bpy)₃Cl₂•6H₂O (7.4 mg, 0.01 mmol, 0.01 equiv), CF₃I (5 mmol, 5 equiv) and DMF (6 mL) were used. The reaction was conducted in a 25 mL round bottom flask. The reaction mixture was then diluted with Et₂O (40 mL), and the resulting mixture was washed with water (2 x 40 mL), saturated aqueous CaCl₂ (1 x 40 mL), and brine (1 x 40 mL) and then dried over magnesium sulfate. The solvent was removed by rotary evaporation at 0 °C, and the product was purified by Kugelrohr distillation at 100 °C at 10 mm Hg. The isolated product **14a** (139.0 mg, 68% yield) was

95% pure, and contained traces (5%) of the corresponding protodeboronation byproduct methyl benzoate, which was not easily separable by chromatography on silica gel. The ^1H , ^{13}C and ^{19}F NMR spectroscopic data were identical to that reported previously in the literature.^{4c}



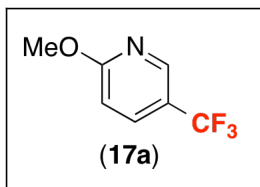
The reaction was performed on a 0.25 mmol scale using 10 mol % of CuOAc (3 mg, 0.025 mmol, 0.1 equiv) under otherwise identical conditions. The ^{19}F NMR spectral data for **15a** matched that of an authentic sample (Matrix Scientific, s, -60.7 ppm). The trifluoromethylated product was formed in 50% yield. The identity of the product was further confirmed by GCMS analysis, where the product peak was observed at 11.90 min.

This reaction of substrate **15** was also conducted on a 1 mmol scale. For the 1 mmol scale reaction, substrate **15** (138 mg, 1 mmol, 1 equiv), CuOAc (12 mg, 0.1 mmol, 0.1 equiv), K_2CO_3 (138 mg, 1 mmol, 1 equiv), $\text{Ru}(\text{bpy})_3\text{Cl}_2 \cdot 6\text{H}_2\text{O}$ (7.4 mg, 0.01 mmol, 0.01 equiv), CF_3I (5 mmol, 5 equiv) and DMF (6 mL) were used. The reaction was conducted in a 25 mL round bottom flask. The reaction mixture was then diluted with Et_2O (40 mL), and the resulting mixture was washed with water (2 x 40 mL), saturated aqueous CaCl_2 (1 x 40 mL), and brine (1 x 40 mL) and then dried over magnesium sulfate. The solvent was removed by rotary evaporation at 0°C , and the product was purified by Kugelrohr distillation at 110°C at 10 mm Hg. Compound **15a** was obtained as a 10:1 mixture with the inseparable protodeboronation product phenol as a clear liquid (69.0 mg in total, 40% yield for **15a**). The ^1H , ^{13}C and ^{19}F NMR spectroscopic data were identical to the authentic sample.

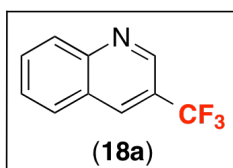


The reaction was performed on a 0.25 mmol scale using 50 mol % of CuOAc (15 mg, 0.125 mmol, 0.5 equiv) and 3 equivalent of CF_3I (0.75 mmol, 3 equiv) under otherwise identical conditions. The ^{19}F NMR spectral data for **16a** matched that of an authentic sample (Matrix Scientific, s, -64.6 ppm). The trifluoromethylated product was formed in 64% yield. The identity of the

product was further confirmed by GCMS analysis, where the product peak was observed at 3.94 min.

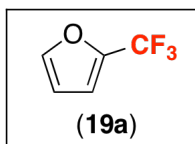


The reaction was performed on a 0.25 mmol scale using the standard procedure. The ^{19}F NMR spectral data for **17a** matched that of an authentic sample (Matrix Scientific, s, -61.1 ppm). The trifluoromethylated product was formed in 66% yield. The identity of the product was further confirmed by GCMS analysis, where the product peak was observed at 8.63 min.

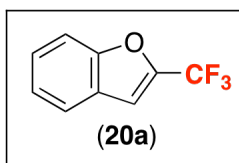


The reaction was performed on a 0.25 mmol scale using the standard procedure. The trifluoromethylated product **18a** was formed in 70% yield. The product showed a ^{19}F NMR signal at -61.4 ppm in DCE (lit. -61.4 ppm in CDCl_3).⁴⁰ The identity of the product was further confirmed by GCMS analysis, where the product peak was observed at 13.28 min.

This reaction of substrate **18** was also conducted on a 1 mmol scale. For the 1 mmol scale reaction, substrate **18** (173 mg, 1 mmol, 1 equiv), CuOAc (24 mg, 0.2 mmol, 0.2 equiv), K_2CO_3 (138 mg, 1 mmol, 1 equiv), $\text{Ru}(\text{bpy})_3\text{Cl}_2 \cdot 6\text{H}_2\text{O}$ (7.4 mg, 0.01 mmol, 0.01 equiv), CF_3I (5 mmol, 5 equiv) and DMF (6 mL) were used. The reaction was conducted in a 25 mL round bottom flask. The reaction mixture was then diluted with Et_2O (40 mL), and the resulting mixture was washed with water (2 x 40 mL), saturated aqueous CaCl_2 (1 x 40 mL), and brine (1 x 40 mL) and then dried over magnesium sulfate. The solvent was removed by rotary evaporation at 0°C , and the product was purified by Kugelrohr distillation at 130°C at 10 mm Hg. The isolated product **18a** (132.0 mg, 67% yield) was 96% pure, and contained traces (4%) of the corresponding protodeboronation byproduct quinoline. Subsequent purification of this sample by column chromatography on silica gel using 2% diethyl ether in pentane as the eluent afforded **18a** as a white solid (108 mg, 55% yield). The ^1H , ^{13}C and ^{19}F NMR spectroscopic data were identical to that reported previously in the literature.⁴⁰

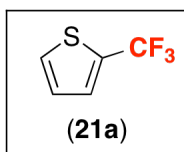


The reaction was performed on a 0.25 mmol scale using 50 mol % of CuOAc (15 mg, 0.125 mmol, 0.5 equiv) at 70 °C under otherwise identical conditions. The trifluoromethylated product **19a** was formed in 44% yield. The product showed a ^{19}F NMR signal at -63.6 ppm in DCE (lit. -64.8 ppm in CD_3CN).⁴¹ The identity of the product was further confirmed by GCMS analysis. The GC oven temperature program was as follows: 30 °C hold 6 min, ramp 20 °C/min to 250 °C, and hold for 3 min. The product peak was observed at 2.08 min.



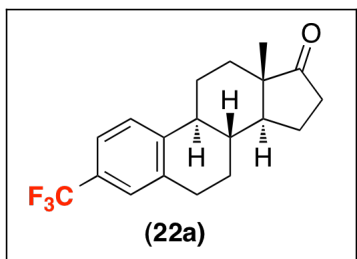
The reaction was performed on a 0.25 mmol scale using 10 mol % of CuOAc (3 mg, 0.025 mmol, 0.1 equiv) at 40 °C under otherwise identical conditions. The trifluoromethylated product **20a** was formed in 72% yield. The product showed a ^{19}F NMR signal at -64.4 ppm in DCE (lit. -64.8 ppm in CDCl_3).^{4c} The identity of the product was further confirmed by GCMS analysis, where the product peak was observed at 10.52 min.

This reaction of substrate **20** was also conducted on a 1 mmol scale. For the 1 mmol scale reaction, substrate **20** (162 mg, 1 mmol, 1 equiv), CuOAc (12 mg, 0.1 mmol, 0.1 equiv), K_2CO_3 (138 mg, 1 mmol, 1 equiv), $\text{Ru}(\text{bpy})_3\text{Cl}_2 \cdot 6\text{H}_2\text{O}$ (7.4 mg, 0.01 mmol, 0.01 equiv), CF_3I (5 mmol, 5 equiv) and DMF (6 mL) were used. The reaction was conducted in a 100 mL round bottom flask. The reaction mixture was then diluted with Et_2O (40 mL), and the resulting mixture was washed with water (2 x 40 mL), saturated aqueous CaCl_2 (1 x 40 mL), and brine (1 x 40 mL) and then dried over magnesium sulfate. The solvent was removed by rotary evaporation at 0 °C, and the product was purified by column chromatography on aluminum oxide using pentane as the eluent. Compound **20a** was isolated as a clear liquid (104.0 mg, 56% yield). The ^1H , ^{13}C and ^{19}F NMR spectroscopic data were identical to that reported previously in the literature.^{4c}



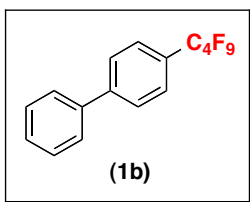
The reaction was performed on a 0.25 mmol scale using 5 mol % of CuOAc (1.5 mg, 0.0125 mmol, 0.05 equiv) under otherwise identical conditions. The trifluoromethylated product **21a** was formed in 54% yield. The product showed a ^{19}F NMR signal at -54.5 ppm in DCE (lit. $-$

55.1 ppm in CDCl₃).⁴² The identity of the product was further confirmed by GCMS analysis, where the product peak was observed at 3.43 min.



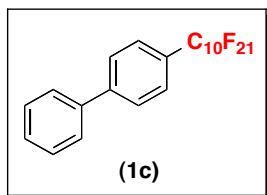
Estrone boronic acid was prepared according to literature procedure.⁴³ The reaction was performed on a 0.25 mmol scale using 50 mol % of CuOAc (6 mg, 0.125 mmol, 0.5 equiv) under otherwise identical conditions. The trifluoromethylated product **22a** was formed in 87% yield by ¹⁹F NMR spectroscopy. The reaction mixture was then diluted with ethyl acetate (20 mL), and the resulting mixture was washed with brine (3 x 30 mL) and then dried over magnesium sulfate. The solvent was removed by rotary evaporation, and the product was purified by column chromatography on silica gel using ethyl acetate/hexane 1:9 as the eluent. Compound **22a** was obtained as white crystalline solid (65.0 mg, 80% yield, mp = 146.4-147.8 °C). ¹H NMR (CDCl₃, 25 °C): δ 7.40-7.38 (m, 2H), 7.36-7.33 (m, 1H), 2.98-2.93 (m, 2H), 2.52 (dd, *J* = 19.1, 9.0 Hz, 1H), 2.47-2.42 (m, 1H), 2.37-2.30 (m, 1H), 2.20-1.96 (m, 4H), 1.70-1.44 (m, 6H), 0.92 (s, 3H). ¹³C NMR (¹H decoupled, CDCl₃, 25 °C): δ 220.59, 143.86, 137.39, 128.24 (q, *J* = 31.8 Hz), 125.92, 125.86 (q, *J* = 4.1 Hz), 124.48 (q, *J* = 272.3 Hz), 122.59 (q, *J* = 3.6 Hz), 50.63, 48.02, 44.58, 37.96, 35.95, 31.66, 29.43, 26.34, 25.76, 21.72, 13.94. ¹⁹F NMR (CDCl₃, 25 °C): δ -62.46 (s, 3F). HRMS EI (m/z): [M]⁺ calcd for C₁₉H₂₁F₃O, 322.1545; measured, 322.1542.

Perfluoroalkylation of Aryl Boronic Acids



In a glovebox, substrate **1** (49.5 mg, 0.25 mmol, 1 equiv), CuOAc (15.3 mg, 0.125 mmol, 0.5 equiv), Ru(bpy)₃Cl₂•6H₂O (1.85 mg, 0.0025 mmol, 0.01 equiv) and K₂CO₃ (35 mg, 0.25 mmol, 1 equiv) were weighed into a 20 mL vial. DMF (1.5 mL) and then C₄F₉I (215 μL, 1.25 mmol, 5 equiv) were added. The vial was sealed with a Teflon-lined cap, removed from the glove box and placed in a clear oil bath at 60 °C with two 26 W compact fluorescent light bulbs (one on either side of the vial about 5 cm away). The reaction mixture was allowed to stir for 12 h. The resulting red reaction mixture was cooled to room temperature and diluted with CH₂Cl₂ (2 mL). 1,3,5-Trifluorobenzene

(0.25 mmol, 1 equiv) was added as an internal standard, and the yield was determined to be 82% by ^{19}F NMR spectroscopy. The reaction mixture was then diluted with Et_2O (20 mL), and the resulting mixture was washed with water (3 x 20 mL) and brine (1 x 20 mL) and then dried over magnesium sulfate. The solvent was removed by rotary evaporation, and the product was purified by column chromatography on silica gel using hexane as the eluent. Compound **1b** was obtained as white crystalline solid (62.0 mg, 67% yield, mp = 50.8-51.6 °C). ^1H NMR (CDCl_3 , 25 °C): δ 7.72 (d, J = 8.0 Hz, 2H), 7.66 (d, J = 8.0 Hz, 2H), 7.62 (d, J = 8.0 Hz, 2H), 7.49 (t, J = 8.0 Hz, 2H), 7.42 (t, J = 8.0 Hz, 1H). ^{13}C NMR (^1H decoupled, CDCl_3 , 25 °C): δ 145.07, 139.79, 129.15, 128.41, 127.70 (t, J = 24.7 Hz), 127.47 (2 carbons), 127.45, 127.40, 118-109 (multiple peaks, perfluoroalkyl chain). ^{13}C NMR (^{19}F decoupled, CDCl_3 , 25 °C): δ 145.07 (m), 139.79 (m), 129.15 (dd, J = 161.8, 7.6 Hz), 128.42 (dt, J = 160.8, 7.8 Hz), 127.72 (t, J = 7.8 Hz), 128-126 (multiple overlapping peaks), 117.67, 116.06 (m), 110.51, 109.15. ^{19}F NMR (CDCl_3 , 25 °C): δ -81.03 (t, J = 9.4 Hz, 3F), -110.82 (t, J = 13.2 Hz, 2F), -122.70 (m, 2F), -125.57 (m, 2F). HRMS EI (m/z): $[\text{M}]^+$ calcd for $\text{C}_{16}\text{H}_9\text{F}_9$, 372.0561; measured, 372.0551.



In a glovebox, substrate **1** (49.5 mg, 0.25 mmol, 1 equiv), CuOAc (30.6 mg, 0.25 mmol, 1 equiv), $\text{Ru}(\text{bpy})_3\text{Cl}_2 \cdot 6\text{H}_2\text{O}$ (1.85 mg, 0.0025 mmol, 0.01 equiv) and K_2CO_3 (35 mg, 0.25 mmol, 1 equiv) and $\text{C}_{10}\text{F}_{21}\text{I}$ (193.8 mg, 0.3 mmol, 1.2 equiv) were weighed into a 20 mL vial. DMF (1.5 mL) was added. The vial was sealed with a Teflon-lined cap, removed from the glove box, and placed in a clear oil bath at 60 °C with two 26 W compact fluorescent light bulbs (one on either side of the vial about 5 cm away). The reaction mixture was allowed to stir for 12 h. The resulting red reaction mixture was cooled to room temperature and diluted with CH_2Cl_2 (2 mL). 1,3,5-Trifluorobenzene (0.25 mmol, 1 equiv) was added as an internal standard, and the yield was determined to be 80% by ^{19}F NMR spectroscopy. The reaction mixture was then diluted with Et_2O (20 mL), and the resulting mixture was washed with water (3 x 20 mL) and brine (1 x 20 mL) and then dried over magnesium sulfate. The solvent was removed by rotary evaporation, and the product was purified by column chromatography on silica gel using hexane as the eluent. Compound **1c** was obtained as white crystalline solid

(119.0 mg, 71% yield, mp = 91.4-94.8 °C). ¹H NMR (CDCl₃, 25 °C): δ 7.72 (d, *J* = 8.0 Hz, 2H), 7.66 (d, *J* = 8.0 Hz, 2H), 7.62 (d, *J* = 7.5 Hz, 2H), 7.48 (t, *J* = 8.0 Hz, 2H), 7.42 (t, *J* = 7.5 Hz, 1H). ¹³C NMR (¹H decoupled, CDCl₃, 25 °C): δ 145.08, 139.82, 129.15, 128.41, 127.87 (t, *J* = 24.8 Hz), 127.52, 127.46 (2 carbons), 127.42, 118-108 (multiple peaks, perfluoroalkyl chain). ¹³C NMR (¹⁹F decoupled, CDCl₃, 25 °C): δ 145.08 (m), 139.82 (m), 129.15 (dd, *J* = 161.8, 7.8 Hz), 128.41 (dt, *J* = 160.8, 7.3 Hz), 127.86 (t, *J* = 7.9 Hz), 128-126 (multiple overlapping peaks), 117.29, 116.21, 111.57, 111.08, 111.04, 110.96, 110.86, 110.34, 108.55. ¹⁹F NMR (CDCl₃, 25 °C): δ -80.88 (t, *J* = 9.4 Hz, 3F), -110.61 (t, *J* = 14.1 Hz, 2F), -121.25 (m, 2F), -121.80 (m, 8F), -121.96 (m, 2F), -122.76 (m, 2F), -126.19 (m, 2F). HRMS EI (m/z): [M]⁺ calcd for C₂₂H₉F₂₁, 672.0369; found, 672.0361.

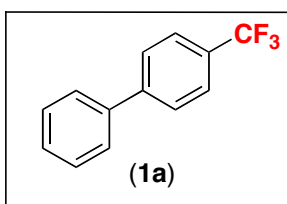
Synthesis and Characterization of Products in Scheme 2.14

Standard Procedure for Trifluoromethylation of Aryl Boronic Acids with NaSO₂CF₃/TBHP

Reaction Conditions A: To a solution of substrate (0.5 mmol, 1 equiv), CuCl (50 mg, 0.5 mmol, 1 equiv), and NaSO₂CF₃ (234 mg, 1.5 mmol, 3.0 equiv) in a mixture of MeOH/DCM/H₂O (1 mL/1 mL/0.8 mL) at 0 °C was slowly added TBHP (70% solution in water, 0.34 mL, 2.5 mmol, 5.0 equiv) with stirring. The reaction was allowed to warm to room temperature and was then stirred for 12 h. Diethyl ether (8 mL) was added, and the organic layer was extracted with saturated aqueous sodium bicarbonate (6 mL) and potassium sulfite (2 mL) solutions. The organic layers were separated and dried over MgSO₄. 1,3,5-Trifluorobenzene (0.5 mmol, 1 equiv) was added as an internal standard, and the reaction was analyzed by ¹⁹F NMR spectroscopy and GCMS. The GC oven temperature program was as follows: 40 °C hold 3 min, ramp 20 °C/min to 250 °C, and hold for 1.5 min.

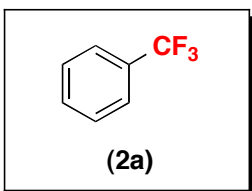
Reaction Conditions B: To a solution of substrate (0.5 mmol, 1 equiv), (MeCN)₄CuPF₆ (186.4 mg, 0.5 mmol, 1 equiv), NaHCO₃ (42 mg, 0.5 mmol, 1 equiv) and NaSO₂CF₃ (234

mg, 1.5 mmol, 3.0 equiv) in MeOH (3 mL) at 0 °C was slowly added TBHP (70% solution in water, 0.28 mL, 2.0 mmol, 4.0 equiv). The reaction was allowed to warm to room temperature and was then stirred for 12 h. Diethyl ether (8 mL) was added, and the organic layer was extracted with saturated aqueous sodium bicarbonate (6 mL) and potassium sulfite (2 mL) solutions. The organic layer was separated, and the aqueous layer was extracted with diethyl ether (3 × 8 mL). The combined organic layers were dried over MgSO₄. 1,3,5-Trifluorobenzene (0.5 mmol, 1 equiv) was added as an internal standard, and the reaction was analyzed by ¹⁹F NMR spectroscopy and GCMS. The GC oven temperature program was as follows: 40 °C hold 3 min, ramp 20 °C/min to 250 °C, and hold for 1.5 min.

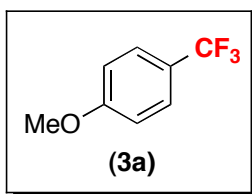


The reaction was performed using reaction condition A on a 0.5 mmol scale (substrate **1**, 99 mg). The trifluoromethylated product **1a** was formed in 95% yield as determined by ¹⁹F NMR spectroscopic analysis. After reaction workup, the solvent was removed by rotary evaporation at 0 °C, and the product was purified by column chromatography on silica gel using pentane as the eluent (*R_F* = 0.72). Compound **1a** was obtained as white crystalline solid (94 mg, 85% yield, mp = 70.2-70.8 °C; literature⁴⁴ = 70-71 °C).

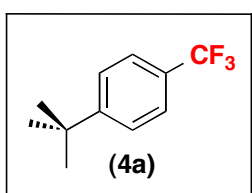
¹H NMR (CDCl₃): δ 7.73 (s, 4H), 7.63 (m, 2H), 7.51 (m, 2H), 7.45 (m, 1H). ¹³C NMR (CDCl₃): δ 144.85, 139.88, 129.48 (q, *J* = 32.5 Hz), 129.12, 128.33, 127.54, 127.40, 125.84 (q, *J* = 3.8 Hz), 124.50 (q, *J* = 272.0 Hz). ¹⁹F NMR (CDCl₃): δ -62.37 (s, 3F). HRMS EI (*m/z*): [*M*]⁺ calcd for C₁₃H₉F₃, 222.0656; measured, 222.0658.



The reaction was performed using reaction conditions A on a 0.5 mmol scale (substrate **2**, 61 mg). The trifluoromethylated product **2a** was formed in 74% yield as determined by ¹⁹F NMR spectroscopic analysis. The ¹⁹F NMR spectral data for **2a** matched that of an authentic sample (Acros, s, -62.3 ppm). The identity of the product was further confirmed by GCMS analysis, where the product peak was observed at 3.58 min.

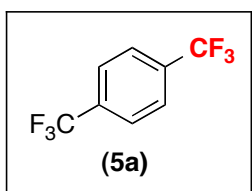


The reaction was performed using reaction conditions A on a 0.5 mmol scale (substrate **3**, 76 mg). The trifluoromethylated product **3a** was formed in 94% yield as determined by ^{19}F NMR spectroscopic analysis. The ^{19}F NMR spectral data for **3a** matched that of an authentic sample (SynQuest Labs, s, -61.0 ppm). The identity of the product was further confirmed by GCMS analysis, where the product peak was observed at 6.99 min.

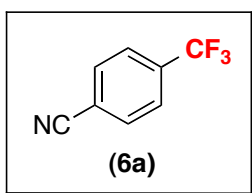


The reaction was performed using reaction conditions A on a 0.5 mmol scale (substrate **4**, 89 mg). The trifluoromethylated product **4a** was formed in 87% yield as determined by ^{19}F NMR spectroscopic analysis. After reaction workup, the solvent was removed by rotary evaporation at $0\text{ }^{\circ}\text{C}$, and the product was purified by column chromatography on silica gel using pentane as the eluent ($R_F = 0.82$). Compound **4a** was obtained as clear liquid (75 mg, 74% yield).

^1H NMR (CDCl_3): δ 7.58 (d, $J = 8.3$ Hz, 2H), 7.52 (d, $J = 8.3$ Hz, 2H), 1.37 (s, 9H). ^{13}C NMR (CDCl_3): δ 155.33, 127.95 (q, $J = 32.3$ Hz), 125.81, 125.15 (q, $J = 3.8$ Hz), 124.60 (q, $J = 271.5$ Hz), 35.10, 31.26. ^{19}F NMR (CDCl_3): δ -62.38 (s, 3F). HRMS EI (m/z): $[\text{M}]^+$ calcd for $\text{C}_{11}\text{H}_{13}\text{F}_3$, 202.0969; measured, 202.0977.



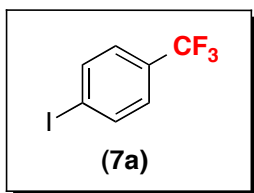
The reaction was performed using reaction conditions B on a 0.5 mmol scale (substrate **5**, 95 mg). The trifluoromethylated product **5a** was formed in 78% yield as determined by ^{19}F NMR spectroscopic analysis. The ^{19}F NMR spectral data for **5a** matched that of an authentic sample (Aldrich, s, -62.8 ppm). The identity of the product was further confirmed by GCMS analysis, where the product peak was observed at 3.50 min.



The reaction was performed using reaction conditions B on a 0.5 mmol scale (substrate **6**, 73.47 mg). The trifluoromethylated

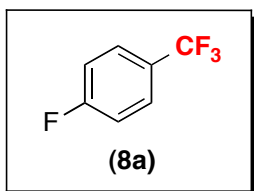
product **6a** was formed in 70% yield as determined by ^{19}F NMR spectroscopic analysis. After reaction workup, the solvent was removed by rotary evaporation at 0 °C, and the product was purified by column chromatography on silica gel using 2% diethyl ether in pentane as the eluent ($R_F = 0.24$). Compound **6a** was obtained as white crystalline solid (53 mg, 62% yield, mp = 35.2-36.4 °C; literature⁴⁵ = 35 °C).

^1H NMR (CDCl_3): δ 7.81 (d, $J = 7.9$ Hz, 2H), 7.76 (d, $J = 7.9$ Hz, 2H). ^{13}C NMR (CDCl_3): δ 134.73 (q, $J = 33.6$ Hz), 132.83, 126.34 (q, $J = 3.7$ Hz), 123.18 (q, $J = 273.1$ Hz), 117.58, 116.22. ^{19}F NMR (CDCl_3): δ -63.56 (s, 3F). HRMS EI (m/z): $[\text{M}]^+$ calcd for $\text{C}_8\text{H}_4\text{F}_3\text{N}$, 171.0296; measured, 171.0301.

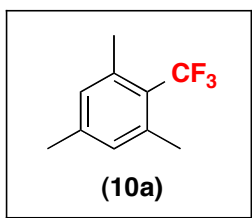


The reaction was performed using reaction conditions A on a 0.5 mmol scale (substrate **7**, 124 mg). The trifluoromethylated product **7a** was formed in 77% yield as determined by ^{19}F NMR spectroscopic analysis. After reaction workup, the solvent was removed by rotary evaporation at 0 °C, and the product was purified by column chromatography on silica gel with pentane as the eluent ($R_F = 0.88$). Compound **7a** was obtained as a colorless liquid (93 mg, 68% yield).

^1H NMR (CDCl_3): δ 7.84 (d, $J = 8.3$ Hz, 2H), 7.35 (d, $J = 8.3$ Hz, 2H). ^{13}C NMR (CDCl_3): δ 138.16, 130.28 (q, $J = 32.9$ Hz), 126.98 (q, $J = 3.8$ Hz), 124.11 (q, $J = 272.2$ Hz), 98.72. ^{19}F NMR (CDCl_3): δ -63.11 (s, 3F). HRMS EI (m/z): $[\text{M}]^+$ calcd for $\text{C}_7\text{H}_4\text{F}_3\text{I}$, 271.9310; measured, 271.9306.

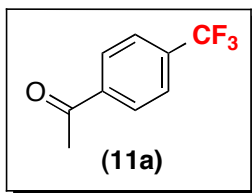


The reaction was performed using reaction conditions A on a 0.5 mmol scale (substrate **8**, 70 mg). The trifluoromethylated product **8a** was formed in 79% yield as determined by ^{19}F NMR spectroscopic analysis. The ^{19}F NMR spectral data for **8a** matched that of an authentic sample (Matrix Scientific, s, 3F, -61.6 ppm; m, F, -107.5 ppm). The identity of the product was further confirmed by GCMS analysis, where the product peak was observed at 3.40 min.



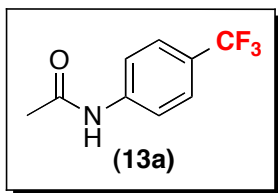
The reaction was performed using reaction conditions A on a 0.5 mmol scale (substrate **10**, 82 mg). The trifluoromethylated product **10a** was formed in 86% yield as determined by ^{19}F NMR spectroscopic analysis. After reaction workup, the solvent was removed by rotary evaporation at 0 °C, and the product was purified by column chromatography on silica gel using 2% diethyl ether in pentane as the eluent ($R_F = 0.79$). Compound **10a** was obtained as colorless liquid (66 mg, 70% yield).

^1H NMR (CDCl_3): δ 6.92 (s, 2H), 2.47 (s, 6H), 2.32 (s, 3H). ^{13}C NMR (CDCl_3): δ 141.00, 137.42 (q, $J = 1.8$ Hz), 130.99, 126.34 (q, $J = 275.7$ Hz), 124.90 (q, $J = 28.4$ Hz), 21.45 (q, $J = 4.0$ Hz), 20.97. ^{19}F NMR (CDCl_3): δ -53.74 (s, 3F). HRMS EI (m/z): $[\text{M}]^+$ calcd for $\text{C}_{10}\text{H}_{11}\text{F}_3$, 188.0813; measured, 188.0814.



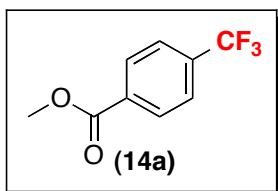
The reaction was performed using reaction conditions B on a 0.5 mmol scale (substrate **11**, 82 mg). The trifluoromethylated product **11a** was formed in 72% yield as determined by ^{19}F NMR spectroscopic analysis. After reaction workup, the solvent was removed by rotary evaporation at 0 °C, and the product was purified by column chromatography on silica gel using 3% diethyl ether in pentane as the eluent ($R_F = 0.18$). Compound **11a** was obtained as a white crystalline solid that melts at very close to room temperature (64 mg, 67% yield). The isolated product **11a** was 96% pure, and contained traces (4%) of 1-(4-chlorophenyl)ethanone, which was not easily separable by chromatography on silica gel.

^1H NMR (CDCl_3): δ 8.06 (d, $J = 8.0$ Hz, 2H), 7.73 (d, $J = 8.0$ Hz, 2H), 2.64 (s, 1H). ^{13}C NMR (CDCl_3): δ 197.11, 139.78, 134.55 (q, $J = 32.7$ Hz), 128.75, 125.81 (q, $J = 3.7$ Hz), 123.72 (q, $J = 272.8$ Hz), 26.93. ^{19}F NMR (CDCl_3): δ -63.16 (s, 3F). HRMS EI (m/z): $[\text{M}]^+$ calcd for $\text{C}_9\text{H}_7\text{F}_3\text{O}$, 188.0449; measured, 188.0451.



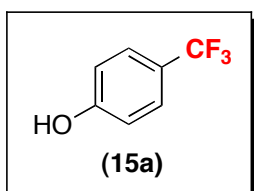
The reaction was performed using reaction conditions A on a 0.5 mmol scale (substrate **13**, 89 mg). The trifluoromethylated product **13a** was formed in 89% yield as determined by ^{19}F NMR spectroscopic analysis. After reaction workup, the solvent was removed by rotary evaporation at 0 °C, and the product was purified by column chromatography on silica gel using 50% diethyl ether in pentane as the eluent ($R_F = 0.22$). Compound **13a** was obtained as white crystalline solid (81 mg, 80% yield, mp = 151.6-152.4 °C; literature⁴⁶ = 153-155 °C).

^1H NMR (CDCl_3): δ 7.63 (d, $J = 8.7$ Hz, 1H), 7.57 (d, $J = 8.7$ Hz, 1H), 7.39 (br s, 1H), 2.21 (s, 3H). ^{13}C NMR (CDCl_3): δ 168.75, 141.03, 126.40 (q, $J = 3.5$ Hz), 126.04 (q, $J = 32.9$ Hz), 124.18 (q, $J = 271.4$ Hz), 119.47, 24.83. ^{19}F NMR (CDCl_3): δ -62.18 (s, 3F). HRMS EI (m/z): $[\text{M}]^+$ calcd for $\text{C}_9\text{H}_8\text{F}_3\text{NO}$, 203.0558; measured, 203.0558.



The reaction was performed using reaction conditions B on a 0.5 mmol scale (substrate **14**, 90 mg). The trifluoromethylated product **14a** was formed in 67% yield as determined by ^{19}F NMR spectroscopic analysis. After reaction workup, the solvent was removed by rotary evaporation at 0 °C, and the product was purified by column chromatography on silica gel using 2% diethyl ether in pentane as the eluent ($R_F = 0.32$). Compound **14a** was obtained as clear liquid (68 mg, 67% yield). The isolated product **14a** was 96% pure, and contained traces (4%) of methyl 4-chlorobenzoate, which was not easily separable by chromatography on silica gel.

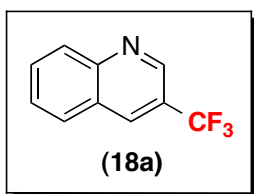
^1H NMR (CDCl_3): δ 8.14 (d, $J = 7.9$ Hz, 2H), 7.70 (d, $J = 7.9$ Hz, 2H), 3.95 (s, 3H). ^{13}C NMR (CDCl_3): δ 165.99, 134.55 (q, $J = 32.4$ Hz), 133.47, 130.10, 125.53 (q, $J = 3.8$ Hz), 123.76 (q, $J = 272.7$ Hz), 52.65. ^{19}F NMR (CDCl_3): δ -63.20 (s, 3F). HRMS EI (m/z): $[\text{M}]^+$ calcd for $\text{C}_9\text{H}_7\text{F}_3\text{O}_2$, 204.0398; measured, 204.0405.



The reaction was performed using reaction conditions A on a 0.5 mmol scale (substrate **15**, 69 mg). The trifluoromethylated product

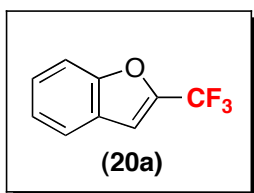
15a was formed in 93% yield as determined by ^{19}F NMR spectroscopic analysis. After reaction workup, the solvent was removed by rotary evaporation at 0 °C, and the product was purified by column chromatography on silica gel using 15% diethyl ether in pentane as the eluent ($R_F = 0.27$). Compound **15a** was obtained as white crystalline solid (68 mg, 84% yield, mp = 41.2-42.2 °C; literature⁴⁷ = 42-43 °C).

^1H NMR (CDCl_3): δ 7.51 (d, $J = 8.5$ Hz, 2H), 6.90 (d, $J = 8.5$ Hz, 2H), 5.20 (s, 1H). ^{13}C NMR (CDCl_3): δ 158.25, 127.35 (q, $J = 3.8$ Hz), 124.49 (q, $J = 271.1$ Hz), 123.37 (q, $J = 32.8$ Hz), 115.58. ^{19}F NMR (CDCl_3): δ -61.58 (s, 3F). HRMS EI (m/z): $[\text{M}]^+$ calcd for $\text{C}_7\text{H}_5\text{F}_3\text{O}$, 162.0293; measured, 162.0291.



The reaction was performed using reaction conditions B on a 0.5 mmol scale (substrate **18**, 86.5 mg). The trifluoromethylated product **18a** was formed in 58% yield as determined by ^{19}F NMR spectroscopic analysis. After reaction workup, the solvent was removed by rotary evaporation at 0 °C, and the product was purified by column chromatography on silica gel using 2% diethyl ether in pentane as the eluent ($R_F = 0.12$). Compound **18a** was obtained as white crystalline solid (54 mg, 55% yield, mp = 43.4-44.0 °C; literature^{4e} = 42-43 °C).

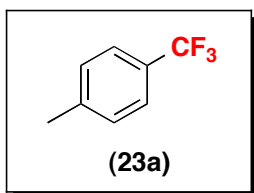
^1H NMR (CDCl_3): δ 9.11 (s, 1H), 8.45 (s, 1H), 8.19 (d, $J = 8.5$ Hz, 1H), 7.93 (d, $J = 8.5$ Hz, 1H), 7.86 (ddd, $J = 8.5, 6.8, 1.4$ Hz, 1H), 7.67 (dd, $J = 8.3, 6.8$ Hz, 1H). ^{13}C NMR (CDCl_3): δ 149.52, 146.18, 134.08 (q, $J = 4.2$ Hz), 131.90, 129.79, 128.74, 128.14, 126.42, 123.83 (q, $J = 272.3$ Hz), 123.76 (q, $J = 32.8$ Hz). ^{19}F NMR (CDCl_3): δ -61.83 (s, 3F). HRMS EI (m/z): $[\text{M}+\text{H}]^+$ calcd for $\text{C}_{10}\text{H}_7\text{F}_3\text{N}$, 198.0525; measured, 198.0524.



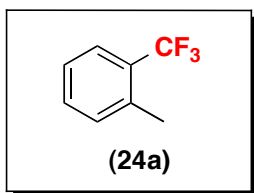
The reaction was performed using reaction conditions A on a 0.5 mmol scale (substrate **20**, 81 mg). The trifluoromethylated product **20a** was formed in 89% yield as determined by ^{19}F NMR spectroscopic analysis. After reaction workup, the solvent was removed by rotary evaporation at 0 °C, and the product was purified by column

chromatography on silica gel using pentane as the eluent ($R_F = 0.69$). Compound **20a** was obtained as colorless liquid (72 mg, 78% yield).

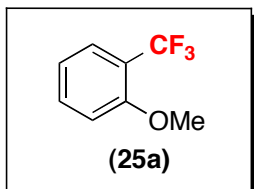
^1H NMR (CDCl_3): δ 7.67 (d, $J = 7.9$ Hz, 1H), 7.58 (d, $J = 8.4$ Hz, 1H), 7.45 (m, 1H), 7.34 (m, 1H), 7.17 (s, 1H). ^{13}C NMR (CDCl_3): δ 155.30, 143.64 (q, $J = 42.1$ Hz), 127.08, 126.16, 124.13, 122.64, 119.48 (q, $J = 267.9$ Hz), 112.26, 108.27 (q, $J = 3.1$ Hz). ^{19}F NMR (CDCl_3): δ -67.44 (s, 3F). HRMS EI (m/z): $[\text{M}]^+$ calcd for $\text{C}_9\text{H}_5\text{F}_3\text{O}$, 186.0292; measured, 186.0301.



The reaction was performed using reaction conditions A on a 0.5 mmol scale (substrate **23**, 68 mg). The trifluoromethylated product **23a** was formed in 86% yield as determined by ^{19}F NMR spectroscopic analysis. The ^{19}F NMR spectral data for **23a** matched that of an authentic sample (Alfa Aesar, s, -61.73 ppm). The identity of the product was further confirmed by GCMS analysis, where the product peak was observed at 5.20 min.

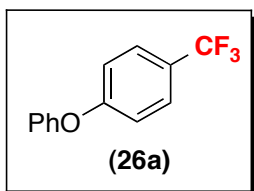


The reaction was performed using reaction condition A on a 0.5 mmol scale (substrate **24**, 68 mg). The trifluoromethylated product **24a** was formed in 95% yield as determined by ^{19}F NMR spectroscopic analysis. The ^{19}F NMR spectral data for **24a** matched that of an authentic sample (Matrix Scientific, s, -61.45 ppm). The identity of the product was further confirmed by GCMS analysis, where the product peak was observed at 5.22 min.



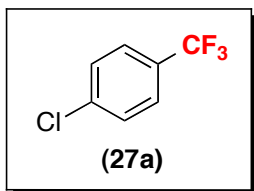
The reaction was performed using reaction conditions A on a 0.5 mmol scale (substrate **25**, 76 mg). The trifluoromethylated product **25a** was formed in 93% yield as determined by ^{19}F NMR spectroscopic analysis. The ^{19}F NMR spectral data for **25a** matched that of an authentic sample (Alfa Aesar, s, -62.5 ppm).

The identity of the product was further confirmed by GCMS analysis, where the product peak was observed at 7.24 min.

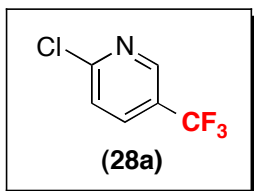


The reaction was performed using reaction conditions A on a 0.5 mmol scale (substrate **26**, 107 mg). The trifluoromethylated product **26a** was formed in 92% yield as determined by ^{19}F NMR spectroscopic analysis. After reaction workup, the solvent was removed by rotary evaporation at 0 °C, and the product was purified by column chromatography on silica gel using pentane as the eluent ($R_F = 0.63$). Compound **26a** was obtained as clear liquid (105 mg, 88% yield).

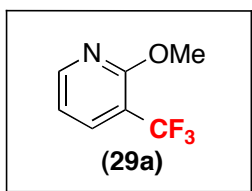
^1H NMR (CDCl_3): δ 7.59 (d, $J = 8.7$ Hz, 2H), 7.41 (m, 2H), 7.21 (m, 1H), 7.06 (m, 4H).
 ^{13}C NMR (CDCl_3): δ 160.67, 155.86, 130.21, 127.25 (q, $J = 3.8$ Hz), 124.98 (q, $J = 32.7$ Hz), 124.48, 124.37 (q, $J = 271.4$ Hz), 120.08, 117.99. ^{19}F NMR (CDCl_3): δ -61.77 (s, 3F). HRMS EI (m/z): $[\text{M}]^+$ calcd for $\text{C}_{13}\text{H}_9\text{F}_3\text{O}$, 238.0606; measured, 238.0611.



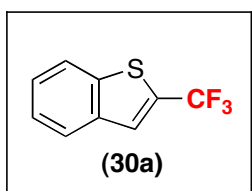
The reaction was performed using reaction conditions A on a 0.5 mmol scale (substrate **27**, 78.18 mg). The trifluoromethylated product **27a** was formed in 68% yield as determined by ^{19}F NMR spectroscopic analysis. The ^{19}F NMR spectral data for **27a** matched that of an authentic sample (AK Scientific, Inc., s, -62.02 ppm). The identity of the product was further confirmed by GCMS analysis, where the product peak was observed at 5.73 min.



The reaction was performed using reaction conditions B on a 0.5 mmol scale (substrate **28**, 78.68 mg). The trifluoromethylated product **28a** was formed in 85% yield as determined by ^{19}F NMR spectroscopic analysis. The ^{19}F NMR spectral data for **28a** matched that of an authentic sample (Matrix Scientific, s, -61.72 ppm). The identity of the product was further confirmed by GCMS analysis, where the product peak was observed at 6.06 min.

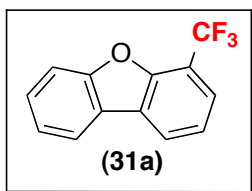


The reaction was performed using reaction conditions A on a 0.5 mmol scale (substrate **29**, 76.5 mg). The trifluoromethylated product **29a** was formed in 96% yield as determined by ^{19}F NMR spectroscopic analysis. The ^{19}F NMR spectral data for **29a** matched that of an authentic sample (Matrix Scientific, s, -63.19 ppm). The identity of the product was further confirmed by GCMS analysis, where the product peak was observed at 6.44 min.



The reaction was performed using reaction conditions A on a 0.5 mmol scale (substrate **30**, 89 mg). The trifluoromethylated product **30a** was formed in 84% yield as determined by ^{19}F NMR spectroscopic analysis. After reaction workup, the solvent was removed by rotary evaporation at $0\text{ }^{\circ}\text{C}$, and the product was purified by column chromatography on silica gel using pentane as the eluent ($R_{\text{F}} = 0.69$). Compound **30a** was obtained as white crystalline solid (78 mg, 77% yield, mp = $53.5\text{-}54.0\text{ }^{\circ}\text{C}$; literature^{4e} = $52\text{-}53\text{ }^{\circ}\text{C}$).

^1H NMR (CDCl_3): δ 7.93 – 7.81 (multiple peaks, 2H), 7.70 (s, 1H), 7.54-7.40 (multiple peaks, 2H). ^{13}C NMR (CDCl_3): δ 140.28, 137.88, 131.39 (q, $J = 38.2$ Hz), 126.70, 125.78 (q, $J = 4.2$ Hz), 125.35, 125.24, 122.69 (q, $J = 269.4$ Hz), 122.75. ^{19}F NMR (CDCl_3): δ -56.32 (s, 3F). HRMS EI (m/z): $[\text{M}]^+$ calcd for $\text{C}_9\text{H}_5\text{F}_3\text{S}$, 202.0064; measured, 202.0063.



The reaction was performed using reaction conditions A on a 0.5 mmol scale (substrate **31**, 106 mg). The trifluoromethylated product **31a** was formed in 92% yield as determined by ^{19}F NMR spectroscopic analysis. After reaction workup, the solvent was removed by rotary evaporation at $0\text{ }^{\circ}\text{C}$, and the product was purified by column chromatography on silica gel using pentane as the eluent ($R_{\text{F}} = 0.54$). Compound **31a** was obtained as white crystalline solid (102 mg, 86% yield, mp = $56.8\text{-}57.6\text{ }^{\circ}\text{C}$).

^1H NMR (CDCl_3): δ 8.09 (d, $J = 7.7$ Hz, 1H) 7.94 (d, $J = 7.7$ Hz, 1H), 7.69 (m, 1H), 7.64 (s, 1H), 7.52 (m, 1H), 7.40 (m, 2H). ^{13}C NMR (CDCl_3): δ 156.58, 152.19 (q, $J = 1.8$ Hz), 128.30, 126.15, 124.51, 124.07 (q, $J = 4.5$ Hz), 123.56, 123.43 (d, $J = 272.1$ Hz), 123.10, 122.51, 120.90, 115.13 (q, $J = 34.0$ Hz), 112.31. ^{19}F NMR (CDCl_3): δ -61.02 (s, 3F). HRMS EI (m/z): $[\text{M}]^+$ calcd for $\text{C}_{13}\text{H}_7\text{F}_3\text{O}$, 236.0449; measured, 236.0451.

2.8 References

1. (a) Schlosser, M. *Angew. Chem., Int. Ed.* **2006**, *45*, 5432; (b) Müller, K.; Faeh, C.; Diederich, F. *Science* **2007**, *317*, 1881; (c) Hagmann, W. K. *J. Med. Chem.* **2008**, *51*, 4359; (d) Kirk, K. L. *Org. Process Res. Dev.* **2008**, *12*, 305; (e) Purser, S.; Moore, P. R.; Swallow, S.; Gouverneur, V. *Chem. Soc. Rev.* **2008**, *37*, 320; (f) Tomashenko, O. A.; Grushin, V. V. *Chem. Rev.* **2011**, *111*, 4475; (g) Roy, S.; Gregg, B. T.; Gribble, G. W.; Le, V. D. *Tetrahedron* **2011**, *67*, 2161.
2. (a) Grushin, V. V.; Marshall, W. J. *J. Am. Chem. Soc.* **2006**, *128*, 4632; (b) Grushin, V. V.; Marshall, W. J. *J. Am. Chem. Soc.* **2006**, *128*, 12644; (c) Grushin, V. V. *Acc. Chem. Res.* **2010**, *43*, 160; (d) Ye, Y.; Ball, N. D.; Kampf, J. W.; Sanford, M. S. *J. Am. Chem. Soc.* **2010**, *132*, 14682; (e) Ball, N. D.; Gary, J. B.; Ye, Y.; Sanford, M. S. *J. Am. Chem. Soc.* **2011**, *133*, 7577.
3. (a) Wang, X.; Truesdale, L.; Yu, J.-Q. *J. Am. Chem. Soc.* **2010**, *132*, 3648; (b) Cho, E. J.; Senecal, T. D.; Kinzel, T.; Zhang, Y.; Watson, D. A.; Buchwald, S. L. *Science* **2010**, *328*, 1679; (c) Mu, X.; Chen, S.; Zhen, X.; Liu, G. *Chem. –Eur. J.* **2011**, *17*, 6039; (d) Loy, R. N.; Sanford, M. S. *Org. Lett.* **2011**, *13*, 2548; (e) Mu, X.; Wu, T.; Wang, H.-Y.; Guo, Y.-L.; Liu, G. *J. Am. Chem. Soc.* **2011**, *134*, 878.
4. (a) Dubinina, G. G.; Furutachi, H.; Vicic, D. A. *J. Am. Chem. Soc.* **2008**, *130*, 8600; (b) Dubinina, G. G.; Ogikubo, J.; Vicic, D. A. *Organometallics* **2008**, *27*, 6233; (c) Chu, L.; Qing, F.-L. *Org. Lett.* **2010**, *12*, 5060; (d) McReynolds, K. A.; Lewis, R. S.; Ackerman, L. K. G.; Dubinina, G. G.; Brennessel, W. W.; Vicic, D. A. *J. Fluorine Chem.* **2010**, *131*, 1108; (e) Senecal, T. D.; Parsons, A. T.; Buchwald, S. L. *J. Org. Chem.* **2011**, *76*, 1174; (f) Zhang, C. P.; Wang, Z. L.; Chen, Q. Y.; Zhang, C. T.; Gu, Y. C.; Xiao, J. C. *Angew. Chem., Int. Ed.* **2011**, *50*, 1896; (g) Tomashenko, O. A.; Escudero, E. C.; Belmonte, M. M.; Grushin, V. V. *Angew. Chem., Int. Ed.* **2011**, *50*, 7655; (h) Morimoto, H.; Tsubogo, T.; Litvinas, N. D.; Hartwig, J. F. *Angew. Chem., Int. Ed.* **2011**, *50*, 3793; (i) Litvinas, N. D.; Fier, P. S.; Hartwig, J. F. *Angew. Chem., Int. Ed.* **2012**, *51*, 536; (j) Zanardi, A.; Novikov, M. A.; Martin, E.; Benet-Buchholz, J.; Grushin, V. V. *J. Am. Chem. Soc.* **2011**, *133*, 20901; (k) Kremlev, M. M.; Mushta, A. I.; Tyrta, W.; Yagupolskii, Y. L.; Naumann, D.; Möller, A. *J. Fluorine Chem.* **2012**, *133*, 67; (l) Khan, B. A.; Buba, A. E.; Goßen, L. J. *Chem. Eur. J.* **2012**, *18*, 1577.
5. (a) Oishi, M.; Kondo, H.; Amii, H. *Chem. Commun.* **2009**, 1909; (b) Shimizu, R.; Egami, H.; Nagi, T.; Chae, J.; Hamashima, Y.; Sodeoka, M. *Tetrahedron Lett.* **2010**, *51*, 5947; (c) Knauber, T.; Arikan, F.; G, R.; Goossen, L. J. *Chem. Eur. J.* **2011**, *17*, 2689; (d) Xu, J.; Luo, D.-F.; Xiao, B.; Liu, Z.-J.; Gong, T.-J.; Fu, Y.; Liu, L. *Chem. Commun.* **2011**, *47*, 4300; (e) Liu, T.; Shen, Q. *Org. Lett.* **2011**, *13*, 2342; (f) Li, Y. C., T.; Wang, H.; Zhang, R.; Jin, K.; Wang, X.; Duan, C. *Synlett* **2011**, *12*, 1713; (g) Liu, T.; Shao, X.; Wu, Y.; Shen, Q. *Angew. Chem., Int. Ed.* **2012**, *51*, 540; (h) Chu, L.; Qing, F.-L. *J. Am. Chem. Soc.* **2011**, *134*, 1298; (i) Jiang, X.; Chu, L.; Qing, F.-L. *J. Org. Chem.* **2012**, *77*, 1251.
6. (a) Akiyama, T.; Kato, K.; Kajitani, M.; Sakaguchi, Y.; Nakamura, J.; Hayashi, H.; Sugimori, A. *Bull. Chem. Soc. Jpn.* **1988**, *61*, 3531; (b) McClinton, M. A.; McClinton, D. A. *Tetrahedron* **1992**, *48*, 6555.
7. (a) Sawada, H.; Nakayama, M. *J. Fluorine Chem.* **1990**, *46*, 423; (b) Kino, T.; Nagase, Y.; Ohtsuka, Y.; Yamamoto, K.; Uraguchi, D.; Tokuhisa, K.; Yamakawa, T. *J. Fluorine Chem.* **2010**, *131*, 98.

8. (a) Nagib, D. A.; Scott, M. E.; MacMillan, D. W. C. *J. Am. Chem. Soc.* **2009**, *131*, 10875; (b) Pham, P. V.; Nagib, D. A.; MacMillan, D. W. C. *Angew. Chem. Int. Ed.* **2011**, *50*, 6119.
9. Nagib, D. A.; MacMillan, D. W. C. *Nature* **2011**, *480*, 224.
10. Langlois, B. R.; Laurent, E.; Roidot, N. *Tetrahedron Lett.* **1991**, *32*, 7525.
11. Ji, Y.; Brueckl, T.; Baxter, R. D.; Fujiwara, Y.; Seiple, I. B.; Su, S.; Blackmond, D. G.; Baran, P. S. *Proc. Natl. Acad. Sci. USA* **2011**, *108*, 14411.
12. Ye, Y.; Sanford, M. S. *J. Am. Chem. Soc.* **2012**, *134*, 9034.
13. Ye, Y.; Künzi, S. A.; Sanford, M. S. *Org. Lett.* **2012**, *14*, 4979.
14. The trifluoromethylated products that are liquids were isolated via Kugelrohr distillation. This isolation procedure typically afforded $\geq 95\%$ pure products (contaminated with traces of protodeboronated material). In many cases (eg, **6a**, **9a**, **18a**, **20a**) $>98\%$ pure products could be obtained via subsequent careful purification by column chromatography, albeit in reduced yields.
15. Hassan, J.; Sévignon, M.; Gozzi, C.; Schulz, E.; Lemaire, M. *Chem. Rev.* **2002**, *102*, 1359.
16. Top Pharmaceuticals Poster Njardarson Group. [http://cbc.arizona.edu/njardarson/group/sites/default/files/Top 200 Pharmaceutical Products by US Retail Sales in 2011_small_0.pdf](http://cbc.arizona.edu/njardarson/group/sites/default/files/Top%20Pharmaceutical%20Products%20by%20US%20Retail%20Sales%20in%202011_small_0.pdf) (accessed Mar. 1st, 2013)
17. The observation that Cu^I salts generally perform better than Cu^{II} salts in this transformation is consistent with this proposal.
18. Campagna, S. P., F.; Nastasi, F.; Bergamini, G.; Balzani, V. *Top. Curr. Chem.* **2007**, *280*, 117.
19. Inorganic Chemistry, 3rd ed.; Housecroft, C. E.; Sharpe, A. G.; Pearson Education: Harlow, England, 2008.
20. (a) Andrieux, C. P. G., L.; Médebielle, M.; Pinson, J.; Saveant, J. M. *J. Am. Chem. Soc.* **1990**, *112*, 3509; (b) Bonesi, S. M. E.-B., R. *J. Chem. Soc., Perkin Trans. 2* **2000**, 1583.
21. The order of steps ii and iii in **Scheme 2.14** could also easily be reversed. Without detailed evidence about the resting state of the Cu-catalyst, we cannot draw definitive conclusions about the species most likely to react with CF₃•.
22. For products **11a** and **14a**, the isolated material contained ~4% of the corresponding chloroarene as an inseparable by-product.
23. Kalyani, D.; McMurtrey, K. B.; Neufeldt, S. R.; Sanford, M. S. *J. Am. Chem. Soc.* **2011**, *133*, 18566.
24. Li, Y.; Wu, L.; Neumann, H.; Beller, M. *Chem. Commun.* **2013**, *49*, 2628.
25. Li, Z.; Cui, Z.; Liu, Z.-Q. *Org. Lett.* **2013**, *15*, 406.
26. Parsons, A. T.; Senecal, T. D.; Buchwald, S. L. *Angew. Chem., Int. Ed.* **2012**, *51*, 2947.
27. Fier, P. S.; Hartwig, J. F. *J. Am. Chem. Soc.* **2012**, *134*, 5524.
28. Cho, E. J.; Buchwald, S. L. *Org. Lett.* **2011**, *13*, 6552.
29. He, Z.; Luo, T.; Hu, M.; Cao, Y.; Hu, J. *Angew. Chem., Int. Ed.* **2012**, *51*, 3944.
30. Janson, P. r. G.; Ghoneim, I.; Ilchenko, N. O.; Szabó, K. l. n. *J. Org. Lett.* **2012**, *14*, 2882.
31. Yasu, Y.; Koike, T.; Akita, M. *Angew. Chem. Int. Ed.* **2012**, *51*, 9567.
32. Zhu, R.; Buchwald, S. L. *J. Am. Chem. Soc.* **2012**, *134*, 12462.

33. Yasu, Y.; Koike, T.; Akita, M. *Chem. Commun.* **2013**, *49*, 2037.
34. Current price of NaTFA = \$104/mol, KTFA = \$167/mol, and CF₃H = \$179/mol. Determined based on the largest quantity of each reagent available from Sigma-Aldrich on March 22, 2013.
35. (a) Matsui, K.; Tobita, E.; Ando, M.; Kondo, K. *Chem. Lett.* **1981**, *10*, 1719; (b) Carr, G. E.; Chambers, R. D.; Holmes, T. F.; Parker, D. G. *J. Chem. Soc., Perkin Trans. I* **1988**, 921; (c) Chang, Y.; Cai, C. *J. Fluorine Chem.* **2005**, *126*, 937; (d) Chang, Y.; Cai, C. *J. Fluorine Chem.* **2005**, *46*, 3161.
36. Depecker, C.; Marzouk, H.; Trevin, S.; Devynck, J. *New J. Chem.* **1999**, *23*, 739.
37. Lai, C.; Mallouk, T. E. *J. Chem. Soc., Chem. Commun.* **1993**, 1359.
38. Tanabe, Y.; Matsuo, N.; Ohno, N. *J. Org. Chem.* **1988**, *53*, 4582.
39. Stavber, S.; Zupan, M. *J. Org. Chem.* **1983**, *48*, 2223.
40. Zhang, C.-P.; Cai, J.; Zhou, C.-B.; Wang, X.-P.; Zheng, X.; Gu, Y.-C.; Xiao, J.-C. *Chem. Commun.* **2011**, *47*, 9516.
41. Naumann, D.; Kischkewitz, J. r. *J. Fluorine Chem.* **1990**, *46*, 265.
42. Knauber, T.; Arikan, F.; Röschenthaler, G.-V.; Gooßen, L. *J. Chem. Eur. J.* **2011**, *17*, 2689.
43. (a) Furuya, T.; Strom, A. E.; Ritter, T. *J. Am. Chem. Soc.* **2009**, *131*, 1662; (b) Ahmed, V.; Liu, Y.; Silvestro, C.; Taylor, S. D. *Bioorg. Med. Chem.* **2006**, *14*, 8564.
44. Han, W.; Liu, C.; Jin, Z.-L. *Organic Letters* **2007**, *9*, 4005.
45. Hatsuda, M.; Seki, M. *Tetrahedron* **2005**, *61*, 9908.
46. Wang, X.-J.; Yang, Q.; Liu, F.; You, Q.-D. *Synth. Commun.* **2008**, *38*, 1028.
47. Sergeev, A. G.; Schulz, T.; Torborg, C.; Spannenberg, A.; Neumann, H.; Beller, M. *Angew. Chem. Int. Ed.* **2009**, *48*, 7595.

CHAPTER 3

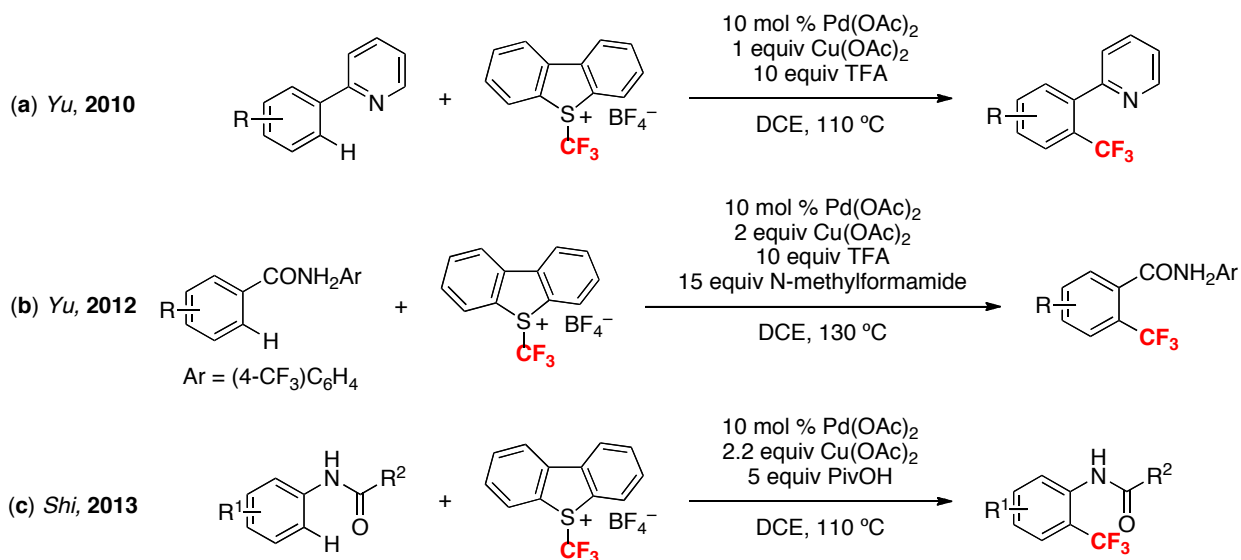
Ag-Mediated Aromatic Trifluoromethylation

3.1 Background

Despite substantial progress in this field of Cu^{1,2} and Pd^{3,4}-based trifluoromethylation, current protocols still have significant limitations. In many cases, expensive “CF₃⁺”,^{1f,2b,d,e,4a} or “CF₃⁻” precursors are required.^{2a,7b} Other methods involve harsh reaction conditions, such as temperatures greater than 100 °C.^{1d,3b,4a,b} In addition, most research efforts have focused on a transition metal catalyzed/mediated cross-coupling strategy, which require substrate prefunctionalization.

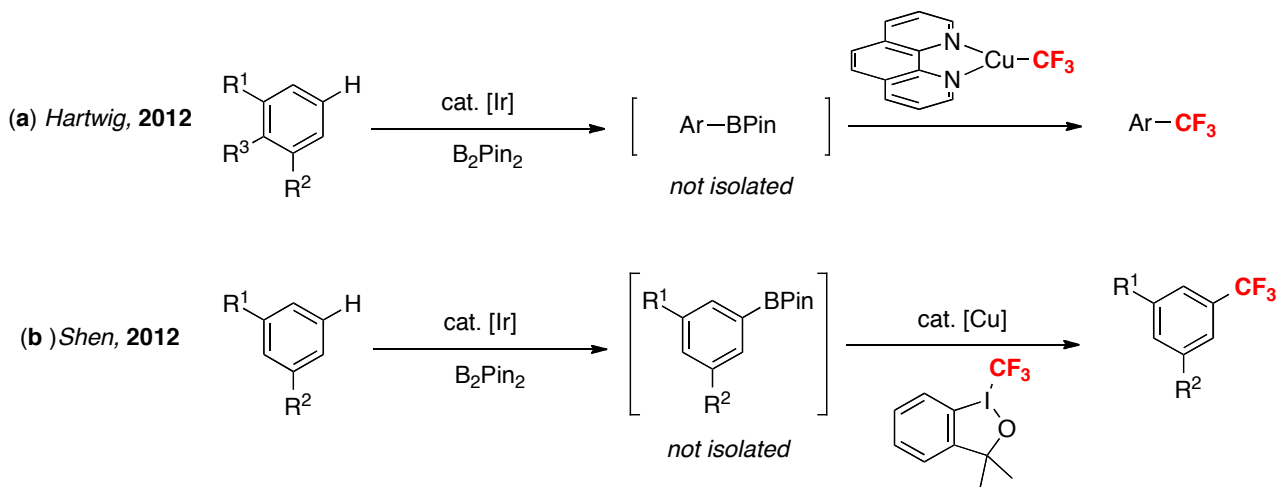
Transition metal catalyzed/mediated direct C–H trifluoromethylation would alleviate the need for pre-functionalized substrates. However, this area also presents significant challenges. In 2010, the Yu group demonstrated the first Pd-catalyzed *ortho*-trifluoromethylation of arenes bearing a nitrogen-based directing group using the Umemoto reagent (**Scheme 3.1a**) (for more discussion of the mechanism of this transformation, see **Chapter 4**).^{4a} Further exploration of this strategy by Yu^{4e} and Shi^{4f} revealed that *N*-arylbenzamides and acetanilides are both viable substrates under similar conditions (**Scheme 3.1b,c**). Both results represent remarkable advances in the field of Pd-catalyzed C–H functionalization, since *N*-arylbenzamides and acetanilides are readily accessible from aromatic carboxylic acids and anilines, and more importantly, could be used as synthetic handles for further functionalization.

Scheme 3.1. Pd-Catalyzed C–H *ortho*-Trifluoromethylation



C–H trifluoromethylation can also be achieved in an indirect fashion, namely through initial C–H functionalization, followed by a second transition-metal catalyzed/mediated cross-coupling reaction. For example, Hartwig^{5a} and Shen^{5b} reported the selective trifluoromethylation of 1,3-disubstituted arenes through a sequence of Ir-catalyzed borylation and subsequent trifluoromethylation (**Scheme 3.2**). Several examples of Pd-catalyzed C–H trifluoromethylation of reactive heterocyclic substrates have also been reported in the literature.⁶

Scheme 3.2. Trifluoromethylation of Aryl–H or Aryl–Br through Arene Borylation



In addition, non-metal mediated free-radical approaches are available for direct arene trifluoromethylation.^{7,8} Despite enabling direct C–H trifluoromethylation of non-prefunctionalized substrates, most current CF₃•-based methods are limited because they require inconvenient electrochemical or photochemical activation procedures^{7b,d,e} or utilize potentially explosive reagents like peroxides at elevated temperatures.^{7c,g} It was not until very recently that several practical, mild and versatile radical trifluoromethylation approaches were reported by Baran, MacMillan, and Cho.⁹ A detailed discussion of these novel strategies can be found in **Chapter 2**.

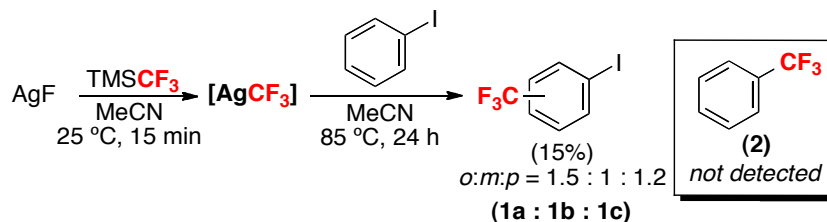
One of our long-term goals was to address the challenges associated with Pd and Cu-based trifluoromethylation by identifying novel transition metal systems that could promote this transformation. Our initial efforts focused on Ag for several reasons. First, Ag^I has the same electronic configuration as Cu^I, which suggests the possibility for similar reactivity. Secondly, Ag has been used for promoting other related organometallic reactions.¹⁰ Finally, despite several recent reports on the synthesis of AgCF₃, this reagent's reactivity is rarely discussed.^{11,12}

In this chapter, we discuss the development, scope, and mechanism of a mild C–H trifluoromethylation protocol using a combination of AgOTf, KF, and TMSCF₃.

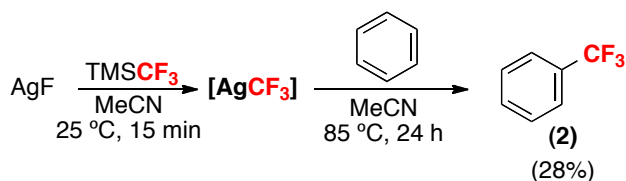
3.2 Reaction Optimization

CuCF₃ complexes are well-known to react with aryl iodides to afford benzotrifluoride products.¹ Thus, we first sought to examine the reactivity of AgCF₃ with PhI (**Scheme 3.3**). AgCF₃ was generated *in situ* from the reaction of AgF with TMSCF₃ in MeCN for 15 min at 25 °C using the procedure of Tyrra and Naumann.¹¹ PhI (20 equiv) was then added, and the reaction was heated at 85 °C for 24 h. ¹⁹F NMR spectroscopic analysis of the crude reaction mixture did not show the presence of PhCF₃. Instead, three isomeric C–H trifluoromethylation products were observed in 15% total yield based on TMSCF₃ (*o* : *m* : *p* ratio = 1.5 : 1 : 1.2). This result clearly demonstrates the orthogonal reactivity of AgCF₃ and CuCF₃ reagents with aryl–H versus aryl–I bonds. Conducting this same procedure with benzene in place of PhI afforded the C–H trifluoromethylation product PhCF₃ in 28% yield (**Scheme 3.4**).

Scheme 3.3. Reaction of AgCF₃ with PhI

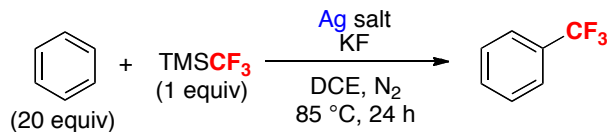


Scheme 3.4. Reaction of AgCF₃ with Benzene



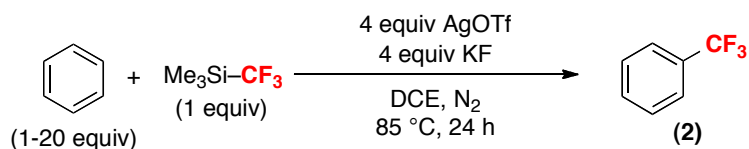
This Ag-mediated C–H trifluoromethylation reaction was optimized using benzene (20 equiv) as the substrate and DCE as the solvent. Since this is a net $2e^-$ oxidation reaction (where Ag^I is presumably acting as the terminal oxidant), our optimization studies began with 2 equiv of various Ag^I salts. As shown in **Table 3.1**, the use of 2 equiv of AgF, AgNO₃, or AgOTf in the presence of 2 equiv of KF afforded trifluorotoluene in modest yield, with AgOTf providing the best result (entries 3-5). When 1 equiv of AgOTf/KF was used, trifluorotoluene was obtained in only 22% yield. AgOAc and Ag₂O generated <10% product under analogous conditions (entries 1 and 2). Moving from 2 equiv to 4 equiv of AgOTf/KF improved the yield from 68 to 87% (entries 5 and 6). Importantly, KF is required for the AgOTf reaction (entry 7), presumably to activate the TMSCF₃.

The use of a large excess of substrate (20 equiv) typically led to higher conversion to the desired CF₃ product; however, excess substrate is not required for this transformation. When the reaction was conducted with 1 equiv of benzene in the presence of 5 equiv TMSCF₃ under otherwise identical conditions, trifluorotoluene was formed in 53% yield (entry 8). Smaller excess amount of substrates (1, 5, or 10 equiv) were also evaluated for this conversion, and the yields are shown in **Table 3.2**.

Table 3.1. Optimization of Trifluoromethylation Reaction^{[a][b]}

entry	metal salt (equiv)	KF equiv	yield (%)
1	AgOAc (2)	2	6
2	Ag ₂ O (2)	2	6
3	AgNO ₃ (2)	2	40
4	AgF (2)	2	45
5	AgOTf (2)	2	68
6	AgOTf (4)	4	87
7 ^[c]	AgOTf (4)	0	0
8 ^[d]	AgOTf (4)	4	53

^[a]General conditions: C₆H₆ (20 equiv), TMSCF₃ (1 equiv) in DCE at 85 °C for 24 h. ^[b]Yields determined by ¹⁹F NMR analysis. ^[c]No KF. ^[d]Conditions: C₆H₆ (1 equiv), TMSCF₃ (5 equiv), AgOTf (4 equiv), KF (4 equiv) in DCE at 85 °C for 24 h.

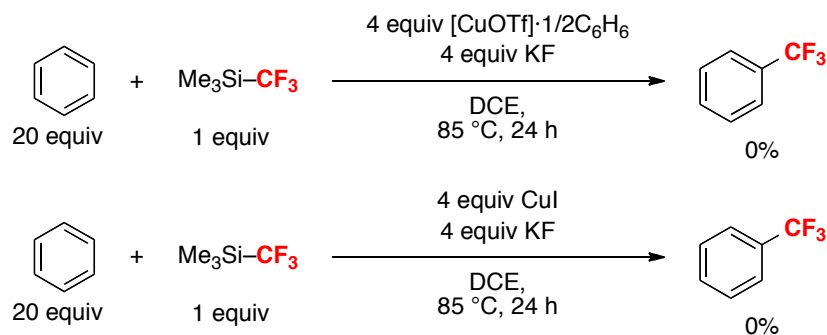
Table 3.2. Trifluoromethylation of Benzene with Different Equivalent of Benzene

entry	C ₆ H ₆ (equiv)	yield (%)
1	1	17
2	5	49
3	10	75
4	20	87

^[a]General conditions: C₆H₆ (1-20 equiv), TMSCF₃ (1 equiv), AgOTf (4 equiv), KF (4 equiv) in DCE at 85 °C for 24 h.

Finally, we examined the reactivity of Cu^I salts such as [CuOTf]·1/2C₆H₆ and CuI under our optimal conditions. As shown in **Scheme 3.5**, they provided none of the C–H trifluoromethylation product, again highlighting the complementarity of this Ag-based method versus more traditional Cu-mediated trifluoromethylation approaches.

Scheme 3.5. Reaction of CuCF₃ with Benzene

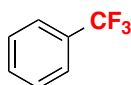
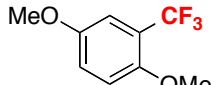
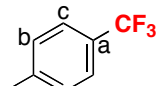
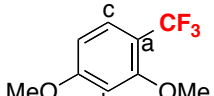
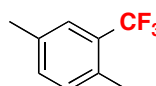
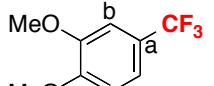
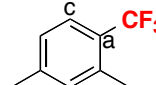
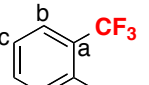
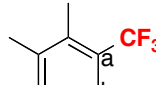
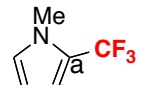
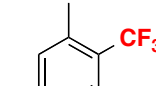
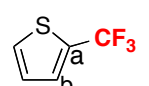
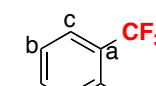
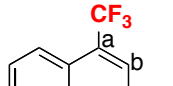


The final optimized conditions (20 equiv of benzene, 4 equiv of AgOTf and KF, 1 equiv of TMSCF₃ at 85 °C for 24 h) were readily scalable, affording trifluorotoluene in 87%, 84%, and 87% yield on 0.08, 0.5, and 1 mmol scales, respectively.

3.3 Substrate Scope

This Ag-mediated C–H trifluoromethylation reaction was applicable to a variety of different arene substrates. As shown in **Table 3.3**, arenes bearing electron-donating alkyl or alkoxy substituents reacted in good to excellent yield (entries 1-10). In general, these transformations proceeded with a modest preference for trifluoromethylation at C–H sites *ortho* and *para* to the electron-donating alkyl and alkoxy groups. Heterocycles like *N*-methyl pyrrole and thiophene were also good substrates for C–H trifluoromethylation and reacted with moderate to excellent selectivity at C2 (entries 12 and 13). Under the optimal conditions PhI afforded a mixture of the *o*, *m*, and *p*-trifluoromethylated isomers in 46% total yield (entry 11). The trifluoromethylation of naphthalene proceeded in good yield with modest selectivity for the α -position (entry 14).

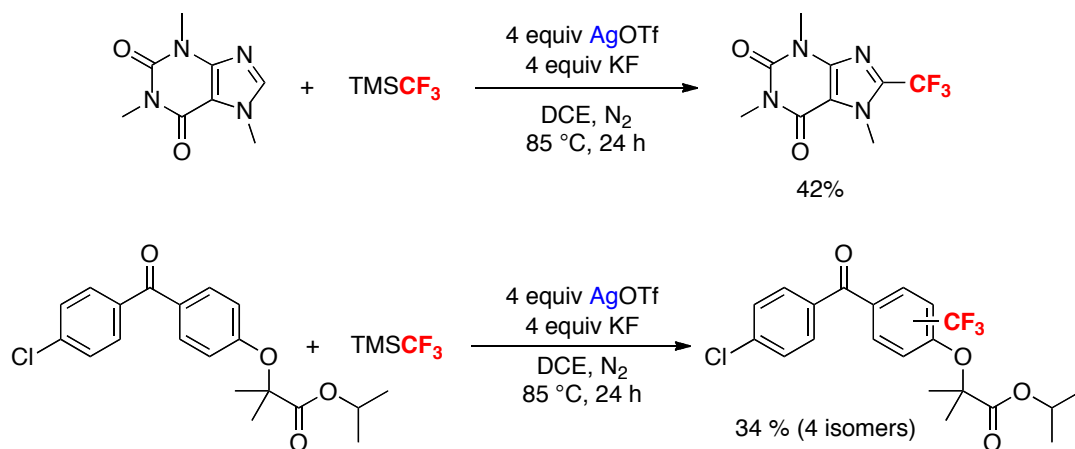
Table 3.3. Substrate Scope of Silver-Mediated Trifluoromethylation^{[a][b]}

entry	major product	yield (%)	isomer ratio	entry	major product	yield (%)	isomer ratio
1 ^[c]		87	---	8 ^[c]		88	---
2		81	a : b : c 2.7 : 1.4 : 1	9		85	a : b : c 13 : 7.3 : 1
3		76	---	10		70	a : b 4 : 1
4		76	a : b : c 5.2 : 3.5 : 1	11 ^[c]		46	a : b : c 1.7 : 1.2 : 1
5		65	a : b 1.4 : 1	12 ^[c]		44	a : b >20 : 1
6		78	---	13		72	a : b 8 : 1
7		87	a : b : c 2.7 : 1.2 : 1	14 ^[d]		70	a : b 4.8 : 1

^[a]General conditions: substrate (10 equiv), TMSCF₃ (1 equiv) in DCE at 85 °C for 24 h. ^[b]Yield and selectivity determined by ¹⁹F NMR analysis of the crude reaction mixtures. ^[c]20 equiv substrate used. ^[d]5 equiv substrate used.

To demonstrate the reactivity and selectivity of this transformation toward biologically relevant molecules, we applied this methodology to the trifluoromethylation of caffeine and Tricor (a commercial cholesterol lowering pharmaceutical) (**Scheme 3.6**). Caffeine showed modest reactivity toward trifluoromethylation at the aromatic C–H bond, leaving the potentially reactive carbonyl groups intact. Tricor contains four aromatic sites that are comparable in electronic character. Thus, as expected, the reaction with Tricor generated four regioisomeric trifluoromethylated products. This transformation is particularly interesting for medicinal chemistry since it has the capability of expediting the assembly and/or late-stage modification of drug targets.

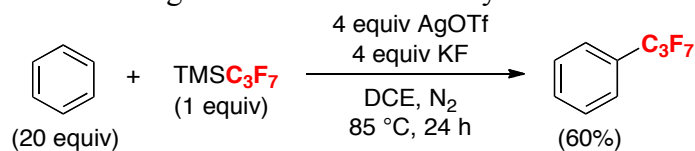
Scheme 3.6 Ag-Mediated Trifluoromethylation of Biological Molecules



One of the limitations of current system is its low reactivity toward electron-deficient, and heterocyclic molecules. A number of other heteroaromatics, including furan (16% yield), 2-methylfuran (7% yield), pyridine (2% yield, 2 isomers), and 1-methylimidazole (3% yield, 3 isomers) were surveyed and afforded low yields of mono-trifluoromethylated products under our standard conditions.

The optimal reaction conditions were also effective for transfer of other perfluoroalkyl groups. For example, the AgOTf/KF-mediated reaction of benzene with TMSC_3F_7 afforded (heptafluoropropyl)benzene in 60% yield (Scheme 3.7).

Scheme 3.7 Ag-Mediated Perfluoroalkylation of Benzene

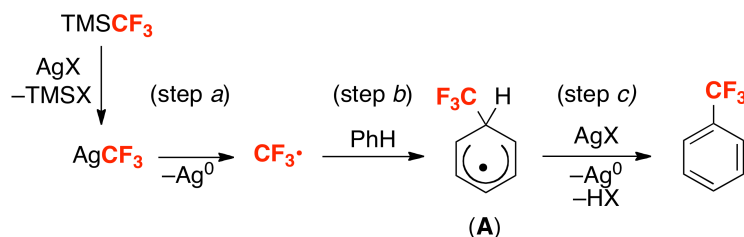


3.4 Mechanistic Investigation

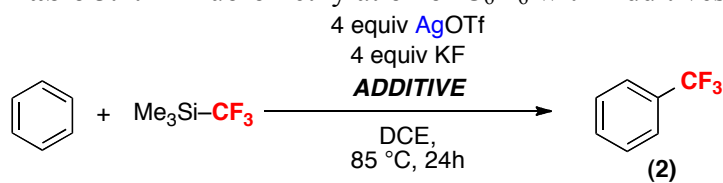
We initially hypothesized that this transformation proceeded via a pathway involving Ag-promoted generation of a trifluoromethyl radical ($\text{CF}_3\cdot$) (Scheme 3.8, step *a*), which then participates in a radical aromatic substitution reaction. Addition of $\text{CF}_3\cdot$ to the aromatic ring to generate intermediate **A** (step *b*) followed by SET from **A** to a second equivalent of Ag^{I} (step *c*) would release the product along with HOTf and Ag^0 . Importantly, free radical arene trifluoromethylation⁷ and perfluoroalkylation⁸ has

significant precedent in the literature. Most commonly, $\text{CF}_3\cdot$ is generated from CF_3Br or CF_3I either photochemically or electrochemically.^{7b,d,e} A more recent report by Yamakawa and coworkers demonstrated radical trifluoromethylation of aromatic compounds using CF_3I , Fe^{II} and H_2O_2 .^{7g} However, to our knowledge, the use of TMSCF_3 as a precursor to radical arene trifluoromethylation has not been reported.

Scheme 3.8 Free Radical Pathway for Ag-Mediated Trifluoromethylation



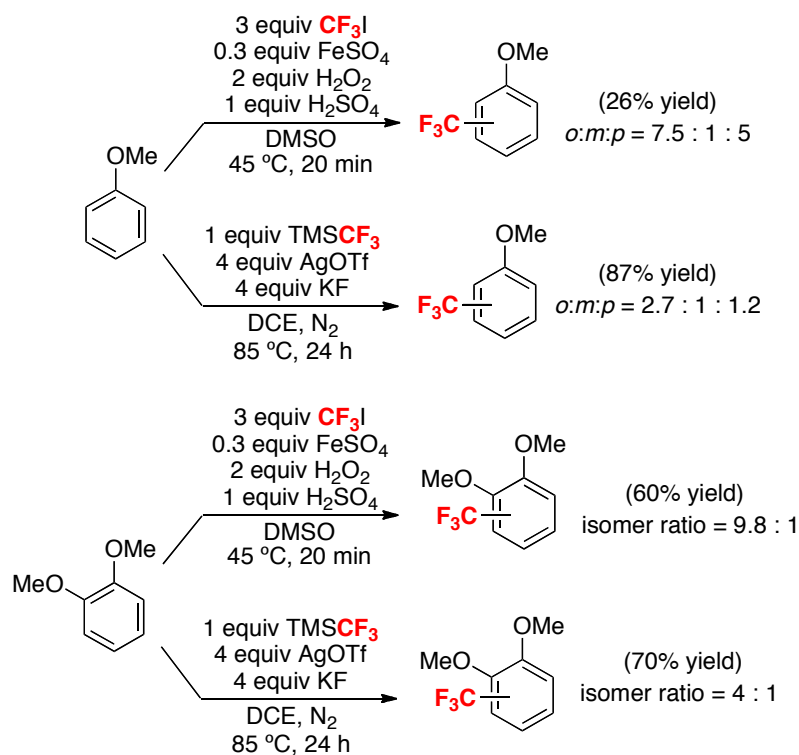
To test for the possibility of $\text{CF}_3\cdot$ intermediates, we examined the reaction of benzene with TMSCF_3 promoted by AgOTf/KF in the presence of a variety of radical initiators/inhibitors. In the presence of light (which is frequently used to promote radical reactions), the reaction proceeded in slightly lower yield (75% versus 87%). This result may be due to the light sensitivity of Ag salts.¹³ The addition of azobisisobutyronitrile (AIBN), a radical initiator, led to a moderate decrease in the overall yield of the reaction. The use of 20 mol % of AIBN resulted in 77% yield of PhCF_3 , while a 57% yield was obtained in the presence of 1 equiv of this additive.¹³ Nitrobenzene has been used previously as an inhibitor of SET transfer steps (like step *c* in **Scheme 3.8**) during free radical trifluoromethylation.^{7a} Interestingly, the addition of 1 equiv of NO_2Ph had little effect on the Ag-mediated reaction of benzene with TMSCF_3 (85% versus 87% yield in the absence of this additive). TEMPO has been utilized in the literature as a trap for $\text{CF}_3\cdot$.^{4c} The addition of 1 equiv of TEMPO led to a dramatic reduction in yield (to 7%) under otherwise analogous conditions.

Table 3.4. Trifluoromethylation of C₆H₆ with Additives

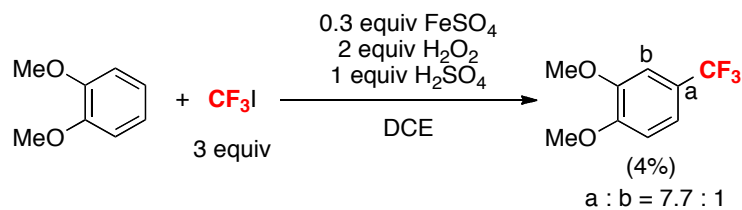
entry	additive	yield (%)
1	20 mol % AIBN	77
2	1 equiv AIBN	57
3	1 equiv nitrobenzene	85
4	1 equiv TEMPO	7

Because the results with the radical inhibitors/initiators were somewhat ambiguous, we next sought to compare the site selectivity of TMSCF₃/AgOTf/KF-mediated trifluoromethylation to that of a known CF₃• reaction. Under the reaction conditions described by Yamakawa and coworkers,^{7g} anisole reacted with *in situ*-generated CF₃• to form a 7.5 : 1 : 5 ratio of *o*:*m*:*p* trifluoromethylated products (**Scheme 3.9**). This reaction shows significantly higher *o/p* selectivity than the analogous Ag-mediated transformation (where *o*:*m*:*p* = 2.7 : 1 : 1.2). Veratrole also reacted with very different site selectivity for trifluoromethylation with CF₃• versus TMSCF₃/AgOTf/KF (**Scheme 3.9**).¹⁴ In order to exclude the solvent effect in radical reactions, we attempted the Yamakawa's radical trifluoromethylation using DCE as solvent.^{7g} However, DMSO proved to be critical for the reactivity in their system (**Scheme 3.10**).

Scheme 3.9. Comparison of Reactivity and Selectivity of Radical Trifluoromethylation



Scheme 3.10. Comparison of Reactivity and Selectivity of Radical Trifluoromethylation



While further studies are needed to gain a complete mechanistic picture of the $\text{TMSCF}_3/\text{AgOTf}/\text{KF}$ -mediated reaction, our results suggest against a purely free-radical pathway for this transformation. The involvement of caged and/or Ag-associated radicals is a likely possibility. Notably, Kamigata has proposed a similar mechanism involving “radical intermediates confined in the coordination sphere of Ru” in related transformations.^{7f}

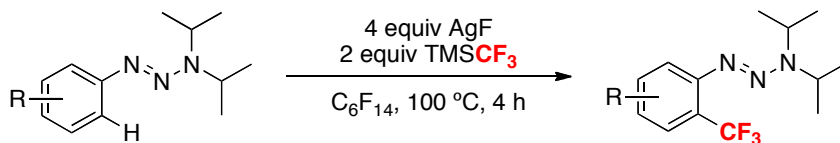
3.5 Conclusions

In conclusion, this report describes the silver-mediated trifluoromethylation of aromatic substrates with TMSCF_3 . These reactions are proposed to proceed via a AgCF_3 intermediate, and preliminary studies suggest against free $\text{CF}_3\cdot$ as an intermediate. Importantly, these Ag-mediated reactions proceed with complementary reactivity to analogous transformations of CuCF_3 reagents. Ongoing studies are focused on probing the mechanism and developing related Ag-catalyzed trifluoromethylation reactions.

3.6 Subsequent Developments

Soon after our report, Bräse and Hafner revealed a closely related AgCF_3 mediated *ortho*-trifluoromethylation of aromatic triazenes (**Scheme 3.11**).¹⁵ This report showed several significant improvements upon our initial system. First, high conversions were achieved using the arene substrate as limiting reagent, making it a much more practical synthetic approach. Second, this transformation is applicable to not only electron-rich, but also electron-poor substrates. This is very exciting, since our system performs poorly on electron-poor arenes. Finally, the triazene motif served as an effective directing group, affording highly *ortho*-selective trifluoromethylation. Although detailed mechanistic studies have not yet been reported, preliminary data suggests $\text{CF}_3\cdot$, derived from AgCF_3 is the reactive species. The high *ortho*-selectivity is presumably a result of chelation between a cage and/or Ag-associated $\text{CF}_3\cdot$ with triazene, which makes the *ortho* C–H bond the most accessible site to the radical.

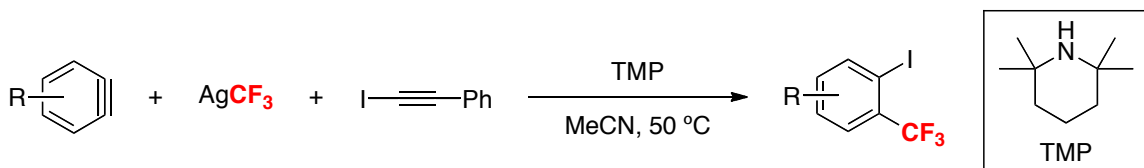
Scheme 3.11. AgCF_3 -Mediated *ortho*-Trifluoromethylation of Aromatic Triazenes



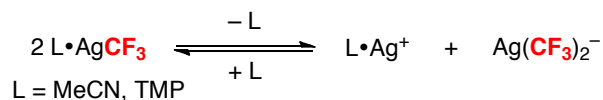
The direct study of AgCF_3 as potential trifluoromethylating reagent is still underdeveloped, due to its poor solubility in most organic solvents, instability in light/air, and the fact that it is usually present in equilibrium with multiple $(\text{L})_n\text{Ag}(\text{CF}_3)_n$ species (L = solvent). Recently, Hu and co-workers reported a AgCF_3 -mediated

trifluoromethylation-iodination of aryne precursors (**Scheme 3.12**).¹⁶ A wide range of trifluoromethylmetallic species (MCF_3) were examined, and AgCF_3 proved optimal, presumably because of its increased stability and softness in comparison with the labile and hard CF_3^- generated from $\text{TMSCF}_3/\text{F}^-$. 2,2,6,6-Tetramethylpiperidine (TMP) was identified as a key additive for this transformation. ^{19}F NMR studies of the reaction of TMP with AgCF_3 in MeCN showed conversion of the $\text{MeCN}\cdot\text{AgCF}_3$ intermediate to a new $\text{TMP}\cdot\text{AgCF}_3$ complex. Moreover, the addition of TMP led to a complete inversion of the equilibrium between the neutral $\text{L}\cdot\text{AgCF}_3$ and ionic $[\text{Ag}(\text{CF}_3)_2]^-$ complexes (**Scheme 3.13**). For instance, subjecting AgF to TMSCF_3 in MeCN results in a 1:3.8 ratio of $\text{MeCN}\cdot\text{AgCF}_3$ and $[\text{Ag}(\text{CF}_3)_2]^-$ species. Addition of only 1 equiv of TMP led to a 18.8:1 ratio of $\text{TMP}\cdot\text{AgCF}_3$ vs $[\text{Ag}(\text{CF}_3)_2]^-$. It is reasonable to assume that the enhanced activity from TMP results from the high concentration of this newly formed $\text{TMP}\cdot\text{AgCF}_3$ intermediate, because the increased electron density on the silver atom should facilitate smooth transfer of CF_3 .

Scheme 3.12. Ag-Mediated Trifluoromethylation-Iodination of Arynes



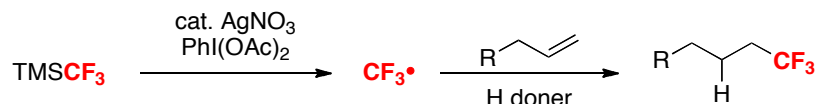
Scheme 3.13. Equilibrium between Neutral $\text{L}\cdot\text{AgCF}_3$ and Ionic $[\text{Ag}(\text{CF}_3)_2]^-$ Complexes



Another example of silver-based trifluoromethylation using TMSCF_3 was reported by Qing and co-workers in the context of the hydrotrifluoromethylation of unactivated alkenes (**Scheme 3.14**).¹⁷ The authors suggested that reaction between AgNO_3 and TMSCF_3 under oxidative conditions led to facile formation of $\text{CF}_3\cdot$. The addition of $\text{CF}_3\cdot$ to the alkene, followed by $\text{H}\cdot$ abstraction generated the final products.

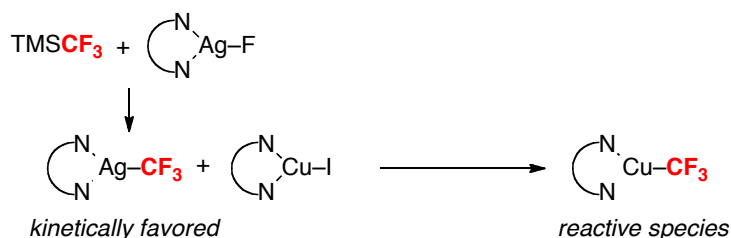
When this hydrotrifluoromethylation reaction was performed in the presence of 1 equiv of TEMPO (a radical scavenger) added, a TEMPO–CF₃ adduct was formed in 80% yield.

Scheme 3.14. Ag-Catalyzed Hydrotrifluoromethylation of Alkenes using TMSCF₃



In **Chapter 2**, we demonstrated that merging Cu-based cross-coupling with CF₃• could lead to mild and facile arene trifluoromethylation. We believe that it is possible (even likely) that many Cu-catalyzed processes that were initially believed to involve CF₃[−] or CF₃⁺ transfer actually involve radical intermediates. For example, several reports have shown that Ag salts serve as promoters for the Cu-catalyzed trifluoromethylation of aryl iodides.^{12,18} The role of Ag has been proposed to involve mediating transmetalation of CF₃[−] from Si (in TMSCF₃) to Cu (**Scheme 3.15**).¹² However, based on the above discussions, we believe that the role of Ag may be to generate CF₃• in these transformations.

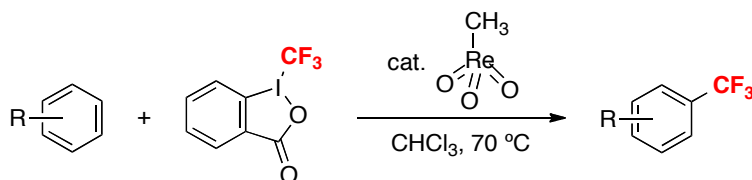
Scheme 3.15. Proposed Corporative Effect of Cu/Ag-Catalyzed Trifluoromethylation



In addition, CF₃⁺ reagents can potentially undergo 1e[−] reduction to form CF₃•,¹⁹ suggesting the possibility that Cu-catalyzed reactions with CF₃⁺ reagents may also involve radical intermediates.^{1f,20} Recently, Togni described a CH₃ReO₃-catalyzed (Lewis acid) trifluoromethylation of arenes and heteroarenes using the Togni reagent (**Scheme 3.16**).²¹ A broad range of arene and heteroarenes were examined. In general, electron-rich substrates reacted to provide the desired products in good yields, whereas electron-poor substrates showed significantly lower reactivity. The observed reactivity along with an *in*

situ EPR study strongly suggested $\text{CF}_3\cdot$ as reactive intermediate. Other examples involving the generation of $\text{CF}_3\cdot$ from a CF_3^+ reagent include Cu-catalyzed allylic trifluoromethylations by Wang^{22a} and Buchwald,^{22b} and Fe^{II} -catalyzed trifluoromethylation of vinyl trifluoroborates.^{22c} Interestingly, Studer group reported a transition-metal free trifluoromethylation of alkenes using the Togni reagent. TEMPONa was used as a single-electron-transfer (SET) reagent for reduction of the hypervalent-iodine- CF_3 reagent.^{22d}

Scheme 3.16. Re-Catalyzed Trifluoromethylation of Arenes and Heteroarenes



Finally, several examples have demonstrated an alternative radical approach for aryl or allylic trifluoromethylation. Instead of reacting the electrophilic $\text{CF}_3\cdot$ with a nucleophilic carbon center, Qing and co-workers investigated the reaction of nucleophilic CF_3^- with radical cation intermediates generated under oxidative conditions. This approach has been successfully realized in the context of Cu-catalyzed trifluoromethylation of terminal alkenes using TMSCF_3 with $\text{PhI}(\text{OAc})_2$.²³ More recently, a metal-free C-H trifluoromethylation of arenes using $\text{TMSCF}_3/\text{PhI}(\text{OAc})_2$ was demonstrated.²⁴ The key to this transformation is the facile formation of the aromatic radical cation intermediates. As a result, the current method is limited to electron-rich substrates.

In conclusion, radical trifluoromethylation has become a rapidly growing field. New development has focused on facile generation of $\text{CF}_3\cdot$ under mild and practical conditions using benign and inexpensive trifluoromethylating reagents. In several examples, the strategy has been applied to complex substrate and showed high efficiency with high regioselectivity. We anticipate a continued fast growing of this approach in the future.

3.7 Experimental Procedures and Characterization Data

General Procedures

NMR spectra were obtained on a Varian vnmrs 700 (699.76 MHz for ^1H ; 175.95 MHz for ^{13}C ; 658.43 for ^{19}F), Varian vnmrs 500 (500.10 MHz for ^1H ; 125.75 MHz for ^{13}C , 470.56 MHz for ^{19}F), Varian Inova 500 (499.90 MHz for ^1H ; 125.70 MHz for ^{13}C), or a Varian MR400 (400.52 MHz for ^1H ; 100.71 for ^{13}C , 376.87 MHz for ^{19}F) spectrometer. ^1H and ^{13}C chemical shifts are reported in parts per million (ppm) relative to TMS, with the residual solvent peak used as an internal reference. ^{19}F NMR spectra are referenced based on the internal standard 4-fluoroanisole, which appears at -125.00 ppm. Multiplicities are reported as follows: singlet (s), doublet (d), doublet of doublets (dd), doublet of doublets of doublets (ddd), doublet of triplets (dt), triplet (t), triplet of doublets (td), triplet of triplets (tt), quartet (q), quintet (quin), multiplet (m), and broad resonance (br). Melting points were determined with a Mel-Temp 3.0, a Laboratory Devices Inc, USA instrument, and are uncorrected. HRMS data were obtained on a Micromass AutoSpec Ultima Magnetic Sector mass spectrometer. GCMS analysis was performed on a Shimadzu GCMS-QP2010 plus gas chromatograph mass spectrometer. The products were separated on a 30 m length by 0.25 mm id, RESTEK XTI-5 column coated with a 0.25 μm film. Helium was employed as the carrier gas, with a constant column flow of 1.5 mL/min. The injector temperature was held constant at 250 $^\circ\text{C}$.

Materials and Methods.

AgF, AgOTf, and 4-fluoroanisole were obtained from Matrix Scientific. Benzene and potassium fluoride were obtained from EMD. Rupert's reagent (TMSCF_3) was obtained from Oakwood Products. AgNO_3 , 1,2-Dimethoxybenzene, 1,3-dimethoxybenzene, 1,4-dichlorobenzene, anisole, iodobenzene, and naphthalene were obtained from Sigma Aldrich. 1,4-Dimethoxybenzene and *o*-xylenes were obtained from TCI America. Trifluorotoluene and *m*-xylenes were obtained from Acros. 1,2-Dichloroethane, *p*-xylene, thiophene, *N*-methylpyrrole and mesitylene were obtained from Alfa Aesar. CDCl_3 was obtained from Cambridge Isotope Laboratories. Authentic samples of the aryl- CF_3 products were purchased from commercial sources unless otherwise stated. Dichloroethane, xylenes, and dimethoxybenzenes were distilled from CaH_2 . Benzene was

distilled from Na and benzophenone. Anisole, *N*-methylpyrrole, mesitylene, and thiophene were distilled from Na. Other chemicals were used as received. All syntheses were conducted using standard Schlenk techniques or in a nitrogen atmosphere glovebox unless otherwise stated.

Experimental Details.

Reactivity of Ag–CF₃ with PhI

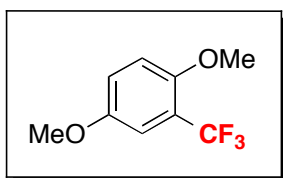
In a glovebox, AgF (10.3 mg, 0.081 mmol, 1 equiv) was weighed into a 4 mL vial and dissolved in MeCN (0.2 mL). TMSCF₃ (12 μL, 0.081 mmol, 1 equiv) was added, and the reaction was stirred at 25 °C for 15 min.¹¹ Iodobenzene (180 μL, 1.62 mmol, 20 equiv) was added to the reaction mixture. The vial was sealed with a Teflon-lined cap and removed from the glovebox. The reaction was heated at 85 °C for 24 h with exclusion of light. The resulting dark brown mixture was cooled to room temperature and diluted with MeCN (1 mL). 4-Fluoroanisole (1 equiv) was added as an internal standard, and the reaction was analyzed by ¹⁹F NMR spectroscopy in MeCN, showing a combined 15% yield of the three isomeric products. The ¹⁹F NMR spectroscopic data matched that of authentic samples of all three isomers (*o*-isomer (Alfa Aesar): s, –62.7 ppm; *m*-isomer (Matrix Scientific): s, –62.9 ppm; *p*-isomer (Matrix Scientific), s, –63.0 ppm).

Reactivity of Ag–CF₃ with Benzene

In a glovebox, AgF (10.3 mg, 0.081 mmol, 1 equiv) was weighed into a 4 mL vial and dissolved in MeCN (0.2 mL). TMSCF₃ (12 μL, 0.081 mmol, 1 equiv) was added, and the reaction was stirred at 25 °C for 15 min.¹¹ Benzene (144 μL, 1.62 mmol, 20 equiv) was added to the reaction mixture. The vial was sealed with a Teflon-lined cap and removed from the glovebox. The reaction was heated at 85 °C for 24 h with exclusion of light. The resulting dark brown mixture was cooled to room temperature and diluted with MeCN (1 mL). 4-Fluoroanisole (1 equiv) was added as an internal standard, and the reaction was analyzed by ¹⁹F NMR spectroscopy in MeCN, showing 28% yield of trifluorotoluene. The ¹⁹F NMR spectroscopic data matched that obtained of an authentic sample of trifluorotoluene (Acros, s, –63.3 ppm).

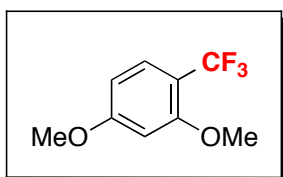
General Procedure for Preparation of Authentic Samples of Previously Unreported Benzotrifluorides

The authentic samples were synthesized following a literature procedure.^{1c} In a glovebox, [Cu(OTf)₂•C₆H₆] (60.4 mg, 0.12 mmol, 0.6 equiv), 1,10-phenanthroline (43 mg, 0.24 mmol, 1.2 equiv), K₃PO₄ (127 mg, 0.6 mmol, 3 equiv), KF (58.1 mg, 1.0 mmol, 5 equiv), Ag₂CO₃ (55.2 mg, 0.2 mmol, 1 equiv), DMF (2.0 mL) and TMSCF₃ (0.15 mL, 0.1 mmol, 5 equiv) were added to a 20 mL reaction vial that was equipped with a stir bar. In a second vial, boronic acid (0.2 mmol, 1 equiv) was dissolved in DMF (2.0 mL). Both vials were sealed with rubber septa and removed from the glovebox. The first vial was heated to 45 °C, and the solution of boronic acid was then added to over 2 h by using a syringe pump under N₂ atmosphere. After addition of the boronic acid solution, the reaction mixture was heated at 45 °C for another 2 h. The reaction was cooled to 0 °C, and water (10 mL) was added. The resulting mixture was extracted with diethyl ether, and the combined organic extracts were washed with water (3 x 50 mL) and brine (1 x 50 mL) and then dried over magnesium sulfate. The solvent was removed by rotary evaporation, and the products were purified by column chromatography on silica gel using pentane as the eluent.



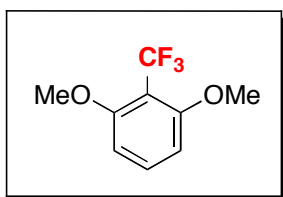
1,4-Dimethoxy-2-(trifluoromethyl)benzene

The general procedure was followed using 2,5-dimethoxyphenylboronic acid (36.4 mg, 0.2 mmol, 1 equiv) as the substrate. The product was obtained as colorless liquid ($R_F = 0.13$ in pentanes). ¹H NMR (CDCl₃, 25 °C): δ 7.12 (s, 1H), 7.02 (d, $J = 9.2$ Hz, 1H), 6.94 (d, $J = 9.2$ Hz, 1H), 3.86 (s, 3H), 3.79 (s, 3H). ¹³C NMR (CDCl₃, 25 °C): δ 153.10, 151.67, 123.56 (q, $J = 271.0$ Hz), 119.54 (q, $J = 30.8$ Hz), 118.23, 113.72, 112.96 (q, $J = 5.5$ Hz), 56.71, 56.03. ¹⁹F NMR (CDCl₃, 25 °C): δ -62.44 (s, 3F). HRMS EI (m/z): [M]⁺ calcd for C₉H₉F₃O₂, 206.0555; found, 206.0563.



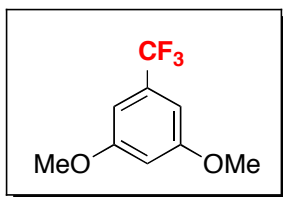
1,3-Dimethoxy-4-(trifluoromethyl)benzene

The general procedure was followed using 2,4-dimethoxyphenylboronic acid (36.4 mg, 0.2 mmol, 1 equiv) as the substrate. The product was obtained as colorless liquid ($R_F = 0.1$ in pentanes). ^1H NMR (CDCl_3 , 25 °C): δ 7.48 (d, $J = 8.7$ Hz, 1H), 6.52 (s, 1H), 6.49 (d, $J = 8.7$ Hz, 1H), 3.87 (s, 3H), 3.84 (s, 3H). ^{13}C NMR (CDCl_3 , 25 °C): δ 163.80, 159.01, 128.41 (q, $J = 5.4$ Hz), 124.12 (q, $J = 270.6$ Hz), 111.70 (q, $J = 31.1$ Hz), 103.84, 99.51, 55.96, 55.65. ^{19}F NMR (CDCl_3 , 25 °C): δ -61.32 (s, 3F). HRMS EI (m/z): $[\text{M}]^+$ calcd for $\text{C}_9\text{H}_9\text{F}_3\text{O}_2$, 206.0555; found, 206.0559.



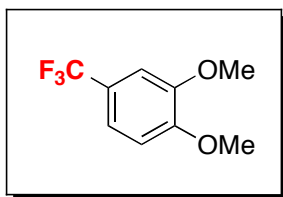
1,3-Dimethoxy-2-(trifluoromethyl)benzene

The general procedure was followed using 2,6-dimethoxyphenylboronic acid (36.4 mg, 0.2 mmol, 1 equiv) as the substrate. The product was obtained as a light yellow viscous solid ($R_F = 0.13$ in pentanes). ^1H NMR (CDCl_3 , 25 °C): δ 7.38 (t, $J = 8.8$ Hz, 1H), 6.61 (d, $J = 8.8$ Hz, 2H), 3.86 (s, 6H). ^{13}C NMR (CDCl_3 , 25 °C): δ 159.44, 133.11, 127.30, 124.22 (q, $J = 275.5$ Hz), 104.96, 56.50. ^{19}F NMR (CDCl_3 , 25 °C): δ -54.97 (s, 3F). HRMS EI (m/z): $[\text{M}]^+$ calcd for $\text{C}_9\text{H}_9\text{F}_3\text{O}_2$, 206.0555; found, 206.0555.



1,3-Dimethoxy-5-(trifluoromethyl)benzene

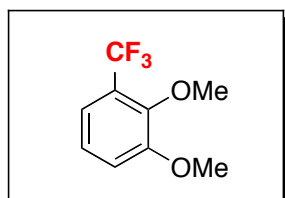
The general procedure was followed using 3,5-dimethoxyphenylboronic acid (36.4 mg, 0.2 mmol, 1 equiv) as the substrate. The product was obtained as colorless liquid ($R_F = 0.23$ in pentanes). ^1H NMR (CDCl_3 , 25 °C): δ 6.74 (s, 2H), 6.60 (s, 1H), 3.82 (s, 6H). ^{13}C NMR (CDCl_3 , 25 °C): δ 161.16, 132.53 (q, $J = 32.3$ Hz), 124.05 (q, $J = 272.3$ Hz), 103.76, 103.42 (q, $J = 3.9$ Hz), 55.67. ^{19}F NMR (CDCl_3 , 25 °C): δ -62.96 (s, 3F). HRMS EI (m/z): $[\text{M}]^+$ calcd for $\text{C}_9\text{H}_9\text{F}_3\text{O}_2$, 206.0555; found, 206.0554.



1,2-Dimethoxy-4-(trifluoromethyl)benzene

The general procedure was followed using 3,4-dimethoxyphenylboronic acid (36.4 mg, 0.2 mmol, 1 equiv) as the substrate. The product was obtained as colorless liquid ($R_F =$

0.1 in pentanes). ^1H NMR (CDCl_3 , 25 °C): δ 7.18 (d, J = 8.4 Hz, 1H), 7.05 (s, 1H), 6.88 (d, J = 8.4 Hz, 1H), 3.89 (s, 6H). ^{13}C NMR (CDCl_3 , 25 °C): δ 151.66, 149.12, 124.40 (q, J = 271.5 Hz), 122.97 (q, J = 32.9 Hz), 118.40 (q, J = 3.6 Hz), 110.65, 108.06 (q, J = 3.6 Hz), 56.04, 56.02. ^{19}F NMR (CDCl_3 , 25 °C): δ -61.67 (s, 3F). HRMS EI (m/z): $[\text{M}]^+$ calcd for $\text{C}_9\text{H}_9\text{F}_3\text{O}_2$, 206.0555; found, 206.0559.



1,2-Dimethoxy-3-(trifluoromethyl)benzene

The general procedure was followed using 2,3-dimethoxyphenylboronic acid (36.4 mg, 0.2 mmol, 1 equiv) as the substrate. The product was obtained as colorless liquid (R_F = 0.12 in pentanes). ^1H NMR (CDCl_3 , 25 °C): δ 7.17-7.08 (multiple peaks, 3H), 3.91 (s, 3H), 3.90 (s, 3H). ^{13}C NMR (CDCl_3 , 25 °C): δ 153.62, 147.72 (q, J = 1.9 Hz), 124.72 (q, J = 30.4 Hz), 123.92, 123.68 (q, J = 273.6 Hz), 118.16 (q, J = 5.1 Hz), 116.24, 61.50, 56.15. ^{19}F NMR (CDCl_3 , 25 °C): δ -61.36 (s, 3F). HRMS EI (m/z): $[\text{M}]^+$ calcd for $\text{C}_9\text{H}_9\text{F}_3\text{O}_2$, 206.0555; found, 206.0559.

General Procedure for Trifluoromethylation of Arenes

In a glovebox, AgOTf (83.2 mg, 0.324 mmol, 4 equiv) and KF (18.8 mg, 0.324 mmol, 4 equiv) were weighed into a 4 mL vial and dissolved in DCE (0.2 mL). The aromatic substrate and TMSCF_3 (12 μL , 0.081 mmol, 1 equiv) were then added. The vial was sealed with a Teflon-lined cap and removed from the glovebox. The reaction was heated at 85 °C for 24 h with exclusion of light. The resulting dark brown mixture was cooled to room temperature and diluted with DCE (1 mL). 4-Fluoroanisole (1 equiv) was added as an internal standard, and the reaction was analyzed by ^{19}F NMR spectroscopy in DCE to determine the yield. GCMS analyses were performed on a Shimadzu GCMS-QP5000 gas chromatograph mass spectrometer. The products were separated on a 30 m length \times 0.25 mm i.d., RESTEK XTI-5 column coated with a 0.25 μm film. The GC oven temperature program was as follows: 30 °C hold 10 min, ramp 20 °C/min to 250 °C, and hold for 3 min. Helium was employed as the carrier gas, with a constant column flow of 1.5 mL/min. The injector temperature was held constant at 250 °C.

Substrate = Benzene: The general procedure was followed using 20 equiv of benzene. The ^{19}F NMR spectroscopic data matched that obtained for an authentic sample of trifluorotoluene (Acros, s, -63.3 ppm). Trifluorotoluene was formed in 87% yield as determined by ^{19}F NMR spectroscopic analysis of the crude reaction mixture.

This reaction was also conducted on 0.5 mmol and 1 mmol scale. For the 0.5 mmol scale reaction, AgOTf (514 mg, 2 mmol, 4 equiv), KF (116 mg, 2 mmol, 4 equiv), TMSCF_3 (73.8 μL , 0.5 mmol, 1 equiv), benzene (0.89 mL, 10 mmol, 20 equiv) and DCE (1.25 mL) were used. The yield of the reaction was 84%. For the 1 mmol scale reaction, AgOTf (1028 mg, 4 mmol, 4 equiv), KF (232 mg, 4 mmol, 4 equiv), TMSCF_3 (147.7 μL , 1 mmol, 1 equiv), benzene (1.78 mL, 20 mmol, 20 equiv) and DCE (2.5 mL) were used. The reaction was conducted in a 20 mL vial, and the yield was 87%.

Substrate = Toluene: The general procedure was followed using 10 equiv of toluene. The ^{19}F NMR spectroscopic data matched that of authentic samples of all three isomers (*o*-isomer, (Matrix Scientific): s, -62.7 ppm; *m*-isomer (Matrix Scientific): s, -62.4 ppm; *p*-isomer (Alfa Aesar), s, -61.7 ppm). The trifluoromethylated products were formed in 81% combined yield with an *o* : *m* : *p* ratio of 1.4 : 1 : 2.7 as determined by ^{19}F NMR spectroscopic analysis of the crude reaction mixture.

Substrate = *p*-Xylene: The general procedure was followed using 10 equiv of *p*-xylene. ^{19}F NMR analysis of the crude reaction mixture showed that 1,4-dimethyl-2-(trifluoromethyl)benzene was formed in 76% yield. The product showed a ^{19}F NMR signal at -61.6 ppm in DCE (lit. -61.6 ppm in CDCl_3).²⁵ The identity of the product was further confirmed by GCMS analysis, where the product peak was observed at 11.8 min.

Substrate = *m*-Xylene: The general procedure was followed using 10 equiv of *m*-xylenes. ^{19}F NMR analysis of the crude reaction mixture showed that the mono-trifluoromethylated product was formed in 76% yield as a mixture of 3 isomers. These products showed ^{19}F NMR signals in DCE at -61.2 ppm (a isomer, lit. -61.2 ppm in CDCl_3),²⁵ -54.1 ppm (b isomer, lit. -54.1 ppm in CDCl_3),²⁵ and -62.6 ppm (c isomer, lit.

–62.6 ppm in CDCl₃).²⁵ The identity of the products was further confirmed by GCMS analysis, where the product peaks were observed at 11.6 min, 11.9 min and 12.2 min.

Substrate = *o*-Xylene: The general procedure was followed using 10 equiv of *ortho*-xylenes. ¹⁹F NMR analysis of the crude reaction mixture showed that the mono-trifluoromethylated product was formed in 65% yield as a 1.4 : 1 mixture of the a and b isomers. These products showed ¹⁹F NMR signals in DCE at –60.4 ppm (a isomer, lit. –60.4 ppm in CDCl₃)²⁵ and –62.3 ppm (b isomer). The ¹⁹F NMR spectroscopic data of b isomer matched that of an authentic sample (SynQuest Laboratories). The identity of the products was further confirmed by GCMS analysis, where the product peaks were observed at 12.3 min and 12.4 min.

Substrate = Mesitylene: The general procedure was followed using 10 equiv of mesitylene. ¹⁹F NMR analysis of the crude reaction mixture showed that 1,3,5-trimethyl-2-(trifluoromethyl)benzene was formed in 78% yield. The product showed a ¹⁹F NMR signal at –53.7 ppm in DCE (lit. –55 ppm in CDCl₃).²⁶ The identity of the product was further confirmed by GCMS analysis, where the product peak was observed at 14.0 min.

Substrate = Anisole: The general procedure was followed using 10 equiv of anisole. The ¹⁹F NMR spectroscopic data matched that of authentic samples of all three isomers (*o*-isomer (Alfa Aesar): s, –62.5 ppm; *m*-isomer (Matrix Scientific): s, –62.8 ppm; *p*-isomer (SynQuest Laboratories), s, –61.5 ppm). The trifluoromethylated products were formed in 87% combined yield with an *o* : *m* : *p* ratio of 2.7 : 1 : 1.2 as determined by ¹⁹F NMR spectroscopic analysis of the crude reaction mixture.

Substrate = 1,4-Dimethoxybenzene: The general procedure was followed using 20 equiv of 1,4-dimethoxybenzene. The ¹⁹F NMR spectroscopic data matched that of the authentic samples of prepared above. 1,4-Dimethoxy-2-trifluoromethylbenzene was formed in 81% yield as determined by ¹⁹F NMR spectroscopic analysis of the crude reaction mixture.

Substrate = 1,3-Dimethoxybenzene: The general procedure was followed using 10 equiv of 1,3-dimethoxybenzene. The ^{19}F NMR spectroscopic data matched that of the authentic samples of prepared above. The three isomeric mono-trifluoromethylated products were formed in 85% yield with an a : b : c ratio of 13 : 7.3 : 1 as determined by ^{19}F NMR spectroscopic analysis of the crude reaction mixture.

Substrate = 1,2-Dimethoxybenzene: The general procedure was followed using 10 equiv of 1,2-dimethoxybenzene. The ^{19}F NMR spectroscopic data matched that of the authentic samples of prepared above. The three isomeric mono-trifluoromethylated products were formed in 71% yield with an a : b ratio of 4 : 1 as determined by ^{19}F NMR spectroscopic analysis of the crude reaction mixture.

Substrate = Iodobenzene: The general procedure was followed using 20 equiv of iodobenzene. The ^{19}F NMR spectroscopic data matched that of authentic samples of all three isomers (*o*-isomer (Alfa Aesar): s, -62.7 ppm; *m*-isomer (Matrix Scientific): s, -62.9 ppm; *p*-isomer (Matrix Scientific), s, -63.0 ppm). The trifluoromethylated products were obtained in 46% combined yield with an *o* : *m* : *p* ratio of 1.7 : 1.2 : 1 as determined by ^{19}F NMR analysis of the crude reaction mixture.

Substrate = *N*-methylpyrrole: The general procedure was followed using 20 equiv of *N*-methylpyrrole. ^{19}F NMR analysis of the crude reaction mixture showed that the mono-trifluoromethylated product was formed in 44% total yield as a >20:1 mixture of the a and b isomers. These products showed ^{19}F NMR signals in DCE at -58.8 ppm (a isomer, lit. -58.3 ppm in CDCl_3)²⁷ and -56.8 ppm (b isomer, lit. -56.6 in CDCl_3).²⁷ The identity of the products was further confirmed by GCMS analysis, where the product peaks were observed at 3.7 min and 4.1 min.

Substrate = Thiophene: The general procedure was followed using 10 equiv of thiophene. ^{19}F NMR analysis of the crude reaction mixture showed that the mono-trifluoromethylated product was formed in 72% total yield as an 8:1 mixture of the a and b isomers. These products showed ^{19}F NMR signals in DCE at -55.1 ppm (a isomer, lit. $-$

55.1 ppm in thiophene)²⁸ and -59.4 ppm (b isomer, lit. -59.5 in thiophene).²⁸ The identity of the products was further confirmed by GCMS analysis, where the product peaks were observed at 3.3 min and 3.5 min.

Substrate = Naphthalene: The general procedure was followed using 5 equiv of naphthalene. ^{19}F NMR analysis of the crude reaction mixture showed that the mono-trifluoromethylated product was formed in 70% total yield as an 4.8 : 1 mixture of the a and b isomers. These products showed ^{19}F NMR signals in DCE at -59.9 ppm (a isomer, lit. -60.1 ppm in CDCl_3)^{4b} and -62.4 ppm (b isomer, lit. -62.1 in CDCl_3).^{1c} The identity of the products was further confirmed by GCMS analysis, where the product peaks were observed at 15.7 min and 15.8 min.

Substrate = Caffeine: The general procedure was followed using 5 equiv of caffeine. ^{19}F NMR analysis of the crude reaction mixture showed that the trifluoromethylated product was formed in 42% yield. The product showed ^{19}F NMR signals in DCE at -62.5 ppm (lit. -62.7 ppm in CDCl_3).^{7h} The identity of the product was further confirmed by GCMS analysis. The GC oven temperature program was as follows: start at 100 °C, ramp 15 °C/min to 250 °C, and hold for 10 min. The product peak was observed at 6.5 min.

Heptafluoropropylation of Arenes

In a glovebox, AgOTf (83.2 mg, 0.324 mmol, 4 equiv) and KF (18.8 mg, 0.324 mmol, 4 equiv) were weighed into a 4 mL vial and dissolved in DCE (0.2 mL). Benzene (144 μL , 1.62 mmol, 20 equiv) was added to the reaction mixture. The vial was removed from the glovebox. In the air, TMSC_3F_7 (16.4 μL , 0.081 mmol, 1 equiv) was added, and the vial was sealed with a Teflon-lined cap. The reaction was heated at 85 °C for 24 h with exclusion of light. The resulting dark brown mixture was cooled to room temperature and diluted with DCE (1 mL). 4-Fluoroanisole (1 equiv) was added as an internal standard, and the reaction was analyzed by ^{19}F NMR spectroscopy in DCE to determine the yield. ^{19}F NMR analysis of the crude reaction mixture showed that heptafluoropropyl-benzene was formed in 60%. The product was identified by comparison to literature ^{19}F NMR data: observed d -80.4 ppm (t, $J = 9.8$ Hz, 3F), -111.8 ppm (q, $J = 9.8$ Hz, 2F), -126.6

ppm (s, 2F) in DCE; lit. -80.2 ppm (t, $J = 9$ Hz, 3F), -111.5 ppm (q, $J = 9$ Hz, 2F), -126.5 ppm (s, 2F) in CDCl_3 .²⁹ The identity of the product was further confirmed by GCMS analysis, where the product peak was observed at 5.0 min.

Trifluoromethylation of C_6H_6 under Light

In a glovebox, AgOTf (83.2 mg, 0.324 mmol, 4 equiv) and KF (18.8 mg, 0.324 mmol, 4 equiv) were weighed into a 4 mL vial and dissolved in DCE (0.2 mL). Benzene (144 μL , 1.62 mmol, 20 equiv) and TMSCF_3 (12 μL , 0.081 mmol, 1 equiv) were added. The vial was sealed with a Teflon-lined cap and removed from the glovebox. A 26-watt fluorescent light source was placed 5 cm from the reaction, and the reaction was heated in a clear oil bath at 85°C for 24 h. The resulting dark brown mixture was cooled to room temperature and diluted with DCE (1 mL). 4-Fluoroanisole (1 equiv) was added as an internal standard, and the reaction was analyzed by ^{19}F NMR spectroscopy, showing 75% yield of trifluorotoluene.

Trifluoromethylation of C_6H_6 Reaction with Additives

In a glovebox, AgOTf (83.2 mg, 0.324 mmol, 4 equiv) and KF (18.8 mg, 0.324 mmol, 4 equiv) were weighed into a 4 mL vial and dissolved in DCE (0.2 mL). Benzene (144 μL , 1.62 mmol, 20 equiv), additive (0.2 equiv or 1 equiv), and TMSCF_3 (12 μL , 0.081 mmol, 1 equiv) were added. The vial was sealed with a Teflon-lined cap and removed from the glovebox. The reaction was heated at 85°C for 24 h with exclusion of light. The resulting dark brown mixture was cooled to room temperature and diluted with DCE (1 mL). 4-Fluoroanisole (1 equiv) was added as an internal standard, and the reaction was analyzed by ^{19}F NMR spectroscopy.

Radical Trifluoromethylation

The radical trifluoromethylation reactions were performed following a literature procedure.^{7g} In air, anisole (109 μL , 1.0 mmol) or veratrole (127 μL , 1.0 mmol), DMSO (2.0 mL), a DMSO solution of H_2SO_4 (0.5 M, 2.0 mL), a DMSO solution of CF_3I (3.0 M, 1.0 mL) and an aqueous solution of FeSO_4 (1 M, 0.3 mL) were combined in a 20 mL vial. A 30% aqueous solution of H_2O_2 (0.2 mL) was added drop-wise at the rate of 0.04

mL/min using a syringe pump. After the addition of H₂O₂, the mixture was stirred at 45 °C for 20 min. After cooling to room temperature, 2,2,2-trifluoroethanol (1 equiv) was added as an internal standard, and the reaction was analyzed by ¹⁹F NMR spectroscopy.

Radical Trifluoromethylation in DCE

The radical trifluoromethylation reactions were performed following a modified literature procedure.^{7g} In air, veratrole (127 μL, 1.0 mmol), DCE (2.0 mL), a DCE solution of H₂SO₄ (0.5 M, 2.0 mL), a DMSO solution of CF₃I (3.0 M, 1.0 mL) and an aqueous solution of FeSO₄ (1 M, 0.3 mL) were combined in a 20 mL vial. A 30% aqueous solution of H₂O₂ (0.2 mL) was added drop-wise at the rate of 0.04 mL/min using a syringe pump. After the addition of H₂O₂, the mixture was stirred at 45 °C for 20 min. After cooling to room temperature, 2,2,2-trifluoroethanol (1 equiv) was added as an internal standard, and the reaction was analyzed by ¹⁹F NMR spectroscopy.

3.8 Reference

¹ Recent examples of Cu-mediated trifluoromethylation reactions: (a) Dubinina, G. G.; Furutachi, H.; Vivic, D. A. *J. Am. Chem. Soc.* **2008**, *130*, 8600. (b) Dubinina, G. G.; Ogikubo, J.; Vivic, D. A. *Organometallics* **2008**, *27*, 6233. (c) Chu, L.; Qing, F.-L. *Org. Lett.* **2010**, *12*, 5060. (d) McReynolds, K. A.; Lewis, R. S.; Ackerman, L. K. G.; Dubinina, G. G.; Brennessel, W. W.; Vivic, D. A. *J. Fluorine Chem.* **2010**, *131*, 1108. (e) Senecal, T. D.; Parsons, A. T.; Buchwald, S. L. *J. Org. Chem.* **2011**, *76*, 1174. (f) Zhang, C.-P.; Wang, Z.-L.; Chen, Q.-Y.; Zhang, C.-T.; Gu, Y.-C.; Xiao, J.-C. *Angew. Chem. Int. Ed.* **2011**, *50*, 1896. (g) Morimoto, H.; Tsubogo, T.; Litvinas, N. D.; Hartwig, J. F. *Angew. Chem. Int. Ed.* **2011**, *50*, 3793. (h) Tomashenko, O. A.; Escudero, E. C.; Belmonte, M. M.; Grushin, V. V. *Angew. Chem. Int. Ed.* **2011**, *50*, 7655.

² Cu-catalyzed trifluoromethylation reactions: (a) Oishi, M.; Konda, H.; Amii, H. *Chem. Commun.* **2009**, 1909. (b) Shimizu, R.; Egami, H.; Nagi, T.; Chae, J.; Hamashima Y.; Sodeoka, M. *Tetrahedron Lett.* **2010**, *51*, 5947. (c) Knauber, T.; Arikan, F.; Röschenthaler, G.-V.; Gooßen, L. J. *Chem. Eur. J.* **2011**, *17*, 2689. (d) Xu, J.; Luo, D.-F.; Xiao, B.; Liu, Z.-J.; Gong, T.-J.; Fu, Y.; Liu, L. *Chem. Commun.* **2011**, *47*, 4300. (e) Liu, T.; Shen, Q. *Org. Lett.* **2011**, *13*, 2342.

³ Recent examples of palladium-mediated arene trifluoromethylation reactions: (a) Grushin, V. V.; Marshall, W. J. *J. Am. Chem. Soc.* **2006**, *128*, 4632. (b) Grushin, V. V.; Marshall, W. J. *J. Am. Chem. Soc.* **2006**, *128*, 12644. (c) Grushin, V. V. *Acc. Chem. Res.* **2010**, *43*, 160. (d) Ball, N. D.; Kampf, J. W.; Sanford, M. S. *J. Am. Chem. Soc.* **2010**, *132*, 2878. (e) Ye, Y.; Ball, N. D.; Kampf, J. W.; Sanford, M. S. *J. Am. Chem. Soc.* **2010**, *132*, 14682. (f) Ball, N. D.; Gary, J. B.; Ye, Y.; Sanford, M. S. *J. Am. Chem. Soc.* **2011**, *133*, 7577.

⁴ Pd-catalyzed arene trifluoromethylation reactions: (a) Wang, X.; Truesdale, L.; Yu, J. Q. *J. Am. Chem. Soc.* **2010**, *132*, 3648. (b) Cho, E. J.; Senecal, T. D.; Kinzel, T.; Zhang, Y.; Watson, D. A.; Buchwald, S. L. *Science* **2010**, *328*, 1679. (c) Mu, X.; Chen, S.; Zhen, X.; Liu, G. *Chem. Eur. J.* **2011**, *17*, 6039. (d) Loy, R. N.; Sanford, M. S. *Org. Lett.* **2011**, *13*, 2548. (e) Zhang, X.-G.; Dai, H.-X.; Wasa, M.; Yu, J.-Q. *J. Am. Chem. Soc.* **2012**, *134*, 11948. (f) Zhang, L.-S.; Chen, K.; Chen, G.; Li, B.-J.; Luo, S.; Guo, Q.-Y.; Wei, J.-B.; Shi, Z.-J. *Org. Lett.* **2012**, *15*, 10.

⁵ (a) Litvinas, N. D.; Fier, P. S.; Hartwig, J. F. *Angew. Chem. Int. Ed.* **2012**, *51*, 536. (b) Liu, T.; Shao, X.; Wu, Y.; Shen, Q. *Angew. Chem. Int. Ed.* **2012**, *51*, 540.

⁶ (a) Chu, L.; Qing, F.-L. *J. Am. Chem. Soc.* **2011**, *134*, 1298. (b) Mu, X.; Chen, S.; Zhen, X.; Liu, G. *Chem. –Eur. J.* **2011**, *17*, 6039.

⁷ Examples of arene/heteroarene trifluoromethylation with CF₃•: (a) Wakselman, C.; Tordeux, M. *J. Chem. Soc., Chem. Commun.* **1987**, 1701. (b) Akiyama, T.; Kato, K.; Kajitani, M.; Sakaguchi, Y.; Nakamura, J.; Hayashi, H.; Sugimori, A. *Bull. Chem. Soc. Jpn.* **1988**, *61*, 3531. (c) Sawada, H.; Nakayama, M. *J. Fluorine Chem.* **1990**, *46*, 423. (d) Langlois, B. R.; Laurent, E.; Roidot, M. *Tetrahedron Lett.* **1991**, *32*, 7525. (e) McClinton, M. A.; McClinton, D.A. *Tetrahedron* **1992**, *48*, 6555. (f) Kamigata, N.; Ohtsuka, T.; Fukushima, T.; Yoshida, M.; Shimizu, T. *J. Chem. Soc., Perkin Trans. 1* **1994**, 1339. (g) Kino, T.; Nagase, Y.; Ohtsuka, Y.; Yamamoto, K.; Uruguchi, D.; Tokuhisa, K.; Yamakawa, T. *J. Fluorine Chem.* **2010**, *131*, 98.

- ⁸ Examples of arene perfluoroalkylation with R_F•: (a) Cowell, A.; Tamborski, C. *J. Fluorine Chem.* **1981**, *17*, 345. (b) Dolbier, W. R. *Chem. Rev.* **1996**, *96*, 1557. (c) Bravo, A.; Bjørsvik, H.-R.; Fontana, F.; Liguori, L.; Mele, A.; Minisci, F. *J. Org. Chem.* **1997**, *62*, 7128. (d) Huang, X.-T.; Long, Z.-Y.; Chen, Q.-Y. *J. Fluorine Chem.* **2001**, *111*, 107. (e) Li, Y.; Li, C.; Yue, W.; Jiang, W.; Kopecek, R.; Qu, J.; Wang, Z. *Org. Lett.* **2010**, *12*, 2374.
- ⁹ (a) Ji, Y.; Brueckl, T.; Baxter, R. D.; Fujiwara, Y.; Seiple, I. B.; Su, S.; Blackmond, D. G.; Baran, P. S. *Proc. Nat. Acad. Sci.* **2011**, *108*, 14411. (b) Nagib, D. A.; MacMillan, D. W. C. *Nature* **2011**, *480*, 224. (c) Iqbal, N.; Choi, S.; Ko, E.; Cho, E. J. *Tetrahedron Lett.* **2012**, *53*, 2005.
- ¹⁰ (a) Teverovskiy, G.; Surry, D. S.; Buchwald, S. L. *Angew. Chem. Int. Ed.* **2011**, *50*, 7312. (b) Huang, C.; Liang, T.; Harada, S.; Lee, E.; Ritter, T. *J. Am. Chem. Soc.* **2011**, *133*, 13308.
- ¹¹ For a review on silver perfluoroalkyl complexes: Tyrre, W. E.; Naumann, D. *J. Fluorine Chem.* **2004**, *125*, 823.
- ¹² Wang, Z.; Lee, R.; Jia, W.; Yuan, Y.; Wang, W.; Feng, X.; Huang, K. W. *Organometallics* **2011**, *30*, 3229.
- ¹³ It is possible that light/AIBN do not have an effect on this system because they are just not capable of promoting the Ag–CF₃ bond homolysis (step *a* in **Scheme 3.8**).
- ¹⁴ The different selectivity with CF₃• does not appear to be a temperature or solvent effect. For example, when the Fe-catalyzed reaction of CF₃• with veratrole was conducted at 85 °C, it afforded 10.2 : 1 selectivity (67% yield). Similarly, when DCE was used as the solvent in place of DMSO, the product was obtained with 7.7 : 1 selectivity (4% yield).
- ¹⁵ Hafner, A.; Bräse, S. *Angew. Chem. Int. Ed.* **2012**, *51*, 3713.
- ¹⁶ Zeng, Y.; Zhang, L.; Zhao, Y.; Ni, C.; Zhao, J.; Hu, J. *J. Am. Chem. Soc.* **2013**, *135*, 2955.
- ¹⁷ Wu, X.; Chu, L.; Qing, F.-L. *Angew. Chem. Int. Ed.* **2013**, *52*, 2198.
- ¹⁸ Li, Y. C., T.; Wang, H.; Zhang, R.; Jin, K.; Wang, X.; Duan, C. *Synlett* **2011**, *12*, 1713.
- ¹⁹ Stanek, K.; Koller, R.; Togni, A. *J. Org. Chem.* **2008**, *73*, 7678.
- ²⁰ Zhang, C.-P.; Cai, J.; Zhou, C.-B.; Wang, X.-P.; Zheng, X.; Gu, Y.-C.; Xiao, J.-C. *Chem. Commun.* **2011**, *47*, 9516.
- ²¹ Mejía, E.; Togni, A. *ACS Catal.* **2012**, *2*, 521.
- ²² (a) Wang, X.; Ye, Y.; Zhang, S.; Feng, J.; Xu, Y.; Zhang, Y.; Wang, J. *J. Am. Chem. Soc.* **2011**, *133*, 16410. (b) Parsons, A. T.; Buchwald, S. L. *Angew. Chem. Int. Ed.* **2011**, *50*, 9120. (c) Parsons, A. T.; Senecal, T. D.; Buchwald, S. L. *Angew. Chem. Int. Ed.* **2012**, *51*, 2947. (d) Li, Y.; Studer, A. *Angew. Chem. Int. Ed.* **2012**, *51*, 8221.
- ²³ Chu, L.; Qing, F.-L. *Org. Lett.* **2012**, *14*, 2106.
- ²⁴ Wu, X.; Chu, L.; Qing, F.-L. *Tetrahedron Lett.* **2013**, *54*, 249.
- ²⁵ DeCosta, D.; Pincock, J. *J. Org. Chem.* **2002**, *67*, 9484.
- ²⁶ Stavber, S.; Zupan, M. *J. Org. Chem.* **1983**, *48*, 2223.
- ²⁷ Chen, Q.-Y.; Li, Z.-T. *J. Chem. Soc., Perkin Trans. 1* **1993**, 645.
- ²⁸ Naumann, D.; Kischkewitz, J. *J. Fluorine Chem.* **1990**, *46*, 265.

²⁹ Gerus, I. I.; Yagupol'skii, Yu. L.; Yagupol'skii, L. M. *Journal of Organic Chemistry USSR (English Translation)*, **1985**, *21*, 1694.

CHAPTER 4

Aryltrifluoromethylation via High-Valent Palladium

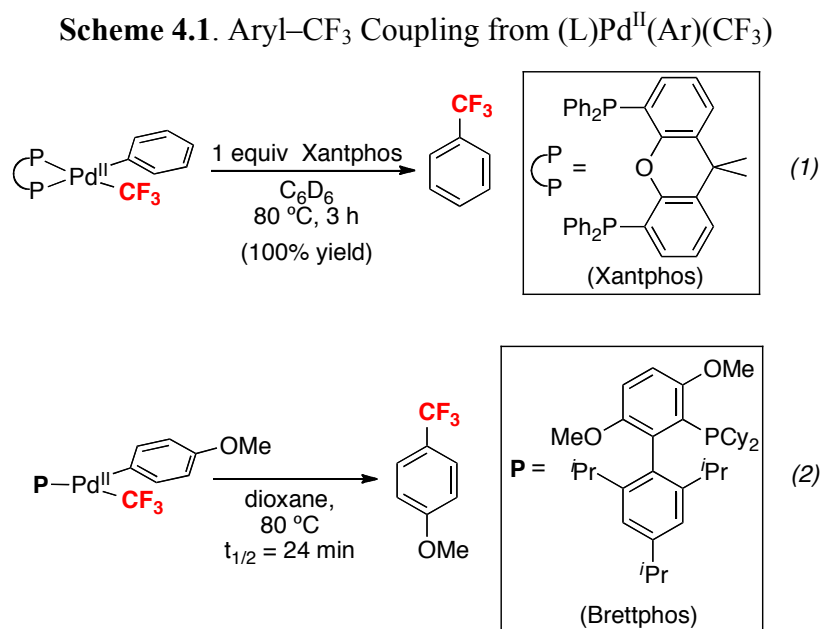
4.1 Background

Molecules featuring aryl-CF₃ motifs have found widespread application in pharmaceuticals, agrochemicals, and materials science.¹ Despite increasing demand for novel methodologies for installing the CF₃ group into target aromatic systems, very few methods exist for direct aryl-CF₃ bond formation under mild conditions.^{1f,2} Consequently, the synthesis of CF₃ containing molecules still heavily relies on the availability of commercially available aryl-CF₃ building blocks derived from traditional functional group interconversion methods, such as the Swarts reaction, which requires reaction temperatures greater than 100 °C and highly reactive fluorinating reagents.³

Transition metal-catalyzed/mediated aromatic trifluoromethylations can serve as desirable alternatives to the Swarts reaction. The presence of a transition metal catalyst could potentially lower the activation barrier and allow trifluoromethylation to proceed with a broad range of substrates under milder reaction conditions.

Pd-catalyzed cross-coupling transformations have emerged as a powerful tool for the construction of a wide variety of C-C bonds.^{4,5} As such, the use of Pd catalysts for aryl-CF₃ bond forming reactions is of particular interest. However, developments in Pd-catalyzed trifluoromethylation have been limited by the challenges associated with a key step of the cross-coupling catalytic cycle, namely, aryl-CF₃ bond-forming reductive elimination from Pd.^{2b,6} In fact, at the time that we initiated this work, only two examples of this transformation had been reported in the literature, and both involved the use of specialized phosphine ligands to induce the desired reactivity. For example, in 2006,

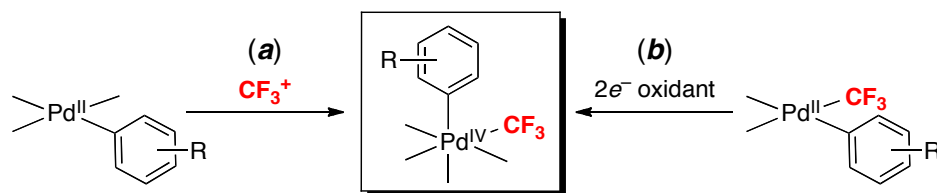
Grushin reported stoichiometric Ph–CF₃ coupling from (Xantphos)Pd^{II}(Ph)(CF₃) (Scheme 4.1, eq. 1).⁷ More recently, Buchwald showed that (Brettphos)Pd^{II}(aryl)(CF₃) also undergoes aryl–CF₃ bond-forming reductive elimination under mild conditions (80 °C, ~30 min) (eq. 2)⁸



4.2 Design Plan

We aimed to achieve aryl–CF₃ coupling from Pd using a different, complementary approach. Rather than modifying the ligands at Pd^{II}, we sought to achieve the desired reactivity by changing the oxidation state of the Pd center from Pd^{II} to Pd^{IV}. This idea was predicted on the fact that Pd^{IV} complexes are well-known to undergo other reductive elimination reactions (eg, C–F, C–Cl, C–I, C–N, C–O) that have proven challenging at Pd^{II} centers.^{4,9} To probe the viability of this strategy, we synthesized and studied the reactivity of Pd^{IV}(aryl)(CF₃) intermediates. Two different synthetic routes were used to access these compounds: the oxidation of Pd^{II}(aryl) complexes with CF₃⁺ reagents (Scheme 4.2a),¹⁰ and the 2e[−] oxidation of pre-formed Pd^{II}(aryl)(CF₃) complexes (Scheme 4.2b).¹¹

Scheme 4.2. Two Synthetic Toutes to Pd^{IV}(aryl)(CF₃) Complexes



4.3 Investigations of Pd^{IV}(Ar)(CF₃) Derived from Oxidation of Pd^{II}-aryl with “CF₃⁺”

Our initial study pursued the synthesis of a Pd^{IV}-CF₃ intermediate through the oxidation of a Pd^{II}-aryl complex with a “CF₃⁺” oxidant. In this case, the oxidant not only changes the oxidation state of the Pd center, but also provides the CF₃ ligand.¹⁰

Exploration of Pd-catalyzed aryl-CF₃ coupling using “CF₃⁺”: We first focused on the Pd(OAc)₂-catalyzed C-H trifluoromethylation of benzo[*h*]quinoline (**1**) with commercial “CF₃⁺” oxidant (**2a-e**) under conditions similar to other C-H functionalization reactions.¹² Our proposed catalytic trifluoromethylation cycle involves: (i) ligand-directed C-H activation to generate a cyclopalladated intermediate, (ii) two-electron oxidation of the palladacycle by a “CF₃⁺” oxidant to generate a Pd^{IV} species, and finally (iii) aryl-CF₃ bond-forming reductive elimination to release the product.

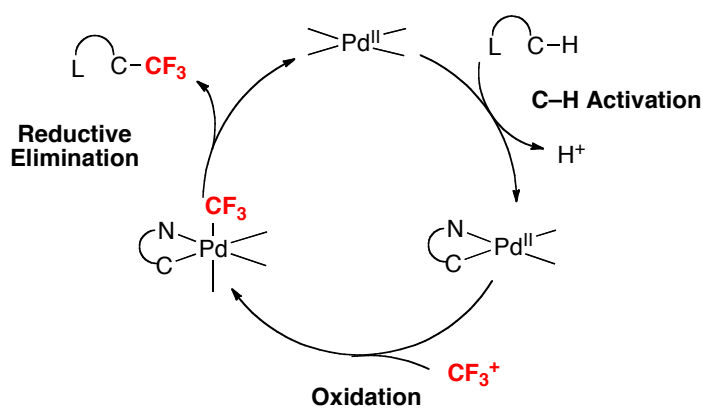
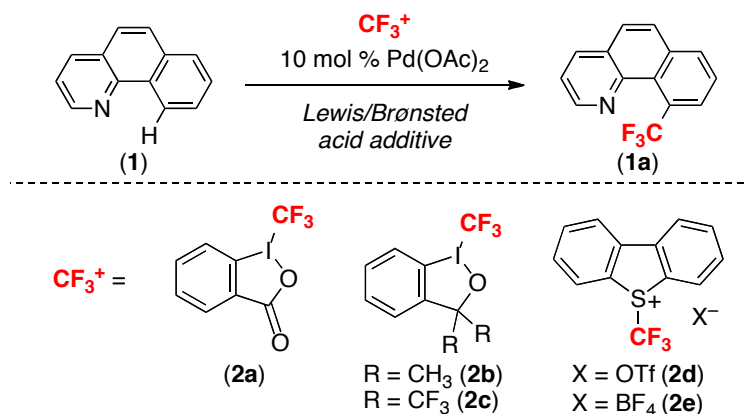


Figure 4.1. Proposed Catalytic Cycle of Pd-Catalyzed C-H Trifluoromethylation

Despite extensive exploration of different reaction conditions, <10% of the desired trifluoromethylated product was observed. Under our best conditions, reaction of

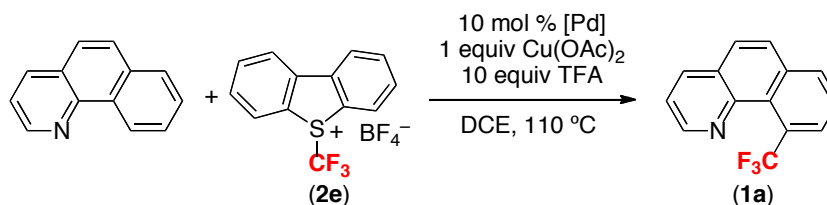
Togni's reagent, **2b**, with substrate **1** in the presence of $\text{Cu}(\text{OTf})_2$ afforded trifluoromethylated product **1a** in only 15% yield (1.5 turnovers of catalyst).

Scheme 4.3. Proposed Pd-Catalyzed C–H Trifluoromethylation using “ CF_3^+ ”



We hypothesized that elucidating the structure and reactivity of catalytically relevant intermediates could potentially help us to rationally address the observed low reactivity. Importantly while we were undertaking these investigations, Yu reported a transformation closely related to the one that we have developed (*vide infra*).¹³ As shown in **Scheme 4.4**, he used the Umemoto reagent **2e** as electrophilic CF_3 source, and the addition of $\text{Cu}(\text{OAc})_2$ and TFA was shown to be critical for achieving high reactivity. Investigation of the catalytic intermediates should provide useful insights to the role of additives like CuOAc and TFA and facilitate the development of Pd-catalyzed C–H trifluoromethylation.

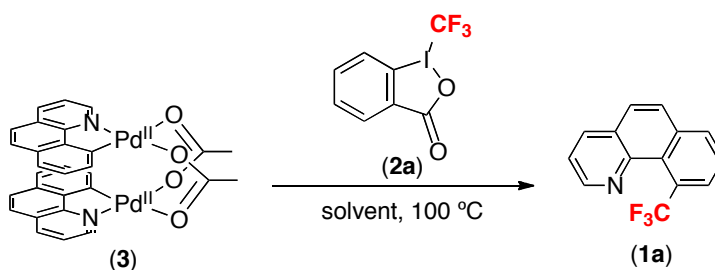
Scheme 4.4. Yu's Pd-Catalyzed C–H Trifluoromethylation with Electrophilic CF_3 Oxidant



Toward this goal, we turned to studying the stoichiometric reaction of a cyclometalated Pd^{II} dimer **3** with “ CF_3^+ ” oxidants. Notably, Pd dimers like **3** can be

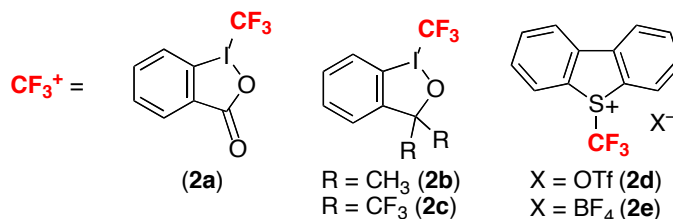
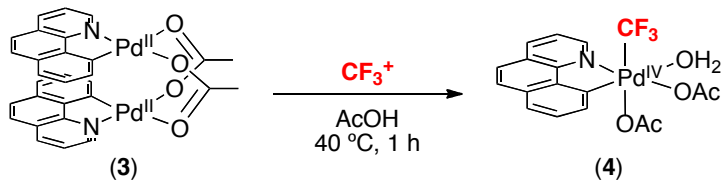
formed under Pd-catalyzed C–H functionalization conditions, and are generally believed to be intermediates during catalysis.^{14,15} The hypervalent iodine(III) CF₃ oxidants (**2a,b**) were chosen because they provided higher yields under the catalytic conditions screened above. Gratifyingly, the stoichiometric reaction of Pd^{II} dimer **3** with **2a** generated **1a** in modest yield in various solvents at 100 °C. This was the first example of achieving aryl–CF₃ bond formation via treatment of a Pd^{II} dimer with an electrophilic CF₃ oxidant.

Table 4.1. Stoichiometric Reaction of **3** and **2a** in Various Solvents



Solvent	Yield
AcOH	33%
CH ₂ Cl ₂	33%
Nitrobenzene	32%
CH ₃ NO ₂	29%
CHCl ₃	27%

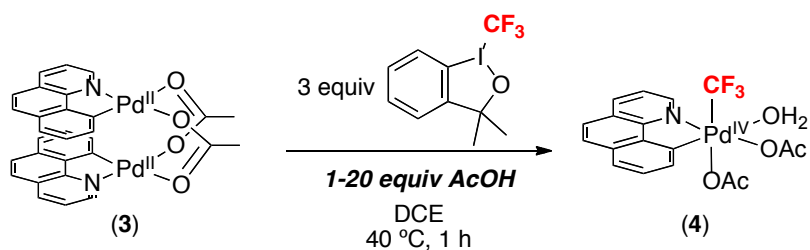
Upon lowering the reaction time and temperature, NMR spectroscopic studies showed the presence of a single Pd–CF₃ intermediate in these reactions. After 1 h at 40 °C **4** was generated in yields ranging from 27-60% (**Table 4.2**). Compared to the Togni reagents (**2a-c**), trifluoromethyl sulfonium oxidants are more stable at high temperature, even in the presence of strong acid (such as TFA). However, only 2-4% of complex **4** was observed in the reactions of Pd^{II} dimer **3** with **2d,e**.

Table 4.2. Oxidation of **3** with Different “CF₃⁺” Reagents^[a]

Entry	Oxidant	Yield 4
1	2a	45%
2	2b	60%
3	2c	27%
4	2d	2%
5	2e	4%

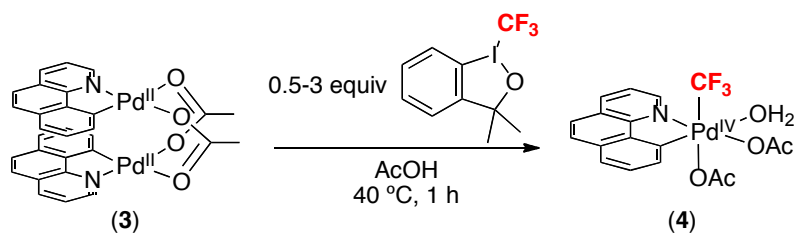
^[a] Conditions: Complex **3** (1 equiv) and “CF₃⁺” reagent (3 equiv) in AcOH (0.4 mL) for 1 h at 40 °C. Yields were determined by ¹⁹F NMR spectroscopy and represent an average of at least two independent runs.

When the solvent was changed to 1,2-dichloroethane, which has been used as a solvent for Pd-catalyzed C–H trifluoromethylation with similar oxidants,¹³ the reaction of **3** with **2b** afforded less than 2% of **4**. However, interestingly, when this same reaction was conducted in the presence of 1-20 equiv AcOH (which is present during catalytic C–H trifluoromethylation, *vide infra*),¹³ **4** was formed in modest to good yield (**Table 4.3**). Complex **4** was isolated in 60% yield as a pale yellow solid from the reaction of **3** with 3 equiv of **2b** in AcOH at room temperature.

Table 4.3. Yield of **4** as a Function of Equiv of AcOH

Entry	Equiv AcOH	Yield 4
1	0	<2%
2	1	48%
3	5	56%
4	20	65%

Complex **4** was the major inorganic product regardless of the equiv of ‘CF₃⁺’ (from 0.5-3) used in this reaction. As shown in **Table 4.4**, lower amounts of oxidant simply led to lower conversion of **3**.

Table 4.4. Yield of **4** as a Function of Equiv of Oxidant

Entry	Equiv 2b	Remaining 3	Yield 4
1	0.5	56%	11%
2	1	62%	38%
3	2	<2%	63%
4	3	<2%	72%

¹H and ¹⁹F NMR spectroscopic analysis of complex **4** at room temperature showed that this molecule contains a cyclometalated benzo[*h*]quinoline, a CF₃ group, and two different acetate ligands. In addition, when samples of **4** were cooled to –40 °C, a

broad ^1H NMR resonance integrating to two protons was observed at 10.45 ppm, implicating the presence of a coordinated water molecule.

The aquo ligand on the Pd center could come from adventitious H_2O in the AcOH solvent. Interesting, only traces of H_2O are required. Nearly identical yield of complex **4** (74% yield as determined by ^{19}F NMR spectroscopy) was observed when the reaction was conducted under inert atmosphere with AcOH solvent freshly dried by distillation over Ac_2O and KMnO_4 .

X-ray quality crystals of **4** were obtained by vapor diffusion of pentanes into a concentrated dichloroethane solution. As shown in **Figure 4.2**, the crystal structure of **4** shows the monomeric Pd^{IV} complex $(\text{bzq})\text{Pd}(\text{CF}_3)(\text{OAc})_2(\text{OH}_2)$. In the solid state, the aquo ligand is *trans* to the aryl group, and it participates in two intramolecular hydrogen bonds with the carbonyl oxygens of the acetate ligands.¹⁶ The $\text{O}_{\text{Ac}}\cdots\text{H}$ bond distances 1.69(5) and 1.82(2) Å are similar to hydrogen bonds reported in $\text{I}^i\text{PrPd}^{\text{II}}(\text{OAc})_2(\text{OH}_2)$ (1.73 and 1.82 Å, I^iPr = 1,3-bis(2,6-diisopropylphenyl)imidazol-2-ylidene).¹⁷ The H-bonding interaction in **4** is also apparent by IR spectroscopy (ν_{OH} (KBr) = 3414 cm^{-1}).

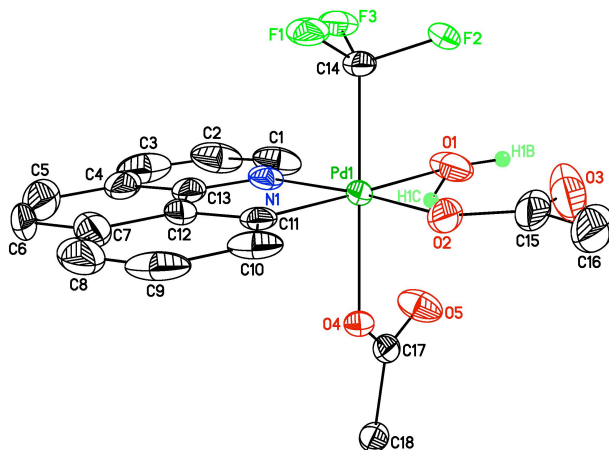
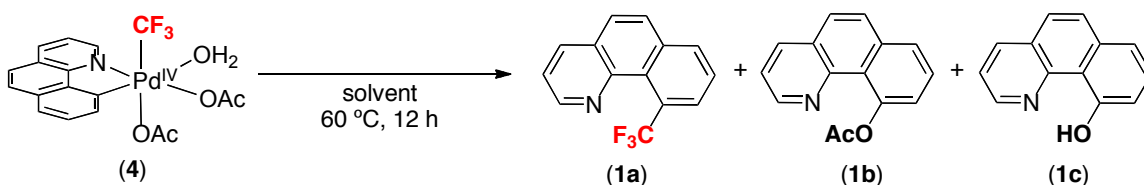


Figure 4.2. ORTEP Drawing of Complex **4**. Thermal ellipsoids are drawn at 50% probability, and hydrogen atoms are omitted for clarity expect for those on the H_2O ligand. The structure was solved as two identical structures in a unit cell (only one is shown for clarity).

Complex **4** is remarkable for several reasons. First, this mono- σ -aryl Pd complex is unusually stable at room temperature. In the solid state, **4** can be stored for at least 1 month without noticeable decomposition; furthermore, the $t_{1/2}$ for decomposition in $\text{CD}_3\text{CO}_2\text{D}$ solution is 16 h at 25 °C. Second, **4** is formed under conditions analogous to those reported for catalytic C–H trifluoromethylation (using CF_3^+ reagents in DCE containing 1-20 equiv of exogenous AcOH),¹³ suggesting the possibility that it is a catalytic intermediate (*vide infra*). Finally, the formation of **4** shows that dimer **3** can be oxidized to afford monomeric Pd^{IV} complexes.

C–CF₃ Bond-Forming Reductive Elimination from 4: Complex **4** could undergo reductive elimination to produce at least three products: bzq–CF₃ (**1a**), bzq–OAc (**1b**), or bzq–OH (**1c**) (Table 4.5). Thus, this system provides an opportunity to assess the relative rates of these different C–CF₃ and C–O bond-forming processes. While C–O bond-forming reductive elimination is well-precedented from palladium(IV)^{9b,18} and many other metal centers/oxidation states,¹⁹ C–CF₃ coupling reactions remain extremely rare in organometallic chemistry.^{11,2b,7-8,20}

Table 4.5. Reductive Elimination from **4** as a Function of Solvent



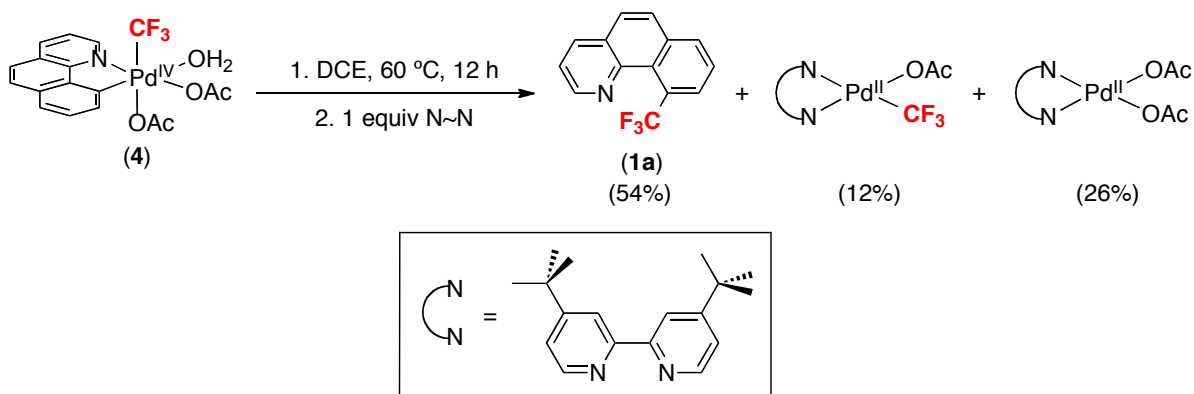
Entry	Solvent	Yield 1a	Yield 1b	Yield 1c
1	AcOH	56%	<2%	<2%
2	DCE	54%	<2%	<2%
3	CHCl_3	62%	<2%	<2%
4	NO_2Ph	57%	<2%	<2%
5	DCE/50 equiv. pyridine	<2%	<2%	84%

Conditions: Complex **6** (1 equiv) in solvent (0.26 mL) for 12 h at 60 °C. Yields were determined by ¹⁹F and ¹H NMR spectroscopy and represent an average of at least two independent runs.

Heating **4** at 60 °C for 12 h in a variety of solvents (AcOH, CHCl₃, DCE, and nitrobenzene) produced trifluoromethylated product **1a** in 54-62% yield along with <2% of **1b** and **1c** (Table 4.5, entries 1-4). We propose that the remarkably high chemoselectivity for C–CF₃ bond formation may be due to hydrogen bonding between the coordinated H₂O and OAc ligands, which slows competing C–O bond coupling. Although no other organic products could be identified in these reactions, we could only account for approximately 60% of the benzo[*h*]quinoline ligand. The only other recognizable benzo[*h*]quinoline-containing product was [(bzoq)Pd(OAc)]₂ (**3**), which was formed in <3% yield.

The inorganic by-products of C–CF₃ bond-forming reductive elimination in DCE were also characterized. After heating **4** to 60 °C for 12 h, di-*tert*-butylbipyridine (dtbpy) was added to trap the Pd-containing species. Stirring the resulting mixture at room temperature for 1 h afforded (*t*-Bu-bpy)(Pd^{II})(CF₃)(OAc) and (*t*-Bu-bpy)(Pd^{II})(OAc)₂ as the major inorganic products (Scheme 4.5).

Scheme 4.5. Characterization of Inorganic Byproduct of Reductive Elimination from **4**

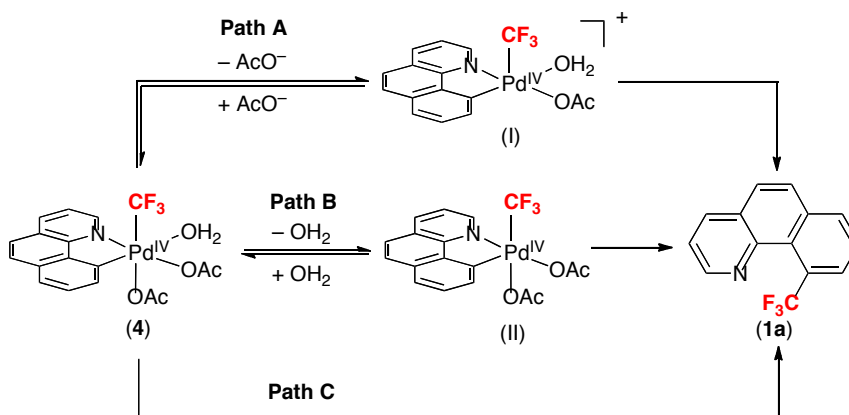


Literature reports have described similarly modest mass balance in other oxidatively-induced reductive elimination reactions from Pd.^{9e,15a,21} In many of these cases, the addition of pyridine (which can bind to highly reactive, coordinatively unsaturated Pd intermediates) led to improved results.^{9e,15a,21} Thus, we also examined the thermolysis of **4** in DCE in the presence of 50 equiv of pyridine. As anticipated, the mass balance improved significantly under these conditions (with 84% of the benzo[*h*]quinoline ligand accounted for). However, intriguingly, the chemoselectivity of

the reaction was reversed, and only the C–O coupled product **1c** was detected by ^1H NMR spectroscopic analysis of the crude reaction mixture (Table 4.5, entry 5). We hypothesize that this dramatic change in selectivity may result from disruption of the H-bonding in **4** (by either deprotonation or displacement of the H_2O ligand by pyridine), which then lowers the activation barrier for C–O bond formation.

Mechanism of C–CF₃ Bond-Forming Reductive Elimination: The most likely mechanisms for C–CF₃ bond-forming reductive elimination from complex **4** are paths **A**, **B**, and **C** in Scheme 4.6. Path **A** involves dissociation of an acetate ligand to afford a five-coordinate cationic intermediate (**I**) followed by C–CF₃ bond-forming reductive elimination to afford **1b**. Path **B** proceeds via dissociation of H_2O to generate a neutral 5-coordinate Pd^{IV} species **II** and subsequent C–CF₃ coupling. Finally, path **C** involves direct reductive elimination from octahedral complex **4**. Notably, ionic dissociative mechanisms (like path **A**),^{22,23} neutral dissociative mechanisms (like path **B**),²⁴ and concerted processes (like path **C**)²⁵ all have significant precedent in reductive elimination reactions from octahedral Pd^{IV} and Pt^{IV} complexes.

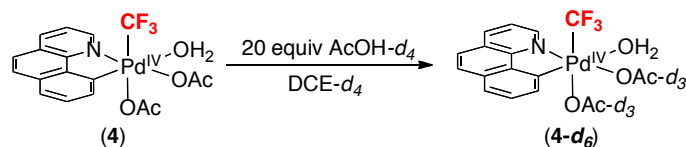
Scheme 4.6. Possible Mechanisms for C–CF₃ Coupling Reductive Elimination from **4**



Our first mechanistic studies probed the viability of carboxylate dissociation/exchange (step i of path **A**). The addition of 20 equiv of $\text{AcOH-}d_4$ or 20 equiv of $\text{NMe}_4\text{OAc-}d_3$ to complex **4** in $\text{DCE-}d_4$ led to complete exchange of both acetate ligands within minutes at room temperature (as determined by ^1H NMR spectroscopic

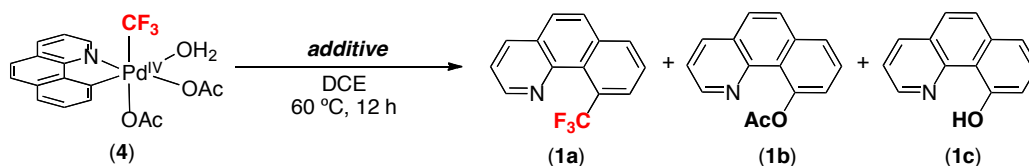
analysis) (**Scheme 4.7**). These results demonstrate that carboxylate ligand substitution is significantly faster than C–CF₃ coupling.

Scheme 4.7. Acetate Dissociation/Exchange on Complex **4**



We next investigated the influence of exogenous NBu₄OAc on C–CF₃ bond-forming reductive elimination from **4**. Interestingly, the addition of 1 equiv of NBu₄OAc almost completely shut down the formation of bzq–CF₃ (**1a**); under these conditions, the major identifiable organic products were oxygenated compounds **1b** and **1c** (**Table 4.6**, entry 3). In the presence of smaller amounts of NBu₄OAc (0.2 equiv), **1a** was formed, but in significantly lower yield than without this additive (26% versus 54% yield, entries 1 and 2, respectively).

Table 4.6. Effect of NBu₄OAc, NBu₄PF₆, and H₂O on Reductive Elimination from **4**^[a]



Entry	Additive	Yield 1a	Yield 1b	Yield 1c
1	None	54%	<2%	<2%
2	0.2 equiv NBu ₄ OAc	26%	<2%	<2%
3	1 equiv NBu ₄ OAc	2%	16%	16%
4	1 equiv NBu ₄ PF ₆	56%	<2%	<2%
5	1 equiv H ₂ O	50%	<2%	<2%
6	10 equiv H ₂ O	50%	<2%	<2%

^[a] Conditions: Complex **4** (1 equiv) and the appropriate additive in DCE (0.26 mL) for 12 h at 60 °C. Yields were determined by ¹⁹F and ¹H NMR spectroscopy and represent an average of at least two independent runs.

Quantitative kinetic analysis of these transformations was complicated by the presence of an induction period. Nonetheless, we found it instructive to compare the reaction profile (yield versus time) in the presence and absence of NBu_4OAc . As shown in **Figure 4.3**, the addition of NBu_4OAc significantly increased the induction period and slowed the rate of bzq-CF_3 coupling. In notable contrast, the addition of NBu_4PF_6 had minimal impact on the yield (**Table 4.6**, entry 4) or reaction profile (**Figure 4.4**) compared to the analogous reaction without additive. This indicates that the dramatic effect of NBu_4OAc is specifically due to the acetate anion.

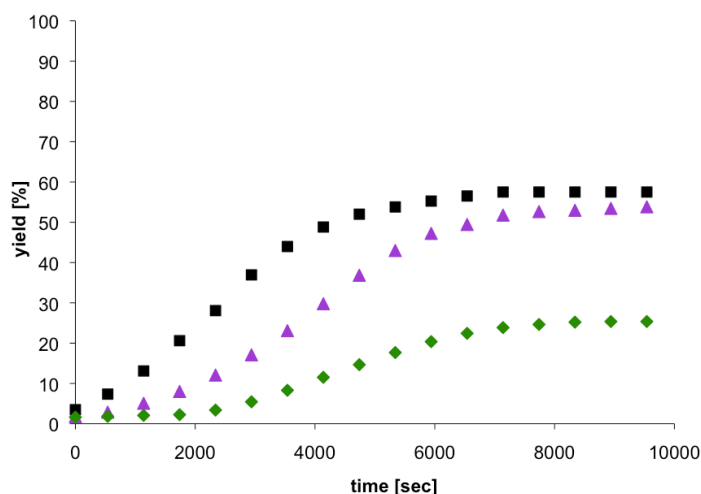


Figure 4.3. Reaction Profile for Reductive Elimination from **4** in DCE at 60 °C in the Presence of No Additive (Black Squares), 1 Equiv of H_2O (Purple Triangles), and 0.2 Equiv of NBu_4OAc (Green Diamonds).

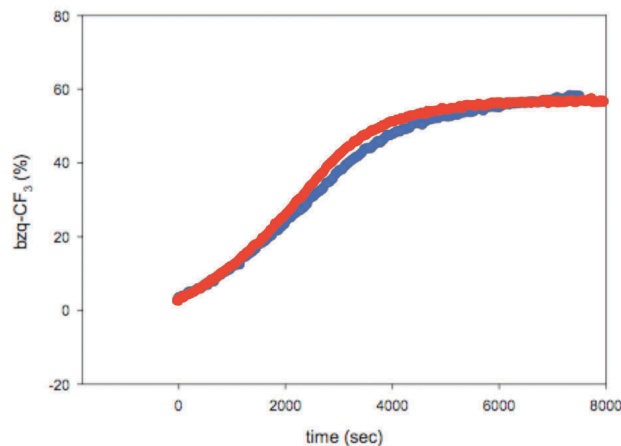


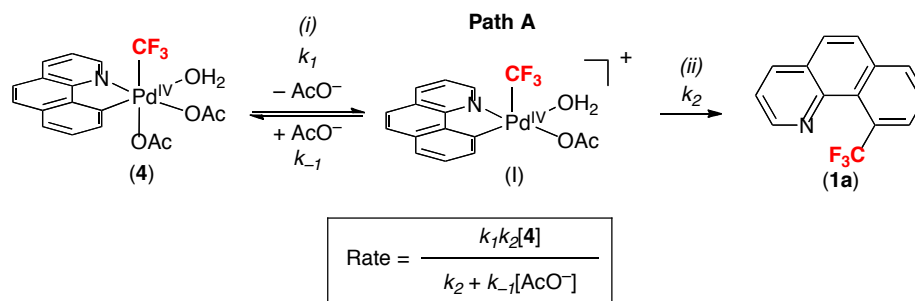
Figure 4.4. Reaction Profile for Reductive Elimination from **4** in DCE at 60 °C in the Presence of 1 Equiv of NBu₄PF₆ (Red Line) and No Additive (Blue Line).

Finally, we examined the influence of H₂O on reductive elimination from **4**. The addition of 1-10 equiv of H₂O had minimal impact on the overall yield of **1a** after 12 h at 60 °C (**Table 4.6**, entries 5 and 6). The presence of 1 equiv of H₂O did slow the rate and increase the induction period for this transformation (**Figure 4.3**); however, this effect was much smaller than that observed with 0.2 equiv NBu₄OAc.

Summary of Mechanistic Data: On the basis of all of this data, we propose that mechanism **A** (involving pre-equilibrium acetate dissociation followed by rate-determining C–CF₃ coupling) is the major pathway for C–CF₃ bond formation from **4**. The AcOH-*d*₄ and NMe₄OAc-*d*₃ exchange experiments indicate that step *i* of path **A** is fast relative to C–CF₃ bond-formation. The inhibition of this reaction by exogenous NBu₄OAc (but not by NBu₄PF₆) is consistent with the expected inverse 1st order dependence on [AcO[−]].

The acetate exchange experiments indicate that step *i* is fast relative to C–CF₃ bond-formation (step *ii*). As such, a rate law for this transformation can be derived using the steady state approximation for 5-coordinate intermediate I. When $k_{-1} > k_2$, this rate law predicts an inverse 1st order dependence on [AcO[−]].

Scheme 4.8. Derivation of Rate Expression of Path A



Importantly, the current data *do not definitively rule out mechanisms B or C as competing pathways*. However, the comparatively small influence of added H₂O on the product distribution, yield, and reaction profile is consistent with mechanism **A** as the most significant contributor to this transformation.

Effects of Additives on C–CF₃ Bond-Forming Reductive Elimination from 4:

On the basis of several literature reports,^{9b,26} we hypothesized that pre-equilibrium dissociation of acetate would be promoted by Brønsted acids [*e.g.*, trifluoroacetic acid (TFA)], Lewis acids (*e.g.*, Yb(OTf)₃), and other reagents that react readily with free AcO[−] [*e.g.*, trifluoroacetic anhydride (TFAA)]. As such, we next examined the effect of these additives on reductive elimination from **4**. As shown in **Figure 4.5**, the addition of 10 equivalent of TFA, TFAA, or 1 equiv of Yb(OTf)₃ eliminated the induction period and provided first order kinetic profiles for bzq–CF₃ coupling.

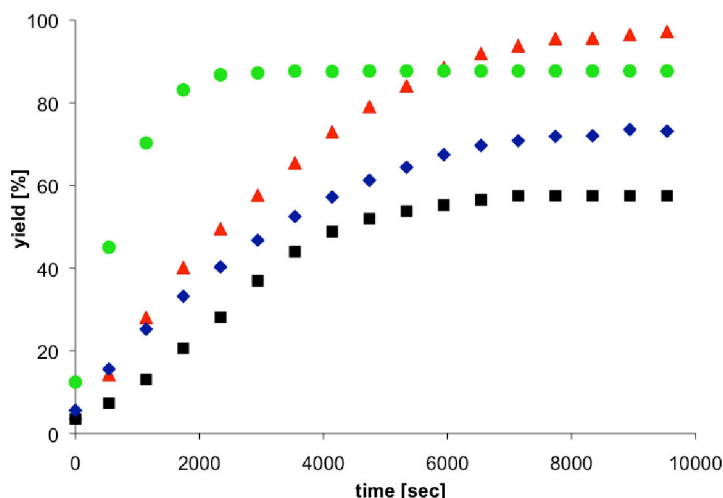
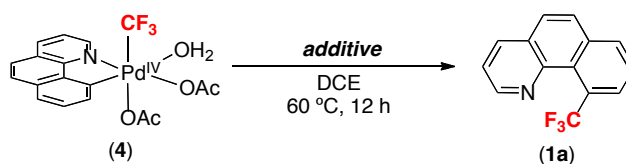


Figure 4.5. Reaction Profile for Reductive Elimination from **4** in DCE at 60 °C in the Presence of No Additive (Black Squares), 10 equiv of TFA (Blue Diamonds), 10 Equiv of TFAA (Green Circles), and 1 Equiv of Yb(OTf)₃ (Red Triangles).

Additionally, these additives led to substantial increases in the yield of C–CF₃ coupled product **1a** (Table 4.7). Most notably, with 1 equiv of Yb(OTf)₃, nearly quantitative yield of **1a** was obtained (compared to 54% in the absence of this additive).

Table 4.7. Effect of Acidic/Electrophilic Additives on Reductive Elimination from **4**



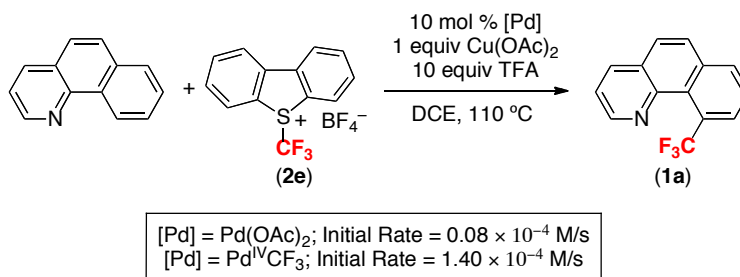
Entry	Additive	k_{obs} (s ⁻¹)	Yield 1a ^[a]
1	None	nd ^[b]	54%
2	10 equiv TFA	$3.31 \pm 0.04 \times 10^{-4}$	73%
3	10 equiv TFAA	$1.43 \pm 0.02 \times 10^{-3}$	84%
4	1 equiv Yb(OTf) ₃	$2.92 \pm 0.03 \times 10^{-4}$	99%

^[a] Conditions: Complex **4** (1 equiv) and the appropriate additive in DCE (0.26 mL) for 12 h at 60 °C. Yields were determined by ¹⁹F and ¹H NMR spectroscopy and represent an average of at least two independent runs. ^[b] k_{obs} could not be determined for this reaction due to an induction period.

These effects provide further support for mechanism **A** (**Scheme 4.6**) as a major pathway for C–CF₃ coupling in this system. Additionally, the observed enhancements in mass balance suggest that the acidic/electrophilic additives may play a role in sequestering reactive, coordinatively unsaturated Pd intermediates formed during the reductive elimination process.

Catalytic Competence of 4 in Pd-Catalyzed C–H Trifluoromethylation: As discussed above, a recent communication by Yu and coworkers demonstrated the Pd(OAc)₂-catalyzed C–H trifluoromethylation of benzo[*h*]quinoline with oxidants **2d**, and **2e** in DCE.¹³ The addition of 1 equiv of Cu(OAc)₂ and 10 equiv of TFA was critical to promote catalytic turnover in these reactions (**Scheme 4.9**); however, no insights were provided regarding the mechanistic role of these additives. In addition, while the authors speculated that a Pd^{II/IV} pathway was plausible in this system, no mechanistic experiments were reported.

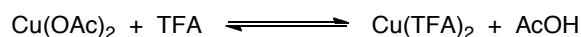
Scheme 4.9. Initial Rates of C–H Trifluoromethylation using Pd(OAc)₂ and Complex **4**



We hypothesized that Pd^{IV} complex **4** might be an intermediate in this catalytic transformation. Using the method of initial rates, we compared the trifluoromethylation of benzo[*h*]quinoline with **2e** using 10 mol % of Pd(OAc)₂ to that with 10 mol % of complex **4** under otherwise identical conditions. As shown in **Scheme 4.9**, the initial rate with **4** was 18-fold faster than that with Pd(OAc)₂. Furthermore, both catalysts provided similar yields of product **1a** when the reactions were followed to completion. These results clearly demonstrate the kinetic competence of **4** and establish the potential viability of this monomeric Pd^{IV} species as a catalytic intermediate.

Role of Promoters in Catalytic C–H Trifluoromethylation: The demonstration that **4** is a catalytically competent intermediate in C–H trifluoromethylation provided a platform for rationalizing the role that the promoters Cu(OAc)₂ and TFA play in the catalytic cycle. All of the studies described above suggest that these additives are important for both the formation of and C–CF₃ reductive elimination from Pd^{IV} complex **4**. As shown in **Table 4.3**, the generation of **4** by oxidation of **3** with CF₃⁺ requires the presence of at least 1 equiv of AcOH. Under the catalytic conditions, the combination of Cu(OAc)₂/TFA would provide an initial source of AcOH through the equilibrium in **Scheme 4.10**.

Scheme 4.10. *In-Situ* Formation of AcOH



The results in **Table 4.7** demonstrate that acidic additives can increase the rate, yield, and mass balance of C–CF₃ bond-forming reductive elimination from **4**. To test whether catalytically relevant quantities of Cu(OAc)₂/TFA have a similar effect, we studied the thermolysis of **4** in the presence of 10 equiv of Cu(OAc)₂ and 100 equiv of TFA. Under these conditions, reductive elimination occurred extremely rapidly and in nearly quantitative yield (94% compared to 54% in the absence of Cu/TFA) (**Figure 4.6**). These results indicate that the added Cu(OAc)₂/TFA could serve to: (i) accelerate reductive elimination from a Pd^{IV} intermediate like **4** and (ii) limit competing unproductive decomposition pathways of this high oxidation state complex that reduce the yield of bzq–CF₃ (**1a**).

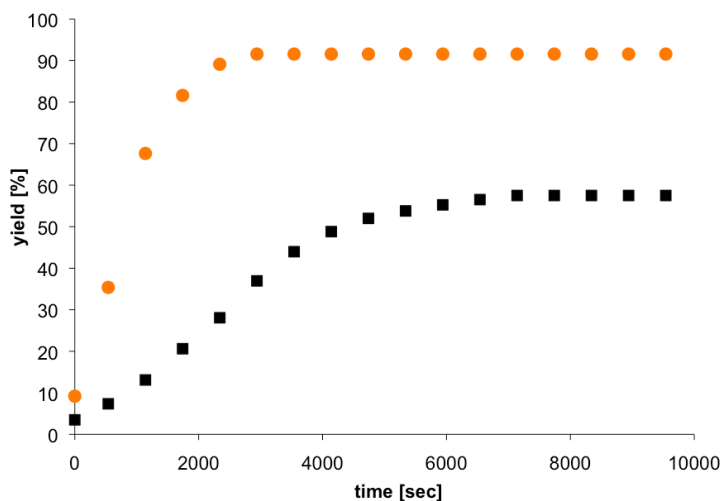


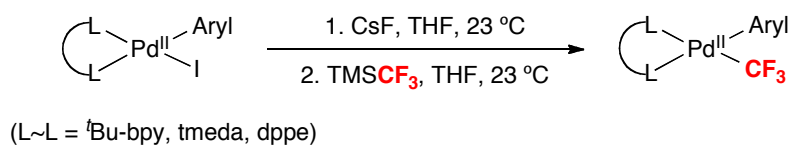
Figure 4.6. Reaction Profile of Reductive Elimination from **4** in the Presence of No Additive (Black Squares) and 10 Equiv Cu(OAc)₂/100 Equiv TFA (Orange Circles).

4.4 Studies of Pd^{IV}(aryl)(CF₃) Generated by Oxidation of Pd^{II}(aryl)(CF₃)

Another way to access Pd^{IV}(aryl)(CF₃) complexes is by oxidation of a Pd^{II}(aryl)(CF₃) species with a 2 e⁻ oxidant.¹¹ This work was done in collaboration with Dr. Nicholas D. Ball and Dr. J. Brannon Gary. Dr. Ball initiated the project and designed and performed the synthesis and characterization of the Pd^{II} and Pd^{IV} complexes. He further studied their reactivity, and investigated the mechanistic details of aryl-CF₃ coupling from these species. Dr. Gary performed the DFT calculations. My contributions focused on exploring the feasibility of accessing Pd^{II}(aryl)(CF₃) intermediates under common Pd-catalyzed reaction conditions. I was also involved in some of the kinetic studies.

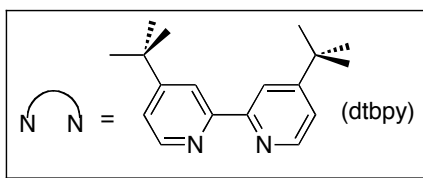
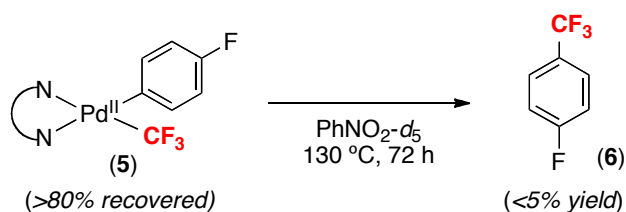
Our plan was to design an isolable Pd^{IV}(aryl)(CF₃) complex to study its reactivity towards aryl-CF₃ coupling. Based on our previous studies of stable Pd^{IV} complexes,^{9c} we chose a variety of rigid, bidentate N- and P-donor ligands to stabilize the potential Pd^{IV} species. As a result, a series of Pd^{II} complexes with general structure (L)₂Pd^{II}(aryl)(CF₃) were prepared by reacting (L)₂Pd^{II}(aryl)(I) intermediates with TMSCF₃ (a CF₃⁻ reagent) and CsF (**Scheme 4.11**).^{7,27}

Scheme 4.11. Synthesis of (L)₂Pd^{II}(aryl)(I) Complexes from (L)₂Pd^{II}(aryl)(CF₃)

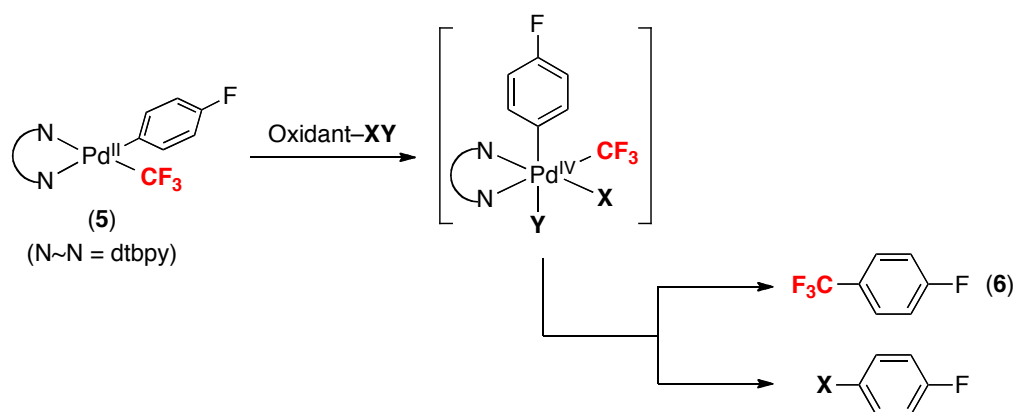


Heating (^tBu-bpy)Pd^{II}(*p*-FC₆H₄)(CF₃) **5** at 130 °C in the absence of an oxidant afforded less than 5% of the desired product and >80% recovered starting material. This observation is consistent with the low reactivity of similar Pd^{II}(aryl)(CF₃) complexes reported in the literature.^{7,27}

Scheme 4.12. Sluggish Aryl–CF₃ Coupling from Pd^{II}(aryl)(CF₃)

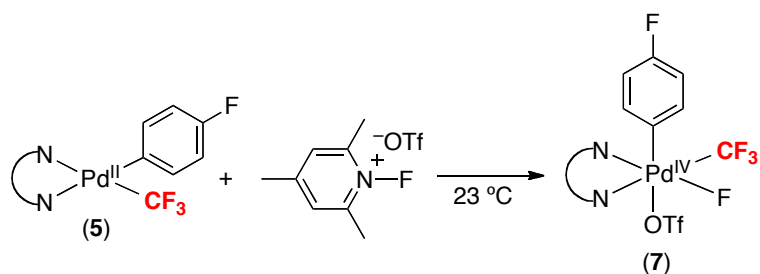


We hypothesized that reaction of a 2 *e*⁻ oxidant with Pd^{II}(aryl)(CF₃) should afford more reactive Pd^{IV}–CF₃ complexes that might lead to the desired aryl–CF₃ reductive elimination products. Subjecting complex **5** to *N*-bromosuccinimide (NBS), *N*-chlorosuccinimide (NCS), or PhI(OAc)₂ led to rapid consumption of the starting complex, but afforded none of the desired aryl–CF₃ product. Instead, aryl–X (X = Br, Cl, or OAc), was generated by competing reductive elimination at the Pd^{IV} center (**Scheme 4.13**).

Scheme 4.13. Competing Reductive Eliminations from Pd^{IV}(aryl)(CF₃)(X)(Y)

We next turned our attention to the use of electrophilic fluorinating oxidants (F⁺ reagents). We reasoned that oxidation of the Pd^{II}(aryl)(CF₃) complex with an F⁺ reagent should introduce a fluoride ligand that might be less kinetically reactive toward reductive elimination than CF₃.^{9c,28} Gratifyingly, reactions between **5** and a variety of F⁺ oxidants generated the aryl–CF₃ coupling products in good to excellent yields after 3 h at 80 °C. *N*-fluoro-1,3,5-trimethylpyridinium triflate (NFTPT) proved to be the optimal oxidant (70% yield of aryl–CF₃). Remarkably, less than 5% of the aryl–F and/or aryl–OTf was generated under these conditions.

In an effort to isolate the high oxidation state Pd intermediate and further study the influence of each reaction partner, we monitored the reaction of **5** with NFTPT at lower temperature (23 °C). A single reaction intermediate was observed and isolated as a yellow solid in 53% yield. An X-ray crystal structure revealed a monomeric Pd^{IV} complex **7** with the aryl group in the axial position and the CF₃ and F ligands on the equatorial plane.

Scheme 4.14. Formation of Pd^{IV} Complex **7**

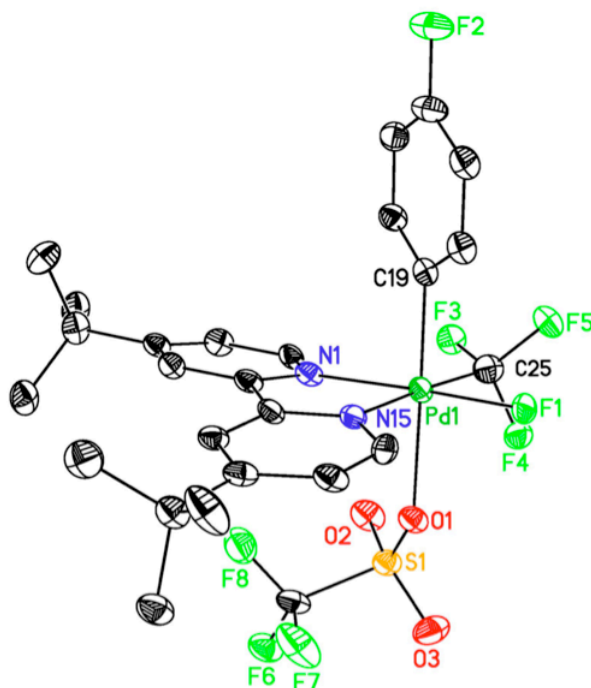
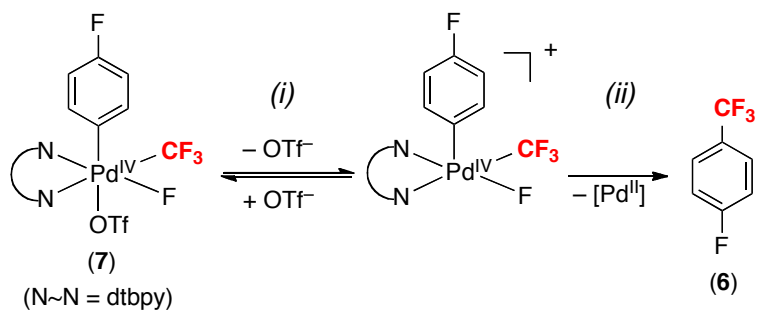


Figure 4.7. ORTEP Drawing of Complex 7. Thermal ellipsoids are drawn at 50% probability, hydrogen atoms are omitted for clarity unless otherwise noted.

A series of mechanistic studies were performed to explore the pathway of the aryl-CF₃ reductive coupling. First, the reaction rate was found to show an inverse first order dependence on [triflate]. Furthermore, enhanced solvent polarity accelerated the aryl-CF₃ coupling. Both mechanistic observations suggested an ionic reaction pathway that involves: (i) initial triflate dissociation to form a new cationic Pd^{IV} intermediate followed by (ii) aryl-CF₃ bond formation from this cationic complex.

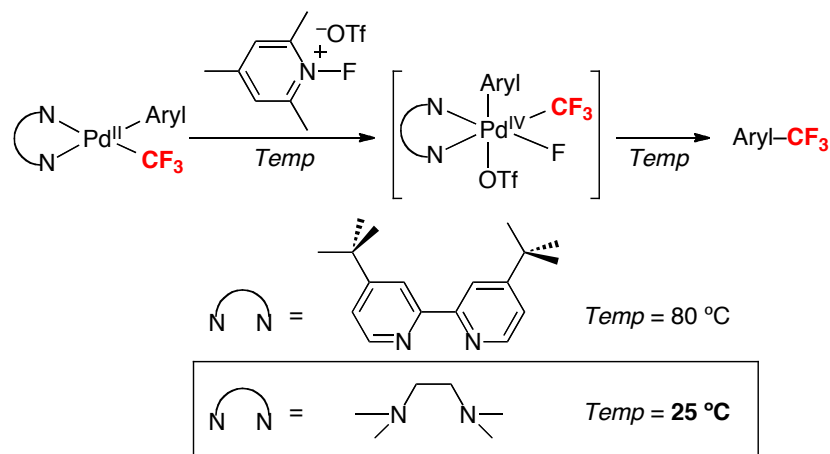
Scheme 4.15. Aryl-CF₃ Coupling Pathway from Pd^{IV} Complex 7



An observation that we cannot explain experimentally is the selectivity for C–CF₃ vs C–F coupling from complex **7**. To fully explore the competing aryl–CF₃ and aryl–F bond formation, we next turned to DFT calculations. Gratifyingly, our DFT model showed slightly lower activation energy for the C–CF₃ coupling than for the C–F bond formation. Moreover, the calculated overall activation enthalpy ($\Delta H_{298}^{\ddagger} = 28.7$ kcal/mol) is in excellent agreement with our experimental value of 29.1 ± 0.2 kcal/mol.

Literature precedent has shown that the use of more flexible tmeda (*N,N,N',N'*-tetramethylethylenediamine) increases the rate of C–C coupling from the related Pd^{IV} complexes (N–N)Pd^{IV}(CH₃)₂(Ph)(I).²⁹ These results led us to propose that replacing the dtbpy ligand with more flexible ligand, such as tmeda, could result in a more facile aryl–CF₃ coupling. DFT calculations further endorsed this hypothesis, showing lower ΔH^{\ddagger} from (tmeda)Pd^{II}(aryl)(CF₃) in both the triflate dissociation and aryl–CF₃ coupling steps. To our delight, experimental studies unambiguously confirmed the predicted reactivity. Subjecting (tmeda)Pd^{II}(Ph)(CF₃) to NFTPT afforded 83% yield of the Ph–CF₃ coupling product at temperatures as low as 23 °C. This is the first example of aryl–CF₃ coupling from a Pd center at room temperature.

Scheme 4.16. Facile Aryl–CF₃ Coupling from (tmeda)Pd^{IV}(Ph)(CF₃)



The study of (L)₂Pd^{IV}(aryl)(CF₃) complexes provides useful mechanistic insights for the development of future catalytic trifluoromethylation systems. However, the requirement of (L)₂Pd^{II}(aryl)(I) intermediates to access the corresponding Pd^{IV}–CF₃

species could be problematic in a catalytic system for several reasons. First, the presence of an iodide ligand could lead to competing aryl–I bond forming reactions. Second, the generation of stoichiometric amounts of iodide waste is not desirable from economic and environmental points of view. To our delight, the tmeda complex can also be prepared by reacting $(\text{tmeda})\text{Pd}^{\text{II}}(p\text{-CF}_3\text{C}_6\text{H}_4)(\text{X})$ ($\text{X} = \text{acetate}$, trifluoroacetate or triflate) with $\text{CsF}/\text{TMSCF}_3$ in THF. This synthetic pathway avoids the requirement for iodine containing starting materials, and is relevant and potentially useful for developing catalytic C–H fluorination reactions using $\text{Pd}(\text{OAc})_2$, $\text{Pd}(\text{TFA})_2$, or $\text{Pd}(\text{OTf})_2$.

Scheme 4.17. Generation of $(\text{tmeda})\text{Pd}^{\text{II}}(\text{aryl})(\text{CF}_3)$ from Potential Intermediates of Pd-Catalyzed Trifluoromethylations



4.5 Conclusions

In this chapter, we have demonstrated that $\text{Pd}^{\text{IV}}(\text{aryl})(\text{CF}_3)$ undergoes facile aryl– CF_3 bond formation under very mild reaction conditions (even at room temperature). Overall, we anticipate that these detailed mechanistic/organometallic investigations will facilitate the rational design of new catalysts, promoters, and reagents for the development of Pd-catalyzed aromatic trifluoromethylation.

Two distinct synthetic approaches were adopted to access the key $\text{Pd}^{\text{IV}}(\text{aryl})(\text{CF}_3)$ complexes via either electrophilic (CF_3^+) or nucleophilic (CF_3^-) transfer of the CF_3 group to the metal center. In the first example, we studied the oxidation of cyclometalated Pd dimer $[(\text{bzq})\text{Pd}(\text{OAc})]_2$ (**3**) with CF_3^+ reagents to generate monomeric Pd^{IV} trifluoromethyl complex **4**. This complex undergoes highly chemoselective C– CF_3 bond-forming reductive elimination that is accelerated by acidic additives. Complex **4** is also a kinetically competent catalyst for the C–H trifluoromethylation of benzo[*h*]quinoline with CF_3^+ reagents. These studies provide new insights into the role of the promoters $\text{Cu}(\text{OAc})_2$ and TFA in the catalytic transformations. Specifically, these additives appear

to: (1) serve as a source of AcOH (which is critical for the oxidation of dimeric [(bzq)Pd(OAc)]₂ **3** to monomeric **4**) and (2) accelerate and enhance mass balance in C–CF₃ coupling from **4**.

More importantly, our studies of generating Pd^{IV}(aryl)(CF₃) with CF₃⁺ reagents predict the viability of catalytic cycles like that in **Figure 4.8** for Pd^{II/IV}-catalyzed trifluoromethylation. This cycle involves initial generation of Pd^{II}(aryl) intermediate **B** via C–H activation or transmetalation (step *i*), oxidation of **B** with CF₃⁺ (step *ii*), and subsequent C–CF₃ coupling (step *iii*), which releases the trifluoromethylated product. The first Pd-catalyzed C–H trifluoromethylation reaction reported by Yu and co-workers is an elegant realization of this mechanistic strategy.¹³ We anticipate that this pathway could prove broadly useful for a number of different Pd-catalyzed transformations for introducing CF₃ groups into organic molecules.

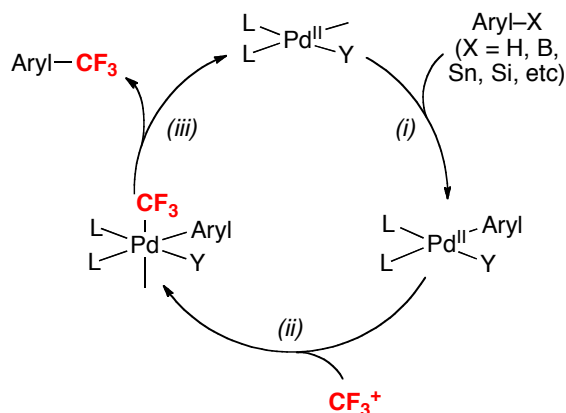


Figure 4.8. General Catalytic Cycle for Pd-catalyzed Oxidative Trifluoromethylation with CF₃⁺ Reagents

In our second approach to access Pd^{IV}(aryl)(CF₃) intermediates, the scope of applicable oxidants is not limited to electrophilic CF₃ reagents. This work provides the basis for the development of many different types of Pd^{II/IV}-catalyzed aryl–CF₃ cross-coupling reactions. A potential catalytic cycle for such transformations is outlined in **Figure 4.9**. Step *i* involves the formation of a Pd^{II}(aryl) complex. This could occur, for example, by C–H activation (X = H) or transmetalation (X = B, Sn, Si). Subsequent reaction with TMSCF₃ (step *ii*) would yield Pd^{II}(aryl)(CF₃). Two-electron oxidation of

this intermediate (step *iii*) followed by aryl–CF₃ bond-forming reductive elimination (step *iv*) would then furnish the trifluoromethylated product and regenerate the catalyst.

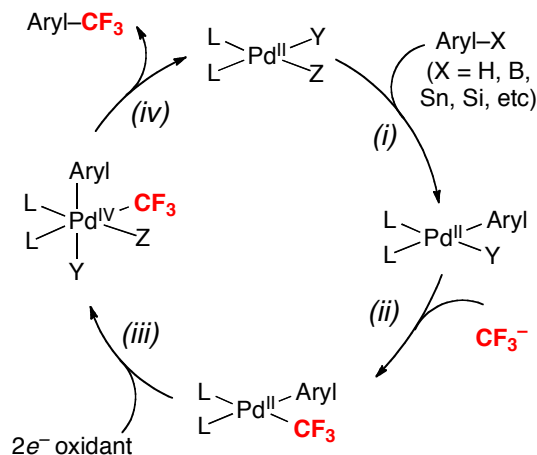
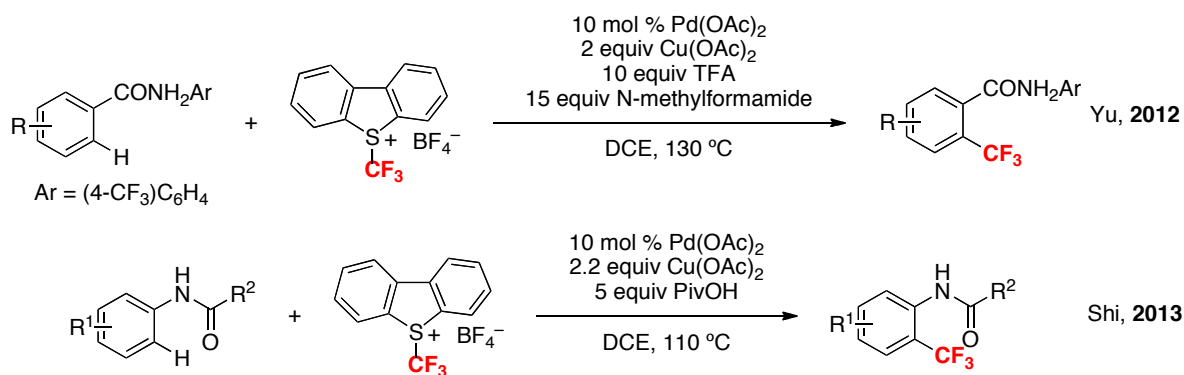


Figure 4.9. General Catalytic Cycle for Pd-Catalyzed Oxidative Trifluoromethylation with CF_3^- Reagents

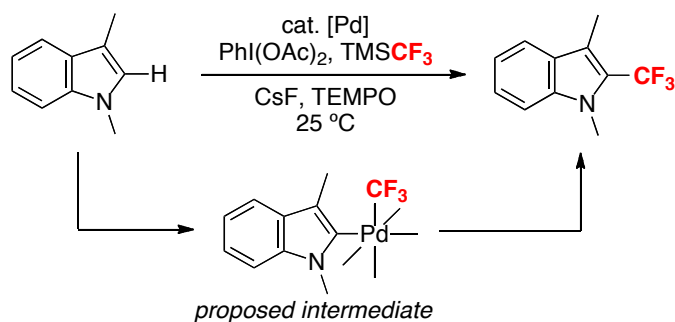
4.6 Subsequent Developments

We anticipate both of our proposed pathways could prove broadly useful for the future development of Pd-catalyzed transformations for introducing CF_3 groups into organic molecules. Indeed, after our initial reports, several synthetically useful Pd-catalyzed trifluoromethylation reactions have been demonstrated. Notably, all of these transformations were conducted under oxidative conditions, and were believed to proceed through a catalytic cycle similar to that proposed in **Figures 4.8** and **4.9**.

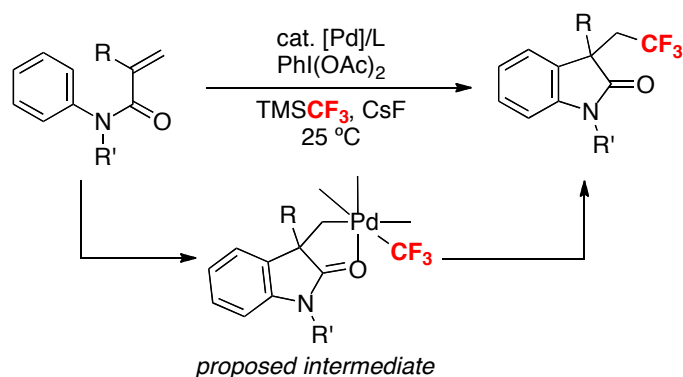
Following Yu's first report of Pd-catalyzed *ortho*-trifluoromethylation of arenes with CF_3^+ reagent, Yu³⁰ and Shi³¹ expanded the substrate scope of this protocol to include *N*-arylbenzamides and acetanilides as transformable directing groups (**Scheme 4.18**). These results are remarkable since *N*-arylbenzamides and acetanilides could be converted to other common functional motifs, whereas the previously studied pyridine based directing groups are not suitable for further elaboration. Notably, Lewis acid additives were essential for achieving high reactivity in both cases, presumably due to their capability to promote aryl–CF₃ coupling from $Pd^{IV}(aryl)(CF_3)$.

Scheme 4.18. Pd-Catalyzed Trifluoromethylation of *N*-Arylbenzamides and Acetanilides

Additionally, several Pd-catalyzed trifluoromethylation reactions have been realized using CF_3^- reagent in the presence of an oxidant. For example, a recent report by Liu and coworkers exploited this strategy for the Pd-catalyzed C–H trifluoromethylation of indoles (**Scheme 4.19**).³² While detailed mechanistic investigations of this transformation have not yet been conducted, the combination of aryl–H (indole), TMSCF_3 , and an oxidant [$\text{PhI}(\text{OAc})_2$] was proposed to react via a similar cycle to that proposed in **Figure 4.9**. Another related pathway has also been proposed for the Pd-catalyzed aryltrifluoromethylation of activated alkenes (**Scheme 4.20**).³³

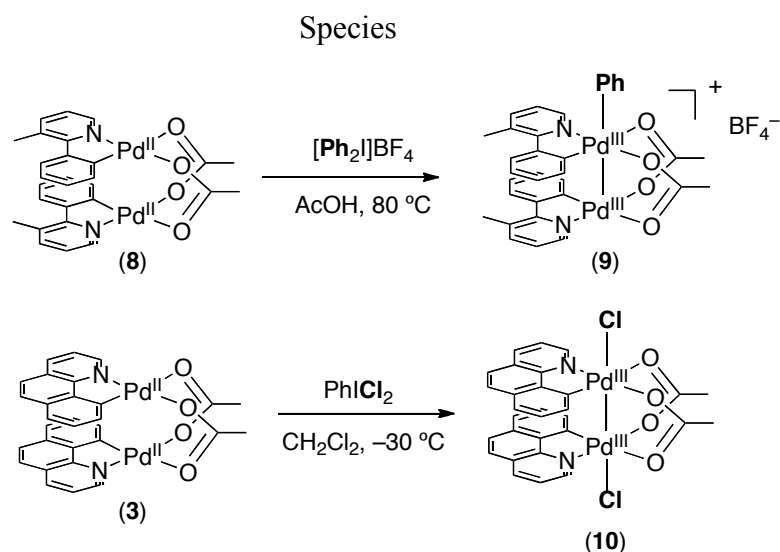
Scheme 4.19. Pd-Catalyzed Oxidative Trifluoromethylation of Indoles

Scheme 4.20. Pd-Catalyzed Oxidative Aryltrifluoromethylation of Activated Alkenes



Our studies into the oxidation of cyclometallated Pd^{II} dimers also have shed some light on the nature of the catalytically active high oxidation state Pd intermediates in Pd-catalyzed C–H functionalization under oxidative conditions. Despite tremendous progress on new reaction development, the nuclearity of the active Pd intermediates in these transformations remains the subject of intense study and discussion.^{9d,34,35} For example, monomeric,^{36,9b,c,9e,9h} dimeric,^{14,15} and trimeric³⁷ Pd complexes in oxidation states ranging from +2 to +4 have all been proposed as catalytically active species.^{9d,34}

Scheme 4.21. Binuclear Pd^{III/IV} or Pd^{III} Complexes from Oxidation of Dimeric Pd^{II}

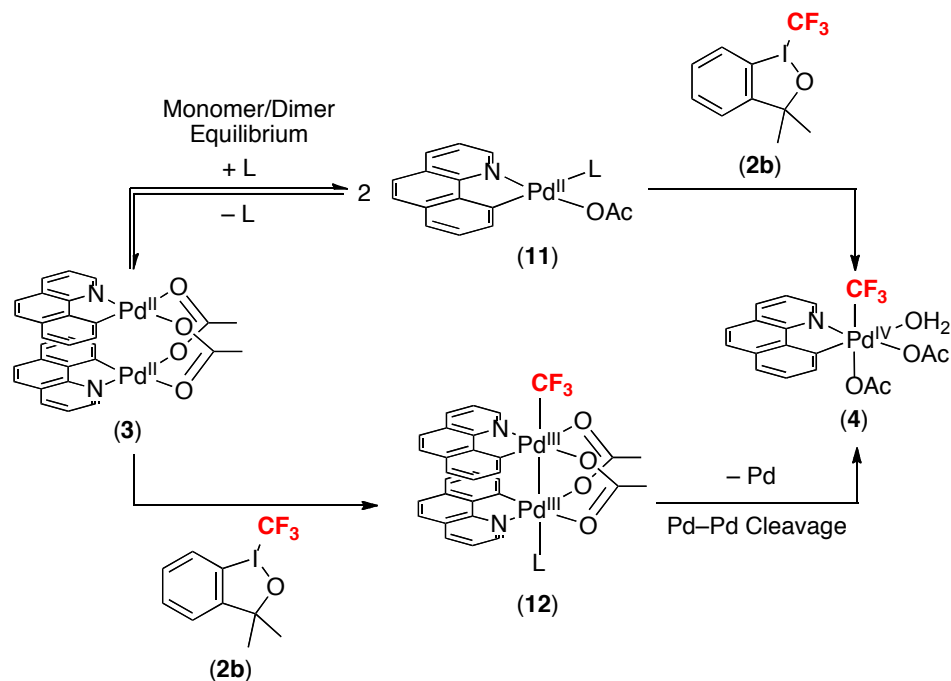


Several recent reports have focused on the role of cyclometallated Pd^{II} dimers like **3** and **8** (Scheme 4.21, eqs 1 and 2) as intermediates in Pd-catalyzed C–H

functionalization.^{14,15} For example, the oxidation of **8** to generate acetate-bridged Pd dimer **9** has been kinetically implicated as the turnover-limiting step in C–H arylation reactions (**Scheme 4.21**, eq. 1).¹⁴ Similar dimeric Pd^{III} adducts **10** have been isolated from the stoichiometric reaction of complex **3** (and analogues) with PhICl₂ and PhI(OAc)₂ (**Scheme 4.21**, eq. 2).¹⁵ Our study on the oxidation of cyclometallated Pd^{II} dimer **3** shows that monomeric Pd^{IV} intermediates such as complex **4** can also be formed under catalytically relevant conditions.¹⁰ We believe this study reiterates the complexities in possible mechanisms for arene functionalization via high oxidation state palladium intermediates.

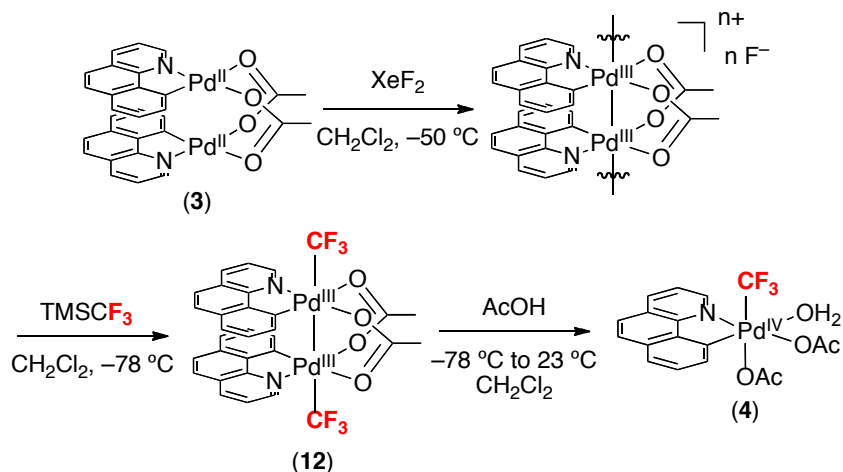
After our initial report on the formation of stable Pd^{IV}(aryl)(CF₃) complex **4** and its reactivity toward selective aryl–CF₃ coupling, we began to focus on understanding the origin of this monomeric Pd^{IV} intermediate from a dimeric Pd^{II} complex **3**. Our initial studies focused on monitoring the formation of Pd^{IV}(aryl)(CF₃) complex at low temperature by ¹⁹F NMR. However, lowering the temperature down to –20 °C didn't show any new Pd–CF₃ species. Moreover, reactions of cyclometallated Pd^{II} adduct **3** with less than 1 equiv of CF₃⁺ reagent did not afford any new fluorine signals. These results tend to suggest that the formation of Pd^{IV}(aryl)(CF₃) complex **4** proceeds via fragmentation of the dimeric Pd^{II} adduct **3** to two mononuclear Pd^{II} complexes **11**, followed by monometallic oxidation. However, it is important to note that our current data cannot rule out an alternative pathway: initial bimetallic oxidation of **3** to a binuclear Pd^{III} intermediate **12**, followed by Pd–Pd bond heterolysis.

Scheme 4.22. Possible Pathways of Pd^{IV}(aryl)(CF₃) Complex **4** Formation from Cyclometallated Pd^{II} Dimer **3**



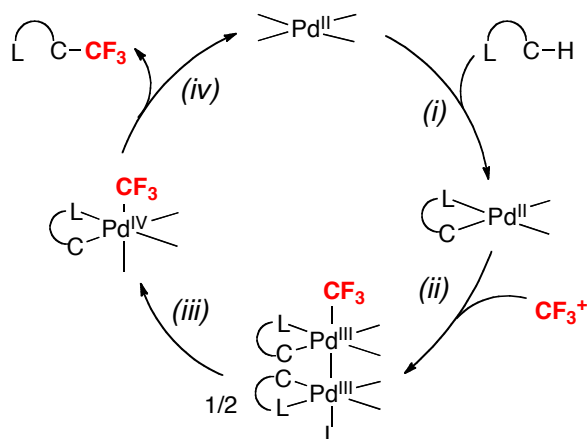
In a joint research effort, Ritter, Sanford, Canty and Yates have reported detailed experimental and computational studies of the oxidation of dimeric Pd^{II} adduct **3**.³⁸ These studies suggest the monomeric Pd^{IV}(aryl)(CF₃) complex **4** is formed by an oxidation-fragmentation pathway. Several key evidences supported this proposed sequence. First, the initial rate of complex **4** formation was $k[\mathbf{2b}][\mathbf{3}][\text{AcOH}]$, suggesting that the dimeric Pd^{II} adduct **3** was intact during the oxidation. Second, since a proposed binuclear Pd^{III} complex **12** was not observed during the initial reaction conditions, presumably due to rapid Pd-Pd cleavage, a related model system was studied to prove the viability of Pd-Pd cleavage step from **12**. Subjecting dimeric complex **3** to XeF₂, followed by treating with TMSCF₃ afforded a new Pd-CF₃ intermediate **12**. Although full characterization of this species was not possible due to its instability, the assignment of this complex to **12** was based on analogous reactions with TMSX (X = Cl, OAc), which generated similar binuclear Pd^{III} complexes that were fully characterized. Finally, DFT calculations support a facile Pd-Pd cleavage step, which has a significantly lower activation barrier compared to that of direct aryl-CF₃ coupling from the binuclear Pd^{III} trifluoromethyl complexes.

Scheme 4.23. Oxidative Trifluoromethylation of Complex **3** with XeF₂ and TMSCF₃



Combining the mechanistic data from our initial study with all the experimental and DFT results reported by Ritter, Canty and Yates, a full mechanistic picture of the Pd-catalyzed C–H trifluoromethylation is shown in **Scheme 4.24**. Ligand directed C–H activation affords the cyclometallated Pd dimer, which reacts with the CF₃⁺ reagent and initially forms the binuclear Pd^{III} intermediate. Facile Pd–Pd cleavage of this unstable bimetallic Pd^{III}–Pd^{III} complex leads to a monomeric Pd^{IV}(aryl)(CF₃) complex (and a cyclometallated Pd^{II} monomer, which recombine with another to reform a dimeric Pd^{II} complex). Finally, reductive elimination from this Pd^{IV} intermediate liberates the desired trifluoromethylated products, and regenerates the catalyst.

Scheme 4.24. Mechanistic Cycle of Pd-Catalyzed C–H Trifluoromethylation



Investigations of the formation and reactivity of high oxidation state Pd–CF₃ intermediates have provided insights that enabled facile aryl–CF₃ coupling from Pd(aryl)(CF₃) complex under unprecedented mild conditions. We anticipate that this strategy could find widespread utility for Pd-catalyzed trifluoromethylation.

4.7 Experimental Procedures and Characterization Data

General Procedures

NMR spectra were obtained on a Varian vnmrs 700 (699.76 MHz for ¹H; 175.95 MHz for ¹³C; 658.43 for ¹⁹F), Varian vnmrs 500 (500.10 MHz for ¹H; 125.75 MHz for ¹³C, 470.56 MHz for ¹⁹F), Varian Inova 500 (499.90 MHz for ¹H; 125.70 MHz for ¹³C), or a Varian MR400 (400.52 MHz for ¹H; 100.71 for ¹³C, 376.87 MHz for ¹⁹F) spectrometer. ¹H, ¹⁹F, and ¹³C chemical shifts are reported in parts per million (ppm) relative to TMS, with the residual solvent peak used as an internal reference. Multiplicities are reported as follows: singlet (s), doublet (d), doublet of doublets (dd), quartet (q), multiplet (m), and broad resonance (br). Elemental analyses were conducted by Atlantic Microlabs in Norcross, Georgia. IR spectra were obtained on a Perkin-Elmer spectrum BX FT-IR spectrometer. Mass spectral data were obtained on a Micromass magnetic sector mass spectrometer or on a Micromass LCT mass spectrometer with an electrospray ionization mode.

Materials and Methods.

The palladium complex [(bzq)Pd(OAc)]₂^{36a} as well as authentic samples of Bzq–OAc (**1b**) and Bzq–OH (**1c**) were prepared according to literature procedures. The electrophilic trifluoromethylating reagents **2a–c** were prepared according to literature procedures,^{12b} while **2d** and **2e** were purchased from Aldrich. NBu₄OAc-*d*₃ was synthesized by reaction of NBu₄OAc with AcOH-*d*₄. Ruppert's reagent (TMSCF₃) was obtained from Matrix Chemicals. Benzo[*h*]quinoline, 2-iodobenzoic acid, 2-(2-iodophenyl)propan-2-ol, and methylmagnesium iodide were obtained from Aldrich or Acros and used as received. Pd(OAc)₂ was obtained from Strem Chemicals and used as received. Pyridine-*d*₅, DCE-

d_4 , TFA- d_1 , AcOH- d_4 , and CDCl_3 were obtained from Cambridge Isotope Laboratories. All other solvents were obtained from Fisher Chemical. Dry acetic acid was distilled from Ac_2O and KMnO_4 .

Experimental Details.

Synthesis of Complex 4: In air, $[(\text{bzq})\text{Pd}(\text{OAc})_2]$ (190 mg, 0.276 mmol, 1 equiv) was weighed into a 20 mL vial and dissolved in AcOH (4 mL). Reagent 5b (274 mg, 0.830 mmol, 3 equiv) was added, and the resulting mixture was stirred at 25 °C for 1 min. The solvent was removed under reduced pressure. The reaction mixture was dissolved in CH_2Cl_2 (1 mL), and hexanes (5 mL) was added to precipitate the product. The precipitate was collected at the top of a plug of Celite and washed with hexanes (50 mL). The product was then eluted through the plug with Et_2O (100 mL), and the solvent was removed under vacuum. Complex 6 was obtained as a light yellow powder (162 mg, 60% yield). ^1H NMR (400 MHz, CDCl_3 , 25 °C, TMS): δ 9.06 (d, $J = 6$ Hz, 1H), 8.53 (d, $J = 8$ Hz, 1H), 8.00-7.92 (multiple peaks, 3H), 7.82-7.73 (multiple peaks, 3H), 2.34 (s, 3H), 1.68 (s, 3H). ^1H NMR (400 MHz, CD_2Cl_2 , -40 °C, TMS): δ 10.45 (br s, 2H), 9.03 (d, $J = 6$ Hz, 1H), 8.6 (d, $J = 8$ Hz, 1H), 8.02-7.98 (multiple peaks, 2H), 7.95 (d, $J = 8$ Hz, 1H), 7.87 (d, $J = 9$ Hz, 1H), 7.82-7.76 (multiple peaks, 2H), 2.30 (s, 3H), 1.58 (s, 3H). ^{13}C NMR (100 MHz, CDCl_3 , 25 °C, TMS): δ 182.40, 180.66, 163.31, 151.13, 147.22, 139.61, 136.13, 135.47, 130.84, 129.34, 128.66, 126.16, 126.06, 124.36, 122.92, 112.61 (q, $J = 380$ Hz), 24.62, 24.28. ^{19}F NMR (376 MHz, CDCl_3 , 25 °C, TMS): δ -23.5 (s, 3F). FTIR (KBr): 3414, 3057, 2930, 2228, 1610, 1407, 1309, 1124, 1064 cm^{-1} . Anal. Calc. for $\text{C}_{18}\text{H}_{16}\text{F}_3\text{NO}_5\text{Pd}$: C, 44.14, H, 3.29, N, 2.86; Found: C, 44.05, H, 3.43, N, 2.71.

Isolation of $(\text{dtbpy})(\text{Pd}^{\text{II}})(\text{CF}_3)(\text{OAc})$: In air, complex 6 (150 mg, 0.306 mmol, 1 equiv) was weighed into a 20 mL vial and dissolved in DCE (7.8 mL). The vial was then sealed with a Teflon-lined cap, and the reaction was heated at 60 °C for 12 h. The resulting mixture was cooled to room temperature. Di-*tert*-butylbipyridine (dtbpy) (82.5 mg, 0.306 mmol, 1 equiv) was added, and the reaction mixture was stirred at room temperature for 1 h. The solvent was removed under reduced pressure, the resulting residue was dissolved

in CH₂Cl₂ (10 mL), and hexanes (50 mL) was added to precipitate the product. The precipitate was collected at the top of a plug of Celite and washed with hexanes (200 mL). The product was then eluted through the plug with DCM (100 mL), and the solvent was removed under vacuum. (dtbpy)(Pd^{II})(CF₃)(OAc) was obtained as a light red powder (18.5 mg, 12% yield). ¹H NMR (400 MHz, CDCl₃, 25 °C, TMS): δ 8.69 (d, *J* = 6 Hz, 1H), 8.28 (d, *J* = 6 Hz, 1H), 7.94 (d, *J* = 2 Hz, 1H), 7.91 (d, *J* = 2 Hz, 1H), 7.50 (dd, *J* = 6 Hz, 2 Hz, 1H), 7.47 (dd, *J* = 6, 2 Hz, 1H), 2.14 (s, 3H), 1.40 (s, 9H), 1.39 (s, 9H). ¹³C NMR (100 MHz, CDCl₃, 25 °C, TMS): δ 177.99, 165.01, 164.69, 156.14, 153.91, 152.78 (q, *J* = 3.5 Hz), 148.70, 124.21, 123.88, 120.62 (q, *J* = 373 Hz), 119.01, 118.25, 35.77, 35.70, 30.40, 30.28, 23.25. ¹⁹F NMR (376 MHz, CDCl₃, 25 °C, TMS): δ -30.93 (s, 3F). Anal. Calc. for C₂₁H₂₇F₃N₂O₂Pd: C, 50.16, H, 5.41, N, 5.57; Found: C, 50.65, H, 5.29, N, 5.41.

Oxidation of 3 with Different Electrophilic Trifluoromethylating Reagents

In air, [(bzq)Pd^{II}(OAc)]₂ (**3**) (20 mg, 0.03 mmol, 1 equiv) was dissolved in CD₃CO₂D (0.4 mL) in a 4 mL vial. The appropriate “CF₃⁺” reagent (0.09 mmol, 3 equiv) was added. The vial was then sealed with a Teflon-lined cap, and the reaction was heated at 40 °C for 1 h. The resulting dark brown mixture was cooled to room temperature, 4-(trifluoromethyl)anisole was added as an internal standard, and the reaction was analyzed by ¹⁹F NMR spectroscopy.

Investigation of the Effect of Additives on the Reaction Profile and Rate of Reductive Elimination from 4

In a N₂-filled drybox, complex **4** (10 mg, 0.0204 mmol, 1.0 equiv), 4-(trifluoromethyl)anisole (50 μL of a stock solution in dry DCE, 0.0204 mmol, 1 equiv), and solid additive were dissolved in dry DCE (0.5 mL) in a 4 mL vial and then transferred to a screw cap NMR tube fitted with a septum. The NMR tube was removed from the glovebox. Liquid additive was then added through the septum. The tube was immediately placed in an NMR spectrometer, and the reaction was allowed to equilibrate for three minutes at 23 °C before acquisition was started. The kinetics of reductive elimination was studied using ¹⁹F NMR spectroscopy by monitoring the appearance of

the product signal. The data was fit to a first order kinetics plot using Sigma Plot 10. Each experiment was carried out in duplicate.

Additive = None. This reaction showed a significant induction period and did not follow a 1st order kinetic profile.

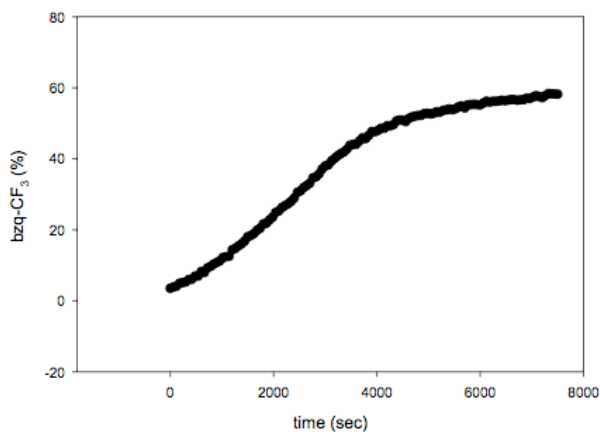


Figure 4.10. Representative Reaction Profile of Reductive Elimination from **4**

Additive = Yb(OTf)₃. The data was fit to the function $f = a*(1-\exp(-b*x))$; $a = 101.42 \pm 0.3523$, $b = 2.918*10^{-4} \pm 2.8745*10^{-6}$, $R^2 = 0.9953$. [$k_{obs} = b$].

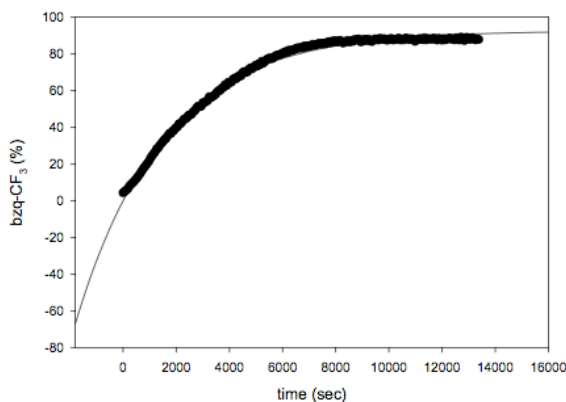


Figure 4.11. Representative Reaction Profile for Reductive Elimination from **4** in the Presence of 1 Equiv of Yb(OTf)₃

Additive = TFA. The data was fit to the function $f = a*(1-\exp(-b*x))$; $a = 83.84 \pm 0.3356$, $b = 3.308*10^{-4} \pm 4.143*10^{-6}$, $R^2 = 0.9904$. [$k_{obs} = b$].

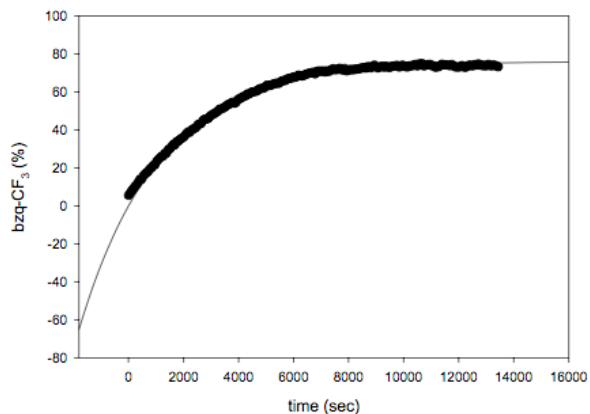


Figure 4.12. Representative Reaction Profile for Reductive Elimination from **4** in the Presence of 10 Equiv of TFA

Additive = (TFA)₂O. The data was fit to the function $f = a*(1-\exp(-b*x))$; $a = 88.80 \pm 0.1990$, $b = 1.430*10^{-3} \pm 1.660*10^{-5}$, $R^2 = 0.9884$. [kobs = b].

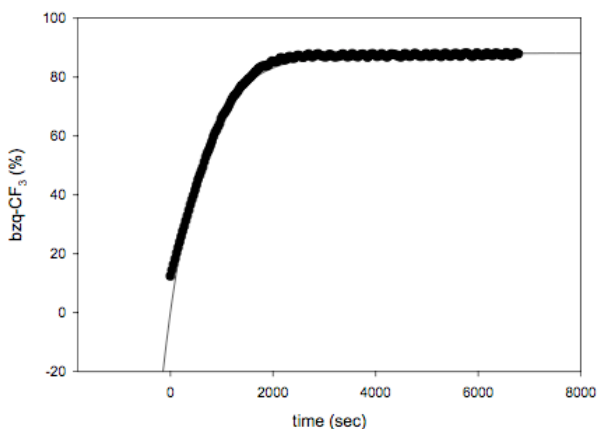


Figure 4.13. Representative Reaction Profile for Reductive Elimination from **4** in the Presence of 10 Equiv of (TFA)₂O

Additive = 10 equiv of Cu(OAc)₂ and 100 equiv of TFA. This reaction showed a induction period and did not follow a 1st order kinetic profile.

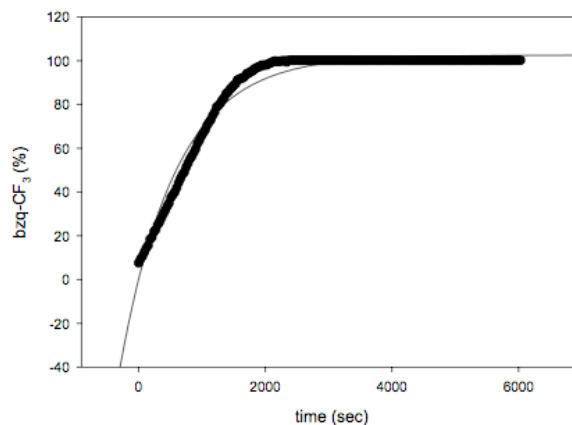


Figure 4.14. Representative Reaction Profile of Reductive Elimination from **4** in the Presence of 10 Equiv of $\text{Cu}(\text{OAc})_2$ and 100 Equiv of TFA

Additive = NBu_4OAc . This reaction showed a significant induction period and did not follow a 1st order kinetic profile.

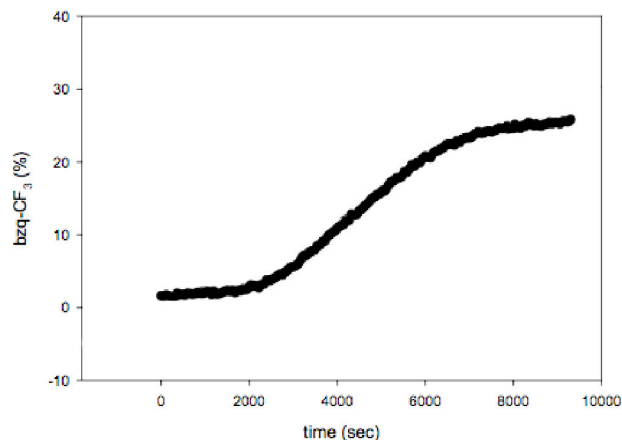


Figure 4.15. Representative Reaction Profile of Reductive Elimination from **4** in the Presence of 0.2 Equiv of NBu_4OAc

Additive = NBu_4PF_6 . This reaction showed a significant induction period and did not follow a 1st order kinetic profile.

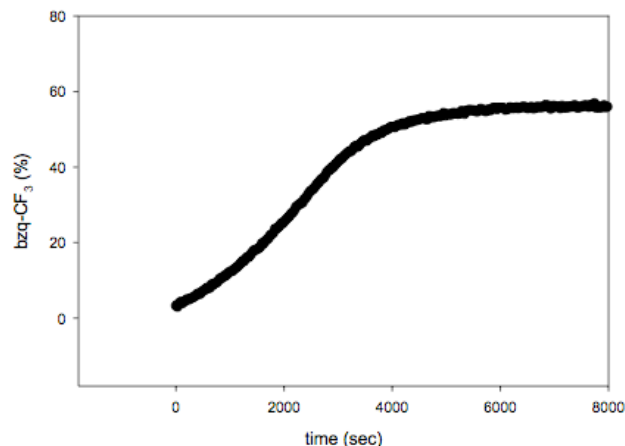


Figure 4.16. Representative Reaction Profile of Reductive Elimination from **4** in the Presence of 1 Equiv of NBu_4PF_6

Additive = H_2O . This reaction showed a significant induction period and did not follow a 1st order kinetic profile.

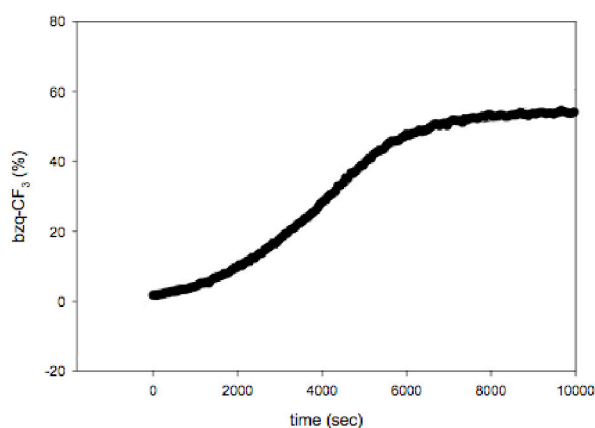


Figure 4.17. Representative Reaction Profile of Reductive Elimination from **4** in the Presence of 1 Equiv of H_2O

Study of Catalytic Competence of 6 using Method of Initial Rates: The reaction kinetics were measured using the method of initial rates. In each experiment, the reaction was monitored to ~20% conversion. Kinetics experiments were run in 4 mL vials sealed with Teflon-lined caps. Each data point represents a reaction in an individual vial, with each vial containing a constant concentration of **2e**, catalyst, beno[*h*]quinoline (bzq), $\text{Cu}(\text{OAc})_2$ and TFA. The vials were each sequentially charged with bzq (5.38 mg, 0.03

mmol, 1 equiv), **2e** (15.3 mg, 0.045 mmol, 1.5 equiv), Cu(OAc)₂ (5.45 mg, 0.03 mmol, 1 equiv), Pd catalyst (10 mol %), dry DCE (0.15 mL) and TFA (22.3 μL, 0.3 mmol 10 equiv). The vials were then heated at 110 °C for various amounts of time. Reactions were quenched by cooling the vial to 0 °C for 10 min. A GC standard (pyrene) was then added, and the reactions were analyzed by gas chromatography

X-ray Crystallographic Analysis

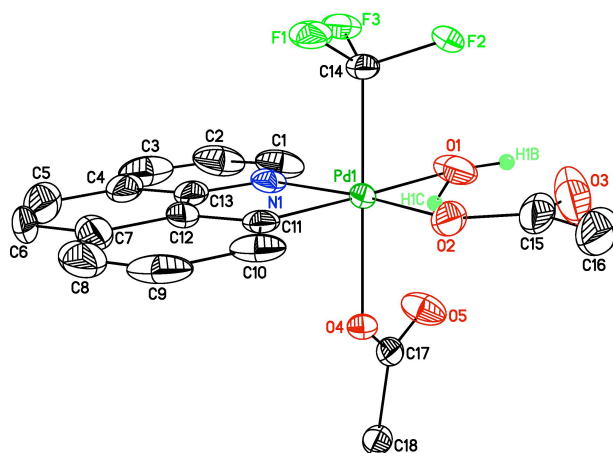


Figure 4.18. X-Ray Crystal Structure of Complex 4 (CCDC 772390)

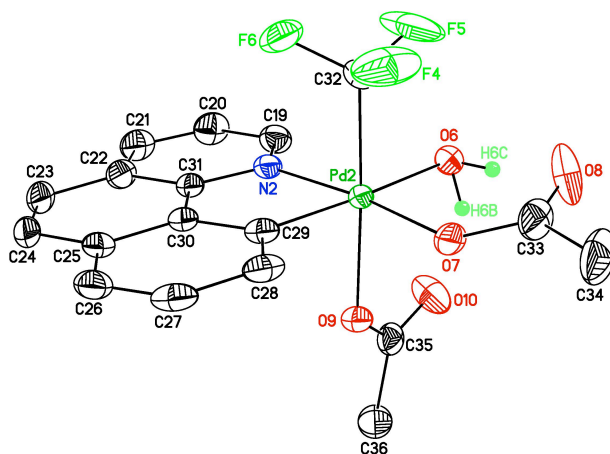


Figure 4.19. X-Ray Crystal Structure of the Other Complex 4 in the Same Unit Cell (CCDC 772390). The structure was solved as two identical structures in a unit cell.

Table 4.8. Hydrogen Bonds for **4** [Å and deg].

D-H...A	d(D-H)	d(H...A)	d(D...A)	<(DHA)
O(1)-H(1B)...O(3)	1.02(4)	1.69(5)	2.624(7)	150(7)
O(1)-H(1C)...O(5)	0.84(4)	1.82(6)	2.547(5)	143(7)
O(6)-H(6B)...O(10)	0.90(4)	1.72(5)	2.531(5)	149(7)
O(6)-H(6C)...O(8)	0.87(4)	1.76(5)	2.607(5)	163(7)

General Procedure for the Synthesis of (tmeda)Pd(Aryl)(I): Under nitrogen, Pd(dba)₂ (2.0 g, 3.48 mmol, 1 equiv) was weighed into a 250 mL round bottom flask and dissolved in THF (50 mL). TMEDA (1.1 g, 9.06 mmol, 2.6 equiv) was added, and the resulting mixture was stirred at 25 °C for 15 min. The appropriate aryl iodide (9.74 mmol, 2.8 equiv) was added, and the reaction was heated at 60 °C for 30 min. In air, the reaction mixture was filtered through a plug of Celite, and the solvent was removed under reduced pressure. The resulting solid was washed with hexanes (3 x 20 mL) and then diethyl ether (3 x 50 mL) to remove all residual dibenzylidene acetone (dba). The product was then dried *in vacuo*.

The product (tmeda)Pd(*p*-CF₃C₆H₄)(I) was isolated as an orange solid (1.02 g, 39% yield). ¹H NMR (CDCl₃): δ 7.35 (d, *J* = 8 Hz, 2H), 7.06 (d, *J* = 8 Hz, 2H), 2.59 (s, 6H), 2.45 (app s, 4H), 2.20 (s, 6H). ¹⁹F NMR (CDCl₃): δ -61.81 (s, 3F). ¹³C NMR (CDCl₃): δ 152.69, 136.48, 124.77 (q, *J* = 271 Hz), 124.56 (q, *J* = 32 Hz), 121.90 (q, *J* = 4 Hz), 61.93, 58.08, 49.76, 49.60. HRMS electrospray (m/z): [M + Na]⁺ calcd for C₁₃H₂₀F₃IN₂Pd, 516.9556; Found, 516.9573.

General Procedure for the Synthesis of (tmeda)Pd(Aryl)(CF₃): Under nitrogen, (tmeda)Pd(Aryl)(I) (1.0 g, 2.02-2.30 mmol, 1 equiv) and CsF (3 equiv) were suspended in THF (0.145 M) in a 25 mL Schlenk flask. This mixture was stirred for 10 min and then Me₃SiCF₃ (2 equiv) was added. The reaction was stirred vigorously for 3 h at 22 °C. The solvent was removed under reduced pressure, CH₂Cl₂ (15 mL) was added to dissolve the

product, and the resulting suspension was filtered through a plug of Celite. The plug was washed with CH₂Cl₂ (2 x 5 mL), the filtrate was concentrated under reduced pressure to (~2 mL), and hexanes (60 mL) was added to precipitate the product. The resulting solid was collected on fritted Buchner funnel, washed with hexanes (3 x 10 mL) and diethyl ether (2 x 2 mL), and dried *in vacuo*. Some substrates were synthesized on a different scale with the same equivalents of materials as described above. These substrates and their scale of synthesis (as determined by amount of (tmeda)Pd(Aryl)(I) used) are noted accordingly.

(tmeda)Pd(*p*-CF₃Ph)(TFA): Under N₂, (tmeda)Pd(*p*-CF₃Ph)(I) (500 mg, 1.01 mmol, 1 equiv) and AgTFA (246 mg, 1.11 mmol, 1.1 equiv) were dissolved in CH₂Cl₂ (5 mL) in a 20 mL vial. The reaction was stirred vigorously for 30 min. The solvent was then removed under reduced pressure. CH₂Cl₂ (50 mL) was added, and the resulting suspension was filtered through a plug of Celite. The filtrate was concentrated under reduced pressure to ~2 mL, and hexanes (30 mL) was added to precipitate the product. The resulting solid was collected on a fritted filter, washed with hexanes (50 mL), and dried *in vacuo*. The product was isolated as a pale-yellow solid (430 mg, 88% yield). ¹H NMR (CDCl₃): δ 7.55 (d, *J* = 8 Hz, 2H), 7.17 (d, *J* = 8 Hz, 2H), 2.76 (m, 2H), 2.59 (m, 2H), 2.58 (s, 6H), 2.50 (s, 6H). ¹⁹F NMR (CDCl₃): δ -21.39 (s, 3F), -61.84 (s, 3F). ¹³C NMR (CDCl₃): δ 161.79 (q, *J* = 37 Hz), 155.23, 134.67, 125.92 (q, *J* = 32 Hz), 124.98 (q, *J* = 271 Hz), 122.43 (q, *J* = 4 Hz), 115.52 (q, *J* = 292 Hz), 63.77, 57.75, 51.68, 47.91. HRMS electrospray (m/z): [M - TFA + MeCN]⁺ calcd for C₁₅H₂₀F₆N₂O₂Pd, 408.0879; Found, 408.0881.

(tmeda)Pd(*p*-CF₃Ph)(OAc): Under N₂, (tmeda)Pd(*p*-CF₃Ph)(I) (500 mg, 1.01 mmol, 1 equiv) and AgOAc (186 mg, 1.11 mmol, 1.1 equiv) were dissolved in CH₂Cl₂ (5 mL) in a 20 mL vial. The reaction was stirred vigorously for 30 min. The solvent was then removed under reduced pressure. CH₂Cl₂ (50 mL) was added, and the resulting suspension was filtered through a plug of Celite. The filtrate was concentrated under reduced pressure to ~2 mL, and hexanes (30 mL) was added to precipitate the product. The resulting solid was collected on a fritted filter, washed with hexanes (50 mL), and

dried *in vacuo*. The product was isolated as a yellow solid (326 mg, 76% yield). ¹H NMR (CDCl₃): δ 7.60 (d, *J* = 8 Hz, 2H), 7.14 (d, *J* = 8 Hz, 2H), 2.71 (m, 2H), 2.59 (s, 6H), 2.56 (m, 2H), 2.46 (s, 6H). ¹⁹F NMR (CDCl₃): δ -61.76 (s). ¹³C NMR (CDCl₃): δ 176.94, 157.53, 135.15, 125.25 (q, *J* = 32 Hz), 125.14 (q, *J* = 272 Hz), 122.09 (q, *J* = 4 Hz), 63.37, 57.92, 51.42, 48.17, 23.83. HRMS electrospray (*m/z*): [M + Na]⁺ calcd for C₁₅H₂₃F₃N₂O₂Pd, 408.0879; Found, 408.0880.

Procedure for the Synthesis of (tmeda)Pd(*p*-CF₃Ph)(CF₃) from (tmeda)Pd(*p*-CF₃Ph)(TFA): Under N₂, (tmeda)Pd(*p*-CF₃Ph)(TFA) (416 mmol, 1 equiv) and CsF (2 equiv) were dissolved in THF (0.04 M) in a 25 mL Schlenk flask. Me₃SiCF₃ (10 equiv) was added. The reaction was stirred vigorously for 2 h at 22 °C. The solvent was then removed under reduced pressure. CH₂Cl₂ (50 mL) was added, and the resulting suspension was filtered through a plug of Celite. The plug was washed with CH₂Cl₂ (40 mL), the filtrate was concentrated under reduced pressure to ~5 mL, and hexanes (60 mL) was added to precipitate the product. The resulting solids were collected on a fritted filter, washed with hexanes (50 mL), and dried *in vacuo* to afford (tmeda)Pd(Aryl)(CF₃) in 56% yield.

Procedure for the Synthesis of (tmeda)Pd(*p*-CF₃Ph)(CF₃) from (tmeda)Pd(*p*-CF₃Ph)(OAc): Under N₂, (tmeda)Pd(*p*-CF₃Ph)(OAc) (469 mmol, 1 equiv) and CsF (2 equiv) were dissolved in THF (0.04 M) in a 25 mL Schlenk flask. Me₃SiCF₃ (10 equiv) was added. The reaction was stirred vigorously for 2 h at 22 °C. The solvent was then removed under reduced pressure. CH₂Cl₂ (50 mL) was added, and the resulting suspension was filtered through a plug of Celite. The plug was washed with CH₂Cl₂ (40 mL), the filtrate was concentrated under reduced pressure to ~5 mL, and hexanes (60 mL) was added to precipitate the product. The resulting solids were collected on a fritted filter, washed with hexanes (50 mL), and dried *in vacuo* to afford (tmeda)Pd(Aryl)(CF₃) in 61% yield.

4.8 Reference

1. (a) Schlosser, M. *Angew. Chem. Int. Ed.* **2006**, *45*, 5432; (b) Müller, K.; Faeh, C.; Diederich, F. *Science* **2007**, *317*, 1881; (c) Hagmann, W. K. *J. Med. Chem.* **2008**, *51*, 4359; (d) Kirk, K. L. *Org. Process Res. Dev.* **2008**, *12*, 305; (e) Purser, S.; Moore, P. R.; Swallow, S.; Gouverneur, V. *Chem. Soc. Rev.* **2008**, *37*, 320; (f) Tomashenko, O. A.; Grushin, V. V. *Chem. Rev.* **2011**, *111*, 4475; (g) Roy, S.; Gregg, B. T.; Gribble, G. W.; Le, V.-D. *Tetrahedron* **2011**, *67*, 2161.
2. (a) Furuya, T.; Kamlet, A. S.; Ritter, T. *Nature* **2011**, *473*, 470; (b) Grushin, V. V. *Acc. Chem. Res.* **2010**, *43*, 160.
3. Swarts, F. *Bull. Acad. R. Belg.* **1892**, *24*, 309.
4. Lyons, T.; Sanford, M. S. *Chem. Rev.* **2010**, *110*, 1147.
5. (a) Hassan, J.; Sévignon, M.; Gozzi, C.; Schulz, E.; Lemaire, M. *Chem. Rev.* **2002**, *102*, 1359; (b) Beccalli, E. M.; Brogini, G.; Martinelli, M.; Sottocornola, S. *Chem. Rev.* **2007**, *107*, 5318; (c) Chen, X.; Engle, K. M.; Wang, D. H.; Yu, J.-Q. *Angew. Chem., Int. Ed.* **2009**, *48*, 5094; (d) McGlacken, G. P.; Bateman, L. M. *Chem. Soc. Rev.* **2009**, *38*, 2447; (e) Daugulis, O.; Do, H. Q.; Shabashov, D. *Acc. Chem. Res.* **2009**, *42*, 1074.
6. (a) Hughes, R. P. *Adv. Organomet. Chem.* **1990**, *31*, 183; (b) Morrison, J. A. *Adv. Organomet. Chem.* **1993**, *35*, 211.
7. Grushin, V. V.; Marshall, W. J. *J. Am. Chem. Soc.* **2006**, *128*, 12644.
8. Cho, E. J.; Senecal, T. D.; Kinzel, T.; Zhang, Y.; Watson, D. A.; Buchwald, S. L. *Science* **2010**, *328*, 1679.
9. (a) Hickman, A. J.; Sanford, M. S. *Nature* **2012**, *484*, 177; (b) Racowski, J. M.; Dick, A. R.; Sanford, M. S. *J. Am. Chem. Soc.* **2009**, *131*, 10974; (c) Ball, N. D.; Sanford, M. S. *J. Am. Chem. Soc.* **2009**, *131*, 3796; (d) Muniz, K. *Angew. Chem. Int. Ed.* **2009**, *48*, 9412; (e) Whitfield, S. R.; Sanford, M. S. *J. Am. Chem. Soc.* **2007**, *129*, 15142; (f) Dick, A. R.; Remy, M. S.; Kampf, J. W.; Sanford, M. S. *Organometallics* **2007**, *26*, 1365; (g) Dick, A. R.; Kampf, J. W.; Sanford, M. S. *J. Am. Chem. Soc.* **2005**, *127*, 12790; (h) Furuya, T.; Benitez, D.; Tkatchouk, E.; Strom, A. E.; Tang, P.; Goddard, W. A.; Ritter, T. *J. Am. Chem. Soc.* **2010**, *132*, 3793.
10. Ye, Y.; Ball, N. D.; Kampf, J. W.; Sanford, M. S. *J. Am. Chem. Soc.* **2010**, *132*, 14682.
11. (a) Ball, N. D.; Gary, J. B.; Ye, Y.; Sanford, M. S. *J. Am. Chem. Soc.* **2011**, *133*, 7577; (b) Ball, N. D.; Kampf, J. W.; Sanford, M. S. *J. Am. Chem. Soc.* **2010**, *132*, 2878.
12. (a) Umemoto, T. *Chem. Rev.* **1996**, *96*, 1757; (b) Eisenberger, P.; Gischig, S.; Togni, A. *Chem. Eur. J.* **2006**, *12*, 2579; (c) Kieltsch, I.; Eisenberger, P.; Stanek, K.; Togni, A. *Chimia* **2008**, *62*, 260.
13. Wang, X.; Truesdale, L.; Yu, J.-Q. *J. Am. Chem. Soc.* **2010**, *132*, 3648.
14. Deprez, N. R.; Sanford, M. S. *J. Am. Chem. Soc.* **2009**, *131*, 11234.
15. (a) Powers, D. C.; Ritter, T. *Nat. Chem.* **2009**, *1*, 302; (b) Powers, D. C.; Geibel, M. A. L.; Klein, J. E. M. N.; Ritter, T. *J. Am. Chem. Soc.* **2009**, *131*, 17050.
16. Hydrogen atoms were placed in idealized positions with the exception of those of the H-bonded waters, which were allowed to refine isotropically with a restrained O–H distance and common U(iso).

17. Jensen, D. R.; Schultz, M. J.; Mueller, J. A.; Sigman, M. S. *Angew. Chem., Int. Ed.* **2003**, *42*, 3810.
18. (a) Canty, A. J.; Denney, M. C.; Skelton, B. W.; White, A. H. *Organometallics* **2004**, *23*, 1122; (b) Yamamoto, Y.; Kuwabara, S.; Matsuo, S.; Ohno, T.; Nishiyama, H.; Itoh, K. *Organometallics* **2004**, *23*, 3898.
19. For other examples of C–O bond-forming reductive elimination, see: (a) Han, R.; Hillhouse, G. L. *J. Am. Chem. Soc.* **1997**, *119*, 8135. (b) Widenhoefer, R. A.; Buchwald, S. L. *J. Am. Chem. Soc.* **1998**, *120*, 6504. (c) Williams, B. S.; Goldberg, K. I. *J. Am. Chem. Soc.* **2001**, *123*, 2576. (d) Stambuli, J. P.; Weng, Z.; Incarvito, C. D.; Hartwig, J. F. *Angew. Chem. Int. Ed.* **2007**, *46*, 7674. (e) Khusnutdinova, J. R.; Newman, L. L.; Zavalij, P. Y.; Lam, Y.-F.; Vedernikov, A. N. *J. Am. Chem. Soc.* **2008**, *130*, 2174.
20. For C–CF₃ bond-formation at Cu/Ni, see: (a) Dubinina, G. G.; Furutachi, H.; Vicic, D. A. *J. Am. Chem. Soc.* **2008**, *130*, 8600. (b) Dubinina, G. G.; Brennessel, W. W.; Miller, J. L.; Vicic, D. A. *Organometallics* **2008**, *27*, 3933. (c) Dubinina, G. G.; Ogikubo, J.; Vicic, D. A. *Organometallics* **2008**, *27*, 6233.
21. Kalyani, D.; Deprez, N. R.; Desai, L. V.; Sanford, M. S. *J. Am. Chem. Soc.* **2005**, *127*, 7330.
22. For examples of mechanisms like path A for reductive elimination from Pd^{IV} see: (a) Byers, P. K.; Canty, A. J.; Crespo, M.; Puddephatt, R. J.; Scott, S. D. *Organometallics* **1988**, *7*, 1363. (b) Ducker-Benfer, C.; van Eldik, R.; Canty, A. J. *Organometallics* **1994**, *13*, 2412. (c) Canty, A. J.; Jin, H.; Skelton, B. W.; White, A. H. *Inorg. Chem.* **1998**, *37*, 3975.
23. For examples of mechanisms like path A for reductive elimination from Pt^{IV}, see: (a) Goldberg, K. I.; Yan, J.; Winter, E. L. *J. Am. Chem. Soc.* **1994**, *116*, 1573. (b) Goldberg, K. I.; Yan, J.; Breitung, E. M. *J. Am. Chem. Soc.* **1995**, *117*, 6889. (c) Ref. 19c. (d) Vedernikov, A. N.; Binfield, S. A.; Zavalij, P. Y.; Khusnutdinova, J. R. *J. Am. Chem. Soc.* **2006**, *128*, 82. (e) Khusnutdinova, J. R.; Zavalij, P. Y.; Vedernikov, A. N. *Organometallics* **2007**, *26*, 3466. (f) Pawlikowski, A. V.; Getty, A. D.; Goldberg, K. I. *J. Am. Chem. Soc.* **2007**, *129*, 10382. (g) Ref. 19e. (h) Khusnutdinova, J. R.; Newman, L. L.; Zavalij, P. Y.; Lam, Y.-F.; Vedernikov, A. N. *J. Am. Chem. Soc.* **2008**, *130*, 2174. (i) Smythe, N. A.; Grice, K. A.; Williams, B. S.; Goldberg, K. I. *Organometallics* **2009**, *28*, 277.
24. For an example of a mechanism like path B for reductive elimination from Pt^{IV}, see: Brown, M. P.; Puddephatt, R. J.; Upton, C. E. E. *J. Chem. Soc., Dalton Trans.* **1974**, 2457.
25. For examples of mechanisms like path C for reductive elimination from Pd^{IV} and Pt^{IV}, see: (a) Crumpton, D. M.; Goldberg, K. I. *J. Am. Chem. Soc.* **2000**, *122*, 962. (b) Crumpton-Bregel, D. M.; Goldberg, K. I. *J. Am. Chem. Soc.* **2003**, *125*, 9442. (c) Arthur, K. L.; Wang, Q. L.; Bregel, D. M.; Smythe, N. A.; O'Neill, B. A.; Goldberg, K. I.; Moloy, K. G. *Organometallics* **2005**, *24*, 4624. (d) Ref. 9b.
26. Williams, B. S.; Goldberg, K. I. *J. Am. Chem. Soc.* **2001**, *123*, 2576.
27. (a) Culkin, D. A.; Hartwig, J. F. *Organometallics* **2004**, *23*, 3398; (b) Grushin, V. V.; Marshall, W. J. *J. Am. Chem. Soc.* **2006**, *128*, 4632.
28. (a) Mei, T. S.; Wang, X.; Yu, J. Q. *J. Am. Chem. Soc.* **2009**, *131*, 10806; (b) Sibbald, P. A.; Rosewall, C. F.; Swartz, R. D.; Michael, F. E. *J. Am. Chem. Soc.* **2009**,

- 131, 15945; (c) Engle, K. M.; Mei, T. S.; Wang, X.; Yu, J.-Q. *Angew. Chem., Int. Ed.* **2011**, *50*, 1478.
29. Markies, B. A.; Canty, A. J.; Boersma, J.; van Koten, G. *Organometallics* **1994**, *13*, 2053.
30. Zhang, X.-G.; Dai, H.-X.; Wasa, M.; Yu, J.-Q. *J. Am. Chem. Soc.* **2012**, *134*, 11948.
31. Zhang, L.-S.; Chen, K.; Chen, G.; Li, B.-J.; Luo, S.; Guo, Q.-Y.; Wei, J.-B.; Shi, Z.-J. *Org. Lett.* **2012**, *15*, 10.
32. Mu, X.; Chen, S.; Zhen, X.; Liu, G. *Chem. –Eur. J.* **2011**, *17*, 6039.
33. Mu, X.; Wu, T.; Wang, H.-Y.; Guo, Y.-L.; Liu, G. *J. Am. Chem. Soc.* **2011**, *134*, 878.
34. (a) Deprez, N. R.; Sanford, M. S. *Inorg. Chem.* **2007**, *46*, 1924; (b) Xu, L. M.; Li, B. J.; Yang, Z.; Shi, Z. J. *Chem. Soc. Rev.* **2010**, *39*, 712; (c) Sehnal, P.; Taylor, R. J. K.; Fairlamb, I. J. S. *Chem. Rev.* **2010**, *110*, 824.
35. Canty, A. J. *Dalton Trans.* **2009**, 10409.
36. (a) Dick, A. R.; Hull, K. L.; Sanford, M. S. *J. Am. Chem. Soc.* **2004**, *126*, 2300; (b) Desai, L. V.; Malik, H. A.; Sanford, M. S. *Org. Lett.* **2006**, *8*, 1141.
37. Giri, R.; Chen, X.; Yu, J. Q. *Angew. Chem., Int. Ed.* **2005**, *44*, 2112.
38. Powers, D. C.; Lee, E.; Ariaifard, A.; Sanford, M. S.; Yates, B. F.; Canty, A. J.; Ritter, T. *J. Am. Chem. Soc.* **2012**, *134*, 12002.

CHAPTER 5

Mild Copper-Mediated Fluorination of Aryl Stannanes and Aryl Trifluoroborates

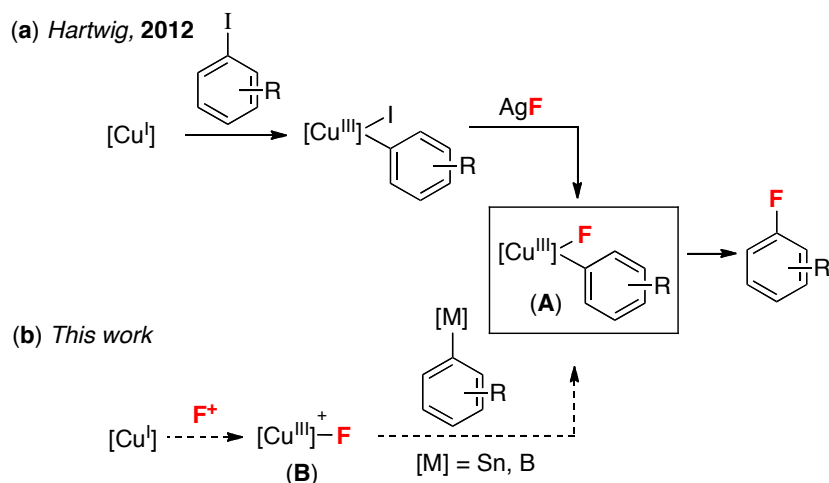
5.1 Background

Aryl fluorides are extremely important structural motifs that feature prominently in pharmaceuticals, agrochemicals, organic materials, and biological imaging agents.¹ As a result, significant recent efforts have focused on the development of new synthetic procedures for the generation of C_{Aryl}-F bonds.² Transition metal-mediated and/or catalyzed aryl-fluoride coupling reactions are of particular interest, because the rate, selectivity, and functional group tolerance of these transformations can often be modulated by changing the metal and its ligand environment.³ Over the past 6 years, several different palladium⁴ and silver-based protocols have been developed to effect aryl-fluoride bond formation via cross-coupling with aryl C-H bonds,^{5,6} aryl triflates,⁷ aryl stannanes,⁸ aryl boronic acids,⁹ and aryl silanes.¹⁰ In several cases, these methods have been successfully applied to the late-stage fluorination of complex molecules. However, despite these significant advances, the reactions remain limited by the requirement for expensive and toxic noble metals.

A key unmet need in the field is a mild and general aryl fluorination protocol mediated by an earth abundant first row metal such as Cu.¹¹ In a seminal report in 2011, Ribas and co-workers demonstrated a proof-of-concept example of aryl-F bond formation at a macrocyclic aryl-Cu(III) complex.^{12,13} More recently, Fier and Hartwig reported the Cu-mediated conversion of a broader scope of aryl iodides to aryl fluorides

using AgF as the fluoride source at 140 °C.^{14,15} As shown in **Scheme 5.1a**, this transformation is also believed to proceed via a Cu^{III}(aryl)(fluoride) intermediate **A** formed by oxidative addition of Ar–I to Cu(I) and subsequent reaction with AgF.

Scheme 5.1. Strategies for Cu-Mediated Aryl–F Coupling



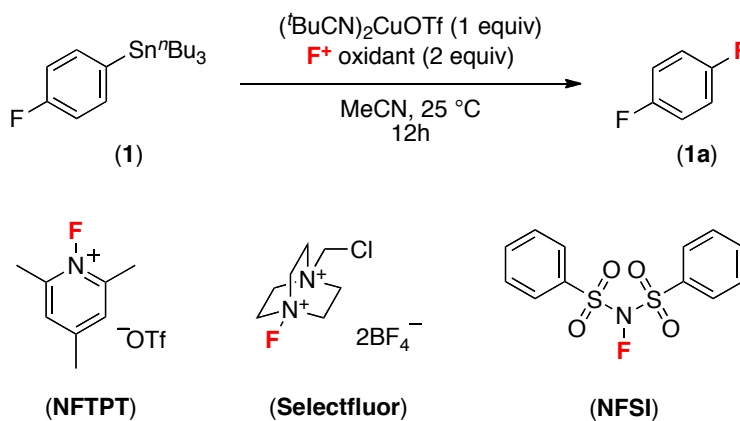
Inspired by these exciting advances, we sought to develop a milder and more versatile Cu(III)-mediated aromatic fluorination protocol. We hypothesized that an intermediate analogous to **A** could be formed under less forcing conditions via the combination of an electrophilic fluorinating reagent (F^+) and an aryl organometallic species (**Scheme 5.1b**).^{5,16} Importantly, literature precedent in Pd- and Ag-catalyzed fluorination reactions has shown that F^+ reagents can serve as fluorine sources without introducing extra ligands that might lead to unproductive competing reductive elimination from the metal center.^{4-6,8-9,10}

5.2 Reaction Optimization and Substrate Scope

To test this hypothesis, we initially explored the Cu-mediated fluorination of aryl stannane **1** with electrophilic fluorinating reagents. We choose aryl stannanes as starting materials based on their known ability to undergo fast transmetalation at transition metal centers. The combination of **1**, $(t\text{BuCN})_2\text{CuOTf}$, and commercial F^+ reagents in MeCN at 25 °C for 12 h afforded modest (7-30%) yield of the desired product (**Table 5.1**). *N*-

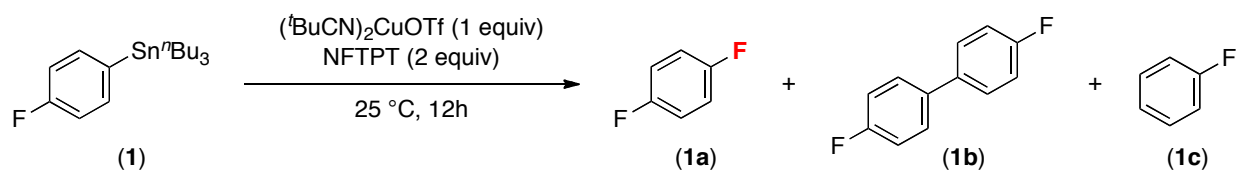
Fluoro-2,4,6-trimethylpyridinium triflate (NFTPT) provided the highest yield and was thus utilized in subsequent reaction optimization.

Table 5.1. F⁺ Oxidants Examined for Cu-Mediated Fluorination of **1**



Entry	F ⁺ Oxidant	Yield of 1a
1	NFTPT	30%
2	Selectfluor	17%
3	NFSI	7%

The major byproducts of this transformation are fluorobenzene and biaryl **1b**, and the ratio of these by-products is highly dependent on the solvent. For example, fluorobenzene **1c** is the major byproduct when MeCN was used as solvent. In fact, stirring stannane **1** and $(t\text{BuCN})_2\text{CuOTf}$ at 25 °C for just 2 h afforded quantitative yield of fluorobenzene, presumably via facile protodestannylation. In contrast, when the reaction was conducted in EtOAc as solvent, biaryl **1b** was formed in 30% yield, presumably resulting from unproductive homocoupling of the aryl stannane. Results of the evaluation of a wide variety of solvents are shown in **Table 5.2**.

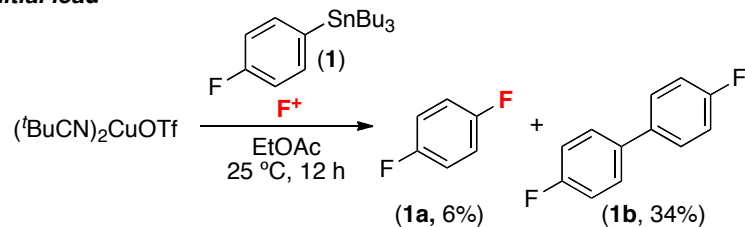
Table 5.2. Solvent Screen for Cu-Mediated Fluorination of **1** with NFTPT

Entry	Solvent	Yield of 1a	Yield of 1b	Yield of 1c
1	DCM	40%	24%	0%
2	MeCN	34%	0%	56%
3	Acetone	30%	17%	0%
4	1,4-Dioxane	20%	27%	4%
5	Toluene	17%	37%	0%
6	EtOAc	12%	30%	0%
7	THF	10%	45%	0%
8	DMF	0%	18%	64%
9	DMSO	0%	12%	76%
10	DMA	0%	16%	57%
11	NMP	0%	14%	54%
12	Diglyme	0%	25%	0%

We reasoned that its formation of biaryl **1b** could be circumvented by initial oxidation of with NFTPT to form putative Cu(III)-F intermediate **B** (Scheme 5.1) followed by addition of the stannane **1**. As shown in Scheme 5.2b, this sequential addition protocol resulted in dramatically improved yield of **1a** (74%) along with <4% of **1b**. Importantly, no detectable amount of fluorobenzene was generated under these conditions.

Scheme 5.2. Cu-Mediated Fluorination of Aryl Stannanes

(a) *Initial lead*



(b) *Sequential addition protocol*

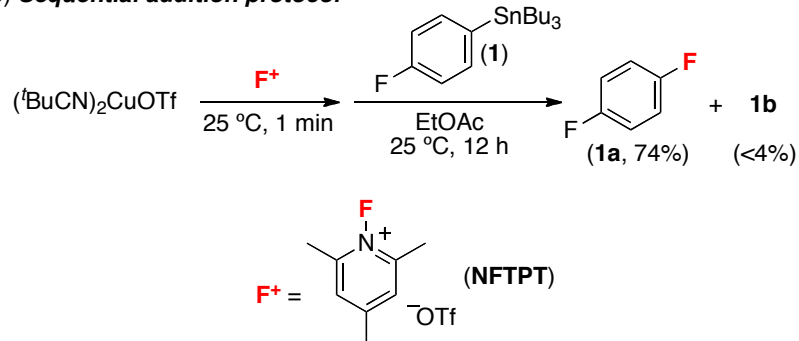
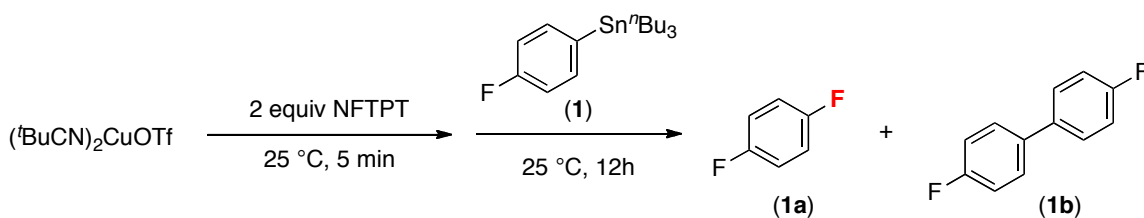


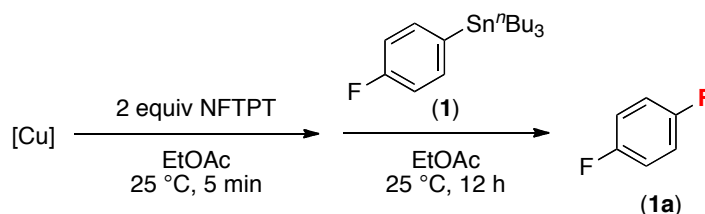
Table 5.3. Solvent Screen for Fluorination of **1** with Sequential Addition Protocol



Entry	Solvent	Yield of 1a	Yield of 1b
1	EtOAc	74%	4%
2	DCM	64%	0%
3	Acetone	48%	5%
4	MeCN	36%	0%
5	1,4-Dioxane	15%	12%
6	Toluene	15%	0%
7	THF	14%	34%
8	DMF	0%	10%
9	DMSO	0%	7%
10	DMA	0%	16%
11	NMP	0%	16%
12	Diglyme	0%	39%

Finally, a wide variety of copper salts were evaluated using our sequential addition protocol. As shown in **Table 5.4**, Cu(I) salts containing non coordinating anions proved to be optimal. Significant amounts of chlorination and acetoxylation products were observed when CuCl and CuOAc were used, respectively.

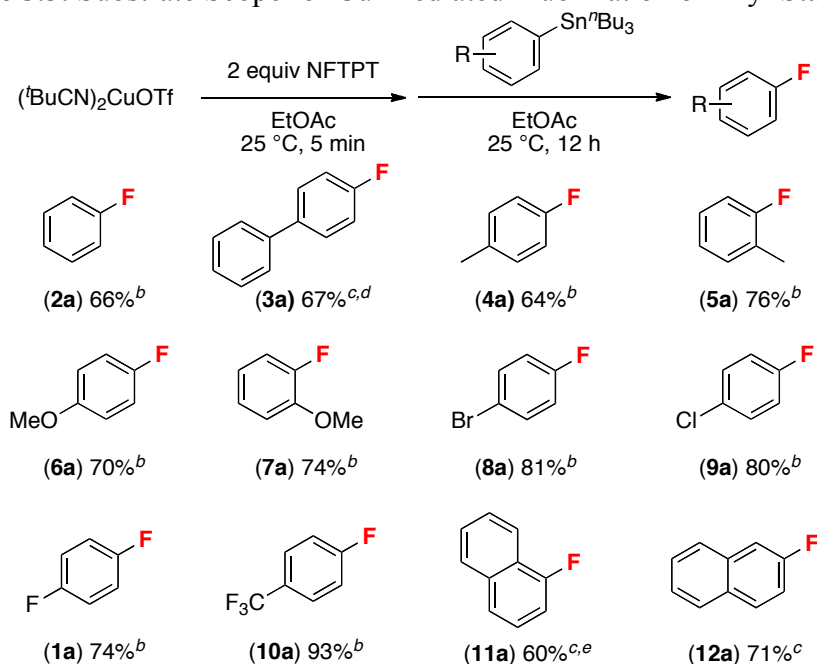
Table 5.4. Copper Screen for Cu-Mediated Fluorination of **1** by NFTPT with Sequential Addition Protocol



Entry	Copper Salt	Yield of 1a
1	(^t BuCN) ₂ CuOTf	74%
2	(MeCN) ₄ CuPF ₆	65%
3	(MeCN) ₄ CuBF ₄	60%
4	Cu(OTf) ₂	23%
5	Cu	15%
6	Cu(OTf)•1/2(C ₆ H ₆)	2%
7	CuCl	1%
8	CuOAc	0%
9	CuF ₂	0%

We next applied this room temperature fluorination protocol to a variety of different aryl stannanes. As shown in **Scheme 5.3**, aryl stannanes bearing electron-donating and withdrawing substituents underwent fluorination in good to excellent yields under these conditions. The presence of *ortho*-substituents was also well-tolerated. Notably, in all of the examples shown in **Scheme 5.3**, no fluorination products were detected in the absence of Cu (see **Table 5.5** for the results of these control experiments).

Scheme 5.3. Substrate Scope for Cu-Mediated Fluorination of Aryl Stannanes^a



^a General conditions: stannane (0.25 mmol, 1 equiv), $(t\text{BuCN})_2\text{CuOTf}$ (1 equiv), NFTPT (2 equiv), EtOAc (0.1 M in stannane), 25 °C, 12 h. Copper salt and NFTPT were pre-stirred in solvent for 5 min, followed by addition of the stannane. ^b Yield determined by ¹⁹F NMR spectroscopy. ^c Isolated yield. ^d Isolated product contained 8% of biphenyl (derived from protodestannylation). ^e 1.2 equiv of $(t\text{BuCN})_2\text{CuOTf}$.

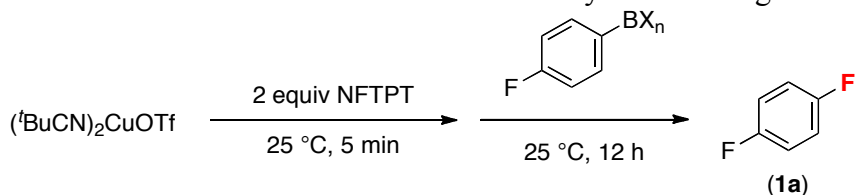
Table 5.5. Reaction of Aryl-SnBu₃ with NFTPT in the Absence of Cu^[a]

Entry	Substrate	Yield	Entry	Substrate	Yield
1		0%	6		0%
2		0%	7		0%
3		0%	8		0%
4		0%	9		0%
5		0%			

^[a] Reaction conditions: substrate (0.025 mmol, 1 equiv) and NFTPT (0.05 mmol, 2 equiv) in EtOAc (0.25 mL) at 25 °C for 12 h. Yields determined by ¹⁹F NMR analysis.

With this proof of principle in hand, we next investigated replacing the aryl stannanes with less toxic aryl–boron reagents. A series of *p*-FC₆H₄BX_n derivatives were examined under identical conditions to those in **Scheme 5.3**. As shown in **Table 5.6**, the aryl boron reagents generally afforded low to modest yields under these conditions. In most cases, the major by-products were either unreacted starting material or fluorobenzene from protodeboronation.¹⁷ The best result (46% yield) was obtained with the aryl trifluoroborate substrate (entry 5).

Table 5.6. Cu-Mediated Fluorination of Aryl Boron Reagents^a

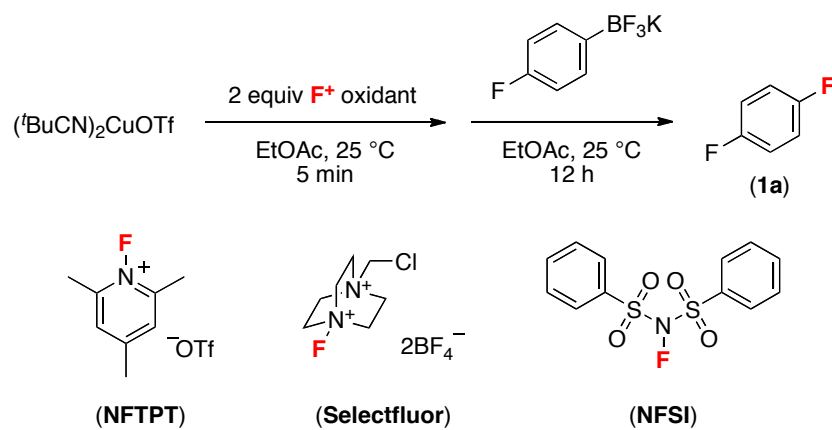


Entry	Substrate	Yield
1		1%
2		3%
3		3%
4		7%
5		46%
6		58% ^b

^a General conditions: stannane (0.025 mmol, 1 equiv), (tBuCN)₂CuOTf (1 equiv), NFTPT (2 equiv), EtOAc (0.1 M in boron reagent), 25 °C, 12 h. Copper salt and NFTPT were pre-stirred in solvent for 5 min, followed by addition of the substrate. Yields determined by ¹⁹F NMR spectroscopy. ^b Reaction conducted using MeCN as solvent.

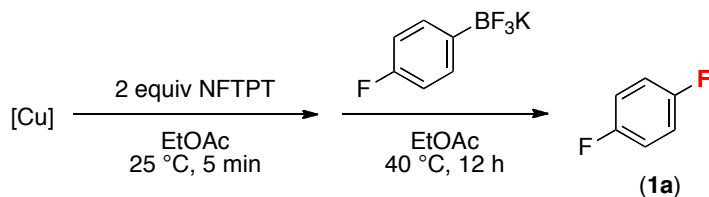
Further optimization studies confirmed that NFTPT and (^tBuCN)₂CuOTf are the best electrophilic fluorinating reagent and copper salt for Cu-mediated fluorination of aryl trifluoroborate (Tables 5.7, 5.8).

Table 5.7. F⁺ Oxidant Screen for Cu-Mediated Fluorination of (4-Fluorophenyl)trifluoroborate



Entry	F ⁺ Oxidant	Yield of 1a
1	NFTPT	46%
2	Selectfluor	9%
3	NFSI	11%

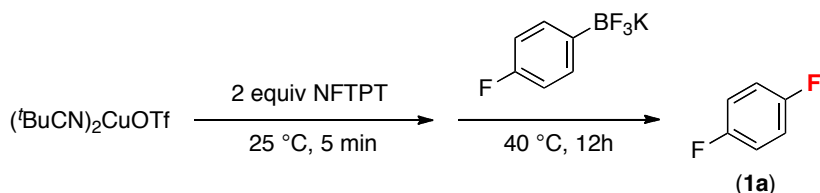
Table 5.8. Copper Screen for Cu-Mediated Fluorination of (4-Fluorophenyl)trifluoroborate



Entry	Copper Salt	Yield of 1a
1	(^t BuCN) ₂ CuOTf	46%
2	(MeCN) ₄ CuBF ₄	46%
3	(MeCN) ₄ CuPF ₆	44%
4	Cu(OTf)•1/2(C ₆ H ₆)	22%
5	Cu(OTf) ₂	12%
6	CuCl	10%
7	Cu	8%
8	CuOAc	0%
9	CuF ₂	0%

Finally, evaluation of a variety of solvents showed that switching from EtOAc to MeCN lead to a significant increase in yield to 58% (**Table 5.9**).

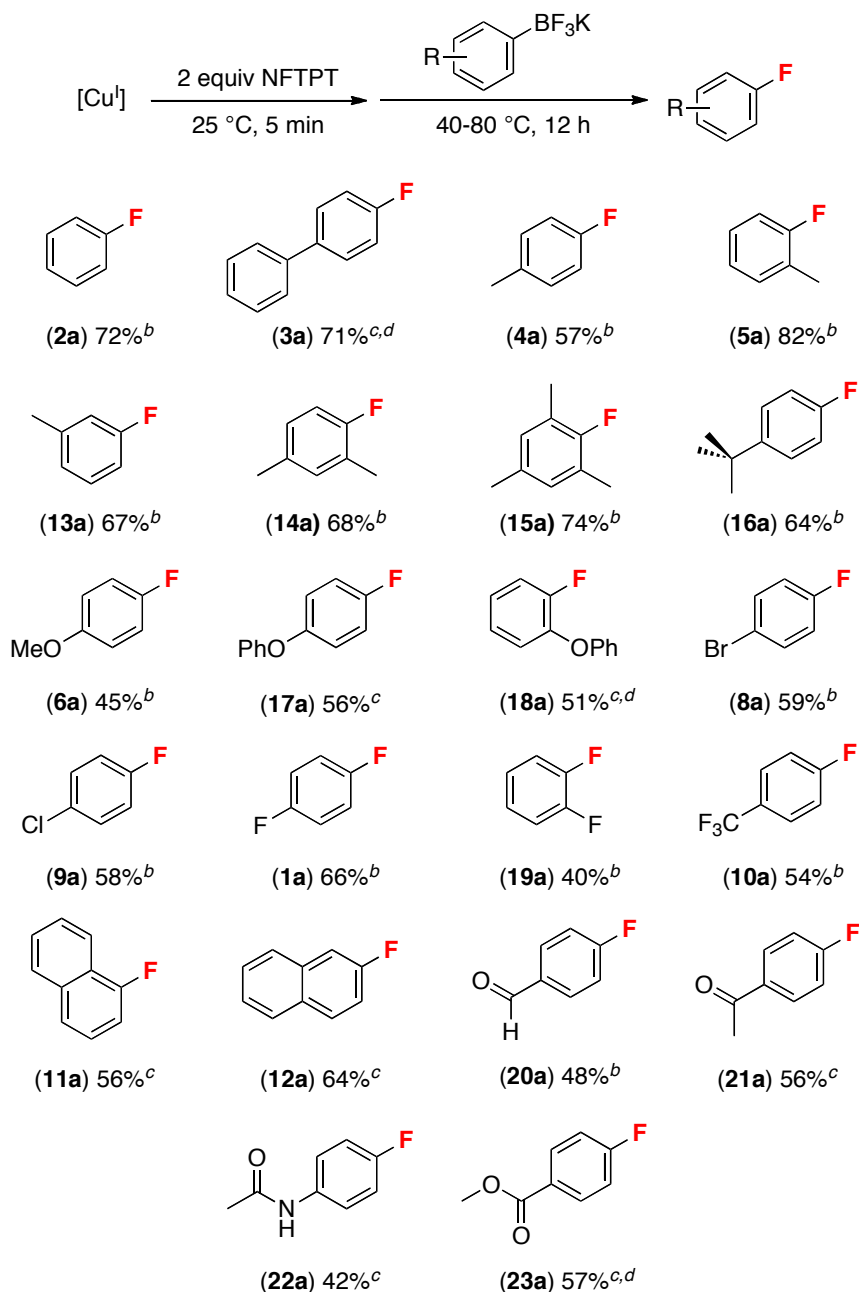
Table 5.9. Solvent Screen for Cu-Mediated Fluorination of (4-Fluorophenyl)trifluoroborate



Entry	Solvent	Yield of 1a
1	MeCN	58%
2	Toluene	48%
3	EtOAc	47%
4	DCM	43%
5	Acetone	21%
6	THF	13%
7	1,4-Dioxane	10%
8	DMF	0%

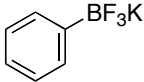
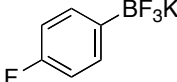
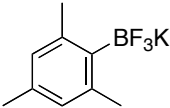
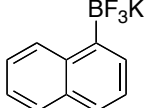
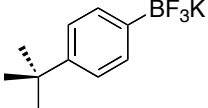
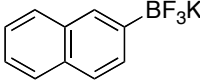
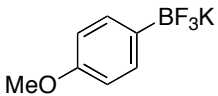
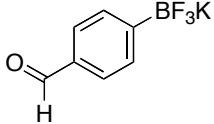
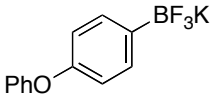
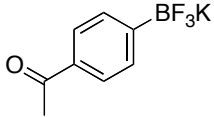
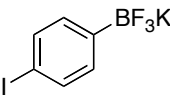
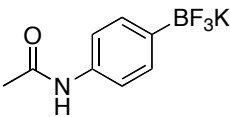
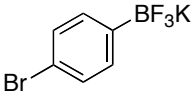
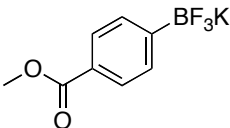
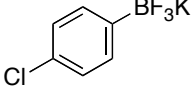
The substrate scope for the copper-mediated fluorination of aryl trifluoroborates is shown in **Scheme 5.4**. Aryltrifluoroborates bearing electron-donating and electron-withdrawing substituents reacted to generate the aryl-F products in good yields. Substrates containing *ortho*-substituents also underwent efficient fluorination under these optimized conditions. This protocol is compatible with a variety of common functional groups. Substrates bearing aryl aldehydes, ketones, amides, and esters produced the aryl fluorides in good yields. Control reactions (without added Cu) were conducted for all of the substrates in **Scheme 5.4**. As shown in **Table 5.10**, the electron deficient aryl trifluoroborates showed no background reaction under these conditions. Furthermore, only traces of background fluorination products (2-6%) were observed with the electron rich substrates *p*-MeOC₆H₄BF₃K, MesBF₃K, and naphthylBF₃K.

Scheme 5.4 Substrate Scope for Cu-Mediated Fluorination of Aryl Trifluoroborates^a



^a General conditions: substrate (0.25 mmol, 1 equiv), (tBuCN)₂CuOTf or (MeCN)₄CuBF₄ (1 to 2 equiv), NFTPT (2 equiv), 40 or 80 °C, 12 h. Copper salt and NFTPT were pre-stirred in solvent for 5 min, followed by addition of the substrate. ^b Yield determined by ¹⁹F NMR spectroscopy. ^c Isolated yield. ^d Isolated products contained small amounts (4-6%) of inseparable protodeboronated side-products.

Table 5.10. Reactions of Aryl–BF₃K with NFTPT^[a]

Entry	Substrate	Yield	Entry	Substrate	Yield
1		0%	9		0%
2		20% ^b	10		3%
3		0%	11		2% ^c
4		6%	12		0%
5		0%	13		0%
6		0%	14		0%
7		0%	15		0%
8		0%			

[a] Reaction conditions: substrate (0.025 mmol, 1 equiv) and NFTPT (0.05 mmol, 2 equiv) in EtOAc at 80 °C for 12 h. Yields determined by ¹⁹F NMR analysis of the crude reaction mixtures. [b] 2% of 2-fluoromesitylene was observed when control reaction was run at 40 °C. [c] 12% of 1-fluoronaphthalene was also observed.

5.3 Mechanistic Investigation

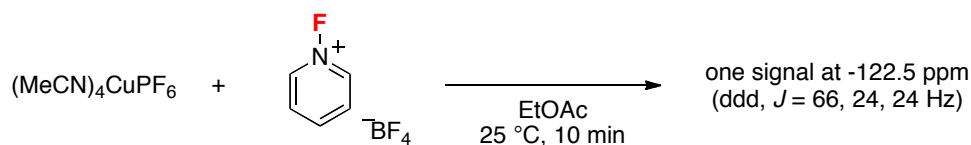
To preliminarily investigate the mechanism of this Cu-mediated fluorination protocol, we conducted a series of NMR spectroscopic studies of the reaction of (t-BuCN)₂CuOTf with NFTPT in EtOAc. After stirring at room temperature for 10 min, ¹⁹F NMR analysis showed the appearance of a resonance at –123.0 ppm, which may

correspond to a Cu(III)–F complex (see **Scheme 5.5**, **Figure 5.1**). However, this species is formed in very low yield (~1%), so it is unclear whether it is responsible for the observed reactivity. As shown in **Figure 5.1**, this signal appears as a doublet of doublet of doublets ($J = 56, 20, 20$ Hz). We initially hypothesized that the observed coupling involved protons on ^tBuCN or 2,4,6-trimethylpyridine, since the Cu-bound fluoride could potentially participate in an intramolecular hydrogen bonding interaction, thereby rendering three methyl hydrogens inequivalent. A similar phenomenon has recently been observed by Hartwig.¹⁵ However, a ¹⁹F NMR study of the oxidation of (MeCN)₄CuPF₆ with 1-fluoro-pyridinium tetrafluoroborate showed a similar doublet of doublet of doublets, suggesting against this proposal (**Scheme 5.6**). Ethyl acetate is a weak ligand, especially compared to MeCN. We tentatively hypothesize that the observed Cu(III)–F complex might contain a labile EtOAc ligand, like complex **24**. However, this possibility remains to be tested experimentally.

Scheme 5.5. Reaction of (^tBuCN)₂CuOTf with NFTPT in Ethyl Acetate



Scheme 5.6. Reaction of (MeCN)₄CuPF₆ with 1-Fluoro-Pyridinium Tetrafluoroborate in Ethyl Acetate

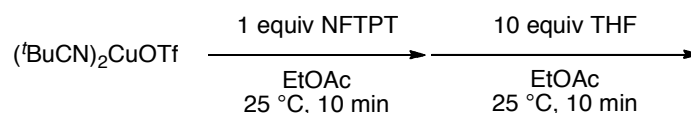


It is also possible that there is another Cu(III)–F species in solution that is undetectable because it shows a broad ¹⁹F NMR resonance due to fast exchange between free and bound EtOAc; however, VT NMR (down to –60 °C) did not provide any conclusive evidence to support or refute this proposal. In addition, attempts to detect Cu intermediates using mass spectrometry were inconclusive, possibly due to weak binding of the putative EtOAc ligand or due to the water sensitivity of these complexes.

We also tried to trap a Cu(III)–(F) intermediate with added ligands. Nitrogen-based mono- or bidentate ligands, such as pyridine, 2,2'-bipyridine, 4,4'-di-*tert*-butyl-2,2'-bipyridine and 1,10-phenanthroline, are commonly used for Cu-based transformations, and their ability to capture reactive transition-metal intermediates is well preceded.^{18,19} However, the addition of 2 equiv of pyridine, or 1 equiv of bidentate nitrogen-donor ligands resulted in immediate formation of blue or white precipitates and thus prevented direct characterization of the Cu(III)–F complex in EtOAc.

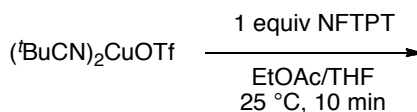
We next examined less coordinating ligands like MeCN and THF. However, a ¹⁹F NMR study of the oxidation of (^tBuCN)₂CuOTf with NFTPT in EtOAc with 10 equiv of MeCN or in MeCN as solvent did not show any Cu(III)–(F) signals. In contrast, the addition of 10 equiv of THF to a pre-stirred mixture of (^tBuCN)₂CuOTf and NFTPT in EtOAc (pre-stirring for 10 min at room temperature) generated a new peak that corresponds to the Cu(III)–(F)(THF) adduct that was reported in a very recent report by Hartwig. However, this species was formed in low (3%) yield in our system (see **Scheme 5.7, Figure 5.2**)¹⁵. For more discussion of Hartwig's similar approach, see **Section 5.5**.

Scheme 5.7. Investigation of Cu^(III)–F Complex using THF as Additive



When this same reaction was conducted in pre-mixed THF and EtOAc (10 equiv of THF) as solvent, the Cu(III)(THF)(F) complex characterized by Hartwig was formed in 18% yield as determined by ¹⁹F NMR spectroscopy (see **Scheme 5.8, Figure 5.3**)¹⁵. Ongoing efforts in our lab are focused on gaining further insights into the organometallic intermediates and the mechanistic complexities of this transformation.

Scheme 5.8. Investigation of Cu^(III)–F Complex using THF as Co-Solvent



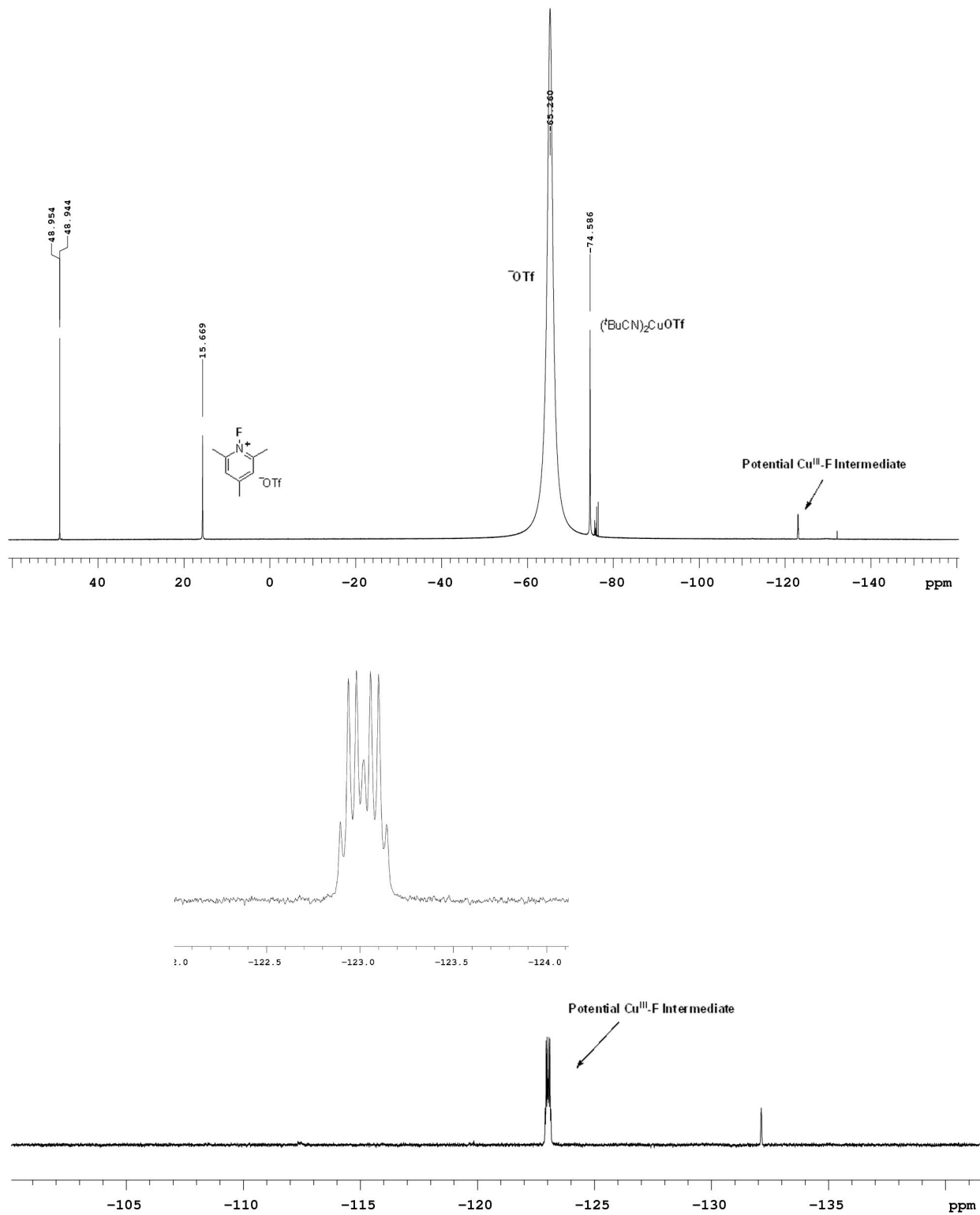


Figure 5.1 Investigation of Putative $\text{Cu}^{\text{III}}\text{-F}$ Intermediate using THF as Additive
(Spectrum Show Reaction before Addition of THF)

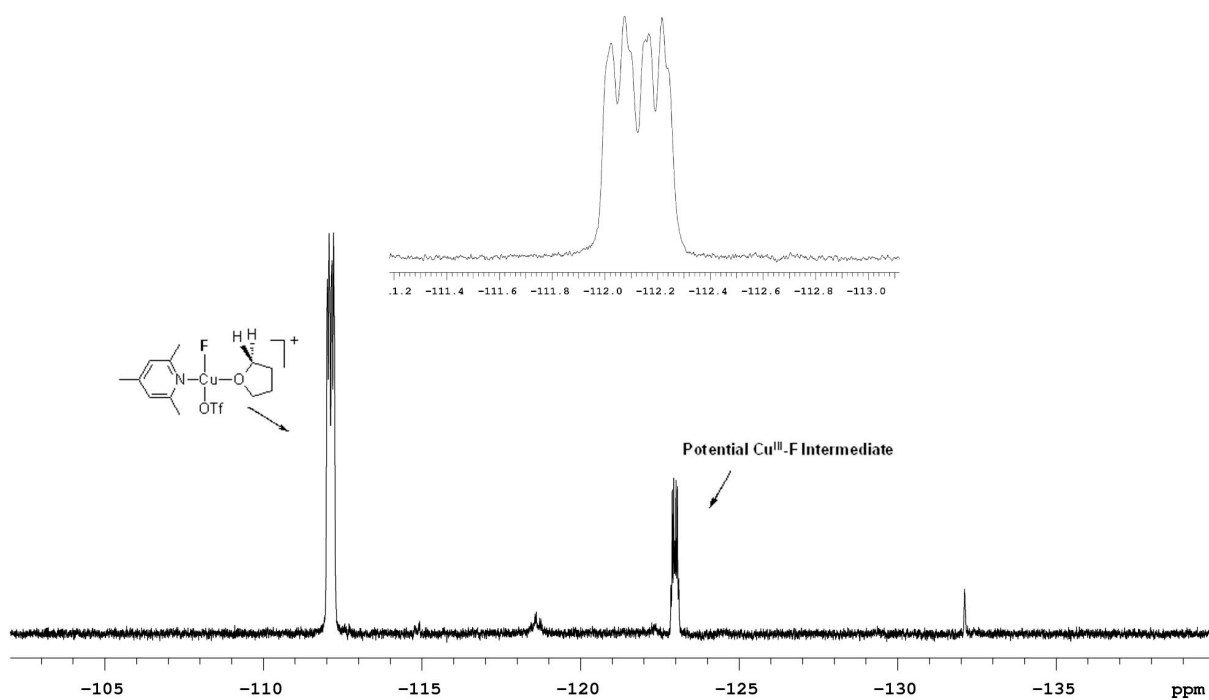
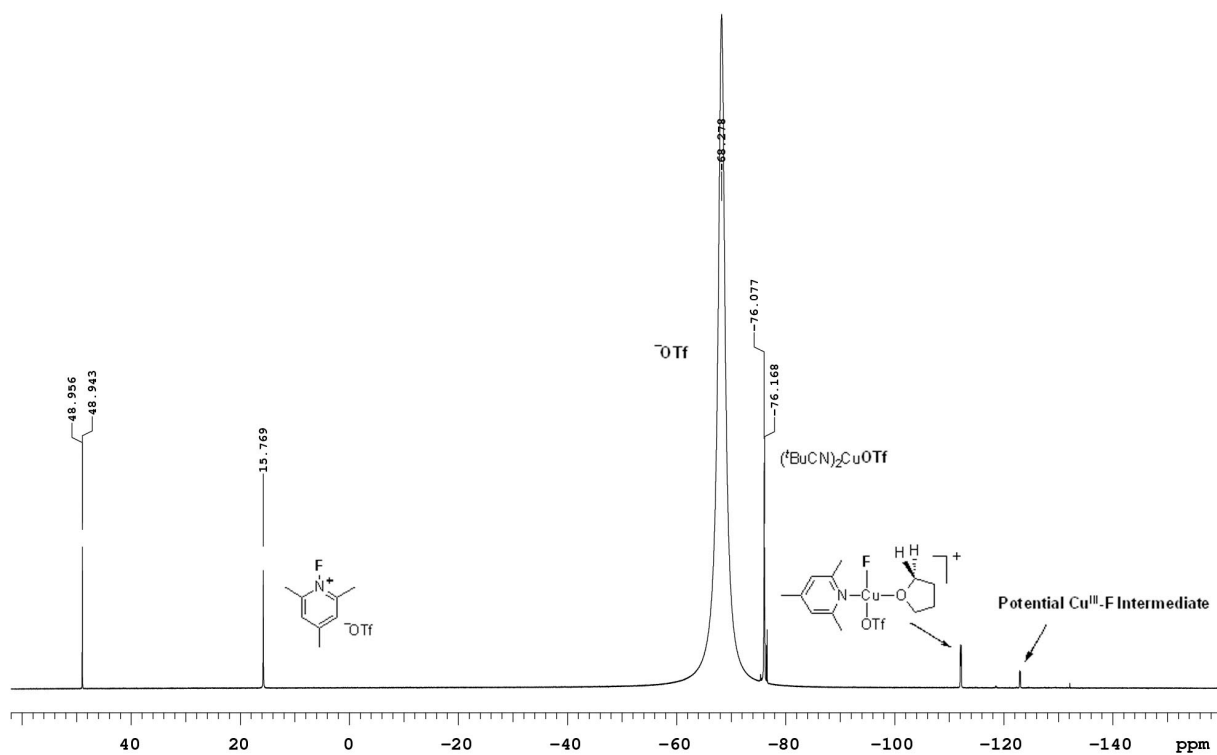


Figure 5.2 Investigation of Putative $\text{Cu}^{\text{III}}\text{-F}$ Intermediate using THF as Additive
 (Spectrum Show Reaction after Addition of THF)

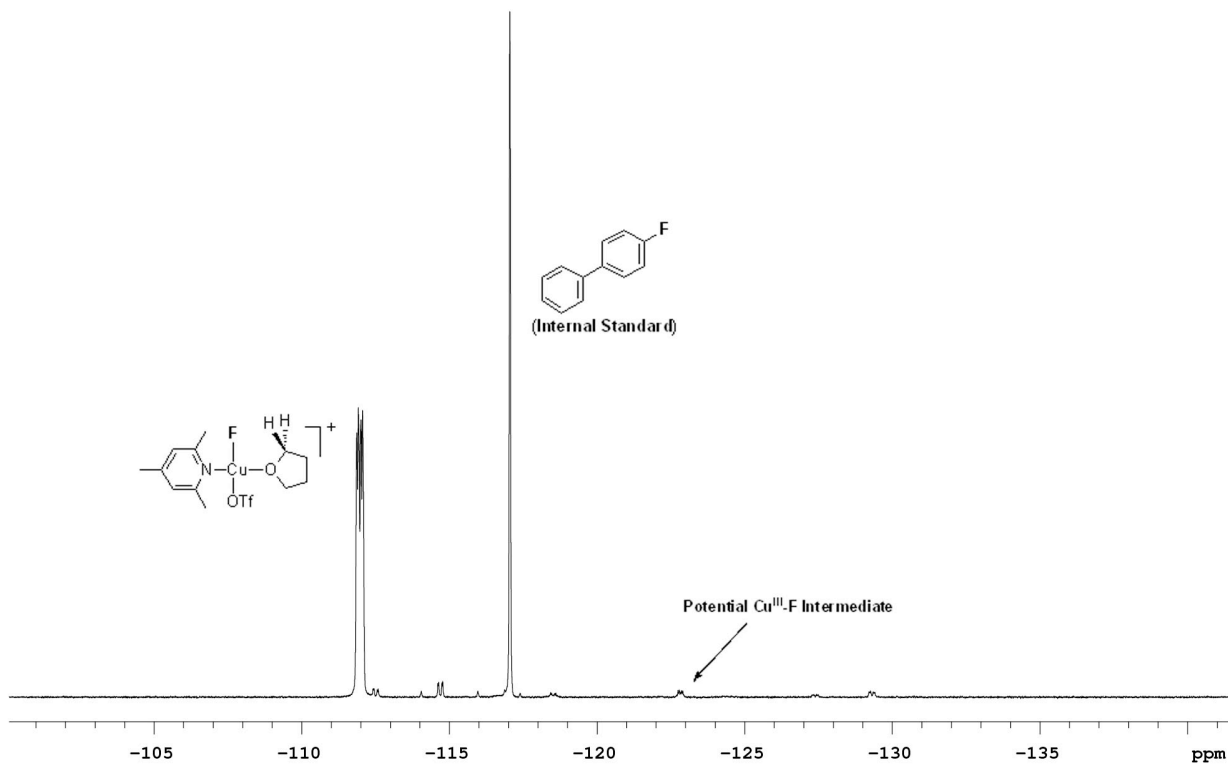
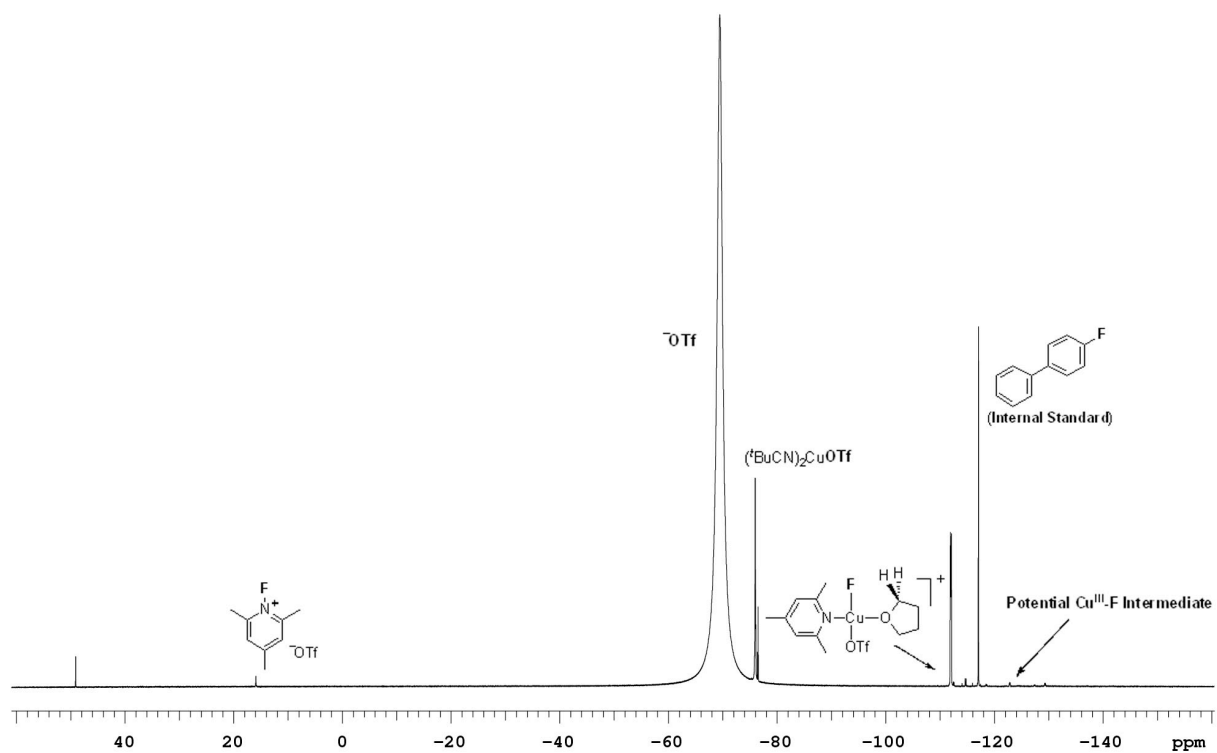


Figure 5.3 Investigation of Putative $\text{Cu}^{\text{III}}\text{-F}$ Intermediate using THF as Co-Solvent

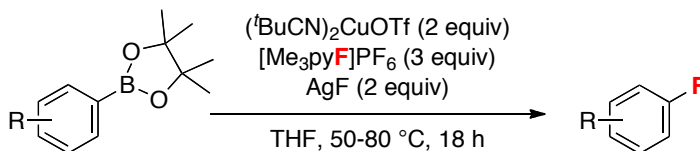
5.4 Conclusions

In summary, this chapter describes a new method for the Cu-mediated fluorination of aryl stannanes and aryl trifluoroborates with an electrophilic fluorinating reagent. The reactions proceed under very mild conditions (in many cases at room temperature) and exhibit a broad substrate scope and functional group tolerance.²⁰ A Cu(I/III) mechanism is proposed with a Cu^{III}(aryl)(fluoride) (**A** in **Scheme 5.1**) serving as a likely intermediate. Importantly, this strategy takes advantage of the dual role of the electrophilic fluorinating reagent as both an oxidant for Cu(I) and a fluorine source.²¹ Ongoing work is focused on effecting analogous fluorination reactions using alternative oxidants in conjunction with nucleophilic fluoride sources.²²

5.5 Subsequent Developments

While our manuscript was under peer review, Hartwig and co-workers reported a Cu-mediated aromatic fluorination that is remarkably similar to this work (**Scheme 5.9**).¹⁵ In particular, both approaches involve an aryl boron reagent as the organometallic substrate, as well as an *N*-fluoropyridinium salt as the F source and oxidant. Moreover, both methods are proposed to proceed via a Cu^{III} mechanism with a Cu^{III}(aryl)(fluoride) as a key intermediate (**A** in **Scheme 5.1**).

Scheme 5.9 Hartwig's Cu-Mediated Fluorination of Arylboronate Esters

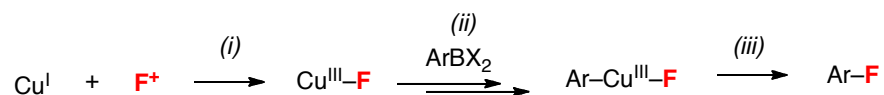


One major difference between Hartwig's and our fluorination method is that his system requires super-stoichiometric quantities of AgF to promote transmetalation of the arylboronate ester to the Cu center. When AgF was excluded from his reaction or was switched to another base, significantly lower yields were observed. On the contrary, our approach circumvents the requirement for this expensive reagent by using a different aryl boron reagent. Importantly, the aryl trifluoroborates used in our reaction can be prepared

in quantitative yield by the reaction of aryl boronic acids with KHF_2 . Aryl trifluoroborates are bench stable, white crystalline solids that participate in facile transmetallation without the addition of a base as promoter.²³ *As such, our approach represents the first mild aromatic fluorination mediated only by an inexpensive, earth abundant, first row transition metal.*

Another important advantage of our method compared to Hartwig's is the straightforward product isolation. Under our optimal conditions, Cu-mediated fluorination of most of the substrates in **Schemes 5.3** and **5.4** afforded the desired fluorinated product with no detectable protodeboronation or protodestannylation. As a result, pure aryl-F products were obtained easily by column chromatography. In only a few cases, small amounts (4-6%) of inseparable protodeboronated side-products were obtained. In contrast, Hartwig's method forms a larger amount of protodeboronated side-products (for example, 12% of the protodeborated by-product was formed in the fluorination of 4-butylphenylboronic acid under his optimal conditions), rendering it impractical for synthetic application.

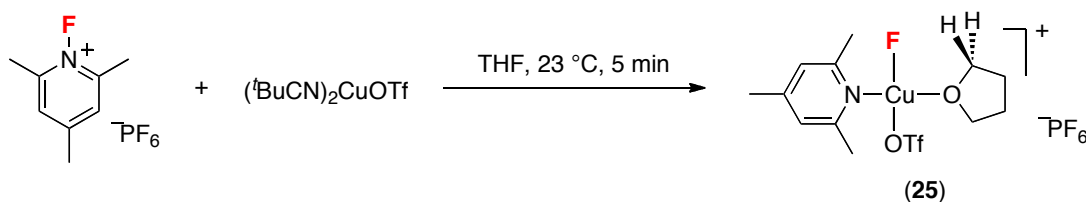
Scheme 5.10 Mechanistic Pathway of Cu-Mediated Fluorination of Aryl Boron Reagent



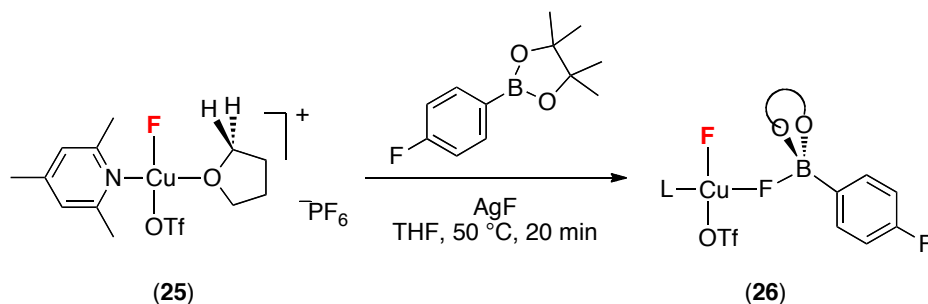
Detailed mechanistic studies by Hartwig suggest the Cu-mediated fluorination occurs through initial oxidation of Cu^{I} with the F^+ oxidant to form a $\text{Cu}^{\text{III}}\text{-F}$ complex (**Scheme 5.10**, step i), followed by AgF-promoted transmetallation of the aryl boronate ester to the Cu^{III} complex (step ii), resulting in a $\text{Cu}^{\text{III}}(\text{aryl})(\text{fluoride})$ intermediate. Fast aryl-F reductive coupling from this reactive $\text{Cu}^{\text{III}}(\text{aryl})(\text{fluoride})$ then liberates the desired fluorinated product. Notably, two $\text{Cu}^{\text{III}}\text{-F}$ intermediates were observed under Hartwig's reaction conditions and were successfully characterized by NMR spectroscopy and ESI-MS. For example, oxidation of $(^t\text{BuCN})_2\text{CuOTf}$ with the *N*-fluoropyridinium reagent in THF formed a new Cu species in full conversion (**Scheme 5.11**). Although the instability of this complex precluded isolation, the authors were able to unambiguously characterize and assign the structure of this intermediate as complex **25**, based on a series of NMR,

ESI-MS and DFT studies. Furthermore, a second Cu^{III}-F intermediate **26** was observed in the reaction of **25** with the aryl boronate ester in the presence of AgF. As discussed earlier, we spent tremendous effort attempting to characterize the Cu^{III} intermediates in our system (which are presumably closely related to complexes **25** and **26**). We believe the more coordinating THF ligand is essential for observing these labile reaction intermediates. Indeed, when THF was added to our reaction mixture of (tBuCN)₂CuOTf with NFTPT in EtOAc, complex **25** was observed, indicating a similar Cu^{III}-F intermediate to complex **24**, is possible in our system.

Scheme 5.11 Reaction of (tBuCN)₂CuOTf with F⁺ Reagent in THF



Scheme 5.12 Reaction of Complex **24** with Aryl-Bpin/AgF in THF



5.6 Experimental Procedures and Characterization Data

General Procedures

NMR spectra were obtained on a Varian MR400 (400 MHz for ¹H; 377 MHz for ¹⁹F; 100 MHz for ¹³C), a Varian vnmrs 500 (500 MHz for ¹H), or a Varian vnmrs 700 (700 MHz for ¹H; 175 MHz for ¹³C) spectrometer. ¹H and ¹³C chemical shifts are reported in parts per million (ppm) relative to TMS, with the residual solvent peak used as an internal reference. ¹⁹F NMR spectra are referenced based on the internal standard 1,3,5-trifluorobenzene or 4-fluoroanisole, which appears at -108.33 ppm and -125.55 ppm,

respectively. ^1H and ^{19}F multiplicities are reported as follows: singlet (s), doublet (d), triplet (t), quartet (q), and multiplet (m). GCMS analysis was performed on a Shimadzu GCMS-QP2010 plus gas chromatograph mass spectrometer. The products were separated on a 30 m length by 0.25 mm id RESTEK XTI-5 column coated with a 0.25 μm film. Helium was employed as the carrier gas, with a constant column flow of 1.5 mL/min. The injector temperature was held constant at 250 $^\circ\text{C}$. The GC oven temperature program was as follows: 32 $^\circ\text{C}$ hold 5 min, ramp 15 $^\circ\text{C}/\text{min}$ to 250 $^\circ\text{C}$, and hold for 1.5 min.

Materials and Methods.

Aryl stannanes were prepared using literature procedures.²⁴ PhSnBu_3 was obtained from Sigma Aldrich. $(^t\text{BuCN})_2\text{CuOTf}$ was prepared according to literature procedures.¹⁴ $(\text{MeCN})_4\text{CuBF}_4$ was obtained from Sigma Aldrich. *N*-fluoro-2,4,6-trimethylpyridinium triflate (NFTPT) was obtained from TCI America. Selectfluor and *N*-fluorobenzenesulfonimide (NFSI) were obtained from Sigma Aldrich. Aryl boronic acids were obtained from Frontier Scientific. Aryl trifluoroborate potassium salts were prepared using literature procedures.²⁵ 1,3,5-Trifluorobenzene and 4-fluoroanisole were obtained from Oakwood Products. Dry DMF, DMA, DMSO, 1,4-dioxane, diglyme and NMP were obtained from Sigma Aldrich. All syntheses were conducted in a nitrogen atmosphere glovebox or using standard Schlenk techniques unless otherwise stated.

Experimental Details.

F⁺ Oxidant Evaluation for Cu-Mediated Fluorination of 1

In a glovebox, substrate **1** (9.6 mg, 0.025 mmol, 1 equiv), $(^t\text{BuCN})_2\text{CuOTf}$ (9.47 mg, 0.025 mmol, 1 equiv), and F^+ oxidant (0.05 mmol, 2 equiv) were weighed into a 4 mL vial. MeCN (0.25 mL) was added as solvent, and the vial was sealed with a Teflon-lined cap. The reaction mixture was allowed to stir at 25 $^\circ\text{C}$ for 12 h. The resulting solution was diluted with CH_2Cl_2 (2 mL). 1,3,5-Trifluorobenzene and 4-fluoroanisole (0.025 mmol, 1 equiv) were added as internal standards, and the reactions were analyzed by ^{19}F NMR spectroscopy and GCMS.

Solvent Screen for Cu-Mediated Fluorination of 1 with NFTPT

In a glovebox, substrate **1** (9.6 mg, 0.025 mmol, 1 equiv), (^tBuCN)₂CuOTf (9.47 mg, 0.025 mmol, 1 equiv), and NFTPT (14.5 mg, 0.05 mmol, 2 equiv) were weighed into a 4 mL vial. Solvent (0.25 mL) was added, and the vial was sealed with a Teflon-lined cap. The reaction mixture was allowed to stir at 25 °C for 12 h. The resulting solution was diluted with CH₂Cl₂ (2 mL). 1,3,5-Trifluorobenzene and 4-fluoroanisole (0.025 mmol, 1 equiv) were added as internal standards, and the reactions were analyzed by ¹⁹F NMR spectroscopy and GCMS.

Solvent Screen for Cu-Mediated Fluorination of 1 by NFTPT with Sequential Addition Protocol

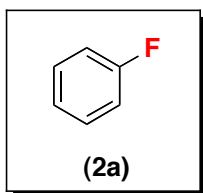
In a glovebox, (^tBuCN)₂CuOTf (9.47 mg, 0.025 mmol, 1 equiv) and NFTPT (14.5 mg, 0.05 mmol, 2 equiv) were weighed into a 4 mL vial. Solvent (0.25 mL) was added, and the vial was sealed with a Teflon-lined cap. The reaction mixture was allowed to stir at 25 °C for 5 min. Then, substrate **1** (9.6 mg, 0.025 mmol, 1 equiv) was added to the reaction mixture, and the reaction was allowed to stir at 25 °C for 12 h. The resulting solution was diluted with CH₂Cl₂ (2 mL). 1,3,5-Trifluorobenzene and 4-fluoroanisole (0.025 mmol, 1 equiv) were added as internal standards, and the reactions were analyzed by ¹⁹F NMR spectroscopy and GCMS.

Copper Screen for Cu-Mediated Fluorination of 1 by NFTPT with Sequential Addition Protocol

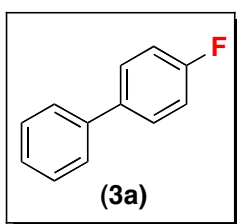
In a glovebox, copper salt (0.025 mmol, 1 equiv) and NFTPT (14.5 mg, 0.05 mmol, 2 equiv) were weighed into a 4 mL vial. EtOAc (0.25 mL) was added, and the vial was sealed with a Teflon-lined cap. The reaction mixture was allowed to stir at 25 °C for 5 min. Then, substrate **1** (9.6 mg, 0.025 mmol, 1 equiv) was added to the reaction mixture, and the reaction was allowed to stir at 25 °C for 12 h. The resulting solution was diluted with CH₂Cl₂ (2 mL). 1,3,5-Trifluorobenzene and 4-fluoroanisole (0.025 mmol, 1 equiv) were added as internal standards, and the reactions were analyzed by ¹⁹F NMR spectroscopy and GCMS.

Standard Procedure for Cu-Mediated Fluorination of Aryl Stannane by NFTPT

In a glovebox, (^tBuCN)₂CuOTf (94.7 mg, 0.25 mmol, 1 equiv) and NFTPT (145 mg, 0.5 mmol, 2 equiv) were weighed into a 20 mL vial. EtOAc (2.5 mL) was added, and the vial was sealed with a Teflon-lined cap. The reaction mixture was allowed to stir at 25 °C for 5 min. The substrate (0.25 mmol, 1 equiv) was then added to the reaction mixture, and the reaction was allowed to stir at 25 °C for 12 h. The resulting solution was diluted with CH₂Cl₂, or EtOAc (5 mL). 1,3,5-Trifluorobenzene and 4-fluoroanisole (0.25 mmol, 1 equiv) were added as internal standards, and the reactions were analyzed by ¹⁹F NMR spectroscopy and GCMS. GCMS analysis was performed on a Shimadzu GCMS-QP2010 plus gas chromatograph mass spectrometer. The products were separated on a 30 m length by 0.25 mm id RESTEK XTI-5 column coated with a 0.25 μm film. Helium was employed as the carrier gas, with a constant column flow of 1.5 mL/min. The injector temperature was held constant at 250 °C. The GC oven temperature program was as follows: 32 °C hold 5 min, ramp 15 °C/min to 250 °C, and hold for 1.5 min.

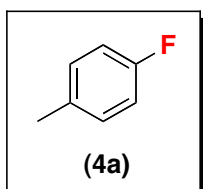


The reaction was performed using tributylphenyltin (92 mg, 0.25 mmol, 1 equiv). The fluorinated product **2a** was formed in 66% yield as determined by ¹⁹F NMR spectroscopic analysis of the crude reaction mixture. The ¹⁹F NMR spectral data for **2a** matched that of an authentic sample (Matrix Scientific, m, -114.07 ppm). The identity of the product was further confirmed by GCMS analysis, where the product peak was observed at 3.63 min.

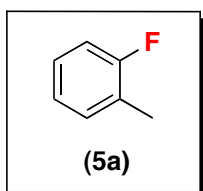


The reaction was performed using 4-(tributylstannyl)biphenyl (110.8 mg, 0.25 mmol, 1 equiv). The fluorinated product **3a** was formed in 68% yield as determined by ¹⁹F NMR spectroscopic analysis of the crude reaction mixture. The reaction mixture was then diluted with Et₂O (10 mL), and the resulting mixture was washed with 2 M aqueous HCl (15 mL) and brine (15 mL) and then dried over magnesium sulfate. The solvent was removed by rotary evaporation at 30 °C, and the product was purified by column chromatography on 10% w/w anhydrous potassium carbonate–silica using 1% triethylamine in pentane as the eluent (R_F = 0.35). Compound **3a** was obtained as white

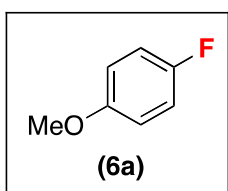
crystalline solid (29.0 mg, 67% yield). Compound **3a** (29 mg) was isolated with 8% of the corresponding protodestannylation byproduct biphenyl, which was not easily separable by chromatography on silica gel. The ^1H , ^{13}C and ^{19}F NMR spectroscopic data were identical to that reported previously in the literature.^{9a} HRMS EI (m/z): $[\text{M}]^+$ calcd for $\text{C}_{12}\text{H}_9\text{F}$, 172.0688; measured, 172.0688.



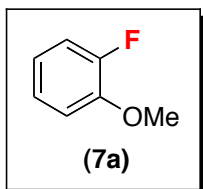
The reaction was performed using (4-methylphenyl)tributylstannane (95.3 mg, 0.25 mmol, 1 equiv). The fluorinated product **4a** was formed in 64% yield as determined by ^{19}F NMR spectroscopic analysis of the crude reaction mixture. The ^{19}F NMR spectral data for **4a** matched that of an authentic sample (Matrix Scientific, m, -119.59 ppm). The identity of the product was further confirmed by GCMS analysis, where the product peak was observed at 6.68 min.



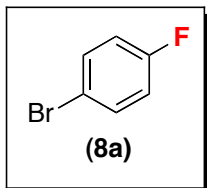
The reaction was performed using (2-methylphenyl)tributylstannane (95.3 mg, 0.25 mmol, 1 equiv). The fluorinated product **5a** was formed in 76% yield as determined by ^{19}F NMR spectroscopic analysis of the crude reaction mixture. The ^{19}F NMR spectral data for **5a** matched that of an authentic sample (Acros Organics, m, -118.63 ppm). The identity of the product was further confirmed by GCMS analysis, where the product peak was observed at 6.62 min.



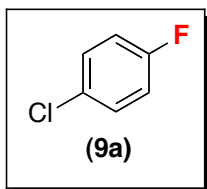
The reaction was performed using (4-methoxyphenyl)tributylstannane (99.3 mg, 0.25 mmol, 1 equiv). The fluorinated product **6a** was formed in 70% yield as determined by ^{19}F NMR spectroscopic analysis of the crude reaction mixture using 1,3,5-trifluorobenzene as an internal standard. The ^{19}F NMR spectral data for **6a** matched that of an authentic sample (Oakwood Products, m, -108.33 ppm). The identity of the product was further confirmed by GCMS analysis, where the product peak was observed at 9.53 min.



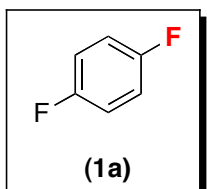
The reaction was performed using (2-methoxyphenyl)tributylstannane (99.3 mg, 0.25 mmol, 1 equiv). The fluorinated product **7a** was formed in 74% yield as determined by ^{19}F NMR spectroscopic analysis of the crude reaction mixture. The ^{19}F NMR spectral data for **7a** matched that of an authentic sample (Matrix Scientific, m, -136.47 ppm). The identity of the product was further confirmed by GCMS analysis, where the product peak was observed at 9.76 min.



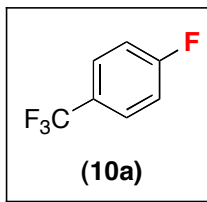
The reaction was performed using (4-bromophenyl)tributylstannane (112 mg, 0.25 mmol, 1 equiv). The fluorinated product **8a** was formed in 81% yield as determined by ^{19}F NMR spectroscopic analysis of the crude reaction mixture. The ^{19}F NMR spectral data for **8a** matched that of an authentic sample (SynQuest Labs, m, -116.25 ppm). The identity of the product was further confirmed by GCMS analysis, where the product peak was observed at 9.48 min.



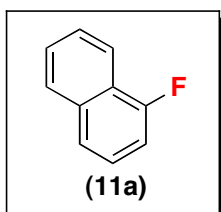
The reaction was performed using (4-chlorophenyl)tributylstannane (100.4 mg, 0.25 mmol, 1 equiv). The fluorinated product **9a** was formed in 80% yield as determined by ^{19}F NMR spectroscopic analysis of the crude reaction mixture. The ^{19}F NMR spectral data for **9a** matched that of an authentic sample (Oakwood Products, m, -116.83 ppm). The identity of the product was further confirmed by GCMS analysis, where the product peak was observed at 8.00 min.



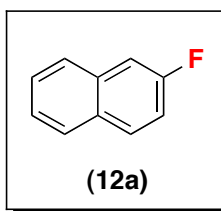
The reaction was performed using (4-fluorophenyl)tributylstannane (96 mg, 0.25 mmol, 1 equiv). The fluorinated product **1a** was formed in 74% yield as determined by ^{19}F NMR spectroscopic analysis of the crude reaction mixture. The ^{19}F NMR spectral data for **1a** matched that of an authentic sample (Alfa Aesar, m, -120.50 ppm). The identity of the product was further confirmed by GCMS analysis, where the product peak was observed at 3.74 min.



The reaction was performed using (4-trifluoromethylphenyl)tributylstannane (108.8 mg, 0.25 mmol, 1 equiv). The fluorinated product **10a** was formed in 93% yield as determined by ^{19}F NMR spectroscopic analysis of the crude reaction mixture using 4-fluoroanisole as internal standard. The ^{19}F NMR spectral data for **10a** matched that of an authentic sample (Matrix Scientific, s, 3F, -62.62 ppm; m, F, -108.44 ppm). The identity of the product was further confirmed by GCMS analysis, where the product peak was observed at 4.28 min.



The reaction was performed using 1-(tributylstannyl)naphthalene (208.6 mg, 0.25 mmol, 1 equiv). In this reaction 1.2 equiv of $(^t\text{BuCN})_2\text{CuOTf}$ (114 mg, 0.30 mmol) was used. The fluorinated product was formed in 66% yield as determined by ^{19}F NMR spectroscopic analysis of the crude reaction mixture. The reaction mixture was then diluted with Et_2O (10 mL), and the resulting mixture was washed with 2 M aqueous HCl (15 mL) and brine (15 mL) and then dried over magnesium sulfate. The solvent was removed by rotary evaporation at $0\text{ }^\circ\text{C}$, and the product was purified by column chromatography on 10% w/w anhydrous potassium carbonate–silica using 1% triethylamine in pentane as the eluent ($R_F = 0.55$). Compound **11a** was obtained as clear liquid (22.0 mg, 60% yield). The ^1H , ^{13}C and ^{19}F NMR spectroscopic data were identical to that reported previously in the literature.^{9a} HRMS EI (m/z): $[\text{M}]^+$ calcd for $\text{C}_{10}\text{H}_7\text{F}$, 146.0532; measured, 146.0531.



The reaction was performed using 2-(tributylstannyl)naphthalene (208.6 mg, 0.25 mmol, 1 equiv). The fluorinated product was formed in 82% yield as determined by ^{19}F NMR spectroscopic analysis of the crude reaction mixture. The reaction mixture was then diluted with Et_2O (10 mL), and the resulting mixture was washed with 2 M aqueous HCl (15 mL) and brine (15 mL) and then dried over magnesium sulfate. The solvent was removed by rotary evaporation at $0\text{ }^\circ\text{C}$, and the product was purified by column chromatography on 10% w/w anhydrous potassium carbonate–silica using 1% triethylamine in pentane as the eluent ($R_F = 0.48$). Compound **12a** was obtained as white crystalline solid (26.0 mg, 71%

yield, mp = 59.8-60.4 °C). ¹H NMR (CDCl₃): δ 7.86-7.82 (multiple peaks, 2H), 7.79 (dd, *J* = 8.4, 1 Hz, 1H), 7.51 (ddd, *J* = 7.5, 7.5, 1 Hz, 1H), 7.46 (m, 1H), 7.45 (ddd, *J* = 7.5, 7.5, 1 Hz, 1H), 7.27 (ddd, *J* = 10.5, 8.4, 1 Hz, 1H). ¹³C NMR (CDCl₃): δ 160.07 (d, *J* = 244.0 Hz), 134.27 (d, *J* = 9.4 Hz), 130.57, 130.42 (d, *J* = 9.6 Hz), 128.02 (d, *J* = 1.4 Hz), 127.40 (d, *J* = 5.4 Hz), 127.00, 125.22 (d, *J* = 2.8 Hz), 116.40 (d, *J* = 25.0 Hz), 111.00 (d, *J* = 20.3 Hz). ¹⁹F NMR (CDCl₃): δ -114.90 (m, 1F). HRMS EI (*m/z*): [M]⁺ calcd for C₁₀H₇F, 146.0532; measured, 146.0531.

Evaluation of Arylboronic Acid Derivatives for Cu-Mediated Fluorination by NFTPT

4-Fluorophenyl boronic acid pinacol ester,²⁶ boroxine,²⁷ and MIDA ester²⁸ were prepared according to literature procedures.

In a glovebox, (tBuCN)₂CuOTf (9.47 mg, 0.025 mmol, 1 equiv) and NFTPT (14.5 mg, 0.05 mmol, 2 equiv) were weighed into a 4 mL vial. EtOAc (0.25 mL) was added as solvent, and the vial was sealed with a Teflon-lined cap. The reaction mixture was allowed to stir at 25 °C for 5 min. Then, the substrate (0.025 mmol based on boron, 1 equiv) was added to the reaction mixture, and the reaction was allowed to stir at 25 °C for 12 h. The resulting solution was diluted with CH₂Cl₂ (2 mL). 1,3,5-Trifluorobenzene and 4-fluoroanisole (0.025 mmol, 1 equiv) were added as internal standards, and the reactions were analyzed by ¹⁹F NMR spectroscopy and GCMS.

F⁺ Oxidant Evaluation for Cu-Mediated Fluorination of (4-Fluorophenyl)trifluoroborate

In a glovebox, (tBuCN)₂CuOTf (9.47 mg, 0.025 mmol, 1 equiv) and F⁺ oxidant (0.05 mmol, 2 equiv) were weighed into a 4 mL vial. EtOAc (0.25 mL) was added, and the vial was sealed with a Teflon-lined cap. The reaction mixture was allowed to stir at 25 °C for 5 min. Then, (4-fluorophenyl)trifluoroborate (5.05 mg, 0.025 mmol, 1 equiv) was added to the reaction mixture, and the reaction was allowed to stir at 25 °C for 12 h. The resulting solution was diluted with CH₂Cl₂ (2 mL). 1,3,5-Trifluorobenzene and 4-

fluoroanisole (0.025 mmol, 1 equiv) were added as internal standards, and the reactions were analyzed by ^{19}F NMR spectroscopy and GCMS.

Copper Screen for Cu-Mediated Fluorination of (4-Fluorophenyl)trifluoroborate by NFTPT

In a glovebox, copper salt (0.025 mmol, 1 equiv) and NFTPT (14.5 mg, 0.05 mmol, 2 equiv) were weighed into a 4 mL vial. EtOAc (0.5 mL) was added, and the vial was sealed with a Teflon-lined cap. The reaction mixture was allowed to stir at 25 °C for 5 min. Then, (4-fluorophenyl)trifluoroborate (5.05 mg, 0.025 mmol, 1 equiv) was added to the reaction mixture, and the reaction was allowed to stir at 40 °C for 12 h. The resulting solution was diluted with CH_2Cl_2 (2 mL). 1,3,5-Trifluorobenzene and 4-fluoroanisole (0.025 mmol, 1 equiv) were added as internal standards, and the reactions were analyzed by ^{19}F NMR spectroscopy and GCMS.

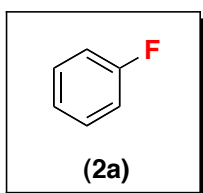
Solvent Screen for Cu-Mediated Fluorination of (4-Fluorophenyl)trifluoroborate by NFTPT

In a glovebox, $(t\text{BuCN})_2\text{CuOTf}$ (9.47 mg, 0.025 mmol, 1 equiv) and NFTPT (14.5 mg, 0.05 mmol, 2 equiv) were weighed into a 4 mL vial. Solvent (0.5 mL) was added, and the vial was sealed with a Teflon-lined cap. The reaction mixture was allowed to stir at 25 °C for 5 min. Then, (4-fluorophenyl)trifluoroborate (5.05 mg, 0.025 mmol, 1 equiv) was added to the reaction mixture, and the reaction was allowed to stir at 40 °C for 12 h. The resulting solution was diluted with CH_2Cl_2 (2 mL). 1,3,5-Trifluorobenzene and 4-fluoroanisole (0.025 mmol, 1 equiv) were added as internal standards, and the reactions were analyzed by ^{19}F NMR spectroscopy and GCMS.

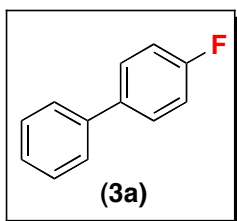
Standard Procedure for Cu-Mediated Fluorination of Aryl Trifluoroborate by NFTPT

In a glovebox, $(t\text{BuCN})_2\text{CuOTf}$ or $(\text{MeCN})_4\text{CuBF}_4$ (0.25-0.5 mmol, 1-2 equiv), and NFTPT (145 mg, 0.5 mmol, 2 equiv) were weighed into a 20 mL vial. EtOAc or MeCN (5 mL) was added, and the vial was sealed with a Teflon-lined cap. The reaction mixture was allowed to stir at 25 °C for 5 min. The substrate (0.25 mmol, 1 equiv) was then added

to the reaction mixture, and the reaction was allowed to stir at 40 or 80 °C for 12 h. The resulting solution was diluted with CH₂Cl₂, or EtOAc (5 mL). 1,3,5-Trifluorobenzene and 4-fluoroanisole (0.25 mmol, 1 equiv) were added as internal standards, and the reactions were analyzed by ¹⁹F NMR spectroscopy and GCMS. GCMS analysis was performed on a Shimadzu GCMS-QP2010 plus gas chromatograph mass spectrometer. The products were separated on a 30 m length by 0.25 mm id RESTEK XTI-5 column coated with a 0.25 μm film. Helium was employed as the carrier gas, with a constant column flow of 1.5 mL/min. The injector temperature was held constant at 250 °C. The GC oven temperature program was as follows: 32 °C hold 5 min, ramp 15 °C/min to 250 °C, and hold for 1.5 min.



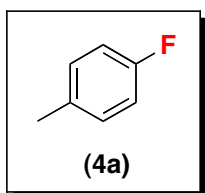
In a glovebox, (tBuCN)₂CuOTf (94.7 mg, 0.25 mmol, 1 equiv) and NFTPT (145 mg, 0.5 mmol, 2 equiv) were weighed into a 20 mL vial. EtOAc (5 mL) was added, and the vial was sealed with a Teflon-lined cap. The reaction mixture was allowed to stir at 25 °C for 5 min. Then, potassium phenyl trifluoroborate (46 mg, 0.25 mmol, 1 equiv) was added to the reaction mixture, and the reaction was allowed to stir at 80 °C for 12 h. The resulting solution was cooled to 25 °C, and diluted with CH₂Cl₂ (5 mL). 1,3,5-Trifluorobenzene and 4-fluoroanisole (0.25 mmol, 1 equiv) were added as internal standards. The fluorinated product **2a** was formed in 72% yield as determined by ¹⁹F NMR spectroscopic analysis of the crude reaction mixture. The ¹⁹F NMR spectral data for **2a** matched that of an authentic sample (Matrix Scientific, m, -114.07 ppm). The identity of the product was further confirmed by GCMS analysis, where the product peak was observed at 3.63 min.



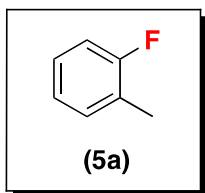
In a glovebox, (MeCN)₄CuBF₄ (94.2 mg, 0.30 mmol, 1.2 equiv) and NFTPT (145 mg, 0.5 mmol, 2 equiv) were weighed into a 20 mL vial. EtOAc (5 mL) was added, and the vial was sealed with a Teflon-lined cap. The reaction mixture was allowed to stir at 25 °C for 5 min. Then, potassium trifluoro(4-phenylphenyl)borate (65 mg, 0.25 mmol, 1 equiv) was added to the reaction mixture, and the reaction was allowed to stir at 80 °C for 12 h. The resulting solution was cooled to 25 °C, and diluted with EtOAc (5 mL). 1,3,5-

Trifluorobenzene and 4-fluoroanisole (0.25 mmol, 1 equiv) were added as internal standards. The fluorinated product **3a** was formed in 71% yield as determined by ^{19}F NMR spectroscopic analysis of the crude reaction mixture. The reaction mixture was then diluted with Et_2O (10 mL), and the resulting mixture was washed with 2 M aqueous HCl (15 mL) and brine (15 mL) and then dried over magnesium sulfate. The solvent was removed by rotary evaporation at 30 °C, and the product was purified by column chromatography on silica gel using pentane as the eluent ($R_{\text{F}} = 0.35$). Compound **3a** was obtained as white crystalline solid.

The isolated product **3a** (30.5 mg, 71% yield) was 94% pure, and contained 6% of the corresponding protodeboronation byproduct, which was not easily separable by chromatography on silica gel. The ^1H , ^{13}C and ^{19}F NMR spectroscopic data were identical to that reported previously in the literature.^{9a} HRMS EI (m/z): $[\text{M}]^+$ calcd for $\text{C}_{12}\text{H}_9\text{F}$, 172.0688; measured, 172.0688.

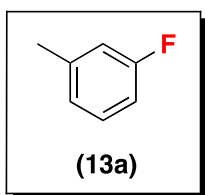


In a glovebox, $(^t\text{BuCN})_2\text{CuOTf}$ (94.7 mg, 0.25 mmol, 1 equiv) and NFTPT (145 mg, 0.5 mmol, 2 equiv) were weighed into a 20 mL vial. EtOAc (5 mL) was added, and the vial was sealed with a Teflon-lined cap. The reaction mixture was allowed to stir at 25 °C for 5 min. Then, potassium (4-methylphenyl)trifluoroborate (49.5 mg, 0.25 mmol, 1 equiv) was added to the reaction mixture, and the reaction was allowed to stir at 80 °C for 12 h. The resulting solution was cooled to room temperature and diluted with CH_2Cl_2 (5 mL). 1,3,5-Trifluorobenzene and 4-fluoroanisole (0.25 mmol, 1 equiv) were added as internal standards. The fluorinated product **4a** was formed in 57% yield as determined by ^{19}F NMR spectroscopic analysis of the crude reaction mixture. The ^{19}F NMR spectral data for **4a** matched that of an authentic sample (Matrix Scientific, m, -119.59 ppm). The identity of the product was further confirmed by GCMS analysis, where the product peak was observed at 6.68 min.

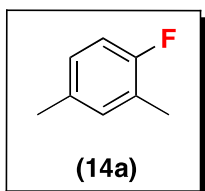


In a glovebox, $(^t\text{BuCN})_2\text{CuOTf}$ (142 mg, 0.375 mmol, 1.5 equiv) and NFTPT (145 mg, 0.5 mmol, 2 equiv) were weighed into a 20 mL vial.

EtOAc (5 mL) was added, and the vial was sealed with a Teflon-lined cap. The reaction mixture was allowed to stir at 25 °C for 5 min. Then, potassium (2-methylphenyl)trifluoroborate (49.5 mg, 0.25 mmol, 1 equiv) was added to the reaction mixture, and the reaction was allowed to stir at 80 °C for 12 h. The resulting solution was cooled to room temperature and diluted with CH₂Cl₂ (5 mL). 1,3,5-Trifluorobenzene and 4-fluoroanisole (0.25 mmol, 1 equiv) were added as internal standards. The fluorinated product **5a** was formed in 82% yield as determined by ¹⁹F NMR spectroscopic analysis of the crude reaction mixture. The ¹⁹F NMR spectral data for **5a** matched that of an authentic sample (Acros Organics, m, -118.63 ppm). The identity of the product was further confirmed by GCMS analysis, where the product peak was observed at 6.62 min.

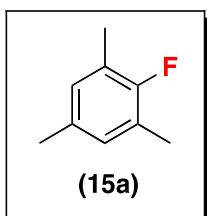


In a glovebox, (tBuCN)₂CuOTf (114 mg, 0.30 mmol, 1.2 equiv) and NFTPT (145 mg, 0.5 mmol, 2 equiv) were weighed into a 20 mL vial. EtOAc (5 mL) was added, and the vial was sealed with a Teflon-lined cap. The reaction mixture was allowed to stir at 25 °C for 5 min. Then, potassium (3-methylphenyl)trifluoroborate (49.5 mg, 0.25 mmol, 1 equiv) was added to the reaction mixture, and the reaction was allowed to stir at 40 °C for 12 h. The resulting solution was diluted with CH₂Cl₂ (5 mL). 1,3,5-Trifluorobenzene and 4-fluoroanisole (0.25 mmol, 1 equiv) were added as internal standards. The fluorinated product **13a** was formed in 67% yield as determined by ¹⁹F NMR spectroscopic analysis of the crude reaction mixture. The ¹⁹F NMR spectral data for **13a** matched that of an authentic sample (Matrix Scientific, m, -115.24 ppm). The identity of the product was further confirmed by GCMS analysis, where the product peak was observed at 6.57 min.

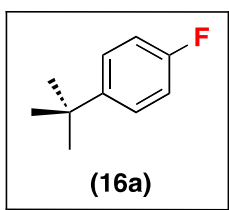


In a glovebox, (MeCN)₄CuBF₄ (94.2 mg, 0.30 mmol, 1.2 equiv) and NFTPT (145 mg, 0.5 mmol, 2 equiv) were weighed into a 20 mL vial. EtOAc (5 mL) was added, and the vial was sealed with a Teflon-lined cap. The reaction mixture was allowed to stir at 25 °C for 5 min. Then, potassium (2,4-dimethylphenyl)trifluoroborate (53 mg, 0.25 mmol, 1 equiv) was added to the reaction mixture, and the reaction was allowed to stir at 80 °C for 12 h. The resulting solution was cooled to room temperature and then diluted with CH₂Cl₂ (5 mL). 1,3,5-

Trifluorobenzene and 4-fluoroanisole (0.25 mmol, 1 equiv) were added as internal standards. The fluorinated product **14a** was formed in 68% yield as determined by ^{19}F NMR spectroscopic analysis of the crude reaction mixture. The ^{19}F NMR spectral data for **14a** matched that of an authentic sample (SynQuest Laboratories, m, -124.10 ppm). The identity of the product was further confirmed by GCMS analysis, where the product peak was observed at 8.84 min.

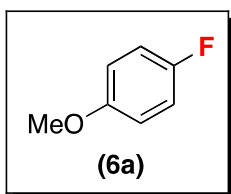


In a glovebox, $(^t\text{BuCN})_2\text{CuOTf}$ (190 mg, 0.50 mmol, 2 equiv) and NFTPT (145 mg, 0.5 mmol, 2 equiv) were weighed into a 20 mL vial. EtOAc (5 mL) was added, and the vial was sealed with a Teflon-lined cap. The reaction mixture was allowed to stir at 25 °C for 5 min. Then, potassium (2,4,6-trimethylphenyl)trifluoroborate (56.5 mg, 0.25 mmol, 1 equiv) was added to the reaction mixture, and the reaction was allowed to stir at 40 °C for 12 h. The resulting solution was diluted with CH_2Cl_2 (5 mL). 1,3,5-Trifluorobenzene and 4-fluoroanisole (0.25 mmol, 1 equiv) were added as internal standards. The fluorinated product **15a** was formed in 74% yield as determined by ^{19}F NMR spectroscopic analysis of the crude reaction mixture. The ^{19}F NMR spectral data for **15a** matched that of an authentic sample (Matrix Scientific, m, -128.52 ppm). The identity of the product was further confirmed by GCMS analysis, where the product peak was observed at 10.46 min.

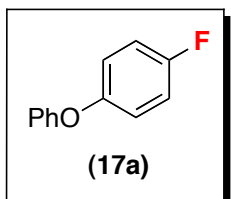


In a glovebox, $(^t\text{BuCN})_2\text{CuOTf}$ (114 mg, 0.30 mmol, 1.2 equiv) and NFTPT (145 mg, 0.5 mmol, 2 equiv) were weighed into a 20 mL vial. EtOAc (5 mL) was added, and the vial was sealed with a Teflon-lined cap. The reaction mixture was allowed to stir at 25 °C for 5 min. Then, potassium (4-*tert*-butylphenyl)trifluoroborate (60 mg, 0.25 mmol, 1 equiv) was added to the reaction mixture, and the reaction was allowed to stir at 80 °C for 12 h. The resulting solution was cooled to room temperature and diluted with CH_2Cl_2 (5 mL). 1,3,5-Trifluorobenzene and 4-fluoroanisole (0.25 mmol, 1 equiv) were added as internal standards. The fluorinated product **16a** was formed in 64% yield as determined by ^{19}F NMR spectroscopic analysis of the crude reaction mixture. The product showed a

^{19}F NMR signal at -119.61 ppm in CDCl_3 (lit. -119.0 ppm in CDCl_3).²⁹ The identity of the product was further confirmed by GCMS analysis, where the product peak was observed at 10.67 min.

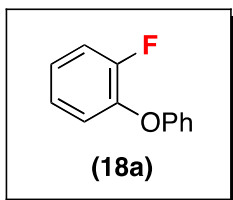


In a glovebox, $(^t\text{BuCN})_2\text{CuOTf}$ (114 mg, 0.30 mmol, 1.2 equiv) and NFTPT (145 mg, 0.5 mmol, 2 equiv) were weighed into a 20 mL vial. EtOAc (5 mL) was added, and the vial was sealed with a Teflon-lined cap. The reaction mixture was allowed to stir at $25\text{ }^\circ\text{C}$ for 5 min. Then, potassium (4-methoxyphenyl)trifluoroborate (53.5 mg, 0.25 mmol, 1 equiv) was added to the reaction mixture, and the reaction was allowed to stir at $80\text{ }^\circ\text{C}$ for 12 h. The resulting solution was cooled to room temperature and then diluted with CH_2Cl_2 (5 mL). 1,3,5-Trifluorobenzene (0.25 mmol, 1 equiv) was added as internal standards. The fluorinated product **6a** was formed in 45% yield as determined by ^{19}F NMR spectroscopic analysis of the crude reaction mixture. The ^{19}F NMR spectral data for **6a** matched that of an authentic sample (Oakwood Products, m, -108.33 ppm). The identity of the product was further confirmed by GCMS analysis, where the product peak was observed at 9.53 min.

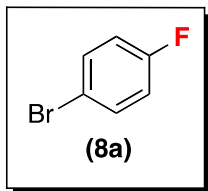


In a glovebox, $(^t\text{BuCN})_2\text{CuOTf}$ (94.7 mg, 0.25 mmol, 1 equiv) and NFTPT (145 mg, 0.5 mmol, 2 equiv) were weighed into a 20 mL vial. EtOAc (5 mL) was added, and the vial was sealed with a Teflon-lined cap. The reaction mixture was allowed to stir at $25\text{ }^\circ\text{C}$ for 5 min. Then, potassium trifluoro(4-phenoxyphenyl)borate (69 mg, 0.25 mmol, 1 equiv) was added to the reaction mixture, and the reaction was allowed to stir at $40\text{ }^\circ\text{C}$ for 12 h. The resulting solution was cooled to $25\text{ }^\circ\text{C}$, and diluted with EtOAc (5 mL). 1,3,5-Trifluorobenzene (0.25 mmol, 1 equiv) was added as internal standards. The fluorinated product **17a** was formed in 60% yield as determined by ^{19}F NMR spectroscopic analysis of the crude reaction mixture. The reaction mixture was then diluted with Et_2O (10 mL), and the resulting mixture was washed with 2 M aqueous HCl (15 mL) and brine (15 mL) and then dried over magnesium sulfate. The solvent was removed by rotary evaporation at $30\text{ }^\circ\text{C}$, and the product was purified by column chromatography on silica gel using

pentane as the eluent ($R_F = 0.24$). Compound **17a** was obtained as clear liquid (26.5 mg, 56% yield). The ^1H , ^{13}C and ^{19}F NMR spectroscopic data were identical to that reported previously in the literature.³⁰ HRMS EI (m/z): $[\text{M}]^+$ calcd for $\text{C}_{12}\text{H}_9\text{FO}$, 188.0637; measured, 188.0631.

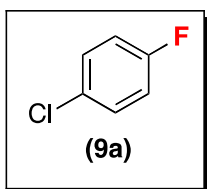


In a glovebox, $(\text{MeCN})_4\text{CuBF}_4$ (78.5 mg, 0.25 mmol, 1 equiv) and NFTPT (145 mg, 0.5 mmol, 2 equiv) were weighed into a 20 mL vial. MeCN (5 mL) was added, and the vial was sealed with a Teflon-lined cap. The reaction mixture was allowed to stir at 25 °C for 5 min. Then, potassium trifluoro(2-phenoxyphenyl)borate (69 mg, 0.25 mmol, 1 equiv) was added to the reaction mixture, and the reaction was allowed to stir at 40 °C for 12 h. The resulting solution was cooled to 25 °C, and diluted with MeCN (5 mL). 1,3,5-Trifluorobenzene (0.25 mmol, 1 equiv) was added as internal standards. The fluorinated product **18a** was formed in 52% yield as determined by ^{19}F NMR spectroscopic analysis of the crude reaction mixture. The reaction mixture was then diluted with Et_2O (10 mL), and the resulting mixture was washed with 2 M aqueous HCl (15 mL) and brine (15 mL) and then dried over magnesium sulfate. The solvent was removed by rotary evaporation at 30 °C, and the product was purified by column chromatography on silica gel using pentane as the eluent ($R_F = 0.24$). Compound **18a** was obtained as clear liquid. The isolated product **18a** (24.0 mg, 51% yield) was 96% pure, and contained traces (4%) of the corresponding protodeboronation byproduct, which was not easily separable by chromatography on silica gel. The ^1H and ^{13}C NMR spectroscopic data were identical to that reported previously in the literature.³¹ HRMS EI (m/z): $[\text{M}]^+$ calcd for $\text{C}_{12}\text{H}_9\text{FO}$, 188.0637; measured, 188.0638.

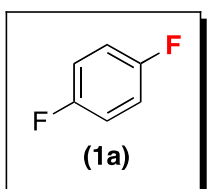


In a glovebox, $(\text{MeCN})_4\text{CuBF}_4$ (94.2 mg, 0.30 mmol, 1.2 equiv) and NFTPT (145 mg, 0.5 mmol, 2 equiv) were weighed into a 20 mL vial. EtOAc (5 mL) was added, and the vial was sealed with a Teflon-lined cap. The reaction mixture was allowed to stir at 25 °C for 5 min. Then, potassium (4-bromophenyl)trifluoroborate (65.7 mg, 0.25 mmol, 1 equiv) was added to the reaction mixture, and the reaction was allowed to stir at 80 °C for 12 h. The resulting

solution was cooled to room temperature and then diluted with CH₂Cl₂ (5 mL). 1,3,5-Trifluorobenzene and 4-fluoroanisole (0.25 mmol, 1 equiv) were added as internal standards. The fluorinated product **8a** was formed in 59% yield as determined by ¹⁹F NMR spectroscopic analysis of the crude reaction mixture. The ¹⁹F NMR spectral data for **8a** matched that of an authentic sample (SynQuest Labs, m, -116.25 ppm). The identity of the product was further confirmed by GCMS analysis, where the product peak was observed at 9.48 min.

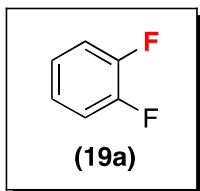


In a glovebox, (MeCN)₄CuBF₄ (94.2 mg, 0.30 mmol, 1.2 equiv) and NFTPT (145 mg, 0.5 mmol, 2 equiv) were weighed into a 20 mL vial. EtOAc (5 mL) was added, and the vial was sealed with a Teflon-lined cap. The reaction mixture was allowed to stir at 25 °C for 5 min. Then, potassium (4-chlorophenyl)trifluoroborate (54.6 mg, 0.25 mmol, 1 equiv) was added to the reaction mixture, and the reaction was allowed to stir at 80 °C for 12 h. The resulting solution was cooled to room temperature and diluted with CH₂Cl₂ (5 mL). 1,3,5-Trifluorobenzene and 4-fluoroanisole (0.25 mmol, 1 equiv) were added as internal standards. The fluorinated product **9a** was formed in 58% yield as determined by ¹⁹F NMR spectroscopic analysis of the crude reaction mixture. The ¹⁹F NMR spectral data for **9a** matched that of an authentic sample (Oakwood Products, m, -116.83 ppm). The identity of the product was further confirmed by GCMS analysis, where the product peak was observed at 8.00 min.

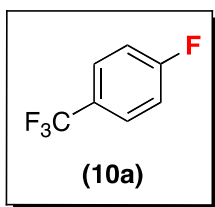


In a glovebox, (MeCN)₄CuBF₄ (94.2 mg, 0.30 mmol, 1.2 equiv) and NFTPT (145 mg, 0.5 mmol, 2 equiv) were weighed into a 20 mL vial. MeCN (5 mL) was added, and the vial was sealed with a Teflon-lined cap. The reaction mixture was allowed to stir at 25 °C for 5 min. Then, potassium (4-fluorophenyl)trifluoroborate (50.5 mg, 0.25 mmol, 1 equiv) was added to the reaction mixture, and the reaction was allowed to stir at 40 °C for 12 h. The resulting solution was cooled to room temperature and diluted with CH₂Cl₂ (5 mL). 1,3,5-Trifluorobenzene and 4-fluoroanisole (0.25 mmol, 1 equiv) were added as internal standards. The fluorinated product **1a** was formed in 66% yield as determined by ¹⁹F

NMR spectroscopic analysis of the crude reaction mixture. The ^{19}F NMR spectral data for **1a** matched that of an authentic sample (Alfa Aesar, m, -120.50 ppm). The identity of the product was further confirmed by GCMS analysis, where the product peak was observed at 3.74 min.

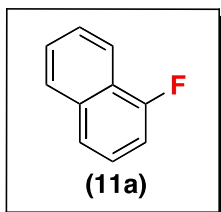


In a glovebox, $(\text{MeCN})_4\text{CuBF}_4$ (94.2 mg, 0.30 mmol, 1.2 equiv) and NFTPT (145 mg, 0.5 mmol, 2 equiv) were weighed into a 20 mL vial. EtOAc (5 mL) and $t\text{BuCN}$ (0.28 mL, 2.5 mmol, 10 equiv) were added, and the vial was sealed with a Teflon-lined cap. The reaction mixture was allowed to stir at 25 °C for 5 min. Then, potassium (2-fluorophenyl)trifluoroborate (50.5 mg, 0.25 mmol, 1 equiv) was added to the reaction mixture, and the reaction was allowed to stir at 40 °C for 12 h. The resulting solution was diluted with CH_2Cl_2 (5 mL). 1,3,5-Trifluorobenzene and 4-fluoroanisole (0.25 mmol, 1 equiv) were added as internal standards. The fluorinated product **19a** was formed in 40% yield as determined by ^{19}F NMR spectroscopic analysis of the crude reaction mixture. The ^{19}F NMR spectral data for **19a** matched that of an authentic sample (Matrix Scientific, m, -139.65 ppm). The identity of the product was further confirmed by GCMS analysis, where the product peak was observed at 4.08 min.

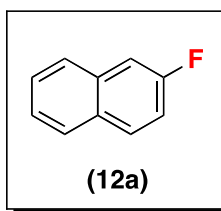


In a glovebox, $(\text{MeCN})_4\text{CuBF}_4$ (118 mg, 0.375 mmol, 1.5 equiv) and NFTPT (145 mg, 0.5 mmol, 2 equiv) were weighed into a 20 mL vial. EtOAc (5 mL) and $t\text{BuCN}$ (0.28 mL, 2.5 mmol, 10 equiv) were added, and the vial was sealed with a Teflon-lined cap. The reaction mixture was allowed to stir at 25 °C for 5 min. Then, potassium (4-trifluoromethylphenyl)trifluoroborate (53.5 mg, 0.25 mmol, 1 equiv) was added to the reaction mixture, and the reaction was allowed to stir at 80 °C for 12 h. The resulting solution was cooled to room temperature and diluted with CH_2Cl_2 (5 mL). 4-Fluoroanisole (0.25 mmol, 1 equiv) was added as internal standards. The fluorinated product **10a** was formed in 54% yield as determined by ^{19}F NMR spectroscopic analysis of the crude reaction mixture. The ^{19}F NMR spectral data for **10a** matched that of an authentic sample (Matrix Scientific, s, 3F, -62.62 ppm; m, F, -108.44 ppm). The identity

of the product was further confirmed by GCMS analysis, where the product peak was observed at 4.28 min.

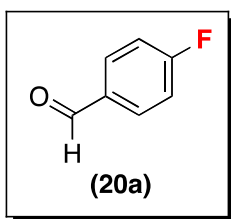


In a glovebox, $(\text{MeCN})_4\text{CuBF}_4$ (94.2 mg, 0.30 mmol, 1.2 equiv) and NFTPT (145 mg, 0.5 mmol, 2 equiv) were weighed into a 20 mL vial. EtOAc (5 mL) and $t\text{BuCN}$ (0.28 mL, 2.5 mmol, 10 equiv) was added, and the vial was sealed with a Teflon-lined cap. The reaction mixture was allowed to stir at 25 °C for 5 min. Then, potassium (1-naphthyl)trifluoroborate (58.5 mg, 0.25 mmol, 1 equiv) was added to the reaction mixture, and the reaction was allowed to stir at 80 °C for 12 h. The resulting solution was cooled to 25 °C, and diluted with EtOAc (5 mL). 1,3,5-Trifluorobenzene and 4-fluoroanisole (0.25 mmol, 1 equiv) were added as internal standards. The fluorinated product **11a** was formed in 62% yield as determined by ^{19}F NMR spectroscopic analysis of the crude reaction mixture. The reaction mixture was then diluted with Et_2O (10 mL), and the resulting mixture was washed with 2 M aqueous HCl (15 mL) and brine (15 mL) and then dried over magnesium sulfate. The solvent was removed by rotary evaporation at 0 °C, and the product was purified by column chromatography on silica gel using pentane as the eluent ($R_F = 0.55$). Compound **11a** was obtained as clear liquid (20.5 mg, 56% yield). The ^1H , ^{13}C and ^{19}F NMR spectroscopic data were identical to that reported previously in the literature.^{9a} HRMS EI (m/z): $[\text{M}]^+$ calcd for $\text{C}_{10}\text{H}_7\text{F}$, 146.0532; measured, 146.0531.

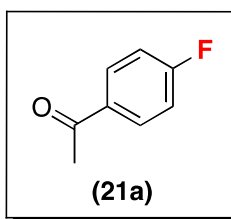


In a glovebox, $(\text{MeCN})_4\text{CuBF}_4$ (78.5 mg, 0.25 mmol, 1 equiv) and NFTPT (145 mg, 0.5 mmol, 2 equiv) were weighed into a 20 mL vial. EtOAc (5 mL) was added, and the vial was sealed with a Teflon-lined cap. The reaction mixture was allowed to stir at 25 °C for 5 min. Then, potassium (2-naphthyl)trifluoroborate (58.5 mg, 0.25 mmol, 1 equiv) was added to the reaction mixture, and the reaction was allowed to stir at 80 °C for 12 h. The resulting solution was cooled to 25 °C, and diluted with EtOAc (5 mL). 1,3,5-Trifluorobenzene and 4-fluoroanisole (0.25 mmol, 1 equiv) were added as internal standards. The fluorinated product **12a** was formed in 66% yield as determined by ^{19}F

NMR spectroscopic analysis of the crude reaction mixture. The reaction mixture was then diluted with Et₂O (10 mL), and the resulting mixture was washed with 2 M aqueous HCl (15 mL) and brine (15 mL) and then dried over magnesium sulfate. The solvent was removed by rotary evaporation at 0 °C, and the product was purified by column chromatography on silica gel using pentane as the eluent (*R*_F = 0.48). Compound **12a** was obtained as white crystalline solid (23.5 mg, 64% yield, mp = 59.8-60.4 °C). ¹H NMR (CDCl₃): δ 7.86-7.82 (multiple peaks, 2H), 7.79 (dd, *J* = 8.4, 1 Hz, 1H), 7.51 (ddd, *J* = 7.5, 7.5, 1 Hz, 1H), 7.46 (m, 1H), 7.45 (ddd, *J* = 7.5, 7.5, 1 Hz, 1H), 7.27 (ddd, *J* = 10.5, 8.4, 1 Hz, 1H). ¹³C NMR (CDCl₃): δ 160.07 (d, *J* = 244.0 Hz), 134.27 (d, *J* = 9.4 Hz), 130.57, 130.42 (d, *J* = 9.6 Hz), 128.02 (d, *J* = 1.4 Hz), 127.40 (d, *J* = 5.4 Hz), 127.00, 125.22 (d, *J* = 2.8 Hz), 116.40 (d, *J* = 25.0 Hz), 111.00 (d, *J* = 20.3 Hz). ¹⁹F NMR (CDCl₃): δ -114.90 (m, 1F). HRMS EI (*m/z*): [*M*]⁺ calcd for C₁₀H₇F, 146.0532; measured, 146.0531.

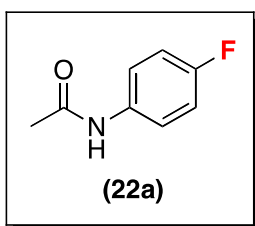


In a glovebox, (MeCN)₄CuBF₄ (118 mg, 0.375 mmol, 1.5 equiv) and NFTPT (145 mg, 0.5 mmol, 2 equiv) were weighed into a 20 mL vial. EtOAc (5 mL) was added, and the vial was sealed with a Teflon-lined cap. The reaction mixture was allowed to stir at 25 °C for 5 min. Then, potassium (4-formylphenyl)trifluoroborate (53 mg, 0.25 mmol, 1 equiv) was added to the reaction mixture, and the reaction was allowed to stir at 80 °C for 12 h. The resulting solution was diluted with CH₂Cl₂ (5 mL). 1,3,5-Trifluorobenzene and 4-fluoroanisole (0.25 mmol, 1 equiv) were added as internal standards. The fluorinated product **20a** was formed in 48% yield as determined by ¹⁹F NMR spectroscopic analysis of the crude reaction mixture. The product showed a ¹⁹F NMR signal at -104.22 ppm in CDCl₃ (lit. -102.9 ppm in CDCl₃).^{9a} The identity of the product was further confirmed by GCMS analysis, where the product peak was observed at 9.94 min.



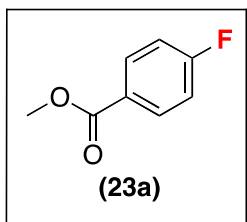
In a glovebox, (MeCN)₄CuBF₄ (94.2 mg, 0.30 mmol, 1.2 equiv) and NFTPT (145 mg, 0.5 mmol, 2 equiv) were weighed into a 20 mL vial. EtOAc (5 mL) was added, and the vial was sealed with a

Teflon-lined cap. The reaction mixture was allowed to stir at 25 °C for 5 min. Then, potassium (4-acetylphenyl)trifluoroborate (56.5 mg, 0.25 mmol, 1 equiv) was added to the reaction mixture, and the reaction was allowed to stir at 80 °C for 12 h. The resulting solution was cooled to 25 °C, and diluted with EtOAc (5 mL). 1,3,5-Trifluorobenzene (0.25 mmol, 1 equiv) was added as internal standards. The fluorinated product **21a** was formed in 60% yield as determined by ¹⁹F NMR spectroscopic analysis of the crude reaction mixture. The reaction mixture was then diluted with Et₂O (10 mL), and the resulting mixture was washed with 2 M aqueous HCl (15 mL) and brine (15 mL) and then dried over magnesium sulfate. The solvent was removed by rotary evaporation at 0 °C, and the product was purified by column chromatography on silica gel using 5% diethyl ether in pentane as the eluent (R_F = 0.25). Compound **21a** was obtained as a clear liquid (19.5 mg, 56% yield). The ¹H, ¹³C and ¹⁹F NMR spectroscopic data were identical to that reported previously in the literature.¹⁰ HRMS EI (m/z): [M]⁺ calcd for C₈H₇FO, 138.0481; measured, 138.0477.



In a glovebox, (t-BuCN)₂CuOTf (114 mg, 0.30 mmol, 1.2 equiv) and NFTPT (145 mg, 0.5 mmol, 2 equiv) were weighed into a 20 mL vial. EtOAc (5 mL) was added, and the vial was sealed with a Teflon-lined cap. The reaction mixture was allowed to stir at 25 °C for 5 min. Then, potassium (4-acetylamino)phenyl)trifluoroborate (60.3 mg, 0.25 mmol, 1 equiv) was added to the reaction mixture, and the reaction was allowed to stir at 80 °C for 12 h. The resulting solution was cooled to 25 °C, and diluted with EtOAc (5 mL). 1,3,5-Trifluorobenzene and 4-fluoroanisole (0.25 mmol, 1 equiv) were added as internal standards. The fluorinated product **22a** was formed in 45% yield as determined by ¹⁹F NMR spectroscopic analysis of the crude reaction mixture. The reaction mixture was then diluted with Et₂O (10 mL), and the resulting mixture was washed with 2 M aqueous HCl (15 mL) and brine (15 mL) and then dried over magnesium sulfate. The solvent was removed by rotary evaporation at 30 °C, and the product was purified by column chromatography on silica gel using 70% diethyl ether in pentane as the eluent (R_F = 0.20). Compound **22a** was obtained as white solid (16 mg, 42% yield, mp = 151.3-152.3 °C). The ¹H, ¹³C and ¹⁹F NMR spectroscopic data were

identical to that reported previously in the literature.^{9a} HRMS EI (m/z): [M]⁺ calcd for C₈H₈FNO, 153.0590; measured, 153.0583.



In a glovebox, (tBuCN)₂CuOTf (114 mg, 0.30 mmol, 1.2 equiv) and NFTPT (145 mg, 0.5 mmol, 2 equiv) were weighed into a 20 mL vial. EtOAc (5 mL) was added, and the vial was sealed with a Teflon-lined cap. The reaction mixture was allowed to stir at 25 °C for 5 min. Then, potassium (4-methoxycarbonylphenyl)trifluoroborate (60.5 mg, 0.25 mmol, 1 equiv) was added to the reaction mixture, and the reaction was allowed to stir at 80 °C for 12 h. The resulting solution was cooled to 25 °C, and diluted with EtOAc (5 mL). 1,3,5-Trifluorobenzene (0.25 mmol, 1 equiv) was added as internal standards. The fluorinated product **23a** was formed in 57% yield as determined by ¹⁹F NMR spectroscopic analysis of the crude reaction mixture. The reaction mixture was then diluted with Et₂O (10 mL), and the resulting mixture was washed with 2 M aqueous HCl (15 mL) and brine (15 mL) and then dried over magnesium sulfate. The solvent was removed by rotary evaporation at 0 °C, and the product was purified by column chromatography on silica gel using 2% diethyl ether in pentane as the eluent (R_F = 0.21). Compound **23a** was obtained as clear liquid. The isolated product **23a** (22.0 mg, 57% yield) was 96% pure, and contained 4% of the corresponding protodeboronation byproduct, which was not easily separable by chromatography on silica gel. The ¹H, ¹³C and ¹⁹F NMR spectroscopic data were identical to that reported previously in the literature.^{9a} HRMS EI (m/z): [M]⁺ calcd for C₈H₇FO₂, 154.0430; measured, 154.0425.

Investigations of High Valent Cu Intermediate using THF as Additive

In a glovebox, (tBuCN)₂CuOTf (38 mg, 0.1 mmol, 1 equiv) and NFTPT (29 mg, 0.1 mmol, 1 equiv) were weighed into a 4 mL vial. EtOAc (0.5 mL) was added, and the vial was sealed with a Teflon-lined cap. The reaction mixture was allowed to stir at 25 °C for 10 min and a ¹⁹F NMR spectrum was recorded. Then, THF (81 μL, 1 mmol, 10 equiv) was added to the reaction mixture, and the reaction was allowed to stir at 25 °C for an additional 10 min. The resulting solution was analyzed by ¹⁹F NMR spectroscopy. The

Cu(III) complex recently characterized by Hartwig¹³ was detected by ¹⁹F NMR spectroscopy in 3% yield.

Investigations of High Valent Cu Intermediate using THF as Co-Solvent

In a glovebox, (tBuCN)₂CuOTf (38 mg, 0.1 mmol, 1 equiv) and NFTPT (29 mg, 0.1 mmol, 1 equiv) were weighed into a 4 mL vial. THF (81 μL, 1 mmol, 10 equiv) and EtOAc (0.5 mL) were pre-mixed in another 4 mL vial before adding into the reaction. The vial was sealed with a Teflon-lined cap, and the reaction mixture was allowed to stir at 25 °C for 10 min. The resulting solution was analyzed by ¹⁹F NMR spectroscopy. The Cu(III) complex recently characterized by Hartwig¹³ was detected by ¹⁹F NMR spectroscopy in 18% yield.

5.7 Reference

1. (a) Jeschke, P. *Pest Manag. Sci.* **2010**, *66*, 10; (b) Purser, S.; Moore, P. R.; Swallow, S.; Gouverneur, V. *Chem. Soc. Rev.* **2008**, *37*, 320; (c) Hagmann, W. K. *J. Med. Chem.* **2008**, *51*, 4359; (d) Jeschke, P. *ChemBioChem* **2004**, *5*, 570.
2. (a) Balz, G.; Schiemann, G. *Ber. Deutsch. Chem. Ges.* **1927**, *60*, 1186; (b) Barnette, W. E. *J. Am. Chem. Soc.* **1984**, *106*, 452; (c) Differring, E.; Wehrli, M. *Tetrahedron Lett.* **1991**, *32*, 3819; (d) Yamada, S.; Gavryushin, A.; Knochel, P. *Angew. Chem., Int. Ed.* **2010**, *49*, 2215; (e) Anbarasan, P.; Neumann, H.; Beller, M. *Angew. Chem., Int. Ed.* **2010**, *49*, 2219.
3. (a) Hollingworth, C.; Gouverneur, V. *Chem. Commun.* **2012**, *48*, 2929; (b) Furuya, T.; Kamlet, A. S.; Ritter, T. *Nature* **2011**, *473*, 470; (c) Grushin, V. V. *Acc. Chem. Res.* **2010**, *43*, 160; (d) Brown, J. M.; Gouverneur, V. *Angew. Chem., Int. Ed.* **2009**, *48*, 8610.
4. For examples of C–F bond formation from Pd(IV)(R)(F) complexes, see: (a) McMurtrey, K. B.; Racowski, J. M.; Sanford, M. S. *Org. Lett.* **2012**, *14*, 4094. (b) Racowski, J. M.; Kampf, J. W.; Sanford, M. S. *Angew. Chem., Int. Ed.* **2012**, *51*, 3414. (c) Ball, N. D.; Kampf, J. W.; Sanford, M. S. *J. Am. Chem. Soc.* **2010**, *132*, 2878. (d) Furuya, T.; Benitez, D.; Tkatchouk, E.; Strom, A. E.; Tang, P.; Goddard, W. A.; Ritter, T. *J. Am. Chem. Soc.* **2010**, *132*, 3793. (e) Lee, E.; Kamlet, A. S.; Powers, D. C.; Neumann, C. N.; Boursalian, G. B.; Furuya, T.; Choi, D. C.; Hooker, J. M.; Ritter, T. *Science* **2011**, *334*, 639.
5. Hull, K. L.; Anani, W. Q.; Sanford, M. S. *J. Am. Chem. Soc.* **2006**, *128*, 7134.
6. (a) Chan, C. S. L.; Wasa, M.; Wang, X.; Yu, J.-Q. *Angew. Chem., Int. Ed.* **2011**, *50*, 9081; (b) Wang, X.; Mei, T. S.; Yu, J.-Q. *J. Am. Chem. Soc.* **2009**, *131*, 7520.
7. (a) Maimone, T. J.; Milner, P. J.; Kinzel, T.; Zhang, Y.; Takase, M. K.; Buchwald, S. L. *J. Am. Chem. Soc.* **2011**, *133*, 18106; (b) Noel, T.; Maimone, T. J.; Buchwald, S. L. *Angew. Chem., Int. Ed.* **2011**, *50*, 8900; (c) Watson, D. A.; Su, M.; Teverovskiy, G.; Zhang, Y.; Garcia-Fortanet, J.; Kinzel, T.; Buchwald, S. L. *Science* **2009**, *321*, 1661.
8. (a) Tang, P.; Furuya, T.; Ritter, T. *J. Am. Chem. Soc.* **2010**, *132*, 12150; (b) Furuya, T.; Strom, A. E.; Ritter, T. *J. Am. Chem. Soc.* **2009**, *131*, 1662.
9. (a) Furuya, T.; Ritter, T. *Org. Lett.* **2009**, *11*, 2860; (b) Furuya, T.; Kaiser, H. M.; Ritter, T. *Angew. Chem., Int. Ed.* **2008**, *47*, 5993.
10. Tang, P.; Ritter, T. *Tetrahedron* **2011**, *67*, 4449.
11. For an example of fluorination of haloarenes by CuF₂/TMEDA, see: Grushin, V. Process for Preparing Fluoroarenes from Haloarenes. U.S. Patent 7,202,388, 2007.
12. Casitas, A.; Canta, M.; Sola, M.; Costas, M.; Ribas, X. *J. Am. Chem. Soc.* **2011**, *133*, 19386.
13. Yao, B.; Wang, Z.-L.; Zhang, H.; Wang, D.-X.; Zhao, L.; Wang, M.-X. *J. Org. Chem.* **2012**, *77*, 3336.
14. Fier, P. S.; Hartwig, J. F. *J. Am. Chem. Soc.* **2012**, *134*, 10795.
15. While this work was under review, a closely related chemistry was reported by Hartwig and co-workers: Fier, P. S.; Luo, J.; Hartwig, J. F. *J. Am. Chem. Soc.* **2013**, *135*, 2552.

16. Engle, K. M.; Mei, T.-S.; Wang, X.; Yu, J.-Q. *Angew. Chem., Int. Ed.* **2011**, *50*, 1478.
17. For metal-free electrophilic fluorination of electron rich aryl trifluoroborates by F-TEDA-BF₄, see: Cazorla, C.; Metay, E.; Andrioletti, B.; Lemaire, M. *Tetrahedron Lett.* **2009**, *50*, 3936.
18. (a) Oishi, M.; Konda, H.; Amii, H. *Chem. Commun.* **2009**, 1909; (b) Knauber, T.; Arikian, F.; Rösenthaller, G. V.; Gooßen, L. J. *Chem. Eur. J.* **2011**, *17*, 2689; (c) Wang, Z.; Lee, R.; Jia, W.; Yuan, Y.; Wang, W.; Feng, X.; Huang, K. W. *Organometallics* **2011**, *30*, 3229; (d) Chu, L.; Qing, F. L. *Org. Lett.* **2010**, *12*, 5060; (e) Senecal, T. D.; Parsons, A. T.; Buchwald, S. L. *J. Org. Chem.* **2011**, *76*, 1174; (f) Liu, T.; Shen, Q. *Org. Lett.* **2011**, *13*, 2342; (g) Xu, J.; Luo, D. F.; Xiao, B.; Liu, Z. J.; Gong, T. J.; Fu, Y.; Liu, L. *Chem. Commun.* **2011**, *47*, 4300; (h) Chu, L.; Qing, F.-L. *J. Am. Chem. Soc.* **2011**, *134*, 1298; (i) Mu, X.; Chen, S.; Zhen, X.; Liu, G. *Chem. –Eur. J.* **2011**, *17*, 6039.
19. (a) Whitfield, S. R.; Sanford, M. S. *J. Am. Chem. Soc.* **2007**, *129*, 15142; (b) Powers, D. C.; Ritter, T. *Nat. Chem.* **2009**, *1*, 302; (c) Powers, D. C.; Geibel, M. A. L.; Klein, J. E. M. N.; Ritter, T. *J. Am. Chem. Soc.* **2009**, *131*, 17050; (d) Kalyani, D.; Deprez, N. R.; Desai, L. V.; Sanford, M. S. *J. Am. Chem. Soc.* **2005**, *127*, 7330; (e) Ye, Y.; Ball, N. D.; Kampf, J. W.; Sanford, M. S. *J. Am. Chem. Soc.* **2010**, *132*, 14682.
20. Inert atmosphere and dry reagents are required for all the reactions in **Schemes 5.3** and **5.4**. Reactions conducted in air with non-dried reagents showed significantly reduced yields.
21. Yin, F.; Wang, Z.; Li, Z.; Li, C. *J. Am. Chem. Soc.* **2012**, *134*, 10401.
22. For related approaches to Ni-mediated fluorination, see: Lee, E.; Hooker, J. M.; Ritter, T. *J. Am. Chem. Soc.* **2012**, *134*, 17456.
23. (a) Darses, S.; Genêt, J.-P.; Brayer, J.-L.; Demoute, J.-P. *Tetrahedron Lett.* **1997**, *38*, 4393; (b) Xia, M.; Chen, Z.-C. *Synth. Commun.* **1999**, *29*, 2457.
24. Satterfield, A. D.; Kubota, A.; Sanford, M. S. *Org. Lett.* **2011**, *13*, 1076.
25. (a) Vedejs, E.; Chapman, R. W.; Fields, S. C.; Lin, S.; Schrimpf, M. R. *J. Org. Chem.* **1995**, *60*, 3020; (b) Molander, G. A.; Biolatto, B. *Org. Lett.* **2002**, *4*, 1867.
26. Morandi, S.; Caselli, E.; Forni, A.; Bucciarelli, M.; Torre, G.; Prati, F. *Tetrahedron: Asymmetry* **2005**, *16*, 2918.
27. Shintani, R.; Takeda, M.; Nishimura, T.; Hayashi, T. *Angew. Chem., Int. Ed.* **2010**, *49*, 3969.
28. Gillis, E. P.; Burke, M. D. *J. Am. Chem. Soc.* **2007**, *129*, 6716.
29. Lothian, A. P.; Ramsden, C. A.; Shaw, M. M.; Smith, R. G. *Tetrahedron* **2011**, *67*, 2788.
30. Kim, H. J.; Kim, M.; Chang, S. *Org. Lett.* **2011**, *13*, 2368.
31. Jalalian, N.; Ishikawa, E. E.; Silva, L. F.; Olofsson, B. *Org. Lett.* **2011**, *13*, 1552.